PATHOGENESIS OF BIOFILM-ISOLATED *LISTERIA MONOCYTOGENES* AND BIOFILMS CONTROL USING FOOD-GRADE NATURAL ANTIMICROBIALS

by

Xingjian Bai

A Dissertation

Submitted to the Faculty of Purdue University

In Partial Fulfillment of the Requirements for the degree of

Doctor of Philosophy

Department of Food Science

West Lafayette, Indiana

May 2021

THE PURDUE UNIVERSITY GRADUATE SCHOOL
STATEMENT OF COMMITTEE APPROVAL

Dr. Arun K. Bhunia, Chair
Department of Food Science

Dr. Bruce M. Applegate
Department of Food Science

Dr. Cindy H. Nakatsu
Department of Agronomy

Dr. Thomas M. Walter
Department of Biological Sciences

Approved by:
Dr. Arun K. Bhunia

Dedicated to my parents and wife

ACKNOWLEDGMENTS

I would like to acknowledge my major professor, Dr. Arun Bhunia, for his mentorship, support, help and patience since my junior year in college. I would not be on this path without the initial opportunity to work in his lab as an undergrad research assistant. I was and will always be inspired by his preciseness, hardworking, and open mindset in research. I would also like to acknowledge Dr. Atul Singh, who guided me through my early time in the lab. He taught me many important lessons, techniques, and the most importantly – a scientific mindset.

Besides, I would like to express my sincere gratitude to my committee members: Dr. Bruce Applegate, Dr. Cindy Nakatsu, and Dr. Thomas Walter. My committee members have consistently offered me guidance, advice, and supports. Whenever I need help, I know that my committee members are always there. Dr. Applegate has always been generous for any materials or equipment I need from his lab and helped me every time I knocked on his door. With her comprehensive experience in microbiology and qRT-PCR research, Dr. Nakatsu provided numerous suggestions for my research and helped me complete experiment designs to address comments from reviewers, which leaded to the publish of my major PhD study. A special thank goes to Dr. Thomas Walter. In addition to his help for my PhD study, his BIOL 221 class not only set a solid foundation for me to build my research but also made me so interested in biology and eventually choose it as a career. His BIOL 529 class pushed me to design experiments and interpret results at a different level. His dedication to work and teaching also motivated me to thrive in my job.

Next, I would like to thank all my lab colleagues and undergraduate researchers who used to work in Bhunia lab. They provided great advice for my research, career, and life. More importantly, I cannot never complete my research without their help and mental support. I appreciated the trust my undergraduate students put in me, listening to my “mini-lectures”.

I would like to thank my parents, Dr. Yuanfeng Zhao and Zhendong Bai. They showed me their unconditional love and support during this journey, especially my mom who encouraged me to pursue a PhD and taught me the importance of consistent study. I would also like to thank my wife and her family for bringing the spirit of optimism, humor, and close-knit relationship to my life. I must also acknowledge Purdue staffs, Mitzi Barnett, Deborah Livengood, Marliese Orr, Stephanie Griswold and Brian Marrs, who helped me on daily basis. I would not have completed

my projects without the funding sources and the wonderful education program offered by Department of Food Science, Purdue University.

Finally, I would like to acknowledge the financial support provided by the Korean Food Research Institute (KFRI grant # E0142102-03), National Academy of Science (NAS) and USAID (AID-263-A-15-00002), the U.S. Department of Agriculture, Agricultural Research Service, under Agreement No. 59-8072-6-001, the USDA National Institute of Food and Agriculture (Hatch Accession No. 1016249), the Center for Food Safety Engineering at Purdue University, Purdue Research Foundation, and Bilsland Dissertation Fellowship. Collaborative research between Purdue University and Assiut University, Egypt (Dr. Talaat El-Khateib, collaborator) funded by USAID is acknowledged.

TABLE OF CONTENTS

LIST OF TABLES

LIST OF FIGURES

ABSTRACT

Foodborne pathogens form biofilms as a survival strategy in various unfavorable environments, and biofilms are known to be the frequent source for infection and outbreaks of foodborne illness. Therefore, it is essential to understand the pathogenicity of bacteria in biofilms and methods to inactivate biofilm-forming microbes from food processing environments, including school cafeteria or other community-based food production facilities, and to prevent foodborne outbreaks. Pathogen transmissions occur primarily through raw or under cooked foods and by cross contamination during unsanitary food preparation practices. Then, pathogens can form biofilms on the surface and become persistent in food production facilities and can be a source for recurrent contamination and foodborne outbreaks. In this study, our first aim was to use *L. monocytogenes* as a model pathogen to study how an enteric infectious pathogen isolated from biofilm modifies its pathogenesis compared to its planktonic counterpart. Both clinical and food isolates with different serotypes and biofilm-forming abilities were selected and tested using cell culture and mouse models. *L. monocytogenes* sessile cells isolated from biofilms express reduced levels of the *lap*, *inlA*, *hly*, *prfA*, and *sigB* and show reduced adhesion, invasion, translocation, and cytotoxicity in the cell culture model than the planktonic cells. Oral challenge of C57BL/6 mice with food, clinical, or murinized-InlA ($InlA^m$) strains revealed that at 12 and 24 h post-infection (hpi), *L. monocytogenes* burdens are lower in tissues of mice infected with sessile cells than those infected with planktonic cells. However, these differences are negligible at 48 hpi. Besides, the expressions of *inlA* and *lap* mRNA in sessile *L. monocytogenes* from intestinal content are about 6.0- and 280-fold higher than the sessile inoculum, respectively, suggesting sessile *L. monocytogenes* can still upregulate virulence genes shortly after ingestion (12 h).

After learning biofilm isolated *L. monocytogenes* cells have similar virulence potential as the planktonic counterparts, our next goal was to effectively prevent or inactivate biofilms using food-grade natural microbials. Since *L. monocytogenes* cells are usually found in multi-pathogen biofilm in nature, I combined two food-grade broad-spectrum natural antimicrobials, chitosan nanoparticles (ChNP) and ε-poly-L-lysine (PL), as ChNP-PL nanoconjugates and tested its function on single or mixed culture biofilms of *L. monocytogenes*, *Staphylococcus aureus*, *Escherichia coli*, *Salmonella enterica* serovar Enteritidis, and *Pseudomonas aeruginosa*. ChNP-PL not only was able to significantly ($P<0.05$) prevent the biofilm formation but also inactivate

pre-formed biofilms when analyzed by crystal violet staining and plate counting. *In vitro* cytotoxicity analysis (LDH and WST-based assays) using an intestinal cell line, indicated ChNP-PL to be non-toxic. In conclusion, our results showed ChNP-PL has strong potential to prevent the formation or inactivation of preformed polymicrobial biofilms of foodborne pathogens in food processing environment. Application of ChNP-PL could inhibit the colonization of foodborne pathogens, minimize cross-contamination during food production, and eventually reduce foodborne outbreaks.

CHAPTER 1. REVIEW OF LITERATURE

1.1 Bacterial biofilm and food safety

Most microbes found in nature exist in biofilms, a well-structured, dynamic, diverse, and protective microbial community (Flemming and Wingender 2010). Biofilm formation is a natural survival strategy of a microbial cell when it tries to colonize a solid surface to compete efficiently with others for space and nutrients and to resist any unfavorable environmental conditions. The solid surface may be comprised of biotic (meat, produce, oral cavity, etc.) or abiotic surface (floors, walls, drains, equipment, or food-contacting surfaces), and microbes adhere to it by producing an extracellular polymeric substance (EPS) forming a three-dimensional biofilm scaffold. Metaphorically, EPS is the "house" that covers and protects bacteria in biofilms, and EPS makes up the majority of the total dry mass of biofilms (Flemming et al. 2007). Although biofilms are solid architecture that can protect bacteria from physical impact, most of the biofilm is still made up of water (Yaron and Romling 2014). About a third of the biofilm's dry weight is bacterial cells, and the remaining weight comes from the bacteria-derived molecules, like polysaccharides, proteins, and DNA, that make up the EPS (Costerton et al. 1999). Biofilms can be comprised of single species or mixed-species cultures. In the food-processing environment, biofilm formation threatens food safety since pathogens can be directly transmitted through contact. After the transmission, pathogens can also form biofilms on food surfaces, for instance *Listeria monocytogenes* found on cantaloupe skin caused a multistate outbreak in 2011 (CDC 2012; Fu et al. 2017). This review focuses on the relationship between bacterial pathogenesis and their biofilm formation.

For bacteria, the microbial attachment and biofilm formation on solid surfaces provide the advantages of living in a protective scaffold against desiccation, resistance to antibiotics or biocides (sanitizers), ultraviolet radiation, metallic cations, and physical impact by washing and cleaning. For instance, Martins et al. (2019) recently showed urinary tract infection causing isolates of *Staphylococcus saprophyticus* were more resistant to several antibiotics in their biofilm status than their planktonic counterparts. *Lactobacillus plantarum*, a commonly used model food spoilage bacterium, in biofilms were more resistant to several stress, including organic acids, ethanol, and sodium hypochlorite, than its planktonic state (Kubota et al. 2009). Bacteria can

acquire and or exchange genetic materials in biofilms. It has been observed that DNA exchanges through both plasmid conjugation and transformation can take place in biofilms (Christensen et al. 1998; Molin and Tolker-Nielsen 2003). The common biofilm-forming microorganisms in different food processing environments may vary and may include *Listeria monocytogenes*, *Micrococcus* spp., *Staphylococcus* spp., *Clostridium* spp., *Bacillus* spp., *Lactobacillus* spp., *Brochothrix thermosphacta*, *Salmonella enterica, Escherichia coli*, *Serratia* spp., *Campylobacter* spp., and *Pseudomonas* spp. (Ray and Bhunia 2007; Di Ciccio et al. 2012).

Biofilm formation occurs in several stages: (i) attachment, (ii) microcolony formation, (iii) maturation with cellular differentiation, and (iv) detachment or dispersion. In biofilms, microorganisms produce fimbriae, curli, flagella, adhesion proteins, and capsules to firmly attach to the surface (Flemming and Wingender 2010). Cells grow in close proximity and cell-to-cell communication (quorum sensing) occurs through the production of autoinducers such as N-acyl homoserine lactone (AI-1) or other molecules, which also regulate gene expression for survival, growth, cell density, resistance to antimicrobials and tolerance to desiccation (Landini et al. 2010). As a microcolony continues to grow, cells accumulate forming a matured biofilm with three-dimensional scaffolding. Loose cells are then sloughed off from matured biofilm and converted into planktonic cells which start the life cycle of a biofilm again by attaching to a new surface exposed to food ingredients or substrates. The cells from biofilms could become a continuous source for food contamination (Ray and Bhunia 2007).

Foodborne pathogens form biofilms as a survival strategy in various unfavorable environments, and biofilms are known to be a frequent source for infections and outbreaks (Flemming and Wingender 2010). Therefore, it is essential to establish effective control measures against biofilm-forming microbes from food production and processing environments, including school cafeterias or other community-based food production facilities to prevent foodborne outbreaks. In this research, our main purpose is to comprehensively study the pathogenic potential of *L. monocytogenes* isolated from biofilm and use natural antimicrobials to develop a solution for mixed culture biofilm control in a food-processing environment.

Pathogen transmission through food and water results in about 1.8 million annual deaths globally (Newell et al. 2010). In the United States alone, foodborne pathogens are responsible for roughly 48 million illnesses, 128,000 hospitalizations, and 3,000 deaths each year, resulting in yearly economic expenses of 78 billion dollars (Scallan et al. 2011). A core set of 31 bacterial

(64%), viral (12%), and parasitic (25%) pathogens have been identified that are responsible for nine million illnesses in the US each year, and the remainder of 39 million illnesses are caused by pathogens or agents whose identities are unknown.

Pathogen transmissions occur primarily through raw uncooked or undercooked foods and by cross-contamination during unsanitary food preparation practices. Pathogens find a harborage site or niche in food production facilities or product surfaces by forming biofilms (Srey et al. 2013), which serve as a major source for foodborne outbreaks, especially in cafeterias, hospitals, cruise ships, and commercial food processing facilities. Therefore, pathogens persist in food production facilities or product surfaces by forming biofilms (Srey et al. 2013), and serve as a major source for foodborne outbreaks. The control of biofilms in a food processing environment is often associated with various challenges. Similar to the use of antibiotic selecting for resistant bacteria, the pathogens that exhibit resistance to disinfectants or sanitizing agents could also be selected for in food processing environments where those chemicals are consistently applied (Shirron et al. 2009). As a result, the resistant ones will survive with less competition since the diversity of commensal bacteria in those environments is reduced by chemicals.

To study biofilms, *in vitro*, *in vivo*, and *ex vivo* models have been developed for biofilms formation from various pathogens (Lebeaux et al. 2013). Here, I will discuss several *in vitro* biofilm formation models since they are most relevant to biofilms formed on food-contact surfaces. Djordjevic et al. (2002) applied a convenient *in vitro* method of using polyvinyl chloride (PVC) 96-well microtiter plates to assess the biofilms formation with *L. monocytogenes* isolates. *L. monocytogenes* cells cultured overnight in tryptic soy broth supplemented with yeast extract (TSBYE) were inoculated in modified Welshimer's broth, a chemically defined minimal medium and incubated in 96-well microtiter plates at 32°C. This method has been well-accepted and used in hundreds of published papers as a high-throughput method to quantify static biofilm formation with *L. monocytogenes*. On the other hand, the method is not applicable for efficiently generating large quantities of sessile bacterial cells or simulating biofilm formation under flowing liquid.

The Calgary biofilm device is a modification of the microtiter plate model, and has also been widely cited by almost two thousand published articles (Ceri et al. 1999). A lid with 96 pins is placed on a 96-well microtiter plate, and the pins are immersed in medium containing bacteria in each well. Biofilms are formed on the pins after incubation, and the lid is transferred to a second microtiter plate. Sessile bacteria in biofilms on those pins can be detached into each well of the

second microtiter plate by sonication. The Biofilm Microfermenter developed at the Pasteur Institute (2015) was applied to investigate biofilm formation under continuously flowing conditions. Toledo-Arana et al. (2005) used the system and showed that *S. aureus* Δ*arlRS* had a higher biofilm-forming capacity than its wildtype counterpart, which provided critical evidence for the role of the *arlRS* system in biofilm formation. Recently, the CDC Biofilm Reactor ® has been used for mimicking biofilm formation by *L. monocytogenes* under a dynamic environment of continuous shear stress and renewing nutrients (Donlan et al. 2001; Mendez et al. 2020). Multiple circular coupons (diameter = 1.27 cm) of metals or plastic are placed in the bioreactor and immersed in medium. After incubation, biofilms formed on those coupons were detached in phosphate buffered saline (PBS) by sonication and enumerated using serial dilution and plate counts (Mendez et al. 2020). Compared to biofilm formation in microtiter plates, the biofilm growth area is significantly improved by using up to 24 coupons in one reactor. Besides, biofilms on coupons can be directly used for microscopic analysis. Mendez et al. (2020) applied both Laser scanning confocal microscopy to image SYTO 9-stained *L. monocytogenes* biofilms and plate count to quantify sessile bacteria in biofilms. Results showed *L. monocytogenes* biofilms formed on polycarbonate coupon at 30°C in TSBYE contained significantly more cells than the biofilms formed under the same conditions at 37°C.

1.2 *Listeria monocytogenes* pathogenesis and biofilm formation

In 1926, a bacterium, which is identified today as *Listeria monocytogenes*, was found to be the cause of monocytosis in laboratory rabbits and guinea pigs (Murray et al. 1926). In the following decades, this pathogen has been further characterized and established to be responsible for both sepsis in infant and meningitis in adults (Gray and Killinger 1966). The earliest recorded human listeriosis outbreaks occurred in Germany and France in 1966 and 1975, respectively (Liu 2008). *L. monocytogenes* is a Gram-positive, non-spore-forming, motile, facultative anaerobic bacterium. Since the 1980s, the understanding of *L. monocytogenes* pathogenesis and treatment for listeriosis has been improved due to significant progress made in molecular biotechnology. Yet, the pathogen still causes invasive and often life-threatening foodborne illnesses around the world, resulting in a tremendous financial burden to individuals and the food industry. Statistics showed that listeriosis is the second most common cause of death among all foodborne infectious diseases in the US, and listeriosis is responsible for 14-15% of all deaths due to food poisoning (Mead et

al. 1999). In the US, *L. monocytogenes* causes nearly 1,600 illnesses and 250 deaths every year (Scallan et al. 2011). The need for transferring listeriosis patients to intensive-care units also made *L. monocytogenes* the third most costly foodborne pathogen after *Clostridium botulinum* and *Vibrio vulnificus* in the US (Scharff 2012). The annual economic loss caused by *L. monocytogenes* is estimated to be over $2 billion (Ivanek et al. 2005). Besides, *L. monocytogenes* is also a global food safety concern and caused 23,150 illnesses and 5,463 deaths worldwide in 2010.

Because *L. monocytogenes* has ubiquitous existence in nature and high tolerance to harsh conditions, the pathogen can contaminate foods at every step from farm to fork. *L. monocytogenes* infection usually causes mild and self-limited symptoms in healthy individuals, yet its infection in immunocompromised hosts, including the elderly, infants, and AIDS patients, often becomes severe or even fatal, while in pregnant women, listeriosis causes fetal death (stillbirth), premature birth or severe neonatal infection. According to the surveillance data from Center for Disease Control and Prevention (CDC), the fatality rate of 1,651 listeriosis cases recorded between 2009 and 2011 was 21% (CDC 2013). The CDC (2021) records of *L. monocytogenes* food outbreaks that happened between 2012 and 2021 are presented in **Table 1.1**. Due to the high risk of listeriosis and mortality, the US regulators implemented "zero tolerance" of *L. monocytogenes* in ready-to-eat foods while the European Union allows a bacterial load of up to 100 CFU of *L. monocytogenes* provided the food does not promote *Listeria* growth throughout its shelf-life. Due to increased numbers of listeriosis cases and low infectious dose (<100 cells) in high-risk populations, the EU regulation may need revision. Thirteen serotypes of *L. monocytogenes* have been identified based on somatic (O) and flagellar (H) antigens, yet three of them (1/2a, 1/2b, and 4b) account for over 95% of listeriosis cases (Liu 2008).

Table 1.1 *L. monocytogenes* outbreaks during 2012-2021*

Year	Cases	Hospitalizations	Deaths	Contaminated food product
2021	11	10	1	Queso Fresco
	12	12	1	Deli meat
2020	36	31	4	Enoki mushroom
	8	5	1	Hard-boiled eggs
2019	24	22	2	Source unidentified
	10	10	1	Deli-slice products
	4	4	0	Pork products
2018	4	4	1	Deli ham
2017	8	8	2	Soft raw milk cheese
2016	9	9	3	Frozen vegetable
	2	2	1	Raw milk
	19	19	1	Packaged salad
2015	30	28	3	Soft cheese
	10	10	3	Blue bell creameries
	35	34	7	Carmel apple
	5	5	2	Soy products
2014	5	4	1	Cheese
	8	7	1	Dairy
2013	6	6	1	Cheese
2012	22	20	4	Cheese
	147	143	44	Cantaloupes

*CDC Report.

1.2.1 Major virulence factors

As a facultative intracellular enteric pathogen, *L. monocytogenes* employs a series of virulence factors to cross the intestinal barrier and to spread systemically from cell-to-cell without being exposed to the immune system (Lopes-Luz et al. 2021). Three major invasive pathways of *L. monocytogenes* from the intestinal lumen into lamina propria have been reported (Drolia and Bhunia 2019). First, *L. monocytogenes* are passively transported by microfold cells (or M cells) in Peyer's patch (Marco et al. 1997). M cells are specialized for sampling antigens from the intestinal lumen and passing them to underlying immune cells, so that the immune system can monitor and respond to various antigens in the lumen (Wang et al. 2014). Like *Brucella abortus*, *Salmonella,*

and other foodborne pathogens, *L. monocytogenes* can be presented to lymphoid tissue underlying villi through transcytosis by M cells.

Second, *L. monocytogenes* directly invade epithelial cells through endocytosis of epithelial cells, triggered by the binding of an invasion protein, Internalin A (InlA) to E-cadherin (Lecuit et al. 1997). InlA belongs to the internalin family which includes 25 proteins with some common structure. For instance, their N terminals start with signal peptide which is followed by a 22-amino-acid leucine-rich repeat (Bonazzi et al. 2009). After being secreted through the cell membrane, bacterial sortase covalently anchors InlA to the cell wall through an LPXTG motif at the C terminal end of InlA (Bierne and Cossart 2007). Although E-cadherin is one of the tight junction proteins located at adherens junctions between epithelial cells, they could be accessible to *L. monocytogenes* in the lumen when cell extrusion or mucus exocytosis creates a transient opening (Drolia and Bhunia 2019). The binding of InlA to E-cadherin triggers a local cytoskeletal rearrangement and eventually causes *L. monocytogenes* to be packaged in a vacuole for entering the epithelial cells (Bonazzi et al. 2009). Although E-cadherin has a generally conserved sequence in mammalian species, a single amino acid difference between the human E-cadherin and mouse or rat E-cadherin dramatically affect the function of InlA-mediated infection (Lecuit et al. 1999b). In permissive species, like human and guinea pigs, E-cadherin has a proline as the 16th amino acid, whereas nonpermissive species, like mouse and rat, has glutamic acid instead (Lecuit et al. 1999a). Due to the lack of InlA-mediated infection in mice, two solutions have been applied to make *L. monocytogenes* pathogenicity studies using the mouse as a model animal more relevant to the pathogenicity in humans. The first approach was to make a transgenic mice that expresses human E-cadherin, and Lecuit et al. (2001) showed the same dose of oral infection with *L. monocytogenes* caused no fatality in wildtype mice and 85% fatality of mice expressing the human E-cadherin. A second approach was to engineer the *L. monocytogenes* InlA so that it has increased binding affinity to mouse E-cadherin (termed murinized InlA, or InlA^{m}). Wollert et al. (2007) showed substitution of two amino acids in InlA, S192N and Y369N, significantly increased its binding affinity with mouse E-cadherin to the level that is similar to the binding between InlA and human E-cadherin. Compared to *L. monocytogenes* expressing the wildtype InlA, the ones expressing murinized InlA had increased *in vitro* invasion on human intestinal epithelial cells and caused more systemic infection three days post infection. However, one drawback is that InlA^{m} strain also

showed increased interaction with N-cadherin and caused enhanced adherens junction disruption (Tsai et al. 2013).

Internalin B (InlB) is another critical virulence factor located on the bacterial cell surface that binds to the hepatocyte growth factor receptor Met and mediates cellular invasion (Hamon et al. 2006). Compared to InlA, InlB is responsible for *Listeria* invasion in more types of cells since Met is more ubiquitously expressed whereas E-cadherin is typically expressed in epithelial cells (Bonazzi et al. 2009). Unlike InlA, InlB is anchored to wall lipoteichoic acid on the bacterial surface via GW modules at the C-terminal end (Bierne and Cossart 2007).

The third method of infection showed that *L. monocytogenes* employs the *Listeria* Adhesion Protein (LAP) independently from InlA to translocate through the epithelial barrier independently from InlA (Drolia et al. 2018). LAP was initially found to help *L. monocytogenes* adhere to intestinal epithelial cells. Later, LAP binding to a host cell receptor, Hsp60 was also proved to mediate translocation through Caco-2 cells (Burkholder and Bhunia 2010). In the mice model, LAP was found to be capable of causing dysfunction in tight junction, which leads to changes in intestinal permeability, resulting in *L. monocytogenes* translocation across the epithelial barrier (Drolia et al. 2018; Drolia and Bhunia 2019).

Once breaking through the intestinal barrier, *L. monocytogenes* causes listeriosis after being systemically disseminated to extraintestinal organs, including spleen, liver, mesenteric lymph node, gall bladder, brain, and placenta in pregnant women (Radoshevich and Cossart 2018). The special strategy of its dissemination is to hide in the cell cytosol and transmit to adjacent cells without being exposed to the extracellular environment. After InlA or InlB of *L. monocytogenes* bind to their corresponding cell receptors, E-cadherin or Met respectively, host cells phagocytosis is triggered and lets the pathogen break through the cell membrane. At this point, the pathogen is still packaged in a vacuole, where it starts to express a pore-forming toxin, Listeriolysin O (LLO) (encoded by gene *hly*), and bacterial phospholipases, PlcA and PlcB to escape from the vacuole. LLO belongs to the family of cholesterol-dependent cytolysins that attack cells by binding to the cell membrane (Mulvihill et al. 2015). Mulvihill and colleagues (2015), using electron microscopy and time-lapse atomic force microscopy and showed LLO oligomerized into “arc- or slit-shaped” assemblies in the membrane. Those assemblies then merged into large rings on membrane which could explain the LLO-mediated vacuole lysis. In vacuoles, LLO also helps *L. monocytogenes* to escape by the inactivation of phagocyte NOX2 (NADPH oxidase) which produces reactive oxygen

species as an antimicrobial strategy (Osborne and Brumell 2017). LLO helps *L. monocytogenes* to escape from the vacuole and enter the host cell cytosol where the bacteria can start replication (Henry et al. 2006). Berche et al. (1987) showed that the concentrations of *hly* deficient *L. monocytogenes* in mice spleens and livers were reduced by about 4 and 3 logs, respectively, compared to the concentrations of their parental wildtype strain (Berche et al. 1987). Furthermore, *hly*-deficient *L. monocytogenes* also induced much less T cell-mediated immunity in mice (Berche et al. 1987). Besides, phosphatidylinositol-specific phospholipase C (PI-PLC) and phosphatidylcholine-specific phospholipase (PC-PLC) are also expressed by *L. monocytogenes* in the endocytic vacuole to facilitate the escape from the phagosome (Camilli et al. 1991). *Lm* can also survives in the vacuole for an extended period, causing latent infection (Kortebi et al. 2017).

In addition, *L. monocytogenes* also suppresses the cellular proinflammatory response using internalin C (InlC) and moves from cell-to-cell by polymerizing host actin protein (ActA) (Portnoy et al. 1992; Gouin et al. 2010; Camejo et al. 2011). ActA is expressed on the surface of *L. monocytogenes* which then triggers host cell cytoskeletal rearrangement and polymerization (Kocks et al. 1992; Lasa et al. 1997; Portnoy et al. 2002). ActA rearranges the host cell actin to form a comet-like tail which propels the bacterium into an adjacent cell without being exposed to the extracellular environment (**Table 1.2**) (Tilney and Portnoy 1989; Tilney et al. 1990). ActA together with PLC help avoid autophagy (Mitchell et al. 2015; Cheng et al. 2018) by stalling autophagosomal structures (Tattoli et al. 2013).

The activation of these virulence genes is regulated under the positive control by the master regulator-PrfA (positive regulatory factor). More specifically, the PrfA regulon directly encodes genes in the *Listeria* pathogenicity island-1 (LIPI-1), including LLO, ActA, PlcA, PlcB, Mpl and PrfA, and three additional chromosomal loci, which are the *inlAB* operon and *inlC* and *hpt* monocistrons. Besides the core regulon, the expression of as many as 145 other *L. monocytogenes* genes may indirectly be regulated by PrfA (de las Heras et al. 2011). The selective activation of PrfA allows *L. monocytogenes* to convert from an environmental saprotroph to a pathogen by taking on many of environmental cues, such as temperature (Leimeister-Wächter et al. 1992), oxidative stress (Sokolovic et al. 1990), carbon sources (Freitag et al. 2009), and low pH (Behari and Youngman 1998) to modulate its virulence. The goal of such regulation is to prevent unnecessary production of PrfA-dependent virulence factors since these factors are not needed during the saprophytic life outside of a host (Kreft and Vázquez-Boland 2001). For example, PrfA-

dependent genes were downregulated by sugar transported through the phosphoenolpyruvate-sugar phosphotransferase system (PTS) (Scortti et al. 2007; Freitag et al. 2009), suggesting the presence of a carbon source-mediated modulation of the PrfA regulon. Another environmental condition that governs the expression of PrfA is a thermoswitch that obscures the ribosome binding site on *prfA* mRNA. When the temperature is below 30°C, a hairpin structure forms at the 5' end of *prfA* mRNA which blocks the binding of the ribosome and resultant translation. When the temperature is at 37°C, translation of the prfA gene is enabled due to the destabilization of the secondary hairpin structure of *prfA* mRNA (de las Heras et al. 2011). PrfA also positively impacts the extracellular environment. Mutants lacking *prfA* were defective in surface-adhered biofilm formation (Lemon et al. 2010). How PrfA regulates biofilm formation is discussed in the following section.

1.2.2 Biofilm and pathogenesis

The ubiquitous existence of *L. monocytogenes* in nature gives it numerous routes to be introduced in a food-processing environment. For instance, *L. monocytogenes* can be introduced into food processing facilities with various fresh produce or raw materials. Prevalence screening of raw salad vegetables from Malaysia showed that 24.2%, 21.9%, and 21.9% of spinach, tomato, and cucumber samples were positive for the pathogen (Ponniah et al. 2010). Another report on vegetables, mushrooms, raw meat, aquatic products, and frozen products collected from multiple major cities in China revealed the total prevalence rate was about 20% (Wu et al. 2015). Once *L. monocytogenes* finds a niche in a food-processing facility, it can attach to several abiotic surfaces, like stainless steel, PVC, and polystyrene, and start to form biofilms, which can be resistant to sanitation and may lead to recurrent food contamination (Borucki et al. 2003; Di Bonaventura et al. 2008; Reis-Teixeira et al. 2017).

Repeated sampling of multiple food processing environments showed that similar *L. monocytogenes* strains can persist for a few months, up to 12 years. Ragimbeau sampled both food and non-food contacting surfaces in a smoked herring plant six times throughout a year (Ragimbeau 2002; Carpentier and Cerf 2011). Results showed four out of ten pulsotypes of *L. monocytogenes* isolates were detected at least four times during sampling (Ragimbeau 2002; Carpentier and Cerf 2011). The persistence of certain *L. monocytogenes* isolates in the food processing environment maybe because that the same strains were consistently introduced by a

raw material, or because sanitation was not effective for some niches. Considering some isolates were collected on food-contacting surfaces, formation of biofilm could be a critical factor that helped *L. monocytogenes* to be persistent and resistant to routine cleaning. Multiple studies have revealed that the biofilm formation also effectively helps *L. monocytogenes* to colonize a surface. Pan and colleagues (2006) simulated how *L. monocytogenes* could go through cycles of incubation, sanitation, and starvation for three weeks in a food processing environment. They found the amounts of bacteria in biofilm were continuously decreasing till about the fifth day and then turned around to increase till the end of three weeks. The simulation results suggested that *L. monocytogenes* in the biofilms may be able to persist on a surface when the surface is repetitively exposed to nutrients from foods and insufficient sanitation.

Virulence factors or regulators are also involved in biofilm formation. As stated above, PrfA of *L. monocytogenes* is a regulator for numerous virulence factors, including InlA, InlB, and LLO, and governs the transition from saprophytic to pathogenic life style (Freitag et al. 2009). Once *L. monocytogenes* infects host cells, PrfA switches to the active status and upregulates the transcription of virulence genes by binding to the promoter regions, referred to as the PrfA box (Lemon et al. 2010). Lemon et al. (2010) also found *L. monocytogenes* without PrfA formed significantly less biofilm than the WT strain did at room temperature, 30°C, and 36°C. Although they did not answer how PrfA is involved in biofilm formation, they excluded the involvement of flagella since both strains showed similar flagellar activities.

Two years later, another research team reported that it was probably ActA which linked PrfA with biofilm formation. As described above, ActA has always been regarded as a critical virulence factor triggering the host cell cytoskeletal rearrangement to propel *L. monocytogenes* in the cytosol, yet Travier et al. (2013a) found that ActA also mediates bacterial aggregation and biofilm formation (**Table 1.2**). The researchers observed that the spontaneous sedimentation was always faster in *L. monocytogenes* (pathogen) than *L. innocua* (nonpathogen), and further investigation found that the sedimentation phenotype was absent in the *prfA* deficient strain. These results inspired the authors to suggest that the aggregation-mediating factor is possibly under the regulation of PrfA. By screening the phenotype of strains with a deficiency in PrfA-controlled genes, the *actA* knockout mutant showed no sedimentation phenotype, similar to the *prfA* mutant, suggesting that ActA is the molecule responsible for *L. monocytogenes* aggregation and sedimentation. Other virulence molecules, including InlA, InlB, and LLO, were not involved in

the bacterial aggregation. Since sedimentation allows the bacteria to contact surfaces, it is usually a prerequisite for adhesion and biofilm formation. The critical role of ActA in proper biofilm formation was established based on the results that the *actA* knockout mutant formed significantly less biofilm biomass than the wildtype did under both static and continuous flow conditions (Travier et al. 2013b). *In vivo* results showed that ActA helped *L. monocytogenes* to aggregate on the surfaces of intestinal epithelial cells and prolonged persistence in mice intestine (Travier et al. 2013b).

Interestingly, a recent study found that recombinant *Lactobacillus casei* expressing LAP from *L. monocytogenes* on the bacterial surface had increased biofilm formation using the microtiter plate assay and improved colonization in the mouse intestine (**Table 1.2**) (Drolia et al. 2018). Although the function of LAP in the pathogenesis of *L. monocytogenes* has been well characterized, results from the recombinant *Lactobacillus casei* highlighted the role of LAP in biofilm formation as well.

1.3 *Staphylococcus aureus* pathogenesis and biofilm formation

Staphylococcus aureus is a Gram-positive opportunistic pathogen and commonly found in natural water sources, earth, animal mucous membrane, and human skin (Miao et al. 2017). *S. aureus* has a remarkably high tolerance to salt under normal conditions at 37°C. Mannitol Salt Agar (MSA), a commonly used selective and differential medium for *S. aureus*, contains 7.5% sodium chloride. High salt tolerance is one of the features that make *S. aureus* a commensal bacterium existing on the skin of about 25% of the total population, which makes humans a common vehicle for the pathogen's transmission to foods. The anterior nares are a common niche where *S. aureus* is commonly isolated (Archer et al. 2011).

S. aureus is also a notorious foodborne pathogen that produces multiple heat-tolerant enterotoxins and causes food poisoning which generally causes symptoms like nausea, vomiting, and stomach cramps. Those symptoms usually develop in 30 min to hours after ingestion and are self-limited in most cases. Improperly handled foods is the most common reason for *S. aureus* contamination (Bennett et al. 2013). In the United States, an annual estimation of 241,000 cases of food poisoning were caused by *S. aureus* (Scallan et al. 2011). Since those symptoms in most cases are mild and self-limited, the number of actual infections could be significantly higher than the recorded number. Rarely, antibiotics are used for intoxication treatment because *S. aureus* does

not usually infect through the gastrointestinal tract. However, antibiotic treatment for skin infection caused by *S. aureus* has become a great challenge because of biofilm formation and widespread antibiotic resistance.

In the food industry, *S. aureus* contamination is a worldwide challenge affecting multiple types of products. Between January 2000 and March 2012, about 14 *S. aureus* outbreaks were recorded in Australia, which affected 429 people including 25 hospitalizations and one death (Pillsbury et al. 2013). About a third of the victims were infected after eating at commercially catered buffet. In Italy, after two individuals suffered from *S. aureus* intoxication, a broad screening of dairy products showed 102 out of 971 samples were positive (Vitale et al. 2015). About 46% of the isolated *S. aureus* cultures contained at least one enterotoxin coding gene.

The development of *S. aureus* biofilm is well programmed by a series of genes. After bacterial adherence to a surface, the next step for biofilm formation is cell-cell binding to form a multilayer structure. Polysaccharide intercellular adhesin (PIA) was initially discovered in *S. epidermidis* as a critical component responsible for cell-cell binding in biofilm formation (Mack et al. 1996). Chemically, PIA is linear β-1,6-linked glycosaminoglycans, and it is synthesized by products from the intercellular adhesion (*ica*) locus, including *icaADB* and *icaC*. Products from *icaA* and *icaD* are responsible for PIA synthesis using UDP-N-acetylglucosamine (Gerke et al. 1998). Cramton et al. (Cramton et al. 1999) reported that the Ica proteins of *S. aureus* share 59-78% identity with those proteins from *S. epidermidis*. Besides, deletion of the *ica* locus in *S. aureus* reduced its ability to form multilayer thick biofilms in microtiter plates, suggesting PIA of *S. aureus* has the same function for cell-cell adhesion. Later, the chemical nature of *S. aureus* PIA was identified to be poly-N-succinyl-β-1,6-glucosamine, yet antibodies generated against PIA of *S. epidermidis* can also probe the PIA of *S. aureus*, which also suggests that PIA has a conserved role in both species (McKenney et al. 1999). Based on the finding that PIA is expressed when *S. aureus* infects the lung of cystic fibrosis patients and partial oxygen pressure is low, Cramton et al. (2001) investigated how oxygen concentration affects the expression of the *ica* operon. In *S. aureus* and *S. epidermidis*, they found that the expression of both PIA and *ica* operon were upregulated. PIA is not only critical in biofilm formation but also plays a significant role in pathogenesis. In a mouse model, Rupp et al. (1999) reported that intravenous infection by *S. epidermidis* with deficience in the *ica* operon is significantly less likely to cause subcutaneous abscess and more likely to be eradicated than the infection caused by the parental strain.

However, another study about the influence of PIA in subcutaneous infection revealed different results. Francois et al. (Francois et al. 2003) studied the infection caused by both wild-type and *ica*-negative *S. aureus* or *S. epidermidis* through subcutaneously implanted tissue cages in guinea pigs. Results showed that bacterial concentrations of either the wildtype or *ica*-mutant strain were similar in tissue fluids or cage-inserted plastic coverslips. Although intravenous infection is not usually caused by foodborne *Staphylococcus*, PIA provides another example of the connection between biofilm formation and virulence; however, the function of PIA in the pathogen during infection may vary based on different infection methods or models. In addition, multiple biofilm-related proteins have been identified as immunogens to the sera of *S. aureus*-infected rabbits (Brady et al. 2006).

On the other hand, *S. aureus* can form biofilm independent of PIA under certain conditions. A two-component system, encoded by *arlRS*, has been found as a repressor for *S. aureus* biofilm formation in Hussain-Hastings-White Modified Medium (HHWm) (Toledo-Arana et al. 2005). After quantifying the biofilm formation in HHWm using the crystal violet staining method, the biofilm formation was doubled for the *arlRS* mutant strain when compared to the parental wildtype (Toledo-Arana et al. 2005). Furthermore, deleting the *ica* operon in the *arlRS* mutant strain did not affect *S. aureus* biofilm formation, suggesting a PIA-independent pathway is responsible for biofilm formation under the specific conditions.

Later, protein A coded by gene *spa* was found to have a similar function for cell-cell adhesin in biofilm development (**Table 1.2**) (Merino et al. 2009). Researchers also reported protein A as an essential component in the biofilm formation by *S. aureus* after using mass spectrometry to analyze proteinaceous components in its biofilms. Consequently, they revealed that the *spa* mutant strain exhibited significantly weakened biofilm formation. Furthermore, an *in vitro* aggregation experiment showed that *S. aureus* cells lacking protein A precipitated much slower than the counterpart expressing protein A, suggesting protein A may be responsible for *S. aureus* cell-cell aggregation (Merino et al. 2009). Surprisingly, they also found that protein A was not required to be covalently anchored on the cell surface to function as an adhesin, since the supplemented exogenous protein A could also trigger the aggregation of a *spa* mutant strain (Merino et al. 2009).

In addition to being a critical proteinaceous component in the biofilm matrix, Protein A also serves as an important virulence factor and helps the bacterium to evade the immune system during infection. Protein A is covalently bound to peptidoglycan through an LPXTG motif, and also binds

to the Fc region of antibodies, thus forcing antibody binding with the F_{ab} portion facing outward from the cell, reducing the chance of opsonization and phagocytosis (Kobayashi and DeLeo 2013). Protein A is also considered a superantigen that binds to the Fab part of the B-cell receptor to induce B cell programmed cell death (apoptosis) (Kobayashi and DeLeo 2013).

Another proteinaceous molecule that works as a cell-cell adhesin in biofilm formation is the biofilm-associated protein (Bap) (**Table 1.2**). Cucarella and colleagues (Cucarella et al. 2001), used random transposon insertion mutagenesis and found two mutants with reduced biofilm-forming abilities. Molecular analysis of both mutant strains revealed an insertion in the *bap* gene that encodes Bap, anchored to the cell wall. *In vivo* biofilm formation showed Bap is responsible for adhesion to inert surfaces. A recent discovery found low pH and low cation concentration are the triggers for the self-assembly of Bap into amyloid aggregates (Taglialegna et al. 2016). A mouse foreign body infection experiment revealed that the *S. aureus* without Bap caused less persistent infection than the wildtype *S. aureus*, suggesting Bap is a virulence factor responsible for persistent infection (Cucarella et al. 2001).

Extracellular DNA (eDNA) is another important component that is involved in biofilm formation independent of PIA in *S. aureus*. The role of eDNA in biofilm formation was first studied in *P. aeruginosa* (Whitchurch et al. 2002). Whitchurch et al. (2002) found that the addition of DNase I in the culture of *P. aeruginosa* could effectively reduce the biofilm forming abilities without affecting the bacterial growth. Furthermore, DNase I treatment for 150 min can significantly reduce a 60-h old biofilm by *P. aeruginosa* (Whitchurch et al. 2002).

CidA (encoded by *cidA* operon), a protein produced by *S. aureus* has been shown to be indirectly involved in biofilm formation. CidA is a murein (bacterial peptidoglycan) hydrolase and facilitates the release of eDNA from cells. CidA shows structural similarity to bacteriophage holins involved in phage-induced cell lysis (Rice et al. 2003). Mutation in the *cidA* gene affected eDNA release and biofilm formation (Rice et al. 2007), suggesting eDNA, released by controlled cell lysis, as a critical component in *S. aureus* biofilm formation. In addition, the high density of bacteria in biofilms also increases the rate of gene exchange (Arciola et al. 2018). The frequency of conjugation happening in biofilms has been reported to be higher than the frequency between planktonic bacteria (Sørensen et al. 2005).

1.4 *Pseudomonas aeruginosa* pathogenesis and biofilm formation

Pseudomonas aeruginosa is a Gram-negative, non-spore-forming, and aerobic rod-shaped bacterium. It is an opportunistic pathogen affecting mostly immunocompromised individuals who also suffering from other illnesses. Its metabolic activity is broad, and growth can occur in either nutrient rich or nutrient-poor conditions. The ability to utilize a wide range of substrates as carbon and nitrogen sources supports the ability of *P. aeruginosa* to colonize in a variety of natural niches, such as any water source and soil. Under laboratory conditions, the bacterium can grow well in a medium containing acetate and ammonium sulfate as carbon and nitrogen source, respectively (Tang and Sails 2014). The bacterium was also shown to grow in distilled water, suggesting a possible mechanism for nosocomial infection and spread in the hospital (Favero et al. 1971). *P. aeruginosa* produce a robust biofilm, which enhances its survival on different surfaces and protects the cells from other harsh conditions and treatments (Klausen et al. 2003). Another major challenge with *P. aeruginosa* is its resistance to multiple classes of antibiotics. In 2017, multidrug-resistant *P. aeruginosa* caused an estimated 32,600 infections among hospitalized patients and 2700 deaths in the U.S. (CDC 2019). In addition, the strong biofilm-forming ability of *P. aeruginosa* makes it even harder for antibiotics to access the cell embedded in biofilms, which significantly reduces the effectiveness of antibiotics to treat infections.

Due to its ubiquity, persistency, and drug resistance, *P. aeruginosa* can be easily spread to humans, especially in a healthcare setting, and cau cause serious acute and chronic infections in immunocompromised people. For example, *P. aeruginosa* is the most important bacterial pathogen causing progressive lung infection in cystic fibrosis patients and causes various symptoms, like high fever, respiratory failure and death. *P. aeruginosa* can cause chronic urinary tract infections and ventilator-associated pneumonia in patients with permanent bladder catheters and intubation, respectively (Ciofu and Tolker-Nielsen 2019). Treatment of *P. aeruginosa* is challenging because it can form infective biofilms after infection, which functions like a barrier protecting bacteria from complement immunity and phagocytosis, and significantly decreases the accessibility of antibiotics (Donelli 2014). Therefore, comprehensive knowledge of *P. aeruginosa* biofilm formation is important for preventing and treating resistant infections. Though *P. aeruginosa* rarely cause foodborne infection, it is the model culture for Gram-negative bacterial biofilm research. Understanding its biofilm formation could help elucidate steps in the control and destruction of biofilms formed by other pathogens. In *P. aeruginosa* biofilms, the highest cell

density is arranged closest to the surface, and cells occupy only a minor fraction (around 2-28%) of the biofilm volume, while EPS occupies the rest. EPS contains mainly biomolecules, exopolysaccharides, extracellular DNA (eDNA), and polypeptides, which provide the architecture of the biofilms (Rasamiravaka et al. 2015). Scanning confocal laser microscopy (SCLM) analysis shows that *Pseudomonas* biofilms have an open and porous structure that may be designed for the transportation of nutrients and waste. Affected by the different rheological characteristics of the living environment, *P. aeruginosa* can form mushroom- or pillar-like matured biofilms (Lawrence et al. 1991). In this section, I will provide up-to-date knowledge of the steps involved in *P. aeruginosa* biofilm formation and associated virulence regulation.

1.4.1 Bacterial surface structures aid in the initial attachment

The biofilm formation process includes the following sequential steps: attachment to a surface, microcolony formation, and maturation of biofilms (Klausen et al. 2003). The polar flagellum on *P. aeruginosa* provides the swimming motility and the responses to chemotactic attractions and also mediates a mode of a social movement referred to as swarming (Rashid and Kornberg 2000; Déziel et al. 2001a). O'Toole et al. (1998) screened the biofilm-forming ability on a polyvinylchloride (PVC) surface of about 2400 random transposon mutants generated from *P. aeruginosa* PA14. From the surface attachment defective mutants, they identified two classes of mutants with a deficiency in the flagella mediated motility or biosynthesis of the type IV pili. Therefore it was concluded that both flagella and pili are necessary for initial attachment. Specifically, the pili-deficient mutants formed a bacterial monolayer but were unable to form microcolonies. The mutant strains with deficient flagella mediated motility were incapable of attaching to the surface (O'Toole and Kolter 1998). Later, Toutain (2007) confirmed the essential role of flagellar motility in biofilm formation by observing that *P. aeruginosa* with a deficiency in either flagellar stators, MotAB or MotCD, showed weakened biofilm formation using both static and flow cell models. Microscopic photos also revealed that surface attachment specifically happened at the polar end of *P. aeruginosa* cells with flagella, supporting the conclusion of flagella-mediated surface attachment.

On the other hand, type IV pili provide twitching motility and, more importantly, type IV pili are considered the principal adhesin to both eukaryotic cells and most abiotic surfaces (Déziel et al. 2001b). In addition, the flagellum has been established as a key infection virulence factor in

several model animals. For instance, flagellum deficient *P. aeruginosa* showed less invasion using the mouse burn wound model and less colonization in the murine intestine (Drake and Montie 1988; Pier et al. 1995). In a neonatal mouse model, *P. aeruginosa* without *fliC* caused no mortality whereas the mortality rate of the wildtype strain was around 30% (Feldman et al. 1998).

Various types of filamentous appendages on the bacterial surface have been studied and classified as pili (Craig et al. 2019). Pili expressed by *P. aeruginosa* belongs to the type IV pilus family, which is assembled by the polymerization of the monomeric major pilin and minor pilin proteins encoded by *pilAEWV* (Craig et al. 2019). Pili-mediated twitching motility for bacterial cells is achieved by polymerization and depolymerization of pili (Clausen et al. 2009; Ellison et al. 2017). *Pseudomonas* pili have a helix structure made up of a single subunit pilin of 18 kDa (Frost and Paranchych 1977). Watts et al. (1982) used octyl-glucoside as a detergent and successfully disassembled purified pili into pilin monomers, and, after removing the detergent, found that the monomers can assemble spontaneously into filaments. They employed an X-ray diffraction study and showed that pili have a hollow cylindrical structure whose outer and inner diameters were approximately 5 nm and 1.2 nm, respectively. After removing the detergent octyl-glucoside, pilins assembled into a filament of 10 to 200 nm in length.

Neisseria gonorrhoeae type IV pili which have an adhesin protein located at the distal tip of the pili, while type IV pili from *P. aeruginosa* does not have a separated minor protein subunit attached to the end, which indicates that the pili themselves are responsible for the adhesion function in *Pseudomonas* (Hahn 1997). The binding specificity of pili is coherently related to their structure and amino acid sequence. The pilin genes identified in different *P. aeruginosa* strains indicate the great heterogeneity in pilin amino acid sequence (Hahn 1997). Without the leader peptide, the length of pilin varies from 145 to 150 amino acids. Genetic research showed that a stretch of 30 aa at the N-terminal end is highly conserved while the rest of the sequences are moderately conserved or highly variable (Hahn 1997). One common structural characteristic found in all *P. aeruginosa* pilin is an intrachain disulfide loop of 12 to 17 amino acids located at the far end of the C-terminal, which is considered to provide the site for specific binding (Hahn 1997).

In addition to being responsible for twitching motility and involved in biofilm formation, pili are also a virulence factors for adhesion to and invasion of epithelial cells. Chi and colleagues (1991) showed around 14 *P. aeruginosa* cells adhered to each A549 cell, a human lung pneumocyte cell line, after 3 h incubation at a MOI of 50. Meanwhile, nonpilated mutants or

mutants with structurally modified or nonpiliated pili showed adhesion that were close to zero, or 10-20 % of the wildtype strain's rate, respectively (Chi et al. 1991). Later, glycosphingolipid asialo-GM1 was identified as the receptor for pili-mediated adhesion using MDCK as a model, and pili were also responsible for the subsequent invasion of the cells (Comolli et al. 1999).

1.4.2 From microcolony formation to biofilm maturation

Both flagella and pili of *P. aeruginosa* are involved in the formation of cell monolayers and the typical mushroom-like structures. By expressing fluorescent proteins of different colors in the wildtype and pili-deficient *P. aeruginosa* strains, researchers visualized the distribution of those two types of bacteria and found only the wildtype strain was located on the cap of the mushroom-like structures, suggesting that functional pili-mediated motility is necessary for forming this type of biofilms (Barken et al. 2008). Similarly, the lack of normal biofilm structure was also observed with the strain expressing malfunctioning flagella (Klausen et al. 2003).

Quorum sensing (QS) systems have a critical role in the organization of cells in biofilms and the formation of rigid biofilm structures, because they allows the bacterial community to globally regulate gene expression and coordinate biological processes in response to population density (Rumbaugh et al. 2000). QS is commonly applied by bacteria to direct a community's behavior using various chemicals. This cell density-dependent cell-to-cell communication system regulates the phenotypic alterations at an early stage of biofilm formation after the attachment (González and Keshavan 2006). Currently, four types of quorum sensing systems have been identified in *P. aeruginosa* that regulate the expression of biofilm formation: the Las, Rhl, PQS, and IQS systems (Maurice et al. 2018). Each system contains at least two major functional elements, one category that is sensing critical concentration of a specific autoinducer (AI), and serves as a transcriptional activator for genes encoding the second category- the cognate AI synthases (Moradali et al. 2017). The Las and RhI systems are triggered by an increase in cell density during the early exponential growth phase, while PQS and IQS systems are activated at the late exponential growth phase (Thi et al. 2020).

The Las system involves the production of an autoinducer N-(3-oxododecanoyl)-L-homoserine lactone (3-O-C_{12}-HSL), which is regulated by the AI synthases LasI, and sensed by the transcription factor LasR. The Rhl system uses the AI synthase RhlI to produce an autoinducer, N-butanoyl-L-homoserine lactone (C_4-HSL), which uses RhlR as its cognate receptor. Research

showed that both Las and RhI are the essential regulating systems for the maturation of *Pseudomonas* biofilm. Davies et al. (1998) revealed that the depth of the cell cluster formed by wild-type *P. aeruginosa* PAO1 in biofilms on glass was significantly larger than the biofilm produced by mutant Δ*lasI* and double-deleted mutant Δ*lasI*Δ*rhlI*. Epifluorescence and scanning microscopy analysis of the biofilm structure after Alcian blue staining (a polysaccharides stain) showed that cells of the *lasI* mutant were almost uniformly distributed on the surface and the height of the cell stack is almost consistent across the surface (Davies et al. 1998). Furthermore, microcolonies separated by water channels were observed only in the WT strain's biofilm while the cells of mutants were spread in a flat-sheet manner. To further verify cell organizations due to the lack of autoinducer encoded by the *lasl* gene, Δ*lasl* mutant cells were incubated on glass together with LasI autoinducer 3-O-C_{12}-HSL, the mutant strain formed biofilms with the similar thickness as biofilms of the wildtype.

To explore the relationship between quorum-sensing systems and biosynthesis of biofilm matrix, another research team focused on the expression of *pel* and the quorum sensing system *las* (Sakuragi and Kolter 2007). The p*el* cluster consists of seven genes that are responsible for the biosynthesis of polysaccharides, a major component making up the extracellular matrix (Vasseur et al. 2005). By screening *P. aeruginosa* transposon mutant strains that cannot form pellicles at the gas-liquid surface, Friedman et al. (2004a) identified the *pel* gene cluster to be responsible for producing and secreting glucose-rich extracellular matrix material. By comparing the biofilm-forming ability of the wildtype and *pel* mutants, the later showed significantly weaker biofilm formation than the former, suggesting that the polysaccharides extracellular matrix is an essential part of biofilms. Later, the same group identified a second genetic locus, *psl*, responsible for producing mannose-rich extracellular materials. *P. aeruginosa* requires at least one of these loci, *pel* or *psl*, to form normal biofilms (Friedman and Kolter 2004b). The evidence that *pel* gene expression is regulated by the *las* quorum sensing system was reported by Sakuragi and Kolter (2007). A transcriptional fusion experiment was conducted to test the possible regulatory relationship between the *las* and *pel* loci. The 785-bp upstream sequence of *pelA* was fused to a promoterless *lacZ* reporter gene and cloned into a vector, which was then introduced in a single copy into the *attB* site of chromosome of the wildtype strain, Δ*rhlR,* and Δ*lasR*Δ*lasI* mutants. After spot inoculation of these cultures and growth on agar plates, colonies were lysed, and the activity of each was tested. The β-galactosidase reporter activity of the wild-type strain colonies increased

linearly after one-day of incubation and remained stable after four days. A similar but lower activity level was observed for the Δ*rhlR* mutant strain. But the activity of β-Galactosidase from the colonies of Δ*lasR*Δ*lasI* mutants remained at a negligible level after 6-days' of incubation. Moreover, complementation with the *lasI* autoinducer restored the expression of *pel* in the *las* deficient mutant. These data suggest that the *las* quorum-sensing system induces the expression of *pel* genes to produce extracellular matrix, and the *rhl* quorum-sensing system may also be involved to a lesser extent in induction of *pel* genes. Later, it was identified that cationic exopolysaccharide Pel binding to negatively charged eDNA plays an essential role in maintaining the integrity of biofilms (Jennings et al. 2015; Flemming et al. 2016).

The PQS, *Pseudomonas* quinolone signal, system is also involved in the release of eDNA and biosurfactants, which are essential for the development of matured biofilms at the late exponential phase (Davies et al. 1998; Tolker-Nielsen 2014). The loci *pqsABCDE*, *pqsL*, *phnAB*, *pqsE*, and *pqsR* are needed to complete the synthesis of PQS, or 2-heptyl-3-hydroxy-4-quinolone (PQS), which is the AI that can be detected by PqsR. The general function of each operon is introduced to briefly explain the correlation between PQS system and biofilm formation. The connection between the PQS systems and biofilm formation was based on the finding that biofilms formed by the *pqsA* mutant contains less eDNA than biofilms formed by their wildtype counterpart (Allesen-Holm et al. 2006). HHQ, 2-heptyl-4-quinolone, is generated through the function of PqsBCD as the precursor of PQS. Eventually, HHQ is transformed into PQS by PqsH (Lee and Zhang 2015). The finding that LasR regulates the expression of *pqsH* showed the interaction between the two quorum-sensing systems, Las and PQS (Schertzer et al. 2009). The function of PqsL was predicated to be a monooxygenase involved in the synthesis of alkyl-quinolones N-oxides, and the lack of PqsL caused PQS to be overproduced (D'Argenio et al. 2002; Lépine et al. 2004). PhnAB is responsible for producing anthranilic acid which is then turned into 4-hydroxy-2-alkylquinolines (HAQs) including HHQ (Lépine et al. 2004). The full function of PqsE is still unknown, except that a *pqsE* mutation did not cause a deficiency in PQS biosynthesis, even though this mutant failed to respond to PQS (McKnight et al. 2002; Diggle et al. 2003; Farrow et al. 2008). PqsR, or MvfR (multiple virulence factor regulator), was also necessary for the synthesis of PQS as a positive regulator of *pqsA* expression by binding to the *pqsA* promoter (Farrow et al. 2008). The binding of PqsR to the promoter was further increased in the presence of PQS, suggesting that PQS may be a cofactor for PqsR. When the function of PqsR is disrupted by mutation, the

expression of *phnAB* and *pqsABCDE* operons were significantly affected, impacting the ability of *P. aeruginosa* to kill nematodes (Gallagher et al. 2002). PqsR controls the synthesis of more than 60 types of secreted anthranilic acids derivatives (Lydon and Rahme 2011). Production of virulence factors, including pyocyanin and hydrogen cyanide (Xiao et al. 2006b), also requires PqsR, which gives PqsR play a key role in both pathogenicity and biofilm formation.

The PQS system is important in virulence factors generation during biofilm development. PQS mutants showed reduced biofilm development and less production of virulence factors, such as pyocyanin, elastase, lectin, and rhamnolipids. The correlation between the PQS system and infection ability has been tested using several *in vivo* models. In burn-wound mouse models, the survival rate of mice infected with *pqsA* mutant strains was about 50% higher than infection with the parental WT (Xiao et al. 2006b). The survival rate of mice infected with *pqsA* mutant strains was about 50% higher than its parental WT (Xiao et al. 2006a). Since *P. aeruginosa* can also be an opportunistic plant pathogen, Cao et al. (2001) showed that a mutant strain with dysfunctional PQS production grew dramatically less than the wildtype strain in *Arabidopsis*, suggesting a critical role of PQS for overall pathogenicity of *P. aeruginosa*.

The IQS (integrated quorum sensing) system is less studied compared to the other three systems. It produces 2-(2-hydroxyphenyl)-thiazole-4-carbaldehydte (aeruginaldehyde) as its cognate AI, while the receptor has not been found. A non-ribosomal peptide synthase gene cluster *ambBCDE* is responsible for IQS synthesis. The disruption led to a decrease in the production of PQS and BHL, along with other virulence factors such as pyocyanin, rhamnolipids, and elastase (Lee and Zhang 2015). However, Cornelis (2020) recently commented that *amb* gene cluster is not responsible for aeruginaldehyde production, since its production is also found in *Pseudomonas* strains lacking the cluster. The recent discovery also confirms the importance of IQS in contributing to the complete virulence of *P. aeruginosa* in animal models. For instance, mice infected by *P. aeruginosa* without *ambB* and *lasI* genes had higher survival rate than either the wildtype or *lasI* knockout mutant strain (Lee et al. 2013). The production of IQS has been found to be related to the availability of phosphate concentration in the host, suggesting IQS system may be responsible for adjusting virulence during infection (Wang et al. 2019). Under iron and phosphate-deficient conditions, both PQS and IQS systems could be enhanced, which will lead to increased virulence factor synthesis, causing increased mortality in the host organism.

In addition, study of mixed-culture biofilms by *P. aeruginosa* and *S. aureus* found that the existence of the latter organism in the biofilm can also increase the expression of exotoxin A (Goldsworthy 2008; Elias and Banin 2012), suggesting that expression of virulence genes by one species in biofilms can be altered by the presence of other species.

1.5 *E. coli* pathogenesis and biofilm formation

E. coli is a Gram-negative, facultatively anaerobic bacterium. Some strains, collectively termed STEC, can cause lethal foodborne diseases. These strains can produce Shiga toxin which might cause hemolytic uremic syndrome (HUS) and lead to kidney failure. On the list of notorious foodborne pathogens, pathogenic *E. coli* and *Salmonella enterica* are associated with the vast majority of outbreaks in fresh produce (Yaron and Romling 2014). For instance, organic fenugreek sprouts were contaminated by a novel Shiga-toxin-producing strain of enteroaggregative *E. coli* in northern Germany in 2011, which caused 3,816 cases of infection including 800 cases of HUS and 53 cases of fatalities (Frank et al. 2011). Patients were identified from Switzerland, Poland, Sweden, and even North America, around whom 800 people had the hemolytic uremic syndrome. In a study investigating the survival of *E. coli* O157:H7 on lettuce (Islam et al. 2004), results showed that waterborne *E. coli* inoculated at a titer of approximately 10^5 CFU/mL can survive on lettuce for as long as 77 days. These findings further support the importance of biofilm control in the food processing environment to prevent contamination from happening.

As one of the pathogens causing the most gastroenteritis cases around the world, *E. coli* is a model bacterium which forms biofilm after well-programmed production of various extracellular molecules. Curli and cellulose are two major components making up the extracellular matrix of both bacteria (Latasa et al. 2005). Curli fimbriae are proteinaceous extracellular fibers expressed by both *E. coli* and *Salmonella* that are responsible for cell-to-cell and cell-to-surface binding (Barnhart and Chapman 2006). Those amyloid nanofibers are made with repeated protein subunits and encapsulate bacteria in a complex network (Nguyen et al. 2014). The signature phenotype of curli-producing bacteria is that their colonies are stained red while growing on a medium containing Congo red (Collinson et al. 1993).

Curli fimbriae of *E. coli* are composed of self-assembled CsgA nucleated by CsgB which is also anchors curli to the bacterial surface (Nguyen et al. 2014). Including the major subunit (CsgA) and nucleation (CsgB), expression of curli fimbriae is achieved by genes in two operons, *csgBAC*

and *csgDEFG*, which are responsible for secretion (CsgC and CsgG), transcription regulation (CsgD), and processing (CsgE and CsgF) (Chapman et al. 2002). The assembly of curli fimbriae requires precipitation of CsgA monomer with CsgB as the nucleator protein (Bian and Normark 1997). The transcription of the two operons for curli biosynthesis is regulated by CsgD (Hammar et al. 1995), OmpR (Vidal et al. 1998), and sigma factors σ^{70} and σ^{S} (Arnqvist et al. 1994) in response to a variety of environmental signals. Under laboratory conditions, the expression of curli is optimal during the stationary phase in an environment with low nutrients and low medium osmolarity at temperature ≤30°C (Olsén et al. 1989). Prigent-Combaret et al. (Prigent-Combaret et al. 2000) acquired electron microscopic images of curli-deficient and WT *E. coli* and showed that curli are required for initial bacterial adhesion to inert surfaces and the development of biofilms. The CsgA-made nanofibers are very resistant to heat and detergents (Nguyen et al. 2014), which may enhance persistence of biofilm in the food processing environment. Analysis of sludge samples from several wastewater treatment plants showed that the biovolume of amyloid fimbriae could make up to 10-40% of biofilm volume (Larsen et al. 2008). During intestinal colonization, curli may not play an essential role in adhesion to the epithelial cells. *E. coli* with *csgA* and *csgD* mutants showed similar adhesion rates on both HeLa and HT-29 cells as the WT counterparts (Saldaña et al. 2009). The authors suggested that it may be because that *E. coli* employs a variety of virulence factors for adhesion to epithelial cells. On the other hand, when CsgD, the curli biosynthesis regulator, was overexpressed, the adhesion of *E. coli* was increased by about five-fold, suggesting curli may still be one of these redundant adhesion factors.

The major exopolysaccharide that *E. coli* secrete in biofilms is cellulose (Zogaj et al. 2001). Cellulose is a (1-4)-β-linked linear glucose chain molecule, and it is the most abundant organic polymer found in nature, which can be produced by plants, microorganisms, and some animals. The role of cellulose in biofilm formation was not discovered until 2001. After screening thirteen thousand mutants, Zogaj et al. (2001) reported that an unknown substance secreted by *E. coli* was closely connected with several genes that are homologous with bacterial cellulose synthesis (*bcs*) genes from *Acetobacter xylinus*. Enzymatic digestion and chemical staining further identified the previously unknown substance in *E. coli* and *Salmonella* biofilm as cellulose. Interestingly, the regulator of the *bcs* operon is AgfD which is homologous with the curli regulator CsgD (Chirwa and Herrington 2003). However, not all *E. coli* biofilm formation depends on curli and cellulose. Enteroaggregative *E. coli* (EAEC) can form thick aggregating biofilm on the intestinal mucosal

surface and cause diarrheal disease (Vial et al. 1988). Upon adhesion to epithelial mucosa, EAEC secretes toxins, including *Shigella* enterotoxin, plasmid-encoded toxin, and enteroaggregative ST-like toxin, that can directly cause cell death and trigger intestinal inflammation (Czeczulin et al. 1999). In the absence of curli, EAEC forms a unique type of biofilm in which cell-to-cell adhesion is solely mediated by aggregative adherence fimbriae (AAF/I and AAF/II). AAF mediates the biofilm formation of EAEC in cell culture medium on two abiotic surfaces, glass and plastic (Sheikh et al. 2001). In addition to their role in interaction with the MUC1 receptor and binding EAEC to epithelial cells, AAF were also identified as a virulence factor in human infection (Czeczulin et al. 1997; Boll et al. 2017). Moreover, the binding between MUC1 and AAF also triggers upregulation of MUC1 in the cells (Boll et al. 2017).

1.6 *Salmonella* pathogenesis and biofilm formation

Salmonella is Gram-negative rod bacterium which is closely related to *E. coli* in evolution. Based on genetic prediction, *Salmonella* diverged from *E. coli* around 100 million years ago (Baker 2018). Like *E. coli*, *Salmonella enterica* also causes outbreaks via contaminated fresh produce (Yaron and Romling 2014). While the whole world was focusing on addressing the COVID-19 pandemic in 2020, an outbreak of foodborne *Salmonella* was happening at the same time. Since the beginning of July 2020, the CDC has reported 1,127 cases of *Salmonella* Newport infection including 167 hospitalizations from 48 states (CDC 2020). What was unique about the outbreak was that a very uncommon produce, red onions, was identified as the primary vehicle for the pathogen, suggesting pathogens very possibly can be adapted to culture new niches, and that it is important not to overlook the safety of any produce.

Not only fresh produce can be contaminated; contamination can occur at any step along the food supply chain, because the bacterium can also survive for an extraordinarily long time on the produce. By studying the pathogen transmission from contaminated water, Kisluk et al. (2012) found *S.* Typhimurium can persist on parsley for at least four weeks when the concentration of the pathogen was above $10^{8.5}$ CFU/mL. Like *E. coli*, curli fimbriae are also a major proteinaceous extracellular fibers expressed by *Salmonella* for cell-to-cell and cell-to-surface binding (Barnhart and Chapman 2006). Two unique phenotypes which helped researchers to identify a curli-expressing *Salmonella* strain are bacterial aggregation and fibronectin binding (Collinson et al. 1993). The adherent fimbriae produced by *Salmonella* Enteritidis can be classified into four types,

SEF14, SEF17, SEF18, and SEF21, according to different molecular weights (Collinson et al. 1993). Specifically, the fimbrial subunits of SEF14, SEF17, SEF18, and SEF21 are expressed from genes *sefA*, *agfA*, *sefD*, and *fimA*, respectively (Collinson et al. 1991). Austin et al. (1998) showed SEF17 is critical for stabilizing cell-to-cell interaction in biofilm formation as the SEF17-deficient mutant cannot form thick cell aggregates on the surface of either polytetrafluoroethylene or stainless steel. Fimbriae are one of the organelles that not only play a critical role in biofilm formation, but also are an important factor for pathogenicity. Collinson et al. (1993) found SEF17 fimbriae but not SEF14 and SEF21 can bind to human fibronectin. Furthermore, SEF17 has been identified as a factor significantly affecting the association and invasion rate of *Salmonella* Enteritidis on epithelial cells. Fuller et al. (1999) showed association and invasion rates of SEF17-deficient mutant were significantly reduced to about 13.7% and 4.2% of the WT strain.

In summary, multifunctional molecules involved in both bacterial pathogenesis and biofilm formation demonstrate a close connection between the two aspects. Although pathogenesis of multiple foodborne pathogens has been comprehensively studied, most of the results were generated using planktonic cultures under laboratory conditions. The actual risk of consuming pathogens in biofilms has not been well characterized. Here, I used *L. monocytogenes* as a model foodborne pathogen to investigate the virulence of the bacteria in biofilms. This study aimed to supplement the understanding about bacterial pathogenesis and biofilm, and also benefit the accurate evaluation of the risks of biofilms in the food processing environment.

Table 1.2 Bacterial factors involved in biofilm formation and pathogenesis

Bacteria	**Factors**	**Function**	
		Biofilm formation	**Pathogenicity**
Listeria monocytogenes	ActA (Actin polymerization protein)	Bacterial aggregation	Rearrange host cytoskeletal and mediate cell-to-cell spread
	LAP (Listeria adhesion protein)	Expression in recombinant *Lactobacillus* enhanced biofilm formation	Epithelial adhesion and translocation through epithelial barrier
	PrfA	Regulate the expression of ActA that is necessary for biofilm formation	Regulatory protein that regulates synthesis of multiple virulence factors
Staphylococcus aureus	BAP	Adhesion to inert surfaces and intercellular adhesion in the development of biofilm formation	Establish persistent infection on a mouse infection model
	Protein A	Cell-cell adhesion in biofilm development; a major proteinaceous component in *S. aureus* biofilms	Help *S. aureus* to evade immune system *in vivo*
	PIA	Cell-cell binding in biofilm formation	Establish persistent *in vivo* infection
Pseudomonas aeruginosa	PqsR	A key component of *Pseudomonas* quinolone signal system	Regulate the production of virulence factors, pyocyanin and hydrogen cyanide.
Salmonella enterica	Fimbria (SEF17)	Cell-to-cell interaction in biofilm formation	Bind to human fibronectin and facilitate cell invasion
E. coli	Curli made with CsgA and CsgB	Adherence to abiotic surfaces	Adhere to epithelial cells when over expressed
Enteroaggregative *E. coli* (EAEC)	Aggregative Adherence Fimbriae (AAF)	Mediate biofilm formation on abiotic surfaces	Bind to MUC1 on epithelial cells

CHAPTER 2. BIOFILM-ISOLATED *LISTERIA MONOCYTOGENES* EXHIBITS REDUCED SYSTEMIC DISSEMINATION AT THE EARLY (12-24 H) STAGE OF INFECTION IN A MOUSE MODEL*

2.1 Abstract

Environmental cues promote microbial biofilm-formation and physiological and genetic heterogeneity. In food production facilities, biofilms produced by pathogens are a major source for food contamination; however, the pathogenesis of biofilm-isolated sessile cells is not well understood. I investigated the pathogenesis of sessile *Listeria monocytogenes* (*Lm*) using cell-culture and mouse models. *Lm* sessile cells express reduced levels of the *lap*, *inlA, hly*, *prfA,* and *sigB* and show reduced adhesion, invasion, translocation, and cytotoxicity in the cell culture model than the planktonic cells. Oral challenge of C57BL/6 mice with food, clinical or murinized-InlA ($InlA^m$) strains reveals that at 12 and 24 h post-infection (hpi), *Lm* burdens are lower in tissues of mice infected with sessile cells than those infected with planktonic cells. However, these differences are negligible at 48 hpi. Besides, the expressions of *inlA* and *lap* mRNA in sessile *Lm* are about 6.0 and 280-fold higher than the planktonic cells, respectively, suggesting sessile *Lm* can still upregulate virulence genes shortly after ingestion (12 h). Similarly, exposure to simulated gastric fluid (SGF, pH3) and intestinal fluid (SIF, pH7) for 13 h shows equal reduction in sessile and planktonic cell counts, but induces LAP and InlA expression and pathogenic phenotypes. Our data show that the virulence of biofilm-isolated *Lm* is temporarily attenuated and can be upregulated in mice during the early stage (12-24 hpi) but fully restored at a later stage (48 hpi) of infection. Our study further demonstrates that *in vitro* cell culture assay is unreliable therefore an animal model is essential for studying the pathogenesis of biofilm-isolated bacteria.

2.2 Introduction

Listeria monocytogenes (*Lm*) is a Gram-positive facultative intracellular pathogen causing listeriosis, notorious for its high fatality (20-30%) among immunocompromised individuals, such as the elderly (65 and older), pregnant women, infants, and the AIDS patients (Swaminathan and

*This article was published in **NPJ Biofilm and Microbiome** in Feb **2021**. (Bai, X., Liu, D., Xu, L., Drolia, R., Gallina, L.F., Cox, A.D., and Bhunia, A.K. 2021. Biofilm-isolated *Listeria monocytogenes* exhibits reduced systemic dissemination at the early (12-24 h) stage of infection in a mouse model. Npj Biofilm and Microbiome 7:18).

Gerner-Smidt 2007). A recent study also showed individuals with damaged intestinal microbiota due to antibiotics or chemotherapy are at higher risk since the commensal microbes are considered the first line of defense against *Lm* infection (Becattini et al. 2017). During foodborne infection, *Lm* crosses the gut barrier utilizing the *Listeria* adhesion protein (LAP), Internalin A (InlA), and M cells (Drolia et al. 2018; Drolia and Bhunia 2019). *Lm* LAP interacts with its cognate epithelial receptor, heat shock protein 60 (Hsp60) (Wampler et al. 2004a; Kim et al. 2006; Jagadeesan et al. 2011), and activates NF-κB and myosin light chain kinase (MLCK) to disrupt the epithelial tight junction barrier for bacterial passage into the lamina propria during the early stage (24-48 h) of infection (Drolia et al. 2018; Drolia et al. 2020). The pathogen also uses InlA for epithelial cell invasion and gut barrier crossing by transcytosis (Nikitas et al. 2011) which plays a significant role possibly at the later stage of infection (72-96 h) on a mouse model of infection (Wollert et al. 2007; Drolia and Bhunia 2019). Another invasion protein, InlB also promotes *Lm* invasion of hepatic and intestinal epithelial cells (Dramsi et al. 1995). After cell invasion, the vacuole-trapped bacterium escapes into the cytoplasm with the aid of listeriolysin O (LLO, encoded in *hly*) and phospholipases (PlcA and PlcB), suppresses cellular proinflammatory response using internalin C (InlC) and moves from cell-to-cell by polymerizing host actin protein (ActA) (Portnoy et al. 1992; Gouin et al. 2010; Camejo et al. 2011). *Lm* also survives in the vacuole for an extended period prompting latent infection (Kortebi et al. 2017). The protein regulatory factor (PrfA) regulates expression of virulence genes (*hly, plc, actA*) located on the *Listeria* pathogenicity island necessary for intracellular survival and spread (de las Heras et al. 2011), while the stress response regulator, SigB regulates virulence genes and other accessory genes required for bacterial survival in the harsh environment of food and the host gut (Kazmierczak et al. 2006; Horn and Bhunia 2018).

Lm existence is ubiquitous in water and earth and can form biofilm on the food-contact surfaces and the food production environment thus biofilms serve as a potential source for contamination and threatens public food safety (Moltz and Martin 2005; Ferreira et al. 2014; Yaron and Romling 2014; Galié et al. 2018; Rodríguez-López et al. 2018). Evolutionarily, *Lm* is well equipped to make the transition from soil/plant/environment-living saprophytic lifestyle to an infective intracellular lifestyle in the human host (Freitag et al. 2009).

Biofilm formation is an essential survival strategy for bacteria by which they manage to colonize on a solid surface, absorb nutrients, proliferate, and communicate with other species through quorum sensing (Weigel et al. 2007; Carpentier and Cerf 2011; Renier et al. 2011).

Furthermore, biofilm formation is also associated with the majority of human infections (Costerton et al. 1999; Hall-Stoodley et al. 2004). Biofilm is generally made up of bacterial cells and extracellular polymeric substances composed of polysaccharide, protein, eDNA, and other inorganic molecules (Donlan 2002; Harmsen et al. 2010). In a biofilm, bacteria are physically protected from harmful environmental factors, for instance, antibiotics, acid or alkali, UV radiation, and osmotic stress (Kokare et al. 2009; Luque-Sastre et al. 2018). Not only surviving in the niche, but bacteria could also be released from biofilms after they are matured (Donlan 2002). Therefore, as long as *Lm* forms a biofilm on a food-contact surface, it could become a consistent contamination source. It has been reported that *Lm* strains with the same pulsotypes have been isolated from a food processing plant multiple times throughout a year (Carpentier and Cerf 2011). Previously, multiple studies have observed significant differences in gene expression between sessile and planktonic *Lm* cells (Tremoulet et al. 2002; Lourenço et al. 2013a; Mata et al. 2015) especially, the reduced expression of InlA, InlC, and LLO in biofilm cells (Lourenço et al. 2013b; Gilmartin et al. 2016). However, none of them examined the pathogenicity of biofilm cells using cell-culture or animal models. Therefore, the question arose - how infective are these *Lm* sessile cells from the biofilm, if a food is consumed immediately after being contaminated with these cells? In addition, can a conventional mammalian cell culture model (Bhunia 2018) that is used routinely in the laboratory predict the nature of infectivity of biofilm isolates accurately? Is there any direct correlation of *in vitro* infectivity data for biofilm-isolated cells with *in vivo* animal experimental data?

To date, various studies have reported the persistence and resistance of *Lm* cells in biofilms to environmental stress and significant change in global gene expression (van der Veen and Abee 2010; Ibusquiza et al. 2011); however, the exact virulence attributes of *Lm* isolated from biofilm has not been fully elucidated. The objective of this study was to assess and compare the pathogenicity of biofilm-isolated and planktonic *Lm* cells using an *in vitro* intestinal epithelial cell culture model and an *in vivo* mouse (C57BL/6) model at different stages of infection (12, 24 and 48 h). Besides, I also analyzed the expression of key virulence proteins (LAP and InlA) that are involved during the early stage of infection (Drolia and Bhunia 2019) and the regulatory genes, *prfA* and *sigB*. The knowledge gained would help understand the pathogenesis and develop an intervention strategy for controlling biofilm-forming bacterial pathogens from causing infection.

2.3 Methods

2.3.1 Bacterial strains

Food (64) and clinical (46) isolates and several mutant *Lm* strains were used in this study (**Table 2.1**). Cultures were stored in brain heart Infusion broth (BHIB, Acumedia) with 25% glycerol at -80°C. To revive cells, the frozen stock cultures were first streaked on a tryptic soy agar plate containing 0.6% yeast extract (TSAYE; Becton Dickinson, Franklin Lakes, NJ), and incubated at 37°C overnight. Then a single colony was inoculated into 4 mL tryptic soy broth supplemented with 0.6% yeast extract (TSBYE), which was further incubated at 37°C for 16 to 18 h to obtain fresh cultures. The cultures of *Lm* 10403S Δ*prfA* and F4244 Δ*inlA* were prepared in the same way, while *lap*$^{-}$ strain in a medium containing erythromycin (10 µg/ml) (Jagadeesan et al. 2010) (**Table 2.2**).

Table 2.1. *Listeria monocytogenes* cultures used in the study

Food-isolates

L. monocytogenes	**Serotype**	**Ribotype**	**Source**[a]
F1	1/2b	DUP-19165	Ground beef, Goias, Brazil, 1990
F2	1/2b	DUP-1042	Chicken, Goias, Brazil,1992
F3	1/2b	DUP-1042	Chicken, Goias, Brazil, 1992
F4	1/2b	DUP-1042	Chicken, Goias, Brazil, 1992
F5	1/2a	DUP-1042	Chicken, Goias, Brazil, 1992
F6	4b	DUP-1042	Chicken, Goias, Brazil, 1992
F7	4b	DUP-18627	Chicken, Goias, Brazil, 1992
F8	4b	DUP-18627	Chicken, Goias, Brazil, 1992
F9	4b	DUP-1042	Chicken, Goias, Brazil, 1993
F10	1/2b	DUP-1042	Chicken, Goias, Brazil, 1993
F11	4b	DUP-1038	Chicken, Goias, Brazil, 1993
F12	4b	DUP-1038	Chicken, Goias, Brazil, 1993
F13	4b	DUP-1042	Chicken, Goias, Brazil, 1993
F14	4b	DUP-1042	Chicken, Goias, Brazil, 1993
F15	4b	DUP-1042	Chicken, Goias, Brazil, 1993
F16	4b	DUP-1042	Chicken, Goias, Brazil, 1993
F17	4b	DUP-1042	Chicken, Goias, Brazil, 1993
F18	4b	DUP-1042	Chicken, Goias, Brazil, 1993
F19	1/2b	DUP-1042	Chicken, Goias, Brazil, 1993
F20	1/2b	DUP-1042	Chicken, Goias, Brazil, 1993
F21	1/2b	DUP-1042	Chicken, Goias, Brazil, 1993

F22	1/2b	DUP-1042	Chicken, Goias, Brazil, 1993
F23	4b	DUP-1038	Chicken, Goias, Brazil, 1993
F24	1/2b	DUP-1042	Chicken, Goias, Brazil, 1993
F25	1/2b	DUP-1042	Chicken, Goias, Brazil, 1993
F26	ND	DUP-1065	Smoked loin, Sao Paulo, Brazil, 2001
F27	1/2b	DUP-18603	Smoked loin, Sao Paulo, Brazil, 2001
F28	4b	DUP-1042	Pizza, Sao Paulo, Brazil, 2001
F29	1/2c	DUP-1051	Sausage, Sao Paulo, Brazil, 2001
F30	4b	DUP-1042	Cooked ham, Minas Gerais, Brazil, 2001
F31	1/2c	DUP-19175	Chicken raw sausage, Minas Gerais, Brazil, 2001
F32	4b	DUP-1042	Pork raw sausage, Minas Gerais, Brazil, 2001
F33	4b	DUP-1042	Mozzarella, Rio Grande do Sul, Brazil, 2002
F34	4b	DUP-18598	Colony cheese, Rio Grande do Sul, Brazil, 2002
F35	4b	DUP-1042	Yellow cheese, Rio Grande do Sul, Brazil, 2002
F36	1/2a	DUP-19174	Frozen cooked beef, Mato Grosso, Brazil, 2005
F37	1/2b	DUP-1046	Cream cheese, Rio de Janeiro, Brazil, 2005
F38	1/2a	DUP-1051	Cheese, Parana, Brazil, 2005
F39	1/2a	DUP-1034	Cheese, Parana, Brazil, 2005
F40	4b	DUP-1042	Ground beef, Sao Paulo, Brazil
F41	1/2a	DUP-19187	Sausage, Sao Paulo, Brazil
F42	1/2c	DUP-1039	Ham, Sao Paulo, Brazil
F43	ND	DUP-15209	Salami, Sao Paulo, Brazil
F44	3c	DUP-1042	Sausage, Sao Paulo, Brazil
F45	1/2b	DUP-1042	Sausage, Sao Paulo, Brazil
F47	1/2c	DUP-19165	Sausage, Sao Paulo, Brazil
F48	3c	DUP-1039	Sausage, Sao Paulo, Brazil
F49	3b	DUP-1042	Ground beef, Sao Paulo, Brazil
F50	4b	DUP-18598	Ground beef, Sao Paulo, Brazil
V7	1/2a	DUP-1039	Raw milk, Massachusetts, USA
V37CE	4b	DUP-1039	Raw milk, Massachusetts, USA
101M	4b	DUP-1044	Salami, USA
103M	1/2a	DUP-1039	Sausage, USA
F4393	4b	DUP-1038	Cheese, USA
ATCC 51414	4b	DUP-1006	Raw milk, Massachusetts, USA
F1057	4b	DUP-1044	Raw milk, USA
F1109	4b	DUP-1044	Raw milk, USA
ATCC 43257	4b	ND	Cheese, California, USA
ATCC 15313	1/2a	ND	Rabbit, Cambridge, England
ATCC 19116	4c	DUP-1061	poultry, USA
ATCC 19118	4e	DUP-1038	poultry USA
ATCC 19114	4a	DUP-1059	bovine brain, USA

Table 2.1 continued

ATCC 19117	4d	DUP-1042	sheep, USA
ATCC 19111	1/2a	ND	Poultry, England

Clinical-isolates

CHLR1	1	DUP-1023	Blood, newborn female, 1984
SLCC 2482	7	DUP-1042	Patient, feces, Copenhagen, Denmark
ATCC 7644	1/2c	DUP-1039	Patient, CSF, Edenborough, Scotland
ATCC 19112	1/2c	DUP-1039	Patient, CSF
Scott A	4b	DUP-1042	Patient, blood, Massachusetts, USA
CHLR10	4	DUP-1038	23-day old female child, meningitis
CHLR8	1	DUP-1053	A 14-day old black female child, meningitis
F4233	1/2b	DUP-1042	CDC, patient, CSF/Blood, USA
C12-S(L)	4	ND	Bovine, feces, Nebraska, USA
CHLR6	1	DUP-1042	CHRL, female, meningitis
171	1/2a	DUP-1023	Patient, blood, USA
CHLR9	4	DUP-1038	CSF
CAP	4b	DUP-1038	Patient, CSf, USA
F4260	1/2b	DUP-1042	Patient, Blood, USA
ATCC 19115	4b	DUP-1042	Patient, CSF, Germany
F4244	4b	DUP-1044	Patient, CSF, USA
CHLR2	1	DUP-1042	CSF, 2-week-old female child
10403S	1/2a	ND	Human skin lesion, USA
ATCC 2540	3b	DUP-1052	Patient, CSF, New Orleans, USA
CHLR7	4	DUP-1024	Human
H6	4b	DUP-18604	CSF, 26-year-old patient, Sao Paulo, 2001
CHLR5	4	DUP-1042	CSF, 11-day old male child
CHLR3	4	DUP-1038	CSF, 2-week-old female child
H11	1/2b	DUP-19175	Blood, 72 years old patient, Sao Paulo, 2005
H9	4b	DUP-1038	Blood, 48 years old patient, Sao Paulo, 2004
H1	4b	DUP-1038	Aorta prosthesis, 69 years old patient, Sao Paulo, 2001
Murray B	4ab	DUP-1042	Patient, Massachusetts, USA
H5	1/2a	DUP-1023	CSF, 71 years old patient, Sao Paulo, 1995
H8	4b	DUP-1042	Blood, 61 years old patient, Sao Paulo, 2003
H16	ND	ND	Blood, 6 days old patient, Sao Paulo, 1998
F4243	4b	ND	Patient, CSF, USA
H12	4b	DUP-1038	CSF, Sao Paulo, 2005
H14	ND	DUP-1042	CSF, Sao Paulo, 2002
H10	1/2a	DUP-19173	CSF, 55 years old patient, Sao Paulo, 2004
H13	ND	DUP-1042	CSF, 16 years old patient, Sao Paulo, 2002
F4263	1/2a	DUP-1060	Patient, CSF/Blood, USA
F4264	4b	DUP-1038	Patient, CSF/Blood, USA

Table 2.1 continued

H7	4b	DUP-1042	Blood, 5 days old patient, Sao Paulo, 2004
SLCC 2482	7	DUP-1042	VICAM, patient, feces, Copenhagen, Denmark
H15	1/2b	DUP-1042	CSF, Sao Paulo, 2005
F4262	4b	DIP-1051	CDC, patient, CSF/Blood, USA
H4	4b	DUP-1042	Blood, 34 years old patient, Sao Paulo, 1998
H3	4b	DUP-19191	CSF, 60 years old patient, Sao Paulo, 1998
ATCC 19113	3a	DUP-1030	Patient, Copenhagen, Denmark
H2	4b	DUP-18604	CSF, 73 years old patient, Sao Paulo, 2000
ATCC 19115	4b	DUP-1042	VICAM, patient, CSF, Germany

[a]CSF, Cerebrospinal fluid; ATCC, American Type Culture Collection; CHLR, Children's Hospital at Little Rock, Arkansas, USA. ND, not determined. Serotypes and ribotypes were identified by Bueno et al. (2010), Jaradat et al. (2002), and Lathrop et al. (2003).

Table 2.2 *L. monocytogenes* mutant strains and growth conditions

L. monocytogenes	**Incubation conditions**	**Source**
F4244 (WT, 4b)	37°C	Our Lab
BL520 (F4244 *inlA*^{m})	37°C	This study
KB208 (F4244 *lap*$^{-}$)	Erythromycin (10 µg/mL), 42°C	Our Lab (Jagadeesan et al. 2010)
AKB301 (F4244 Δ*inlA*)	37°C	Our Lab (Burkholder and Bhunia 2010)
10403S (WT, 1/2a)	37°C	Dr. Daniel Portnoy, UC Berkley, USA
10403S Δ*prfA*	37°C	Dr. Nancy Freitag, University of Illinois, Chicago, USA
10403S Δ*hly*	37°C	Dr. Daniel Portnoy, UC Berkley, USA

2.3.2 Development of *Lm* F4244 expressing murinized Internalin A (InlA^{m})

Murinization of InlA in F4244 (4b) was accomplished by following a method described before (Wollert et al. 2007) and outlined in **Fig 2.14**. Briefly, the sequence between nucleotide 494 and 1485 of the *inlA* gene in *Lm* F4244 (GenBank: CP015508.1) (Bailey et al. 2017) including mutations for the two amino acids substitution was synthesized by GenScript and amplified using Q5 high-fidelity polymerase (New England BioLabs). The other two fragments, upstream 800 base pairs to *inlA* nt 493 and *inlA* nt 1486 to downstream 800 base pairs, were individually amplified using *Lm* F4244 gDNA as the template. Then, a mixture of the three segments was used as the templates, amplified, and combined into a whole fragment by PCR. The whole fragment and a temperature-sensitive suicide plasmid, pHoss1 (Addgene), were digested by *NcoI* and *SalI* and

ligated using T4 ligase (New England BioLabs). Ligated pHoss1::*inlA*^{m} was transformed and maintained in *E. coli* DH5α (Invitrogen). Purified pHoss1::*inlA*^{m} was electroporated into electrocompetent *Lm* F4244 Δ*inlA* at 2,000V (BTX Electroporation System), and transformants were selected on BHI agar plates supplemented with 10 μg/mL erythromycin (Rychli et al. 2014). The *inlA*^{m} knock-in mutant strain was selected as before (Abdelhamed et al. 2015) and the specific mutation in *inlA*^{m} ORF was confirmed by Sanger sequencing (Eurofin) using four primers of both directions (**Fig. 2.14**). Colony PCR to screen the knock-in mutant was conducted using the Platinum II Hot-Start PCR Master Mix (Invitrogen). The expression of InlA^m in the whole-cell extract was verified in Western blot by using anti-InlA mAb-2D12(Mendonca et al. 2012). The surface expression of InlA^m was also confirmed by whole-cell ELISA as before (Kim et al. 2006).

2.3.3 Mammalian cells

Caco-2 cell line (ATCC, Manassas, VA) was seeded and incubated in T-25 tissue culture flasks (TPP, Switzerland) with high glucose Dulbecco's' modified Eagles' medium (DMEM: HyClone, Logan, UT) and 10% (vol/vol) fetal bovine serum (D10F: Atlanta Biologicals) at 37°C with 7% CO_2, and 95% relative humidity until the confluence was achieved (Burkholder and Bhunia 2010). The cell monolayer in the flask was trypsinized (Hyclone) and about 1-2 x 10^4 cells were seeded in each well of 24-well tissue culture plates (TPP, Switzerland) or Transwell inserts with 3.0 μm pores, respectively, for 14-21 days until 95% confluence and polarization were achieved (Burkholder and Bhunia 2010; Drolia et al. 2018). HCT-8 (ATCC) human ileocecal cell line was prepared with the same procedures with minor adjustments. Cells (4.5 ×10^4/ 500 μl) were seeded in each well of a 48-well tissue culture plate (TPP, Switzerland) and incubated for 4 to 5 days (Jagadeesan et al. 2011). Ped-2E9 cell line, a B cell hybridoma(Bhunia et al. 1994), was cultured in the same conditions and incubated in the 75-cm^2 flask (TPP, Switzerland) for 3 to 4 days before being used for experiments (Bhunia et al. 1994; Gray et al. 2005).

2.3.4 Biofilm assay and the preparation of biofilm and planktonic culture

The microtiter plate biofilm assay (Djordjevic et al. 2002). was followed to quantify biofilm formation with slight modification. Optical density (OD) of overnight grown *Lm* TSBYE culture was measured at 595 nm and standardized to 1.2. Then, the culture was diluted with

Modified Welshimer's Medium (MWB, Himedia) by 1 to 40 and 150 µL MWB was aliquoted into six wells on a 96-well tissue culture-treated microtiter plate (Corning, NY) and incubated at 30°C for 48 h (Borucki et al. 2003). To quantify the formation of biofilm in each well, supernatant media was removed and each well was washed thrice with 10 mM sterile phosphate-buffered saline (PBS) to remove loosely attached cells. After air-drying the microtiter plate for 15 min, 150 µl of 0.1% crystal violet (CV) solution was added to each well to stain the biofilm cells and incubated for 45 min at room temperature. Further, each well was washed three times with sterile water to remove residual CV stain, and, after air-drying wells for 15 min, an aliquot of 200 µL of 95% ethanol was added into each well and incubated for 15 min under ambient temperature to destain the biofilms. Finally, the ethanol solution from each well was transferred to a fresh flat-bottom microtiter plate to measure absorbance at 595 nm.

To collect sessile bacteria, the MWB culture (40 ml) was prepared in the same way but inoculated into a tissue culture treated petri dish with 60.1 cm^2 growth surface area (TPP, Switzerland). After growth at 30ºC, each plate was rinsed with 5 mL sterile PBS twice and 5 mL PBS was added before detaching biofilm by 15 min sonication in a water bath (iSonic, Chicago, IL). Planktonic bacteria were prepared by incubating the MWB culture in test tubes under the same conditions (at 130 rpm for 24 h).

2.3.5 *In vitro* bacterial adhesion, invasion, translocation and cytotoxicity assays

Bacterial adhesion and invasion were examined using Caco-2 (colon) and HCT-8 (ileocecal) cell lines. *Lm* planktonic and biofilm cultures were prepared as described above, washed thrice with sterile PBS and diluted in D10F (Burkholder and Bhunia 2010) to proper concentrations. Both sessile and planktonic bacteria in D10F were diluted and added to epithelial cell monolayers in a well at a multiplicity of infection (MOI) 10. For adhesion assays, monolayers were washed once after 30 min infection(Wampler et al. 2004b) and bacteria were released from mammalian cells into 500 µl sterile 0.1% Triton X-100, serially diluted and enumerated by plating on BHI agar plates (BHIA). For invasion assays, cells were incubated for 2 h (Yamada et al. 2006), washed, and then monolayers were incubated with D10F containing 50 µg/ml gentamicin to eliminate extracellular bacteria before lysing mammalian cells by 0.1% Triton X-100. The amount of invaded *Lm* was enumerated by plating on BHIA. Adhesion and invasion rates were calculated by dividing bacterial cell numbers from lysed cells by the number of inoculums.

Translocation assays were performed using Caco-2 cells seeded in a Transwell set up for 14-21 days as described before (Burkholder and Bhunia 2010; Drolia et al. 2018). Briefly, washed bacterial cells were added to the apical well at an MOI of 100 and incubated at 37ºC for 4 h in a CO_2 incubator. The liquid (500-µl aliquot) from the basal well was removed, diluted and plated on BHIA for enumeration. The transepithelial electrical resistance (TEER) values of each well were measured before and after translocation experiments to monitor the integrity of cell monolayers. The wells with TEER values between 400-600 (200 Ω/cm^2) were used for experiments.

For cytotoxicity assays, freshly grown Ped-2E9 cells were counted by Trypan blue staining and resuspended in 500 µl D10F with the final cell concentration of approx. 10^6 cell/ml. Bacteria were added to achieve an MOI of 10 and incubated at 37ºC for 2 h (Bueno et al. 2010). Ped-E9 cells were stained with Annexin V-PE and 7-AAD (BD, Franklin Lakes, NJ) following the vendor's protocol. The Ped-2E9 cells which were viable, in the early apoptosis phase or dead were recognized as both Annexin V and 7-AAD negative, Annexin V positive and 7-AAD negative, and both positive Annexin V and 7-AAD positive, respectively. Labeled cells were analyzed by BD Accuri™ C6 that detects Annexin V-PE in FL-2 and 7-AAD in FL-3, and at least 10,000 events were collected from each sample. As blank controls, two samples of Ped-2E9 cells went through all the labeling procedures the same as the testing samples but without bacterial infection. The percentage of Annexin V positive events of each sample was calculated by subtracting the average percentage of Annexin V positive events in blank controls from the same experiment. To confirm proper labeling, bacteria-treated Ped-2E9 cells were also examined under a fluorescence microscope (Leica, Buffalo Grove, IL) after staining with Annexin V-FITC and 7-AAD, respectively(Bueno et al. 2010; Mannarreddy et al. 2017).

Cytotoxicity was also tested on a Caco-2 cell line by assessing intracellular LDH release (Singh et al. 2018). Caco-2 cells in 24-well plates were incubated with sessile or planktonic *Lm* at MOI of 10 for 2 h at 37ºC. Released LDH in the supernatant was quantified using Pierce LDH Cytotoxicity Kit (Thermo Scientific, Frederick, MD). Supernatant from non-treated cell monolayers and cells lysed with 0.1% Triton X-100 were used as negative and positive controls to determine 0 and 100% cytotoxicity, respectively.

2.3.6 Protein extraction and Western blotting

The whole-cell protein, secreted protein, cell wall protein, and intracellular proteins were extracted and analyzed separately using Western blot to compare the expression of key virulence genes in biofilm-isolated and planktonic *Lm* (Burkholder et al. 2009). Briefly, to extract whole-cell protein, approximately 1×10^8 to 1×10^9 biofilm-isolated or planktonic *Lm* cells were harvested, washed and resuspended into 100 µl PBS. Then, the bacterial cultures were kept in ice and sonicated for three 15s cycles. After centrifugation (14,000 g for 10 min at 4°C), whole-cell protein in the supernatant was collected. Protein from the cell wall, intracellular and supernatant fractions were also extracted (Burkholder et al. 2009) and quantified using BCA (Thermo Scientific) to standardize loading amount. To collect supernatant protein secreted by *Lm* in biofilms, biofilms were incubated in tissue culture-treated Petri dish (TPP) for 24 h, rinsed to remove loosely attached bacteria and replenished with the same volume of fresh MWB medium for another 16 h at 30ºC. Secreted protein in the supernatant from biofilm cells was extracted from the MWB medium after 48 h while from planktonic cells after 24 h at 30ºC. After standardizing the loading amount, quality and quantity of protein samples were analyzed using sodium dodecyl sulfate-polyacrylamide gel electrophoresis (SDS-PAGE;10% acrylamide). Proteins were transferred to a hydrophobic membrane (PVDF) and immunoprobed with antibodies to LAP, and InlA, (all from our lab, **Table 2.2**) and LLO (Cat # ab200538; Abcam, Cambridge, UK). All blots/gels derive from the same experiment and were processed in parallel. See supplementary information for original blots.

2.3.7 RNA extraction and quantitative reverse transcription PCR

Isolation and quantification of mRNA from biofilm-isolated *Lm* from the intestinal chymus were performed as described before (Oozeer et al. 2005) with some modifications. Chymus from the ileum, cecum, and colon were collected into a 2 mL screw-cap tube (BioSpec) pre-filled with 1 mL cold PBS and 2 glass beads (5 mm diameter) (BioSpec), and homogenized using FastPrep 5G (2 cycles of 6 m/s treatment for 40s; MP Biomedicals) to release bacteria. The homogenate was then combined into 9 mL of cold PBS and centrifuged (250 g, 5 min) and the supernatant containing bacteria was filtered through a sterile cell strainer (mesh size 40 µm, Fisher), diluted, and plated on MOX to quantify *Lm*. The filtrate was centrifuged (8,000 g, for 5 min at 4°C), rinsed twice with cold PBS, resuspended into 1 mL TRIzol, and stored at -80°C. RNA was extracted and

purified using Direct-zol™ RNA Miniprep Plus kit (Zymo Research), treated with DNase and purity was assessed using NanoDrop™ 2000 (Thermo Fisher Scientific). cDNA was synthesized using RNA (2-500 ng, A_{260}/ A_{280}~2.0, A_{260}/ A_{230}>2.0) and Maxima H Minus Reverse Transcriptase (Thermo Scientific) and random hexamer primers. To quantify the copy number of target genes in cDNA, I first constructed standard curves of gene copy numbers and Ct values. DNA with known copy numbers of each gene was prepared by PCR (**Table 2.3, Fig 2.8**), purified, quantified using NanoDrop, serially diluted (about 10 to 10^9 copy/μL) and used as templates for quantitative PCR (qPCR) using PowerUp SYBR® Green Master Mix (Applied Biosystems) and qPCR-specific primers (**Table 2.3**) in a StepOnePlus™ Real-Time PCR System (Applied Biosystems). The qPCR primers were all self-designed, and their potential secondary structures were predicted using the OligoAnalyzer Tool (IDT). The relative expressions of virulence (*inlA* and *lap*) and regulator (*prfA* and *sigB*) genes in biofilm-isolated *Lm* from intestinal chymus 12 or 48 hpi were compared with those expressed in the same culture before oral infection using the following equation:

$$\text{Relative expression} = \frac{\text{Total copy\# of target genes in chymus (12 or 48 hpi)}}{\text{CFU of Lm in chymus (12 or 48 hpi)}} * \frac{\text{CFU of biofilm}}{\text{Total copy \# of the target gene in biofilm}} \quad (1)$$

where "biofilm" denotes biofilm-isolated *Lm* before infection.

To compare virulence gene expression between biofilm-isolated and planktonic *Lm* from non-intestinal samples, cultures were prepared as described above and approximately 10^8 CFU was collected after washing twice with PBS (8,000g for 3 min at 4°C) and resuspended in 1 mL of TRIzol® reagent. Then, RNA extraction and cDNA quantification were carried out as above. The relative expression of *lap, inlA, prfA,* and *sigB* in biofilm-isolated cells compared to planktonic cells were calculated using the following equation:

$$\text{Relative expression} = \frac{\text{Total copy \# of target gene in biofilm}}{\text{CFU of biofilm}} * \frac{\text{CFU of planktonic}}{\text{Total copy \# of the target gene in planktonic}} \quad (2)$$

where, "biofilm" and "planktonic" denote biofilm-isolated and planktonic cells.

Table 2.3 Plasmid, primers, and antibodies used in the study

qPCR Oligonucleotides Primers	**Sequence**	**Source**
pHoss1	Available at Addgene.org	Addgene
inlAm5	AGACCCGCTTAAAAACCTAACAAATTTAAATCGGCTAGAACTATCT	This study
inlAm3	GAAACTTAGCATTAAAAATTGCCTTAAGTGGCTGCGTCACTGT	This study
inlA.up.5 (*NcoI*)	cacaagggtttgaatcattagatcccatggATCCGATTATTGTAGTGGCTT	This study
inlA.up.3	ATAGTTCTAGCCGATTTAAATTTGTTAGGTTTTTAAGCGGGTCT	This study
inlA.down.5	CGCAGCCACTTAAGGCAATTTTTAATGCTAAGTTTCA	This study
inlA.down.3 (*SalI*)	gatatcggatccatatgacgtcgacCTAAACAATTCTAAAACA	This study
InlA_3(RT)[a]	GCATTATAGCTATCGCCAGT	This study
inlA_5(RT)[a]	ACAAAACTAACTGAGTTAAAACTGG	
qInlA_3[b]	GTTGTTACACCGTCATTATCCAAGGTTGCTG	This study
qInlA_5[b]	ATTGACTGAACCAGCTAAGCCTGTAAAAGAAGG	
Lap_3(RT)[a]	TCAAACACCTTTGTAAGCTT	This study
Lap_5(RT)[a]	GAACGCGTATTTATCGTAACT	
qLap_3[b]	CGCATTTGCAAACGCCATACCAGC	This study
qLap_5[b]	CCAGATGTTGCGATTGTCGATGCAC	
prfA_3(RT)[a]	TTTTCCCCAAGTAGCAGG	This study
prfA_5(RT)[a]	ATGAACGCTCAAGCAGAA	
qprfA_3[b]	GCTAGGCTGTATGAAACTTGTTTTTGTAGG	This study
qprfA_5[b]	AGAAGTCATTAGCGAACAGGCTACCGC	
SigB_3(RT)[a]	TTACTCCACTTCCTCATTCTG	This study
SigB_5(RT)[a]	ATGCCAAAAGTATCTCAACC	
qSigB_3[b]	CCCATTTCCATTGCTTCTAAAACTTCTTCCTCC	This study
qSigB_5[b]	AATTAGGTCCGAAAATTAAAAATGCCGTAGAAGAG	
inlA-F[c]	GAACCAGCTAAGCCCGTAAAAG	(Werbrouck et al. 2006)
inlA-R[c]	CGCCTGTTTGGGCATCA	
prfA-F[c]	TCATTAGCGAGCAGGCTACC	(Camejo et al. 2009)
prfA-R[c]	GCAAATAGAGCCAAGCTTCC	
Antibodies	**Description**	**Source**
mAb-H7	Mouse monoclonal anti-LAP antibody	Our lab
mAb-2D12	Mouse monoclonal anti-InlA antibody	(Mendonca et al. 2012)
pAb anti-LLO	Rabbit polyclonal anti-LLO pAb	Abcam (Cat # ab200538)
IgG (HRP-linked)	Goat anti-rabbit IgG (HRP-linked)	Cell Signaling (Cat # 7074)
IgG (HRP-linked)	Horse anti-mouse IgG (HRP-linked)	Cell Signaling (Cat # 7076)

[a]Primers used to generate amplicons for generating qPCR standard curves. [b]qPCR primers used for quantifying gene copy numbers. [c]qPCR primers are used for detecting the presence or absence of *Lm* in mouse tissues.

2.3.8 Mouse pathogenicity assay

The animal experiment protocol (No. 1201000595) was approved by the Purdue University Animal Care and Use Committee. C57BL/6 male and female mice (8-10 weeks old) from our breeding colony were used. To characterize the *in vivo* pathogenicity of $InlA^m$ strain, mice (n = 5-6/treatment) were orally gavaged with 100 µl of freshly prepared cultures (5×10^9 CFU in PBS) of *Lm* F4244 WT, $InlA^m$, or ΔinlA using a stainless steel ball-end needle (Popper) (Drolia et al. 2018) and sacrificed 96 hpi.

To determine the pathogenicity of sessile and planktonic *Lm* strains, F4244 (WT), $InlA^m$ or F45, each mouse was orally challenged with 100 µl of freshly prepared cultures (1×10^9 CFU in PBS/mouse). In a separate experiment, mice were pretreated with streptomycin (5 mg/mL) in the drinking water for 32 h followed by 16 h without antibiotics until bacterial gavage (Becattini et al. 2017; Louie et al. 2019). Food was withdrawn 8 h before gavage. Mice (n = 4-9/treatment) were sacrificed 12, 24 and 48 h after infection by CO_2 asphyxiation. Blood was collected through cardiac puncture and 100 µL of blood was mixed with 400 µL 0.4% sodium citrate solution as an anticoagulant and further diluted to enumerate by plating. Extra-intestinal organs were collected and homogenized in 4.5 ml (mesenteric lymph node, spleen, and kidney) or 9 mL (liver) buffered *Listeria* enrichment broth (BLEB: Neogen) supplemented with 0.1% Tween-20 and antimicrobial supplement (Neogen). After sectioning the intestine into jejunum, ileum, cecum, and colon, internal contents were removed, and the intestinal sections were split open before washing (2X) and incubation in sterile D10F containing 50 µg/ml gentamicin at ambient temperature for 2 h to eliminate extracellular bacteria. Then, each part of the intestine was individually homogenized in 1 ml BLEB, diluted in PBS, and plated on Modified Oxford plates (MOX; Neogen) to enumerate invaded bacterial load.

Since the viable bacterial counts in most organs from 12 h infected mice were lower than the detection limit by a standard plating method, the presence of *Lm* in these samples was determined by culture enrichment followed by quantitative PCR. Homogenized samples in BLEB were incubated at 37ºC overnight and 100-µL of each culture was plated on MOX plates. Colonies producing black pigment on MOX plates were transferred into 4 mL BHI broth incubated at 37ºC overnight for the final enrichment. DNA was extracted from cultures using the boiling method, and qPCR using SYBR® Green Master Mix (Applied Biosystems) and targeting two specific virulence genes (*prfA* and *inlA*) (**Table 2.3**) were performed to determine the presence of *Lm.* For

the samples that did not form colonies on MOX plates, DNA was directly extracted from enriched BLEB samples before qPCR.

For histopathology analysis, a small section of the spleen, liver, and parts of the intestine was fixed in formalin (10%) and stained with hematoxylin and eosin to be microscopically examined and scored by a board-certified veterinary pathologist, Dr. Abigail Cox from Purdue University, as before (Drolia et al. 2018).

2.3.9 Bacterial survival and virulence after exposure to simulated gastrointestinal fluids

To assess the survival of biofilm-isolated and planktonic *Lm* in gastrointestinal conditions, simulated gastric fluid (SGF) and simulated intestinal fluid (SIF) was prepared as before (Mathipa and Thantsha 2015) with an exception. Luria-Bertani (LB) was substituted with distilled water as the solvent for SIF. Biofilm-isolated and planktonic bacteria were rinsed once with sterile deionized (DI) water, resuspended in SGF (pH 2), and incubated at 37°C with the agitation of 120 rpm for 1 h. Viable bacterial counts were enumerated at 0- and 60-min post-SGF treatment by diluting and plating on BHIA. After SGF treatment, bacterial cultures were rinsed once with sterile DI water, resuspended in SIF (pH 7) for another 12 h incubation at the same conditions, and enumerated after SIF treatment.

Adhesion, invasion, and transepithelial translocation of SGF and SIF-treated or non-treated sessile and planktonic bacteria were tested on Caco-2 cell monolayers as above. At the same time, whole-cell proteins were extracted from treated and non-treated cultures to assess the expression of LAP and InlA using immunoblotting. Instead of SGF (pH 2), bacteria for *in vitro* virulence tests and immunoblotting were treated with SGF (pH 3) to ensure the availability of an adequate number of viable cells for the experiment. Other conditions remained the same as the survival test.

2.3.10 Statistical analysis

Experimental data were analyzed using GraphPad Prism (La Jolla, CA) software. P values and the type of statistical analysis performed are described in the figure legends. The Mann-Whitney test was used to determine statistical significance for mouse microbial counts and data are presented as median. In other experiments, comparisons between treatment and control were performed using the unpaired Student *t*-test, or by one-way or two-way analysis of variance with

Tukey's multiple-comparison test, and data are presented as the mean ± standard error of the mean (SEM).

2.4 Results

2.4.1 Food-isolated *L. monocytogenes* strains have higher biofilm-forming capability than clinical isolates

The biofilm-forming capability of over 100 *Lm* isolates of food and clinical origin on polystyrene surface was assessed after 48 h using crystal violet staining (Djordjevic et al. 2002) to choose for representative food and clinical strains to investigate the pathogenic potential in *in vitro* cell culture and *in vivo* mouse models. Biofilm-forming capacity varied widely among the strains at 48 h. I found food isolates (65 strains) had significantly ($P < 0.05$) higher biofilm-forming capability than the clinical isolates (45 strains) (**Fig. 2.1a-c**). Furthermore, isolates of serotype 1/2a and 1/2c (Lineage II) had greater biofilm-forming capabilities than serotypes 1/2b or 4b (Lineage I) (**Fig. 2.1a,c**). Isolates were arbitrarily grouped into high, moderate, and low biofilm-producing groups (**Fig. 2.1b**) and representative strains with high (F40 and F45) or moderate (F33, F4244, and 10403S) biofilm-forming capabilities were chosen for further characterization. These isolates (two clinical; F4244 (4b) and 10403S 1/2a) and three food; F40 (4b), F45 (1/2b) and F33 (4b) represent serotypes 4b, 1/2b and 1/2a (**Table 2.1**) which are responsible for a majority of human listeriosis cases (Doumith et al. 2004; Swaminathan and Gerner-Smidt 2007). Light microscopic images revealed the formation of typical honeycomb-like structures of biofilms consistent with the previous observation (Guilbaud et al. 2015) with varying sizes of the biofilm clusters (**Fig. 2.2a**). Furthermore, there is no apparent difference in individual cell lengths between sessile and planktonic cells (**Fig. 2.2b**). Collectively, these data reveal that food-isolated *Lm* strains have higher biofilm-forming capabilities than clinical isolates.

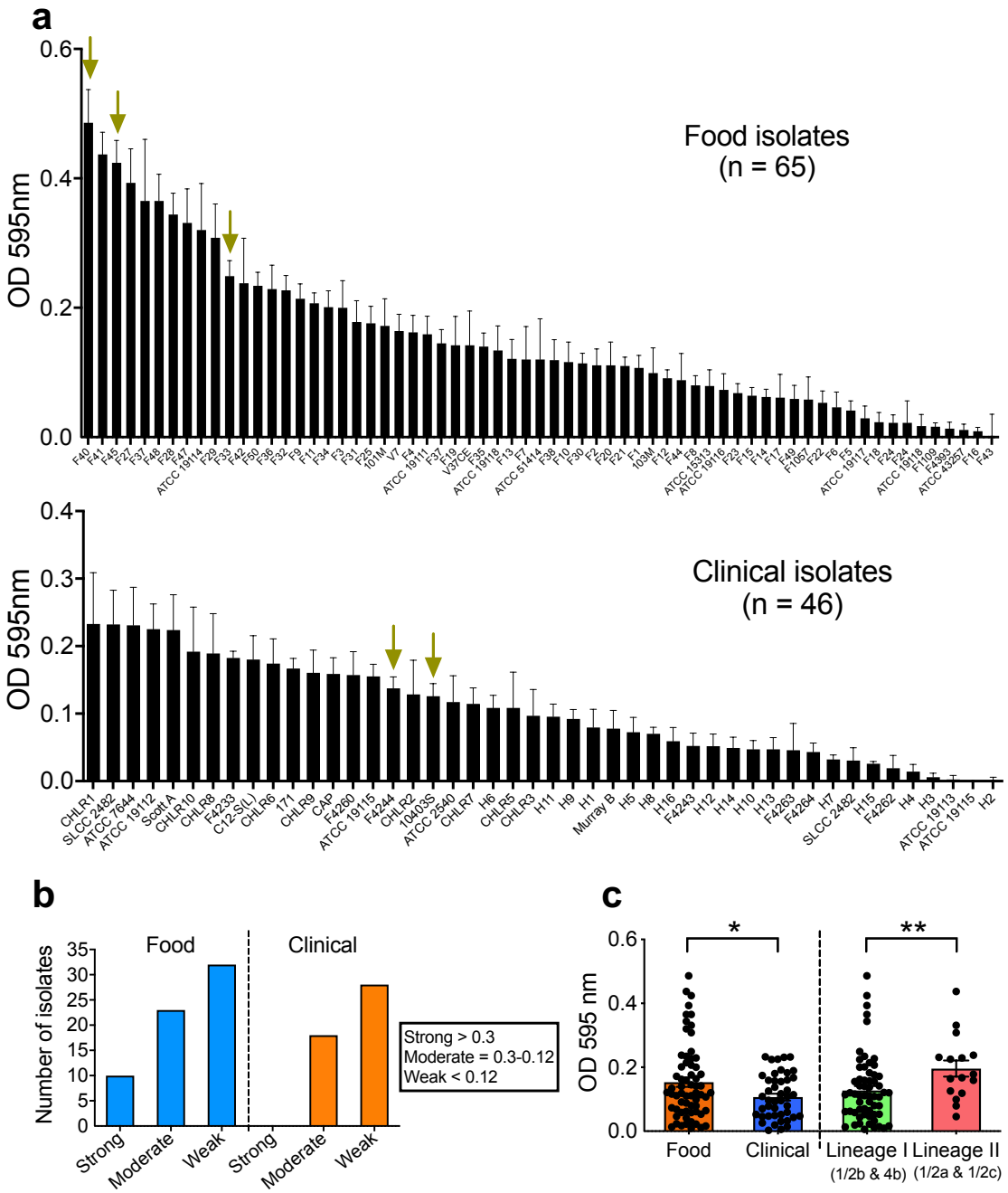

Figure 2.1. Quantification of *L. monocytogenes* (*Lm*) biofilm formation and morphological analysis. (a) The biofilm-forming capabilities of over 100 food-(top-panel) or clinical-isolated (bottom panel) *Lm* strains were tested using crystal violet staining assay. Arrows indicate the strains selected for further characterization. (b) Assemblage (strong, moderate and weak) of isolates based on their ability to form biofilms. (c) Comparison of biofilm formation by food and clinical isolates and isolates of lineage I and II. Food isolates have significantly higher biofilm-forming capability than the clinical isolates, and isolates of lineage II also have a significantly higher capacity than isolates of lineage I. Mann-Whitney test was used for statistical analysis. **P < 0.005; *P < 0.05.

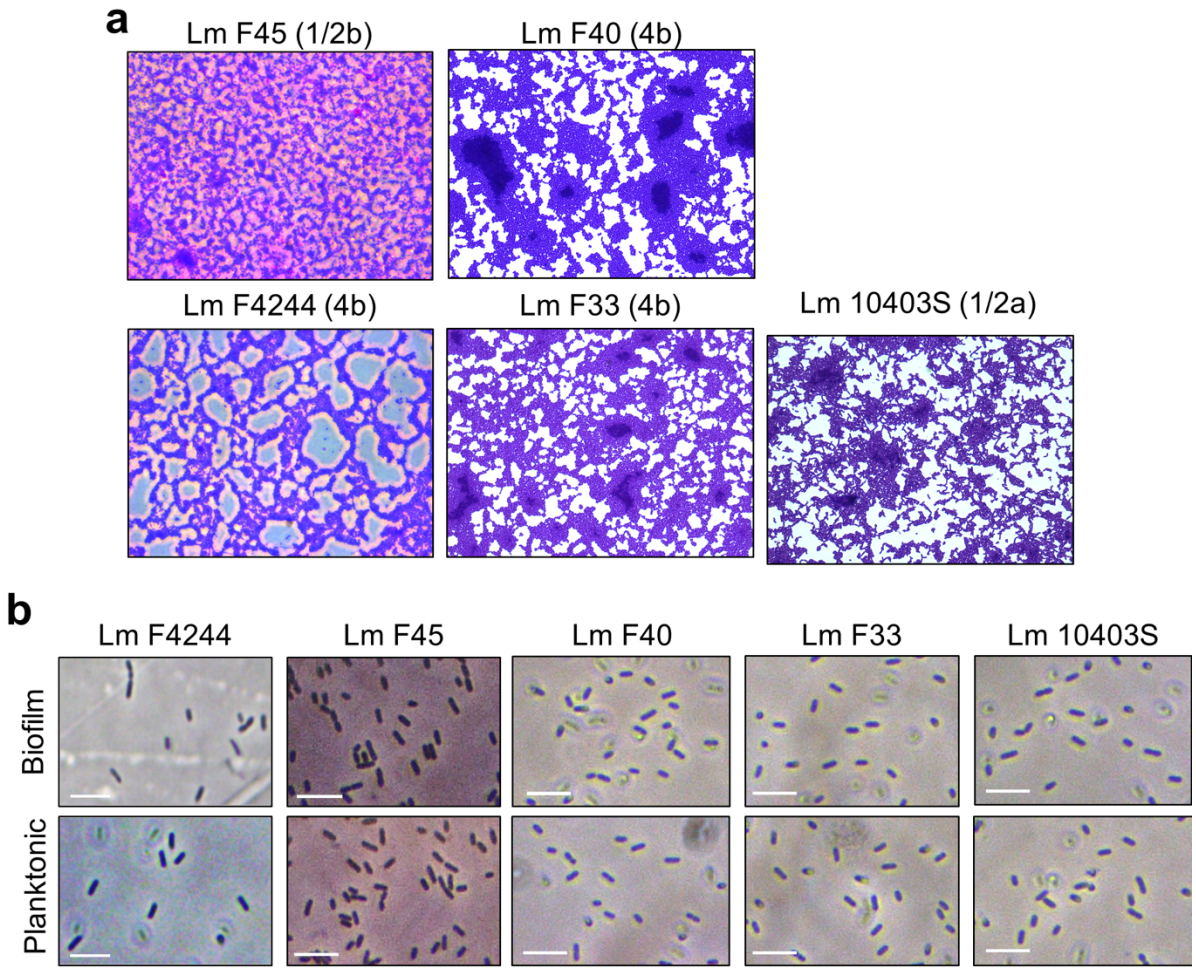

Figure 2.2. (a) Visualization of biofilm formation by high (*Lm* F45 and F40) and moderate (F4244, F33, and 10403S) biofilm forming strains of *L. monocytogenes* isolates on glass slides after crystal violet staining. (b) Morphological comparison of biofilm-isolated and planktonic *Lm* F4244, F45, F40, F33, and 10403S cells using phase-contrast microscopy shows no significant difference in cell length. Scale bars represent 5 µm.

2.4.2 Biofilm-isolated *L. monocytogenes* has attenuated adhesion, invasion, and translocation capability to intestinal epithelial cell lines *in vitro*

To compare the bacterial adhesion, invasion and transmigration characteristics of 48 h-old biofilm-isolated sessile and 24 h-old planktonic *Lm* cells, two human intestinal epithelial cell lines, Caco-2 (colonic cells) and HCT-8 (Ileocecal junctional cells) were used. Sessile cells of all five strains (F40, F45, F33, F4244, and 10403S) tested showed a significantly ($P < 0.05$) decreased adhesion to Caco-2 (**Fig. 2.3a**) and HCT-8 (**Fig. 2.3b**) cells than that of their planktonic counterparts. Likewise, sessile cells showed significantly lower invasion than the planktonic cells

into Caco-2 (**Fig. 2.3c**) and HCT-8 (**Fig. 2.3d**) cells. Sessile cells also showed significantly ($P < 0.05$) lower transepithelial translocation than the planktonic cells in a Transwell setup (**Fig. 2.3e**). Altogether, reduction in adhesion, invasion and transepithelial migration between sessile and planktonic cultures was over 50%. Additionally, planktonic cells of wild-type (WT) *Lm* F4244 strain showed significantly higher adhesion and invasion than that of the planktonic cells of an isogenic *lap*$^{-}$ or Δ*inlA* mutant strains used as controls (**Fig. 2.3**). Note, during this experiment, the growth of both sessile and planktonic *Lm* cells were negligible in mammalian cell culture medium (D10F; Dulbecco's modified Eagles medium with 10% fetal bovine serum) after 3 h and there is no significant difference ($P < 0.05$) between two cultures (**Fig. 2.4**), suggesting the differences in bacterial interaction with mammalian cells are not influenced by their growth during the assay period. Taken together, these *in vitro* results suggest that the biofilm-isolated *Lm* strains have impaired ability to adhere, invade, or translocate across the epithelial cells than that of their planktonic counterparts thus possibly have reduced virulence potential.

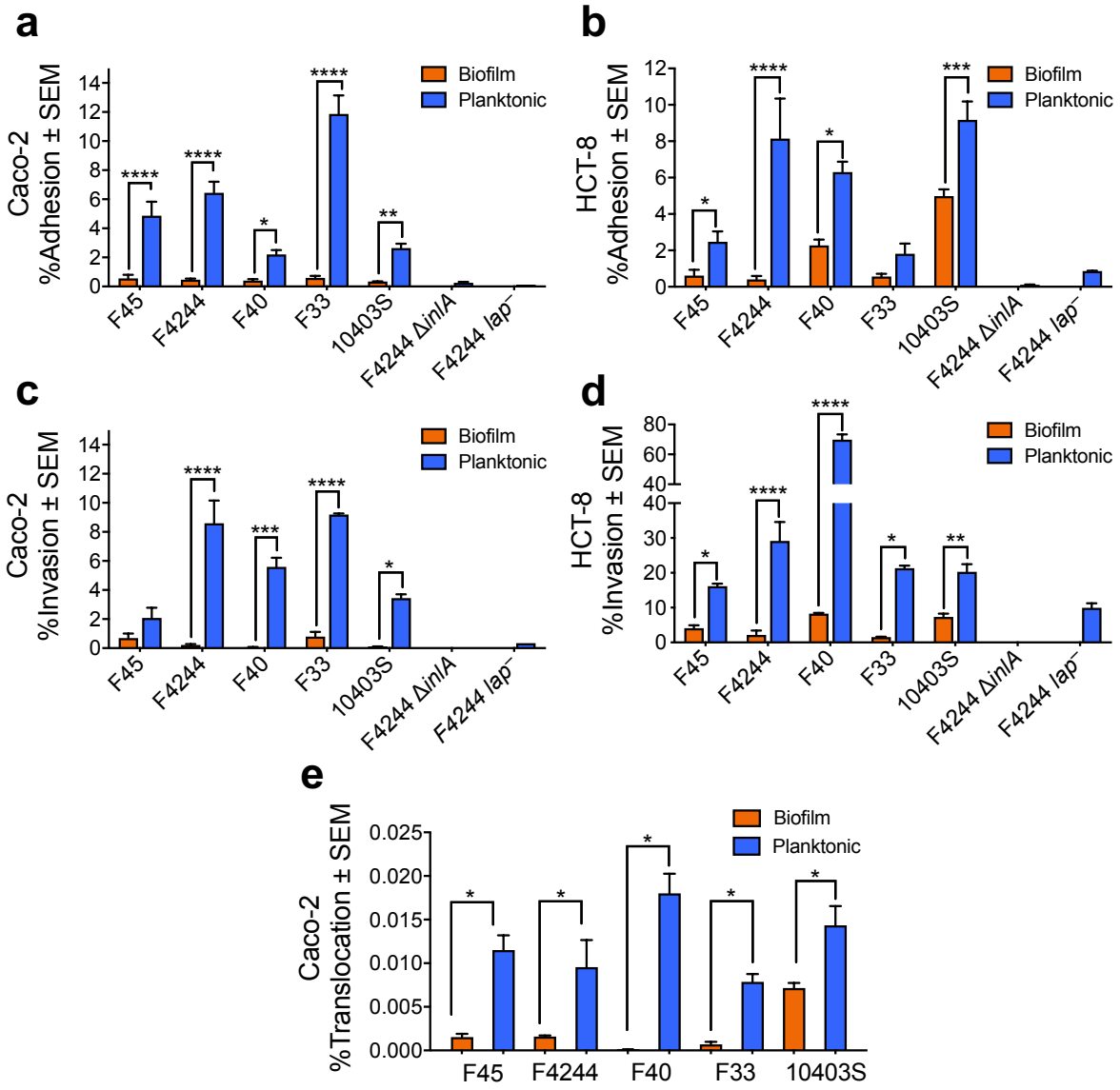

Figure 2.3. Adhesion, invasion and translocation characteristics of biofilm-forming sessile and planktonic cells on the cultured cell line. Comparison of adhesion (a and b) and invasion (c and d) in Caco-2 and HCT-8 cells and transepithelial translocation across Caco-2 cells (e) between *L. monocytogenes* biofilm-isolated sessile and planktonic cells on Caco-2 and HCT-8 cells. The percentage was calculated by dividing the amounts of adhered, invaded, or translocated bacteria by the amounts of bacteria in the inoculum. Data are the average of at least three independent experiments performed in triplicate. All error bars represent SEM. Pairwise Student's t-test was used for statistical analysis. ****P < 0.0001; ***P < 0.0005; **P < 0.005; *P < 0.05.

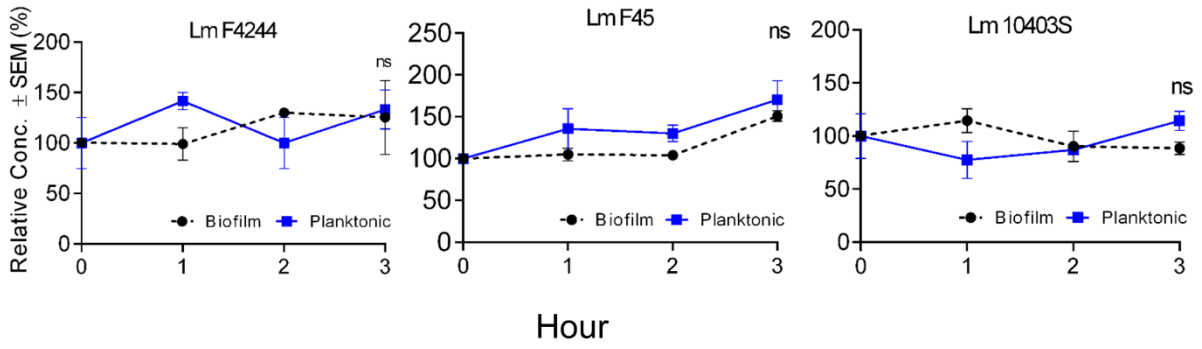

Figure 2.4. Counts of biofilm-isolated or planktonic *Lm* F4244, F45, and 10403S cells in mammalian cell culture medium (D10F; Dulbecco's modified Eagles medium containing 10% fetal bovine serum) remained no significantly different over 3 h period.

2.4.3 Biofilm-isolated *L. monocytogenes* were less cytotoxic to Ped-2E9 and Caco-2 cells than the planktonic bacteria

To characterize pathogenic attributes of biofilm-isolated cells, Ped-2E9 (a hybrid murine B lymphocyte line)-based *in vitro* cytotoxicity assay was conducted (Bhunia et al. 1994; Banerjee and Bhunia 2010). Ped-2E9 has been established to be a sensitive model to respond to the apoptosis triggered by *Lm* (Bhunia and Feng 1999a; Gray et al. 2005; Bueno et al. 2010). I used Annexin V and 7-AAD labeling method to distinguish Ped-2E9 cells in the early or late apoptosis and analyzed them using flow cytometry and fluorescence microscopy. Biofilm-isolated and planktonic cells of *Lm* strains F4244 and 10403S and their corresponding isogenic mutant strains were analyzed (**Fig. 2.5a**). The damage caused by bacteria to Ped-2E9 cells was quantitatively compared by the sum percentage of Annexin V positive events, which include cells in the early and the late stage (dead) of apoptosis (**Fig. 2.6**). Firstly, all planktonic WT strains (F45, F4244 and 10403S) caused significantly more cell damage than the corresponding biofilm-isolated cells (**Fig. 2.5a,b**). Secondly, the microscopic analysis confirmed that the planktonic strains (F4244, 10403S and F45) are responsible for more apoptotic or dead Ped-2E9 cells than the sessile cells. Thirdly, as expected, planktonic 10403S cells caused significantly more damage than the isogenic Δ*prfA* mutant strain whose virulence cannot be upregulated by the major regulator, PrfA (de las Heras et al. 2011) (**Fig. 2.5a,b**). I used the Δ*prfA* mutant as a negative control since *hly*, *plcA* and *plcB* are regulated by PrfA and whose gene products are responsible for Ped-2E9 cell membrane damage and cytotoxicity (Menon et al. 2003b; Bueno et al. 2010) Fourthly, F4244 Δ*inlA* and *lap*$^{-}$ mutant strains did not show a significant difference in cell death than that of the WT planktonic cultures,

suggesting the cytotoxicity reduction in biofilm-isolated bacteria was not affected by InlA or LAP (**Fig. 2.5a,b**). Finally, *L. innocua* F4248, a nonpathogenic strain, did not induce any cytotoxicity (**Fig. 2.5a,b**). In addition, using Caco-2 cells as a second model, I observed planktonic cultures of five WT *Lm* strains (F45, F4244, F40, F33 and 10403S) to induce a significantly more lactate dehydrogenase (LDH) release than the sessile cultures, suggesting that planktonic *Lm* cells are more cytotoxic than the sessile cells (**Fig. 2.5c)**. In sum, Ped-2E9 and Caco-2-based *in vitro* cytotoxicity data were consistent with the observation that biofilm-isolated bacteria have attenuated virulence compared to the planktonic bacteria on cultured cell lines.

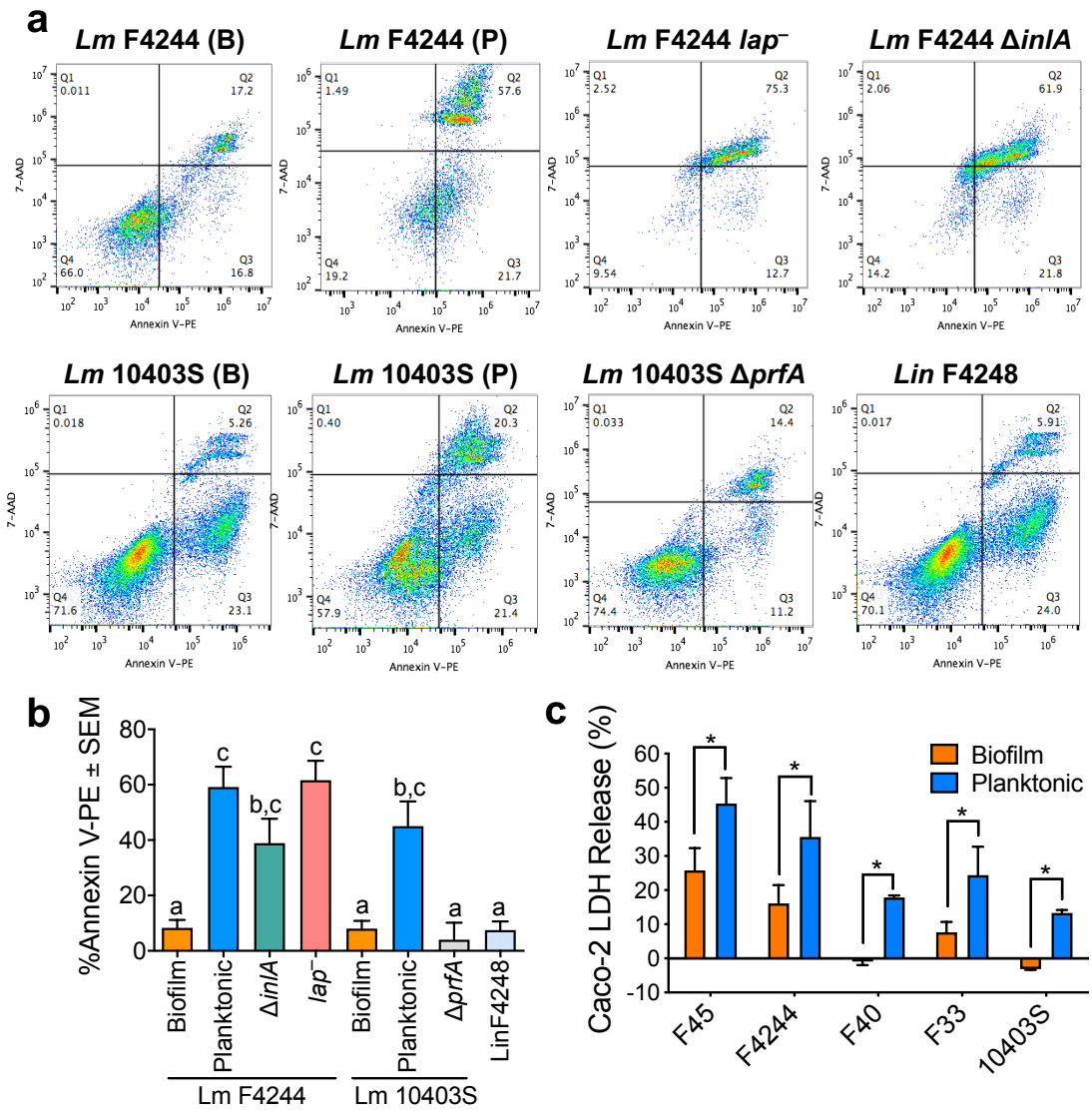

Figure 2.5. Cytotoxicity assessment of biofilm-forming sessile and planktonic *L. monocytogenes*. (a) Flow cytometric analysis of Ped-2E9 (B cell hybridoma) cells treated with biofilm-isolated (B) and planktonic (P) cells of *L. monocytogenes* (*Lm*) F4244 and 10403S and corresponding mutant strains at MOI of 10. Annexin V-PE positive and 7-AAD negative events (Q3) were identified as cells in the early phase of apoptosis. Events with both Annexin V-PE and 7-AAD positive (Q2) or both negative (Q4) were identified as dead or live cells, respectively. *L. innocua* (*Lin*) F4248 was also tested as a nonpathogenic negative control. (b) Quantitative comparison of overall damage of Ped-2E9 caused by bacteria. Each bar represents the percentage of Annexin V-PE positive events, which included early apoptosis (Q3) or dead (Q2) cells. Biofilm-isolated bacteria of both strains were significantly less cytotoxic than their planktonic counterparts. Bars marked with different letters are significantly different at $P < 0.05$. (c) Lactate dehydrogenase (LDH) released from Caco-2 cells (a colorectal adenocarcinoma) treated with both sessile or planktonic cells. Bacteria were incubated with cells at MOI of 10 at 37°C for 2 h. Data are the average of at least three independent experiments performed in triplicate. All error bars represent SEM. A pairwise student t-test was used for statistical analysis. *$P < 0.05$.

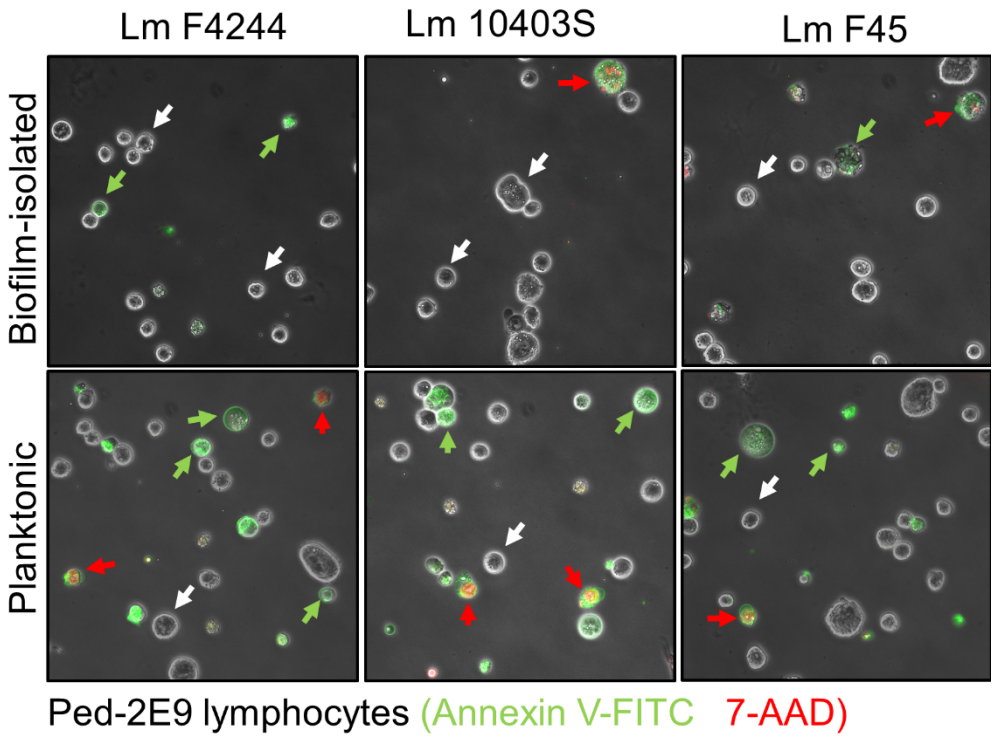

Figure 2.6. Representative merged fluorescence photomicrograph of Ped-2E9 cells showing pro-apoptotic and apoptotic cells. Live (white arrows) cells, early apoptotic (green arrows), or dead (red arrows) cells were observed after Annexin V-FITC and PI staining.

2.4.4 Key virulence factors were downregulated in biofilm-isolated bacteria on both transcription and translation levels

Next, to unravel the underlying reduced *in vitro* adhesion, invasion, translocation and cytotoxic phenotypes in sessile cells, I assessed the expression of mRNA and protein of key virulence factors using reverse transcriptional PCR and Western blot in two representative strains: F4244 (clinical) and F45 (food). Western blot data showed that in biofilm-isolated cells, LAP, and InlA levels were all downregulated in the whole cells (**Fig. 2.7a**). Proteins in bacterial cells could be asymmetrically distributed in cytosol and cell wall, and the virulence molecules expressed on cell surface are responsible for interacting with epithelial cells. Therefore, I specifically compared the amount of those proteins in different cellular fractions. In cell wall (CW) and intracellular (IC) fractions, the amount of InlA and LAP were all significantly reduced in biofilm-isolated cells compared to those in the planktonic cells (**Fig. 2.7b**). At the same time, biofilm-isolated cultures also secreted significantly ($P < 0.05$) lower LLO in the supernatant compared to the planktonic cultures for strains F4244 and F45 (**Fig. 2.7c**). As a control for the anti-LLO antibody, the

planktonic culture of 10403S showed a positive reaction with secreted LLO while an isogenic Δ*hly* strain was negative (**Fig. 2.7c**). The protein samples were standardized with Bicinchoninic acid assay method before loading onto the SDS-PAGE gel (**Fig. 2.8a**).

To quantify the transcription of the major virulence genes, I first generated the standard curves for each gene's copy number and Ct values and validated the specificity of qPCR primers. Standard curves for genes with copy numbers of approximately $10^1 – 10^9$ copy/μL and Ct values were generated with each qPCR primer sets (**Table 2.3**). All the standard curves had R^2 values greater than 0.99 and a similar slope between -3.04 and -3.40 (**Fig. 2.8b,c**). Besides, each primer pairs amplicon showed a sharp and single-peak melting curve (**Fig. 2.8d**) suggesting that the qPCR primers are suitable for quantifying the target genes.

The gene-specific mRNA expression analysis in F4244 and F45 strain showed dramatic downregulation of both *lap* and *inlA* (~95-99%) in biofilm-isolated cells than that of the planktonic cells while both regulatory genes, *prfA,* and *sigB*, were downregulated by about 25% in the biofilm-isolated cells, except for the *prfA* in F45 (**Fig. 2.7d**). Compared to planktonic F45 cells, the amount of *prfA* mRNA is almost similar in biofilm-isolated F45 cells (**Fig. 2.7d**). These data suggest that the attenuated adhesion, invasion, transepithelial translocation and cytotoxicity of biofilm-isolated *Lm* cells were possibly due to low expression of corresponding virulence genes at both mRNA and protein levels.

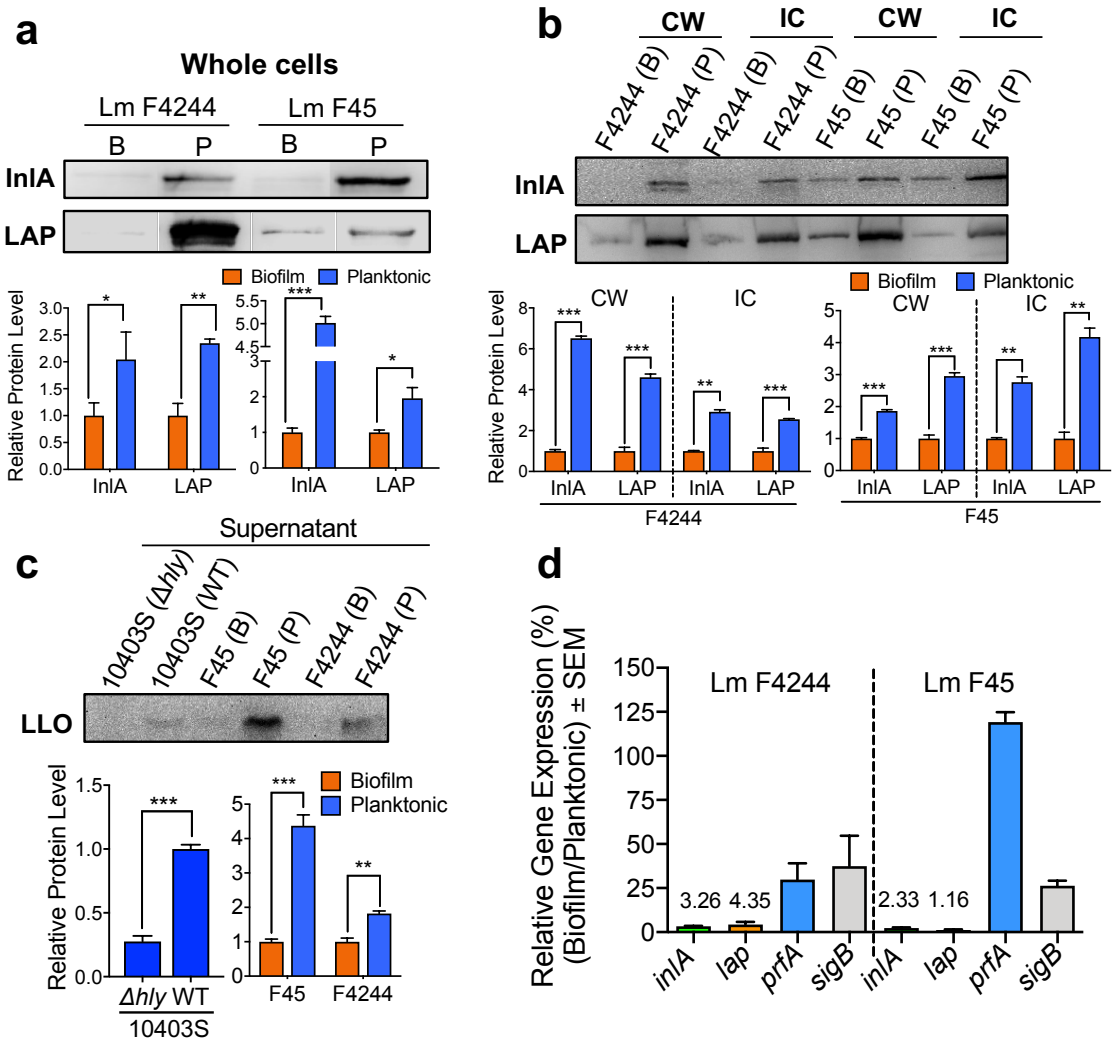

Figure 2.7. Comparison of virulence protein expression in biofilm-isolated (B) and planktonic (P) *L. monocytogenes* cells. (a and b) Immunoblot (top-panel) and densitometry (bottom panels) of InlA, LAP, and InlB in the whole cell (a), cell wall, and intracellular fractions (b) of biofilm-isolated and planktonic cultures of *Lm* F4244 and F45. Immunoblots are representative of three independent experiments. (c) Immunoblot of LLO in the secreted protein fraction of biofilm-isolated and planktonic *Lm* F4244 and F45. Immunoblots are representative of three independent experiments. (d) Relative mRNA expression of virulence genes (*inlA* and *lap*) and virulence regulators (*prfA* and *sigB*) in biofilm-isolated and planktonic cells of F4244 and F45 by RT-PCR. The student's t-test was used for statistical analysis. ***P < 0.0005; **P < 0.005; *P < 0.05.

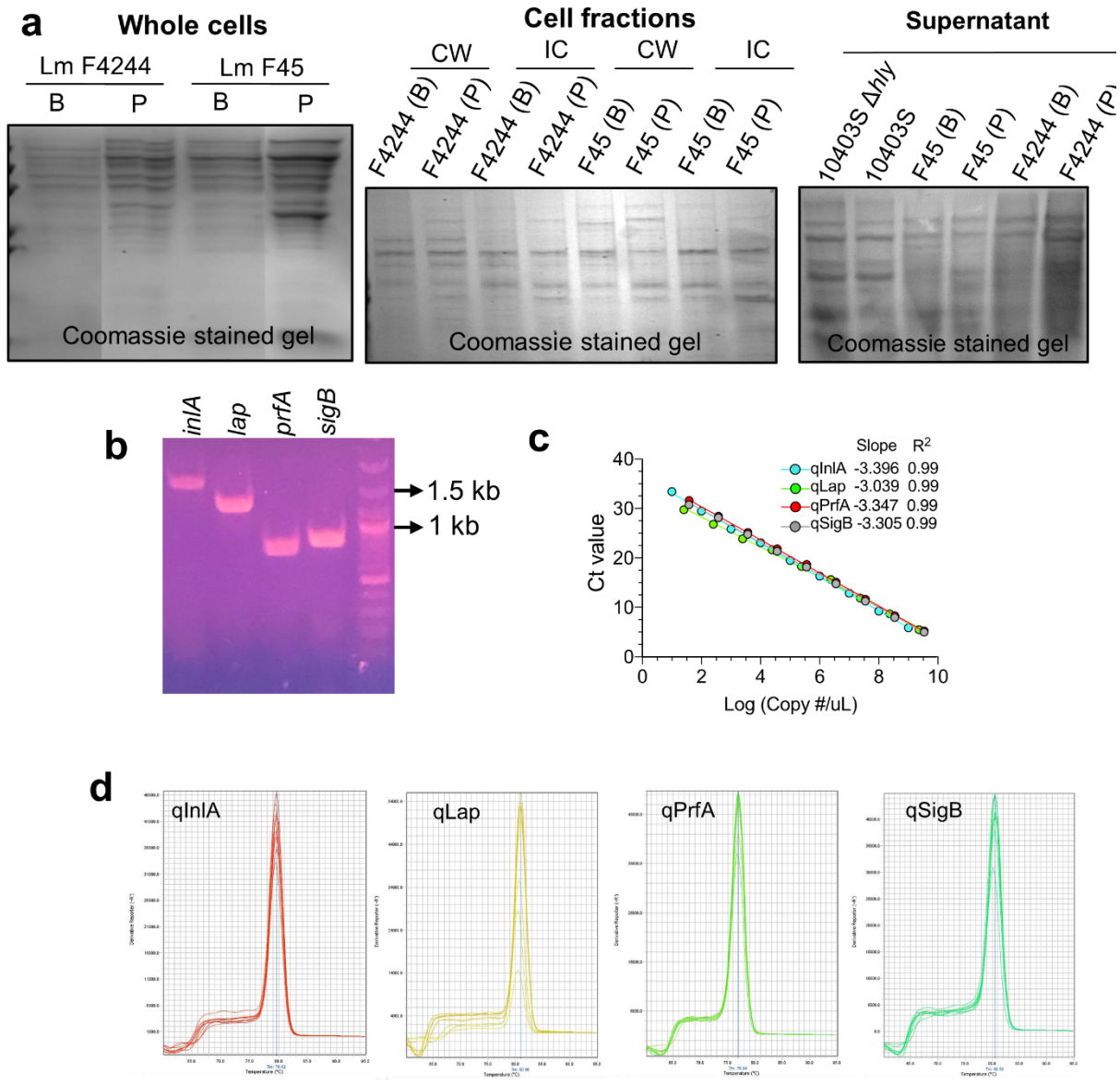

Figure 2.8. (a) Coomassie-stained gels loaded with the same protein samples used in Fig. 4a, 4b, and 4c, respectively. (b) Agarose gel showing PCR amplicons of gene *inlA* (1,436 bp), *lap* (1,136 bp), *prfA* (705 bp), and *sigB* (780 bp) that were extracted from the gel (Thermo Fisher Scientific) and used as templates for (c) qPCR standard curves. (d) Melting curves of respective qPCR amplicons.

2.4.5 In mouse bioassay, biofilm-isolated *Lm* showed reduced tissue burden at the early stage of infection (12-24 h), but similar to planktonic bacteria after 48 h post-infection

In vitro cell culture experiments suggest that biofilm-isolated *Lm* irrespective of food or clinical sources have a significantly lower capacity to adhere, invade and translocate across the intestinal epithelial cells and lower cytotoxicity on B-lymphocytes and Caco-2 cells than the planktonic bacteria. However, the actual virulence of *Lm* in these two physiological states (sessile vs planktonic) cannot be accurately compared without observing their pathogenicity *in vivo*. Therefore, I orally infected 8-10 weeks old male and female C57BL/6 mice with both biofilm-isolated or planktonic *Lm* strains representing clinical (F4244) and food (F45) isolates with 1×10^9 CFU/mouse and analyzed intestinal and extra-intestinal tissues for bacterial dissemination at 12, 24 and 48 h post-infection (hpi).

At 12 hpi, the bacterial burden in mice tissues was below the detection limit when a standard plating method was used. Therefore, I enriched the tissue samples in buffered *Listeria* enrichment broth (BLEB for 24 h) followed by isolation on the Modified Oxford (MOX) agar plate to determine the presence or absence of *Lm* in mice tissues. The select isolates were further verified by qPCR assay (**Table 2.4**). To test the sensitivity of the detection method, I inoculated *Lm* (F4244 or F45) at 1.4 ± 0.2 or 1.2 ± 0.2 CFU/mL BLEB, respectively and incubated at 37°C for 24 h. Aliquots (10 µl) of each culture was streaked on MOX plates, and colonies with the black center were further verified by PCR, suggesting the two-step selective enrichment combined with PCR can detect approximately 1 CFU/mL of *Lm* in BLEB (**Fig. 2.9**). None of the jejunal or ileal tissues of mice (n = 4-6) were positive for *Lm* after challenge with the sessile or planktonic cells (**Table 2.5**). However, only one of five (20%) cecum or colonic tissues were positive when mice were challenged with F4244 sessile cells compared to 50-100% positive when mice were challenged with the planktonic cells (**Table 2.5**). Likewise, no *Lm* cells were detected from the cecum and colon of mice when challenged with F45 sessile bacteria, whereas 80% (4/5) and 100% (5/5) were positive when challenged with planktonic bacteria, respectively (**Table 2.5**). Analysis of extra-intestinal organs/tissues; mesenteric lymph nodes (MLN), liver and spleen of mice revealed that all the animals (n = 5) receiving F4244 sessile cells were negative while 16-50% mice (n = 6) were positive when infected with the planktonic cells (**Table 2.5**). Similarly, all mice receiving F45 sessile cells were negative in extra-intestinal organs, while 20-60% mice were positive when receiving planktonic cells (**Table 2.5**). None of the blood or kidney samples were positive when

infected with either sessile or planktonic cells for both *Lm* strains at this early stage of infection. Nevertheless, these data indicate that bacterial intestinal invasion and subsequent systemic dissemination was lower for sessile cells than the planktonic cells for both *Lm* strains in mice after 12 hpi.

Table 2.4. Confirmation of mouse tissue/organ (12 hpi) for *L. monocytogenes* by qPCR

	Ct values, Biofilm-isolated *Lm* F4244										**Ct values, Planktonic *Lm* F4244**											
Mouse #	1		2		3		4		5		1		2		3		4		5		6	
Target gene	*inlA*	*prfA*	*inlA*	*prfA*	*inlA*	*prfA*	*inlA*	*prfA*	*inlA*	*prfA*	*inlA*	*prfA*	*inlA*	*prfA*	*inlA*	*prfA*	*inlA*	*prfA*	*inlA*	*prfA*	*inlA*	*prfA*
Jejunum	31 (-)	32 (-)	31 (-)	31 (-)	31 (-)	33 (-)	31 (-)	29 (-)	31 (-)	31 (-)	31 (-)	32 (-)	32 (-)	31 (-)	30 (-)	31 (-)	32 (-)	31 (-)	NT	NT	NT	NT
Ileum	33 (-)	32 (-)	31 (-)	32 (-)	30 (-)	32 (-)	31 (-)	32 (-)	32 (-)	31 (-)	33 (-)	32 (-)	31 (-)	31 (-)	32 (-)	30 (-)	29 (-)	32 (-)	NT	NT	NT	NT
Cecum	31 (-)	33 (-)	13 (+)	13 (+)	31 (-)	31 (-)	30 (-)	32 (-)	32 (-)	30 (-)	13 (+)	13 (+)	12 (+)	13 (+)	13 (+)	12 (+)	13 (+)	12 (+)	NT	NT	NT	NT
Colon	33 (-)	32 (-)	12 (+)	13 (+)	32 (-)	31 (-)	29 (-)	30 (-)	29 (-)	30 (-)	11 (+)	13 (+)	33 (-)	30 (-)	13 (+)	12 (+)	31 (-)	31 (-)	NT	NT	NT	NT
MLN	31 (-)	31 (-)	32 (-)	32 (-)	32 (-)	31 (-)	30 (-)	32 (-)	31 (-)	30 (-)	29 (-)	32 (-)	11 (+)	12 (+)	13 (+)	12 (+)	11 (+)	12 (+)	31 (-)	31 (-)	31 (-)	32 (-)
Spleen	31 (-)	32 (-)	31 (-)	31 (-)	31 (-)	32 (-)	32 (-)	29 (-)	32 (-)	32 (-)	31 (-)	32 (-)	31 (-)	29 (-)	12 (+)	13 (+)	32 (-)	30 (-)	31 (-)	32 (-)	31 (-)	31 (-)
Liver	32 (-)	32 (-)	30 (-)	31 (-)	30 (-)	31 (-)	30 (-)	29 (-)	31 (-)	30 (-)	12 (+)	13 (+)	31 (-)	29 (-)	31 (-)	31 (-)	30 (-)	32 (-)	11 (+)	12 (+)	13 (+)	13 (+)
Kidney	32 (-)	31 (-)	31 (-)	31 (-)	30 (-)	31 (-)	32 (-)	32 (-)	31 (-)	32 (-)	30 (-)	31 (-)	31 (-)	30 (-)	30 (-)	31 (-)	31 (-)	32 (-)	31 (-)	32 (-)	30 (-)	32 (-)

Table 2.4 continued

	Ct values, Biofilm-isolated *Lm* F45										**Ct values, planktonic *Lm* F45**									
Mouse #	1		2		3		4		5		1		2		3		4		5	
Target gene	*inlA*	*prfA*	*inlA*	*prfA*	*inlA*	*prfA*	*inlA*	*prfA*	*inlA*	*prfA*	*inlA*	*prfA*	*inlA*	*prfA*	*inlA*	*prfA*	*inlA*	*prfA*	*inlA*	*prfA*
Jejunum	29 (-)	28 (-)	30 (-)	31 (-)	30 (-)	30 (-)	29 (-)	30 (-)	29 (-)	30 (-)	30 (-)	31 (-)	32 (-)	30 (-)	29 (-)	30 (-)	31 (-)	30 (-)	31 (-)	30 (-)
Ileum	30 (-)	32 (-)	29 (-)	30 (-)	28 (-)	30 (-)	31 (-)	29 (-)	31 (-)	30 (-)	29 (-)	31 (-)	30 (-)	32 (-)	31 (-)	29 (-)	29 (-)	31 (-)	30 (-)	29 (-)
Cecum	30 (-)	29 (-)	31 (-)	32 (-)	30 (-)	31 (-)	28(-)	28(-)	30 (-)	29 (-)	17 (+)	19 (+)	31 (-)	30 (-)	19 (+)	14 (+)	19 (+)	19 (+)	15 (+)	16 (+)
Colon	29 (-)	29 (-)	32 (-)	29 (-)	31 (-)	31 (-)	32 (-)	29 (-)	31 (-)	31 (-)	15 (+)	15 (+)	18 (+)	18 (+)	16 (+)	16 (+)	15 (+)	14 (+)	11(+)	11(+)
MLN	32 (-)	31 (-)	32 (-)	30 (-)	30 (-)	31 (-)	31 (-)	32 (-)	30 (-)	30 (-)	29 (-)	30 (-)	16 (+)	17 (+)	29 (-)	30 (-)	28 (-)	30 (-)	14 (+)	15 (+)
Spleen	31 (-)	31 (-)	31 (-)	28 (-)	29 (-)	32 (-)	30 (-)	28 (-)	30 (-)	32 (-)	17 (+)	19 (+)	31 (-)	30 (-)	16 (+)	16 (+)	37 (-)	33 (-)	12 (+)	11 (+)
Liver	30 (-)	31 (-)	31 (-)	31 (-)	30 (-)	31 (-)	29 (-)	29 (-)	29 (-)	30 (-)	13 (+)	15 (+)	30 (-)	29 (-)	29 (-)	30 (-)	30 (-)	31 (-)	13 (+)	14 (+)
Kidney	31 (-)	31 (-)	30 (-)	30 (-)	31 (-)	30 (-)	31 (-)	31 (-)	31 (-)	30 (-)	33 (-)	31 (-)	32 (-)	33 (-)	29 (-)	31 (-)	31 (-)	31 (-)	30 (-)	31 (-)

	Ct values, Biofilm-isolated *Lm* F4244 InlA^m										**Ct values, planktonic *Lm* F4244 InlA^m**									
Mouse #	1		2		3		4		5		1		2		3		4		5	
Target gene	*inlA*	*prfA*	*inlA*	*prfA*	*inlA*	*prfA*	*inlA*	*prfA*	*inlA*	*prfA*	*inlA*	*prfA*	*inlA*	*prfA*	*inlA*	*prfA*	*inlA*	*prfA*	*inlA*	*prfA*
Jejunum	30 (-)	28 (-)	30 (-)	28 (-)	30 (-)	30 (-)	12 (+)	15 (+)	14 (+)	15 (+)	30 (-)	31 (-)	15 (+)	15 (+)	29 (-)	30 (-)	14 (+)	15 (+)	31 (-)	30 (-)
Ileum	28 (-)	28 (-)	29 (-)	29 (-)	29 (-)	30 (-)	31 (-)	30 (-)	30 (-)	30 (-)	31 (-)	30 (-)	15 (+)	14 (+)	31 (-)	29 (-)	29 (-)	31 (-)	15 (+)	16 (+)
Cecum	31 (-)	30 (-)	30 (-)	31 (-)	31 (-)	31 (-)	29 (-)	28 (-)	30 (-)	30 (-)	17 (+)	16 (+)	31 (-)	30 (-)	17 (+)	14 (+)	18 (+)	19 (+)	15 (+)	15 (+)
Colon	30 (-)	29 (-)	31 (-)	29 (-)	29 (-)	30 (-)	32 (-)	30 (-)	31 (-)	31 (-)	14 (+)	15 (+)	17 (+)	17 (+)	16 (+)	17 (+)	31 (-)	29 (-)	31 (-)	29 (-)
MLN	31 (-)	28 (-)	31 (-)	31 (-)	28 (-)	30 (-)	32 (-)	32 (-)	31 (-)	30 (-)	16 (+)	15 (+)	30 (-)	31 (-)	29 (-)	29 (-)	30 (-)	30 (-)	15 (+)	15 (+)

Table 2.4 continued

Spleen	32 (-)	32 (-)	30 (-)	32 (-)	32 (-)	32 (-)	30 (-)	30 (-)	30 (-)	31 (-)	14 (+)	15 (+)	30 (-)	30 (-)	15 (+)	15 (+)	32 (-)	32 (-)	13 (+)	13 (+)
Liver	30 (-)	28 (-)	30 (-)	31 (-)	31 (-)	31 (-)	29 (-)	29 (-)	30 (-)	30 (-)	31 (-)	29 (-)	13 (+)	13 (+)	14 (+)	15 (+)	16 (+)	16 (+)	29 (-)	32 (-)
Kidney	31 (-)	31 (-)	31 (-)	31 (-)	30 (-)	30 (-)	29 (-)	29 (-)	31 (-)	31 (-)	31 (-)	31 (-)	32 (-)	32 (-)	31 (-)	29 (-)	31 (-)	31 (-)	30 (-)	30 (-)
Mouse #	6		7		8		9				6		7		8		9			
Target gene	*inlA*	*prfA*	*inlA*	*prfA*	*inlA*	*prfA*	*inlA*	*prfA*			*inlA*	*prfA*	*inlA*	*prfA*	*inlA*	*prfA*	*inlA*	*prfA*		
Jejunum	29 (-)	28 (-)	15 (+)	15 (+)	30 (-)	30 (-)	29 (-)	30 (-)			16 (+)	16 (+)	16 (+)	15 (+)	30 (-)	30 (-)	14 (+)	14 (+)		
Ileum	31 (-)	31 (-)	33 (-)	30 (-)	15 (+)	14 (+)	30 (-)	29 (-)			31 (-)	32 (-)	29 (-)	29 (-)	29 (-)	31 (-)	30 (-)	29 (-)		
Cecum	30 (-)	31 (-)	31 (-)	32 (-)	15 (+)	16 (+)	30(-)	28(-)			13 (+)	14 (+)	14 (+)	14 (+)	29 (-)	31 (-)	29(-)	28(-)		
Colon	28 (-)	29 (-)	30 (-)	30 (-)	13 (+)	15 (+)	14 (+)	14 (+)			30 (-)	29 (-)	30 (-)	29 (-)	14 (+)	14 (+)	14 (+)	15 (+)		
MLN	32 (-)	32 (-)	32 (-)	30 (-)	31 (-)	31 (-)	32 (-)	31 (-)			30 (-)	31 (-)	31 (-)	30 (-)	30 (-)	30 (-)	31 (-)	30 (-)		
Spleen	31 (-)	31 (-)	31 (-)	31 (-)	30 (-)	32 (-)	30 (-)	30 (-)			14 (+)	15 (+)	15 (+)	15 (+)	30 (-)	30 (-)	31 (-)	31 (-)		
Liver	31 (-)	31 (-)	30 (-)	31 (-)	13 (+)	14 (+)	14 (+)	15 (+)			31 (-)	31 (-)	30 (-)	31 (-)	14 (+)	14 (+)	15 (+)	14 (+)		
Kidney	31 (-)	31 (-)	31 (-)	31 (-)	30 (-)	30 (-)	31 (-)	30 (-)			31 (-)	31 (-)	30 (-)	30 (-)	31 (-)	31 (-)	31 (-)	31 (-)		

*Each Ct value is the average of two replicate qPCR. +, positive; -, negative

Table 2.5. *Listeria monocytogenes* strains (F45, F4244, and F4244 InlA^{m}) translocation in C57BL/6 mice organs/tissues 12 h after oral infection.

Source	Tissues	Number of mouse tissues positive for *L. monocytogenes*/# mouse tested (%)[a]					
		F4244 (WT)		F45 (WT)		F4244 (InlA^{m})[b]	
		Biofilm	Planktonic	Biofilm	Planktonic	Biofilm	Planktonic
Intestinal	Jejunum	0/5 (0)	0/4 (0)	0/5 (0)	0/5 (0)	3/9 (33)	5/9 (56)
	Ileum	0/5 (0)	0/4 (0)	0/5 (0)	0/5 (0)	1/9 (11)	2/9 (22)
	Cecum	1/5 (20)	4/4 (100)	0/5 (0)	4/5 (80)	1/9 (11)	6/9 (67)
	Colon	1/5 (20)	2/4 (50)	0/5 (0)	5/5 (100)	2/9 (22)	5/9 (57)
Extra-Intestinal	MLN	0/5 (0)	3/6 (50)	0/5 (0)	2/5 (40)	0/9 (0)	2/9 (22)
	Liver	0/5 (0)	3/6 (50)	0/5 (0)	2/5 (40)	2/9 (22)	5/9 (56)
	Spleen	0/5 (0)	1/6 (16)	0/5 (0)	3/5 (60)	0/9 (0)	5/9 (56)
	Kidney	0/5 (0)	0/6 (0)	0/5 (0)	0/5 (0)	0/9 (0)	0/9 (0)

[a] Mice (both male and female) were orally gavaged with 1×10^{9} CFU/mouse. Mouse tissue samples were enriched in buffered *Listeria* enrichment broth for 24 h, plated on modified Oxford agar plate for 48 h, and 1-2 colonies per sample were verified by qPCR (see supplementary Table 2.3).
[b] These animals received streptomycin (5 mg/ml) in water for 32 h, followed by 16 h antibiotic-free water before oral gavage with *Lm*.

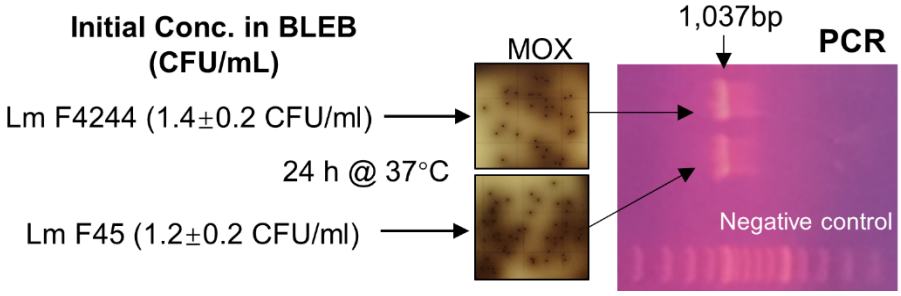

Figure 2.9. Verification of detection of low levels of *Lm*. *Lm* F4244 or F45 were inoculated into BLEB and incubated at 37°C for 24 h. The cultures were inoculated on MOX from where colonies with black centers were verified by PCR using primers targeting InlA (inlAm5 and inlAm3, see Table 2.3) as *Lm*.

At 24 hpi, I was able to enumerate *Lm* in most mice organs and tissues by a standard plating method. In the intestinal tissues, there were no significant differences in bacterial counts between sessile and planktonic cells-challenged mice with the exception of the cecum, where sessile cells had significantly ($P < 0.05$) higher colonization than the planktonic cells (**Fig. 2.10a-d**). However, in the extra-intestinal organs (MLN, spleen, and liver) planktonic cells exhibited significantly (*P*

< 0.05) higher bacterial burdens than the sessile cells (**Fig. 2.10e-g**). In fact, F4244 sessile cells were undetectable in these organs as determined by a plating method suggesting that the sessile cells were either unable or translocated and/or disseminated in blood/lymphatic circulation at levels that are below our detection limits at 24 hpi. In the kidney, counts for both sessile and planktonic cells were below the detection limit with the exception of one mouse, which was showing the planktonic burden of about two logs (**Fig. 2.10h**). Altogether, planktonic F4244 cell-challenged mice had significantly ($P < 0.005$) higher total *Lm* burden than the sessile cell-challenged mice in the extra-intestinal organs while there was no significant difference in total bacterial burden in whole intestinal tissues combined at 24 hpi (**Fig. 2.10i**). Likewise, total *Lm* burdens in the intestine and extraintestinal organs of mice challenged with sessile or planktonic cells of strain F45 are similar to F4244-challenged mice. I did not observe any significant difference in intestinal *Lm* counts for F45 strain; however, significantly ($P < 0.05$) more planktonic cells were found in extra-intestinal organs than the sessile cells (**Fig. 2.10j**). In particular, significantly ($P < 0.05$) more planktonic F45 than biofilm-isolated bacteria were detected in the cecum, but not in other sections of the intestine (jejunum, ileum and colon) (**Fig. 2.10a-e**). Whereas in the extraintestinal organs, infection by planktonic F45 resulted in significantly ($P < 0.05$) more *Lm* counts in MLN and spleen than in the liver (**Fig. 2.10e-g**). Furthermore, the presence of biofilm-isolated *Lm* in MLN of three mice and spleen of one mouse could not be detected even after culture enrichment followed by qPCR (**Fig. 2.10e,g**). Comparing the overall *Lm* burden in the intestine or extra-intestinal organs between F4244 (clinical isolate) and F45 (food isolate) indicates that F4244 had 1-2 log higher counts, hence it is more invasive than F45 in a mouse model of infection (**Fig. 2.10i,j**). These data further reveal that while biofilm-isolated cells are in the process of translocating through the intestinal tissues, planktonic *Lm* cells have already disseminated to the extra-intestinal sites at 24 hpi.

At 48 hpi, F4244 cell burden in both intestinal and extra-intestinal tissues for both sessile cell- and planktonic cell-challenged mice were alike (**Fig. 2.10a,b,d,e,h**) except for the cecum (**Fig. 2.10c**) and spleen (**Fig. 2.10f**) where planktonic counts were significantly ($P < 0.05$) higher than the sessile cells. Comparing the total bacterial burden in the whole intestine and extra-intestinal tissues, no significant difference in total bacterial burden in extra-intestinal tissues was observed between planktonic or sessile bacteria-challenged mice (**Fig. 2.10i**). Likewise, in F45 infected

mice, the burden of planktonic or sessile cells had no significant difference in all intestinal or extra-intestinal organs examined at 48 hpi (**Fig. 2.10a-j**).

Collectively these data demonstrate that the biofilm-isolated *Lm* has temporarily attenuated capacity to translocate across the gut barrier and/or to disseminate in the blood/lymphatic circulation during the early phase of infection (12-24 h), while both planktonic and biofilm-isolated *Lm* were able to disseminate to extra-intestinal tissues similarly at 48 hpi.

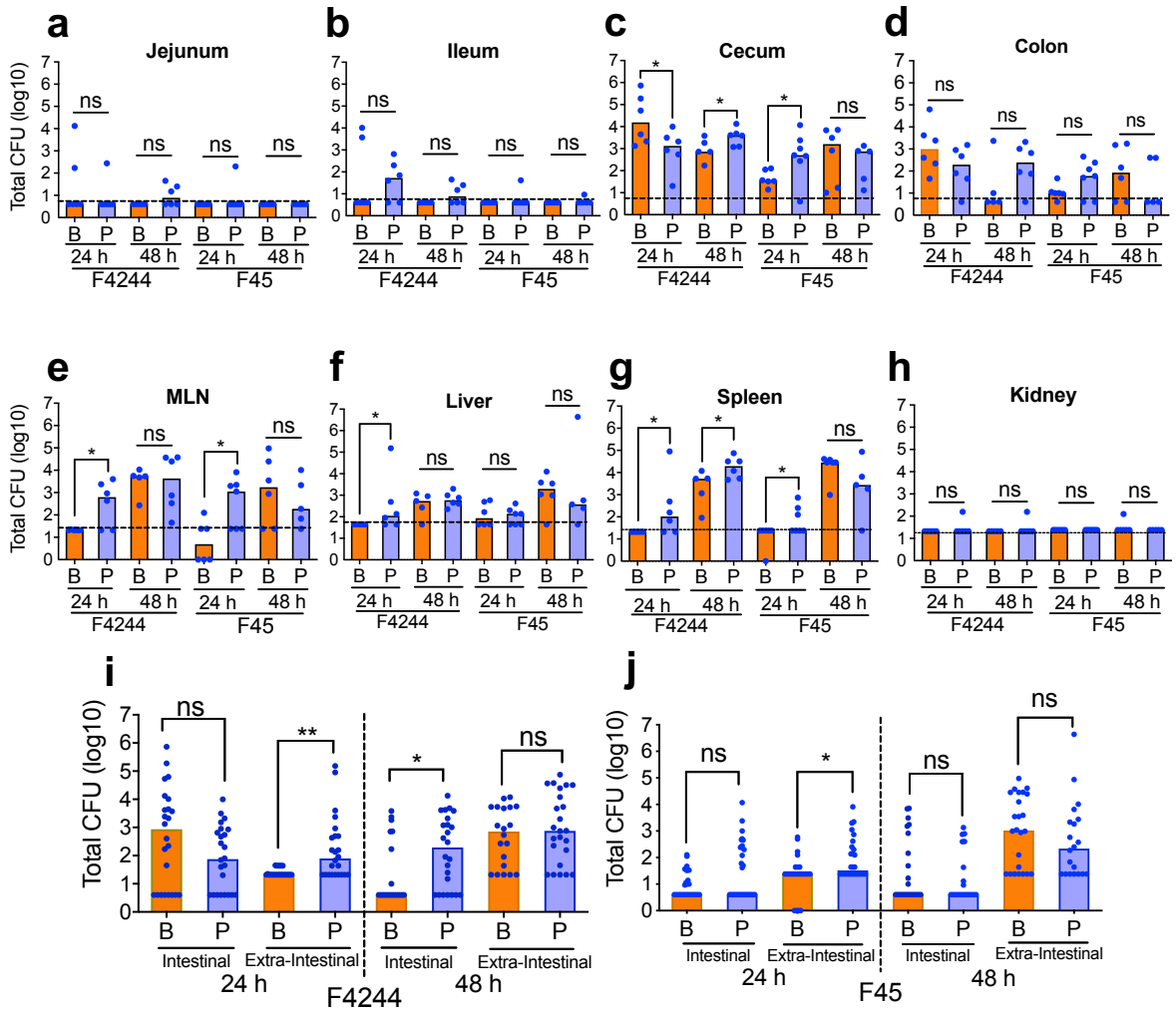

Figure 2.10. Mouse bioassay to compare the pathogenesis of biofilm-isolated sessile and planktonic *L. monocytogenes* cells. *Lm* burden in intestinal (a, b, c, and d) and extra-intestinal tissues (e, f, g, and h) after oral inoculation of mice (C57BL/6, male-female, 8-10 weeks old) with 1×10^9 CFU/mouse of sessile (B) and planktonic (P) cells of F4244 or F45 at 24 and 48 hpi. (i and j) Comparison of the number of bacteria in all intestinal and extra-intestinal tissues at 24 and 48 hpi. Bars represent the median values of each group (B or P). Dashed lines indicate detection limits by a plating method. Mann-Whitney test was used for statistical analysis. **P < 0.005; *P < 0.05

2.4.6 Histopathology shows the increased inflammatory response for planktonic cells than the sessile cells

At 24 hpi, histopathological analysis of planktonic F4244 infected intestinal tissues revealed more polymorphonuclear and mononuclear cells infiltrating villi in mice than the sessile bacteria-infected tissues (**Fig. 2.11a**). At the same time, an increased amount of single-cell necrosis and higher inflammation scores were observed in the liver and spleen of planktonic F4244 challenged mice, suggesting planktonic bacteria caused more inflammatory lesions in extra-intestinal organs than the sessile bacteria at 24 hpi (**Fig. 2.11a,b**). At 48 hpi, a similar inflammatory lesion was observed in both intestinal and extra-intestinal organs of mice challenged with either planktonic or sessile cells of F4244 (**Fig. 2.11a**). The sessile and planktonic cells of the F45 strain also showed similar results as F4244 but the overall inflammatory response was much lower than F4244 (**Fig. 2.12**). Overall inflammation scores showed that sessile bacteria caused much more lesions in the spleen and liver at 48 hpi compared to 24 hpi, which is consistent with the increased bacterial burdens in these organs (**Fig. 2.11**).

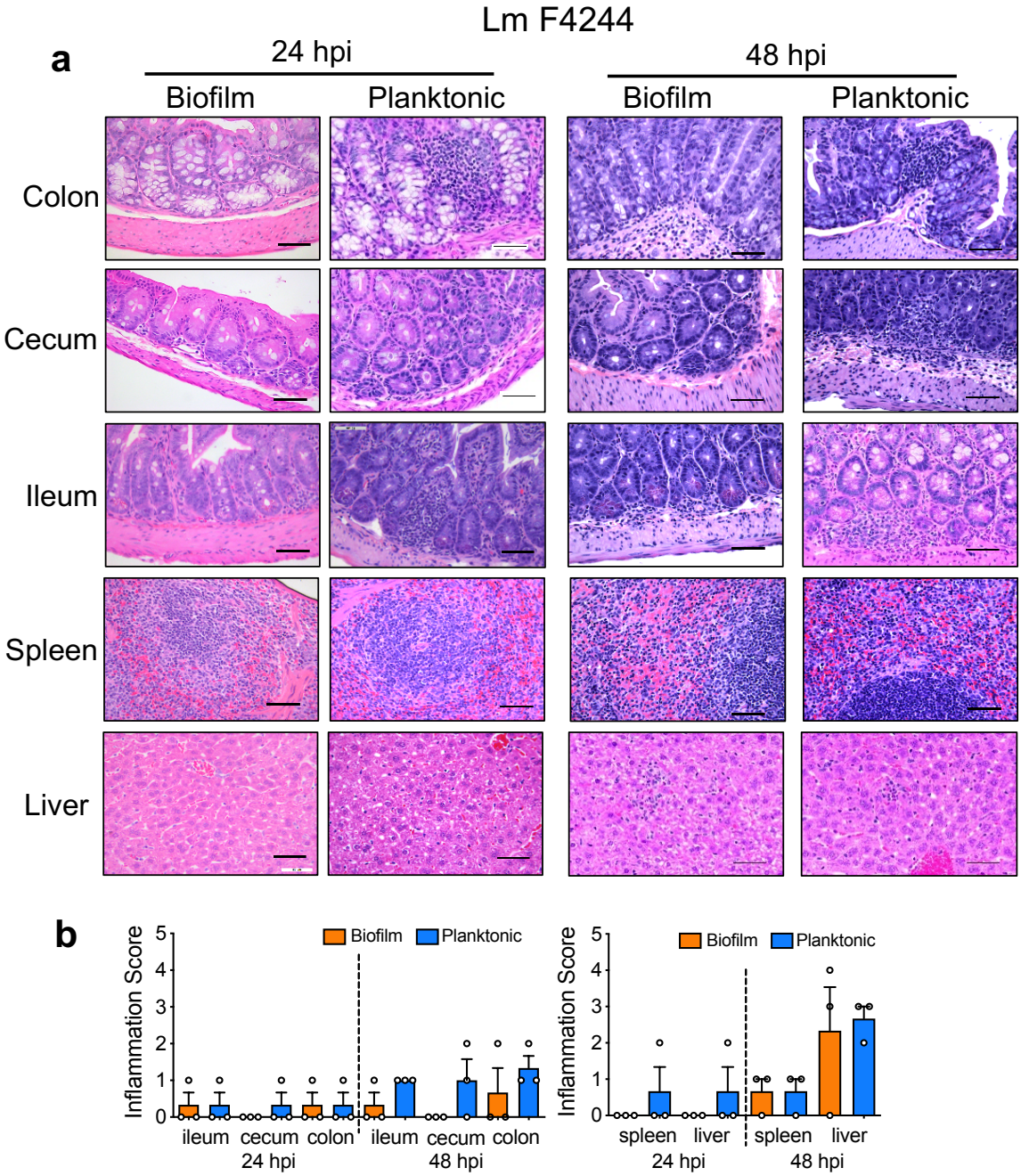

Figure 2.11. Histopathology analysis of mouse tissues for inflammation. Representative images of hematoxylin and eosin-stained tissue sections of mice challenged with 1×10^9 CFU of F4244 sessile (B) or planktonic (P) cells at 24 and 48 hpi (a) and a graph representing histopathological inflammation scores at 24 hpi (b, left panel) and 48 hpi (b, right panel). Scale bars represent 50 µm.

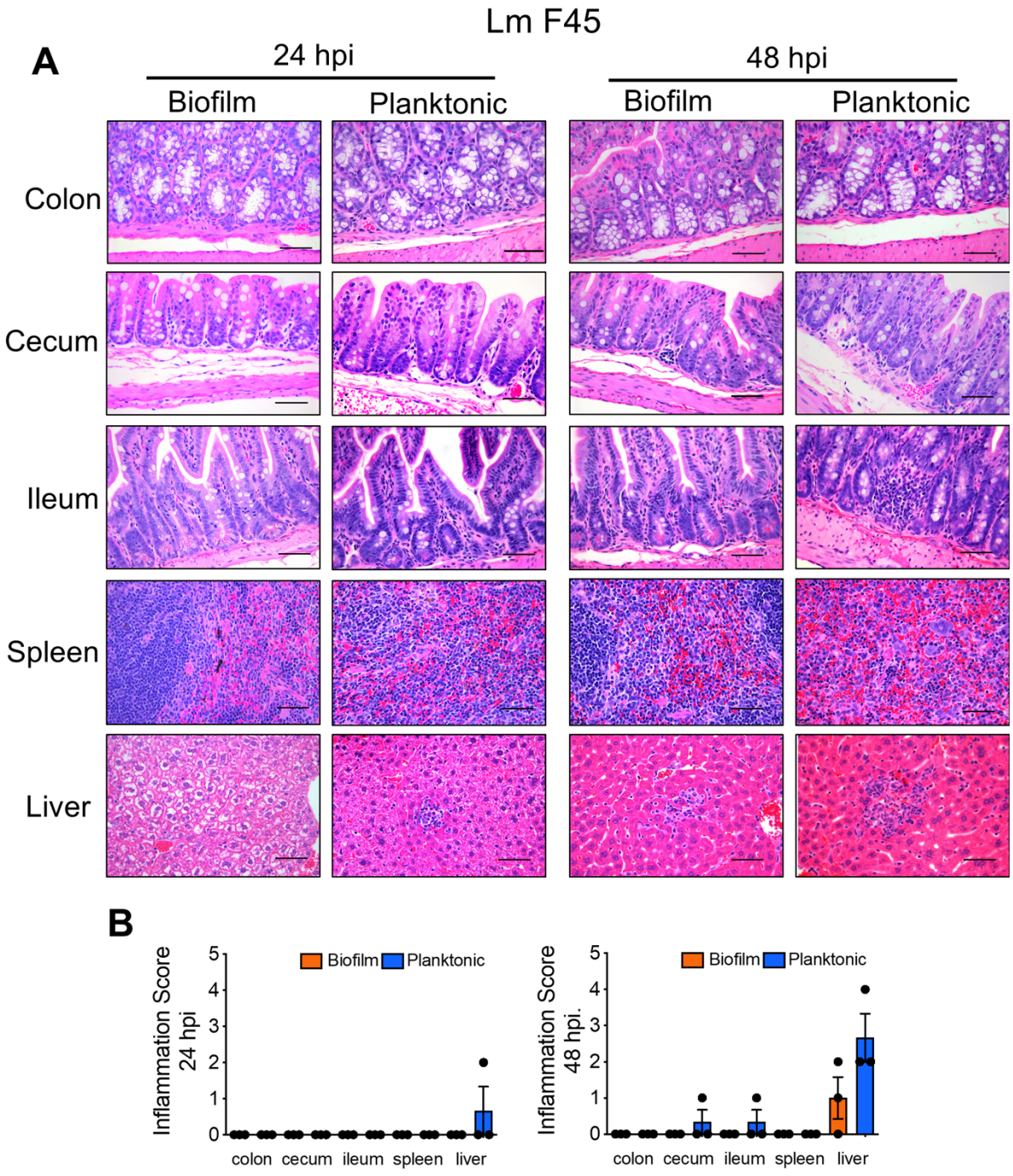

Figure 2.12. Representative images of hematoxylin and eosin-stained tissue sections of mice challenged with *Lm* F45 sessile (B) or planktonic (P) cells @ 1×10^9 CFU/mouse at 24 and 48 hpi (A) and a graph representing histopathological inflammation scores at 24 hpi (B, left panel) and 48 hpi (B, right panel). Scale bars represent 50 μm.

2.4.7 Sessile and planktonic *Lm* with murinized internalin A ($InlA^m$) showed similar pathogenicity and systemic dissemination as the wild type strain

To verify the role of InlA in *Lm* pathogenesis in biofilm-isolated sessile cells in the mouse model, I created murinized inlA ($InlA^m$) in F4244 by substituting two specific amino acids, S192N and Y369S (**Fig. 2.13**) (Wollert et al. 2007). The *inlA*^{m} gene sequencing (**Fig. 2.14a-d, Fig. 2.13a**), Western blotting (**Fig. 2.13b**) and ELISA (**Fig. 2.13c**) confirmed the expression of InlA in the $InlA^m$ strain. Besides, $InlA^m$ strain also showed significantly ($P < 0.05$) higher invasion into intestinal epithelial HCT-8 cells than the WT (F4244) strain (**Fig. 2.13d**) consistent with the results reported for Caco-2 cells (Wollert et al. 2007). In the mouse experiment, $InlA^m$ strain also showed significantly ($P < 0.05$) higher invasion of large intestinal tissues and translocation to the liver after 96 hpi compared to the WT strain (**Fig. 2.13e**) as observed before (Wollert et al. 2007).

We then examined adhesion and invasion of planktonic (P^M) and biofilm-forming sessile cells (B^M) of $InlA^m$ strain *in vitro*, and the planktonic cells showed significantly higher adhesion and invasion into HCT-8 cells than the sessile cells (**Fig. 2.13f**) similar to WT F4244 cells (**Fig. 2.2**). Next, aiming to observe increased invasion and *Lm* tissue burdens in the mouse model of infection, I pretreated the mice with streptomycin (5 mg/ml) for 32 h in drinking water(Louie et al. 2019) before oral challenge with sessile and planktonic $InlA^m$ strains at 1×10^9 CFU/mouse. The sensitivity of $InlA^m$ strain to streptomycin was tested before animal administration and was determined to be 2.5 µg/ml (**Fig. 2.14e**).

At 12 hpi, as before, *Lm* could not be enumerated by the plating method hence the tissue samples were tested for the presence or absence of *Lm*. In the intestinal tissue samples, only 11-33% of mice (n = 9) were positive when challenged with sessile cells while 22-67% of mice (n = 9) were positive for planktonic cells. In the extraintestinal tissues, sessile cells were isolated only from the liver of two mice (22%) while all other tissues (MLN & spleen) were negative. In contrast, 22-56% of mice were positive when challenged with planktonic cells (**Table 2.4**).

At 24 hpi, planktonic cells showed significantly ($P < 0.05$) higher invasion into the cecum and spleen than the sessile cells. While in the colon and liver there were no differences (**Fig. 2.13g**). These data further demonstrate that even though InlA-dependent invasion was restored in the mouse model, the sessile cells still showed delayed invasion and tissue distribution.

At 48 hpi, there was no statistical difference in planktonic and sessile cells of $InlA^m$ strain in the mouse intestinal and extraintestinal tissues (**Fig. 2.13h**). I also compared the tissue

distribution patterns of sessile and planktonic cells of both WT (data from Fig. 5) and InlA^{m} strain (data from Fig. 7h) at 48 hpi and no significant differences were observed between these two strains in the spleen and liver except for planktonic cells of InlA^{m} strain in the liver which showed higher ($P < 0.05$) invasion (**Fig. 2.13i**). Overall, these data show a consistent trend in tissue invasion for sessile and planktonic cells of InlA^{m} and the WT strain confirming the attenuation of translocation of biofilm-forming sessile cells during the early stage (12-24 h) of infection.

Figure 2.13. In mouse bioassay, biofilm-isolated and planktonic *L. monocytogenes* with murinized InlA ($InlA^m$) display differential tissue distribution. (a) PCR confirmation of the insertion of $inlA^m$ gene in the chromosome of *Lm* F4244 Δ*inlA* using primers inlA.up.5 and inlA.down.3 (Table 2.3). WT (F4244) was used as a positive control. (b) Immunoblots showing expression profile of InlA, and LAP in whole-cell extracts of WT, $inlA^m$ and Δ*inlA*. (c) ELISA showing the positive reaction of anti-InlA mAb to whole-cell preparation of WT, $inlA^m$ and reduced reaction with ΔinlA. (d) Percent invasion of WT, $inlA^m$ and ΔinlA to HCT-8 cells. Bars represent mean, and a pairwise student t-test was used for statistical analysis. (e) *Lm* WT, $inlA^m$ and ΔinlA strain burdens in the large intestine, MLN, spleen, and liver of mice (n=5-6) 96 h after oral challenge (5 x 10^9 CFU/mouse). Mann-Whitney test was used for statistical analysis. (f) Percent adhesion and invasion of biofilm-isolated and planktonic cells of InlAm strain to HCT-8 cells. Bars represent mean, and a pairwise student t-test was used for statistical analysis. (g and h) *Lm* burdens in tissues of mice (C57BL/6, male and female, 8-10 weeks old) challenged with murinized $InlA^m$ (1×10^9 CFU/mouse) strain of biofilm-isolated (BM) or planktonic (PM) cells at 24 (g) or 48 (h) hpi. Mice were pretreated with streptomycin (5 mg/ml) in drinking water for 32 h followed by 16 h in antibiotic-free water before the *Lm* challenge. (i) Comparison of tissue (spleen and liver) burden between WT and $InlA^m$ strain for biofilm-isolated (B^{WT} vs B^M) and planktonic (P^{WT} vs P^M) cells at 48 hpi. Data for WT was taken from Fig 5. Bars represent median values, and the Mann-Whitney test was used for statistical analysis in (e, g, h). ****$P < 0.0001$; ***$P < 0.0005$; **$P < 0.005$; *$P < 0.05$; ns, no significance.

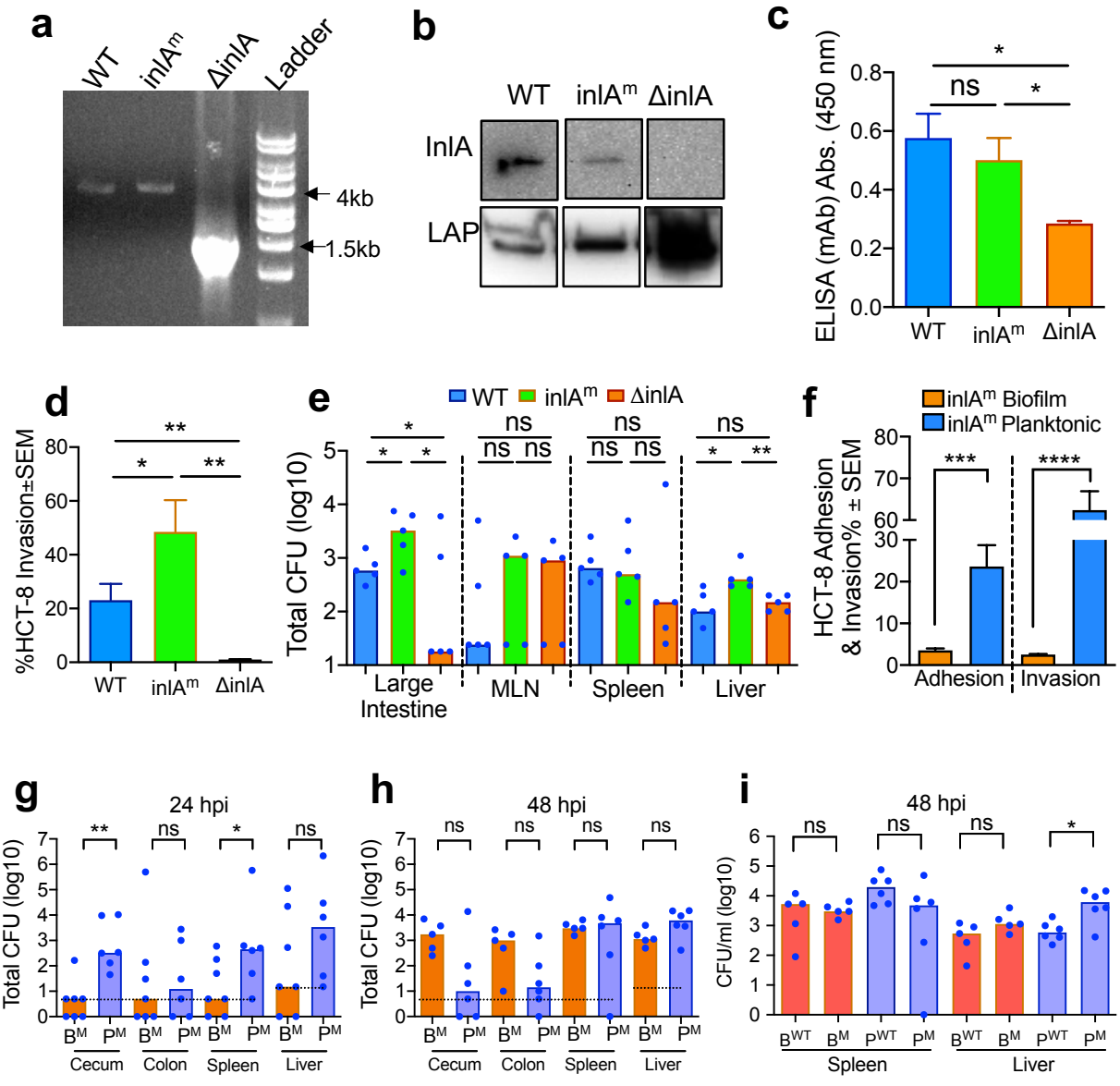
a
WT
inlA^m
ΔinlA
Ladder
4kb
1.5kb
b
WT
inlA^m
ΔinlA
InlA
LAP
c
ELISA (mAb) Abs. (450 nm)
ns
WT
inlA^m
ΔinlA
d
%HCT-8 Invasion±SEM
WT
inlA^m
ΔinlA
e
WT
inlA^m
ΔinlA
Total CFU (log10)
Large Intestine
MLN
Spleen
Liver
f
inlA^m Biofilm
inlA^m Planktonic
HCT-8 Adhesion & Invasion% ± SEM
Adhesion
Invasion
g
24 hpi
Total CFU (log10)
Cecum
Colon
Spleen
Liver
h
48 hpi
Total CFU (log10)
Cecum
Colon
Spleen
Liver
i
48 hpi
CFU/ml (log10)
Spleen
Liver

Figure 2.14. The molecular approach in generating *Lm* F4244 expressing InlA^{m}. (a) Schematic showing the construction of inlA^{m} knock-in fragment. Segment ii (yellow), located between nucleotide 494 and 1485 of *Lm* F4244 *inlA* ORF and contains three mutated nucleotides (green), was synthesized by GenScript and amplified using primers inlAm5 and inlAm3 (Table 3). The mutations resulted in the substitution of amino acids 192 and 369 of InlA from S and Y to N and S, respectively. A XapI cutting site was created after the mutation and used for rapid identification. Segment i, the upstream (gray) and beginning regions (blue) of *inlA* ORF, was amplified using WT *Lm* F4244 gDNA as templates and primers inlA.up.5 and inA.up.3 (Table 2.3). Segment ii, the ending (blue) and downstream (gray) region, was amplified with primers inlA.down.5 and inlA.down.3 (Table 2.3). The three segments were mixed and used as the template to amplify the complete knock-in fragment with NcoI and SalI sites added to 5' and 3' ends, respectively, using primers inlA.up.5 and inlA.down.3. The knock-in fragment was ligated into pHoss1 and electroporated into *Lm* F4244 Δ*inlA* to insert *inlA^{m}* gene in the chromosome. (b) Schematic showing the selection of chromosomal *inlA*^{m} knock-in mutant through two-step homologous recombination. (c) Confirmation of mutation in nucleotide sequence (boxed areas, arrows) by Sanger sequencing using four primers of two directions. Red and gray arrows represent the four sequencing results of *inlA^{m}* and sequence of WT. SnapGene program was used to generate this schematic. (bottom) Nucleotides marked with green represent the mutation site in *inlA^{m}* gene. (d) Confirmation of nucleotide sequence showing a mutation in *inlA^{m}* gene. (e) Analysis of the sensitivity of *Lm* F4244 *InlA^{m}* and 10403S (as reference strain) to streptomycin and tetracycline (as control). Two-hundred microliter BHI containing approx. 1×10^{6} CFU/mL of *Lm* 10403S or InlA^{m} in 96-well microtiter plates were added with serial diluted streptomycin (0.25-1,000 μg/mL) or tetracycline (0.0025-10 μg/mL) and incubated at 37°C for 48 h. Bacterial growth was measured using a microtiter plate reader. *Lm* 10403S was able to grow in 1,000 μg/mL streptomycin (black arrow) while *Lm* F4244 InlA^{m} can grow 1 μg/mL (red arrow), suggesting InlA^{m} is significantly more sensitive to streptomycin than *Lm* 10403S. Meanwhile, the same strains were sensitive to tetracycline when used as a control.

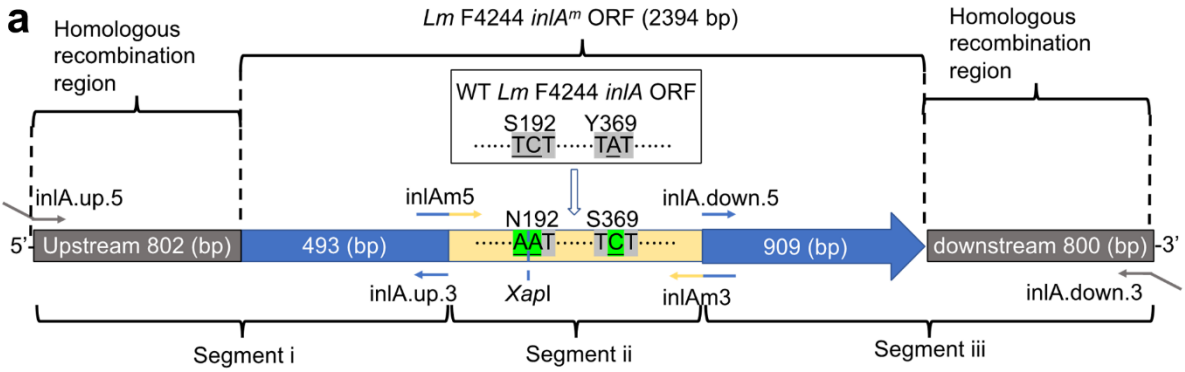

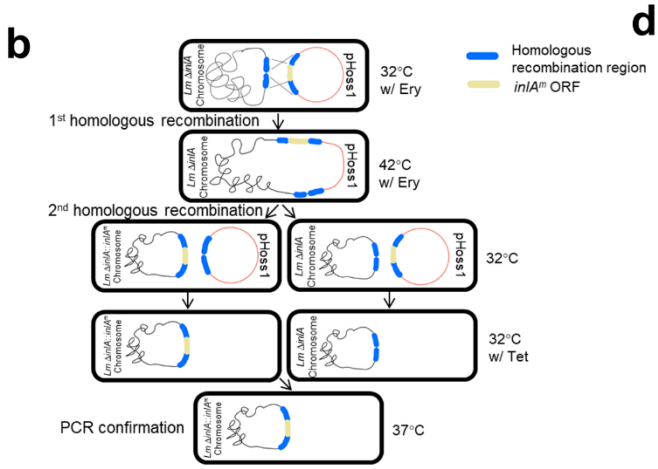

d

(538)AGTGCGCTTTCAGGTTTAACTAGTCTAC
AGCAATTAAATTTTGGTAATCAAGTGACAGAT
TTAAAACCATTAGCTAATTTAACAACACTAGA
ACGACTAGATATTTCAAGTAATAAGGTGTCG
GATATTAGTGTTCTGGCTAAATTAACCAATTT
AGAAAGTCTTATCGCTACTAACAACCAAATAA
GTGATATAACTCCACTTGGGATTTTAACAAAT
TTGGACGAATTATCCTTAAATGGTAACCAGTT
AAAAGATATAGGCACATTGGCGAGTTTAACA
AACCTTACAGATTTAGATTTAGCAAATAACCA
AATTAGTAATCTAGCACCACTGTCGGGTCTA
ACAAAACTAACTGAGTTAAAACTGGGAGCTA
ACCAAATAAGTAACATCAGTCCCCTAGCTGG
TCTAACCGCCCTCACTAACTTAGAGCTAAAT
GAAAATCAGTTAGAAGATATTAGCCCAATTTC
TAACTTGAAAAATCTCACATATTTAACGTTGT
ACTTTAATAATATAAGTGATATAAGCCCAGTT
TCTAGTTTAACAAAGCTTCAAAGATTATTTTT
CTCTAATAACAAGGTAAGTGACGTAAGCTCG
CT(1136)

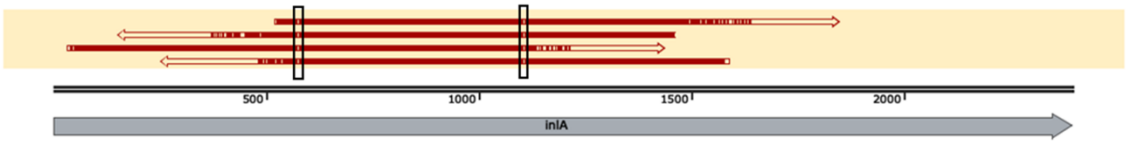

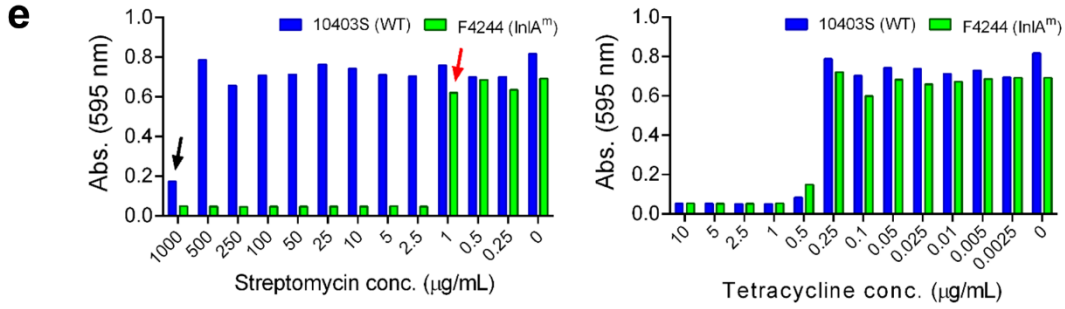

2.4.8 LAP and InlA expression were significantly upregulated in planktonic cells than the sessile cells after exposure to simulated gastrointestinal fluids for 13 h

In vivo data revealed late dissemination of sessile cells to extra-intestinal tissues, therefore, I hypothesized that the sessile cells are either more susceptible to intestinal conditions than that of the planktonic cells or the intestinal condition may suppress the expression of key virulence factors in sessile cells. To verify the first event, I tested the survivability of both biofilm-isolated and planktonic *Lm* cells exposed to simulated gastric fluid (SGF) and simulated intestinal fluid (SIF). Both sessile and planktonic cell viability was decreased by about three logs after 60 min of exposure to SGF and there was no significant difference in cell viability between the two (**Fig. 2.15a**). I then examined the adhesion, invasion, and translocation properties of these bacterial cells through Caco-2 cells and analyzed the expression of LAP and InlA proteins. Interestingly, SGF and SIF-exposed sessile cells of both F4244 and F45 strains showed significantly increased adhesion, invasion, and transepithelial translocation through Caco-2 cells compared to the sessile cells that are not exposed to simulated gastrointestinal fluids (**Fig. 2.15b-d**). These results further indicate that exposure to gastrointestinal conditions increased virulence attributes in *Lm* sessile cells. In contrast, planktonic cells showed mixed results showing slightly decreased or the same levels of adhesion, invasion, and translocation with or without exposure to SGF and SIF (**Fig. 2.15b-d**). Overall, planktonic cells displayed significantly higher adhesion, invasion and translocation than that of the sessile cells thus supporting the hypothesis that virulence of planktonic bacteria is significantly higher in the gastrointestinal environment than the sessile bacteria at the very early (12-24 h) stage of infection (**Fig. 2.15c,d**).

Immunoblot analysis confirmed a significant increase (2-3 fold) in the expression of LAP and InlA in sessile cells in both F4244 and F45 strains after exposure to SGF and SIF (**Fig. 2.15e,f**). Furthermore, significantly increased expression of these proteins was also observed in planktonic cells of the F4244 strain but not in the F45 strain. Overall, the expression of these proteins was significantly higher in planktonic cells than in the sessile cells in F4244 strains (**Fig. 2.15f**). Taken together, these data show that overall reduced expression of LAP and InlA in sessile cells relative to the protein expression by planktonic cells may be responsible for decreased adhesion, invasion, and transepithelial migration during the very early stage (12-24 h) of infection.

To validate the hypothesis that sessile cells upregulate virulence genes after oral infection, I quantified the transcriptional expression of virulence genes in sessile $InlA^m$ cells from mice

intestinal chymus 12 and 48 hpi and compared them with the expression in the same cells before infection. I observed a 5-fold higher *inlA* expression in $InlA^m$ at both 12 hpi and 48 hpi compared to that of control ($InlA^m$ cells before infection) (**Fig. 2.15g**). Interestingly *lap* expression was 250-fold and 70-fold higher at 12 hpi and 48 hpi, respectively (**Fig. 2.15g**). The *sigB* expression was 10-fold higher at 12 hpi and maintained at a similar level at 48 hpi (**Fig. 2.15g**). In contrast, *prfA* expression remained unchanged at 12 hpi, and it was below the detection limit at 48 hpi (**Fig. 2.15g**). These data indicate that the delayed invasion of sessile cells in mice at 24 hpi was possibly because of their lower expression of virulence factors, LAP and InlA, than their planktonic counterparts. Besides, the intestinal environment positively upregulates *lap* and *inlA* expression in sessile cells in the intestine, which could allow the sessile cells to be as invasive as planktonic cells at 48 hpi.

Figure 2.15. Survival and virulence of biofilm-isolated and planktonic *L. monocytogenes* strain suspended in simulated gastrointestinal fluid. (a) Survival of sessile and planktonic *Lm* F4244 and F45 after sequential exposure to simulated gastric fluid (SGF, pH 2) for 1 h and simulated intestinal fluid (SIF, pH7) for 12 h. (b, c, and d) Comparison of adhesion (b), invasion (c) and translocation (d) rates on Caco-2 cells of SGF (pH 3) and SIF (pH7)-treated biofilm-isolated and planktonic *Lm* F4244 and F45. (e and f) Immunoblot showing LAP and InlA expression in sessile and planktonic cells after exposure to SGF (pH 3) and SIF (pH7). Immunoblots are representative of three independent experiments. (g) Relative mRNA expression of virulence genes (*inlA* and *lap*) and virulence regulators (*prfA* and *sigB*) in biofilm-isolated InlAm from mice intestinal chymus at 12 or 48 hpi and the same cells before infection using RT-PCR. A pairwise student t-test was used for statistical analysis. ***$P < 0.0005$; **$P < 0.005$; *$P < 0.05$.

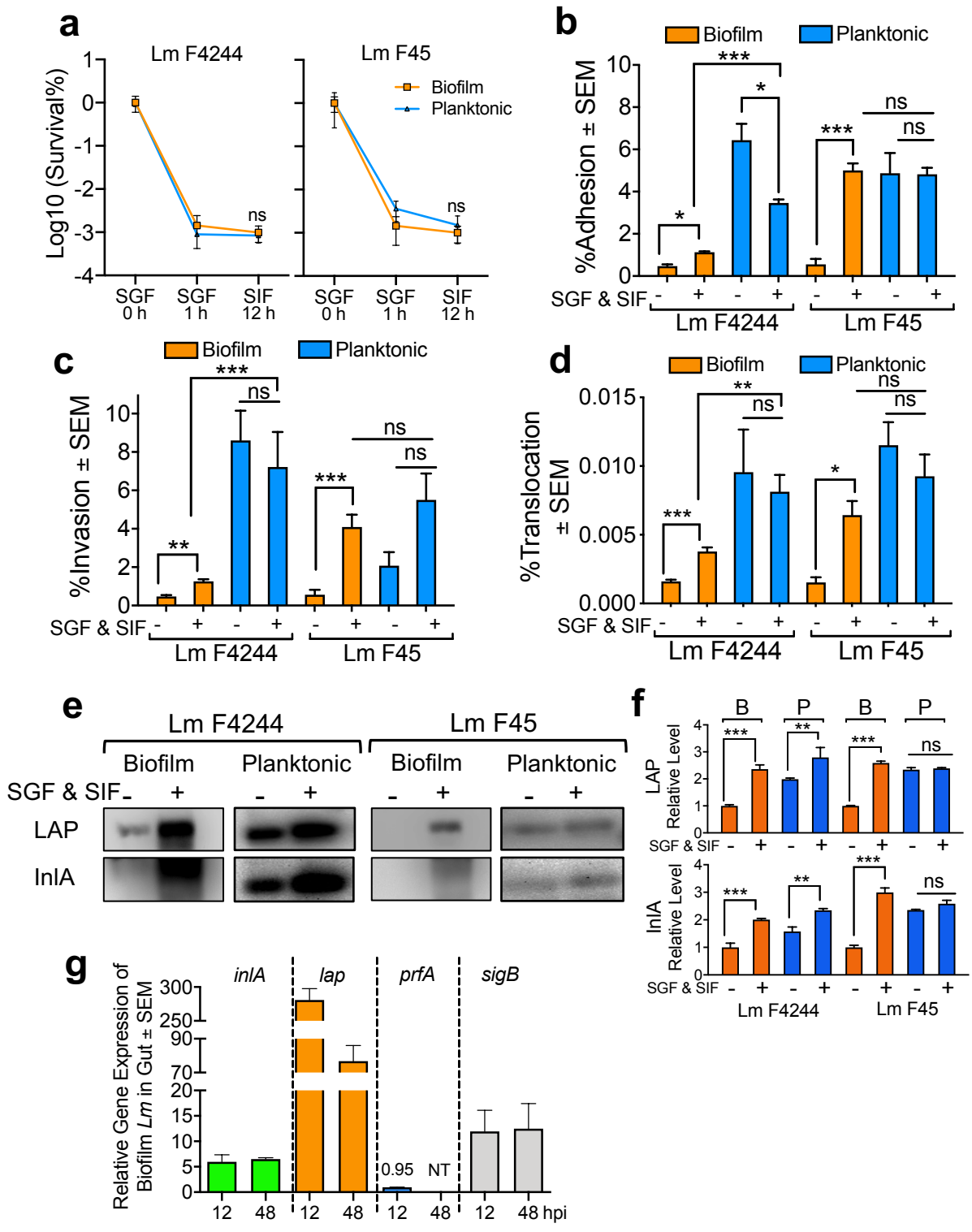
a
Lm F4244
Lm F45
Biofilm
Planktonic
Log10 (Survival%)
SGF 0 h
SGF 1 h
SIF 12 h
ns
b
%Adhesion ± SEM
SGF & SIF
Lm F4244
Lm F45
c
%Invasion ± SEM
d
%Translocation ± SEM
e
LAP
InlA
f
LAP Relative Level
InlA Relative Level
B
P
g
Relative Gene Expression of Biofilm Lm in Gut ± SEM
inlA
lap
prfA
sigB
0.95
NT
12
48
48 hpi

2.5 Discussion

The biofilm-forming ability gives *Lm* the advantage of persistence even for many years on various surfaces in a food processing/production environment, which presumably serves as a primary source for food contamination (Moltz and Martin 2005; Ferreira et al. 2014; Yaron and Romling 2014; Galié et al. 2018). *Lm* has been routinely isolated from meat and dairy(Charlton et al. 1990) processing plants. The persistence of pathogens on the abiotic surface is facilitated by their ability to form a biofilm, in which cells experience a wide range of stress thus show physiological and genetic heterogeneity allowing them to be more resistant to antimicrobials, and to survive in limited nutrient and oxygen tensions(Stewart and Franklin 2008; Renier et al. 2011; Luo et al. 2013). Although several studies have reported reduced expression of virulence genes in sessile cells, the pathogenic potential of these cells hasn't been tested using either *in vitro* or *in vivo* models. Therefore, I studied the virulence of biofilm-isolated sessile cells of *Lm* using both cell culture and animal models, and the expression of virulence genes to support the observed phenotype, especially between 12 - 48 hpi.

The biofilm-forming capability of over 100 *Lm* strains was screened and all formed biofilms of varying degrees on a polystyrene surface; and food isolates in general, had significantly higher biofilm-forming capacity than the clinical isolates (**Fig. 2.1**). These observations agree with the previous studies (Borucki et al. 2003; Renier et al. 2011; Barbosa et al. 2013). Among the different serotypes examined, isolates of serovar ½a and ½c (Lineage II) are stronger biofilm formers than the isolates of ½b and 4b (Lineage I), which are in accordance with another study (Borucki et al. 2003). I also observed that many strains were weak biofilm-former and their persistence on surfaces may be doubtful; however, studies have demonstrated that mixed-species biofilms possibly facilitate the persistence of such weak biofilm-forming pathogens (Carpentier and Chassaing 2004; Pan et al. 2009).

Biofilm–forming cells experience stress and exhibit physiological and genetic heterogeneity (Stewart and Franklin 2008), thus I were curious about their dynamics of infectivity in cell culture and mouse models. Five *Lm* strains of food and clinical origins representing the major outbreak causing serotypes with diverse biofilm-forming phenotypes were selected for *in vitro* cell culture experiments. All biofilm-isolated cells I tested irrespective of food or clinical origins were less adhesive, invasive and cytotoxic and showed reduced ability to traverse across the Caco-2 epithelial barrier than the planktonic cells suggesting these cells are less virulent compared to the

planktonic cells (**Figs. 2.3** and **2.5**). I analyzed the expression of key virulence proteins (LAP, InlA and LLO) that are responsible for *Lm* invasion, paracellular translocation, and intracellular persistence. I observed significantly reduced expression of these proteins in sessile cells at the transcriptional and translational levels (**Figs. 2.5** and **2.7**), which may explain the reason for reduced virulence of sessile cells in *in vitro* cell culture experiment. However, the contribution of other virulence factors including ActA cannot be ignored. ActA, a PrfA and SigB regulated protein known to contribute to biofilm formation and intestinal colonization (Tiensuu et al. 2013; Travier et al. 2013b) may also be affected in sessile cells for the delayed invasion and tissue distribution in mice. Furthermore, reduced *inlA* expression in sessile cells is in agreement with others who also observed similar reduced InlA expression in biofilm-isolated cells(Mata et al. 2015; Gilmartin et al. 2016). Besides, mRNA of gene *sigB*, coding a stress response regulator, was also downregulated to around 25% in sessile cells of both *Lm* strains compared to their planktonic counterparts (**Fig. 2.7**). SigB has been implicated in *Lm* biofilm formation (van der Veen and Abee 2010) and it also regulates InlA expression (McGann et al. 2007). The observed suppression of SigB and consequent InlA expression in sessile cells possibly is responsible for reduced *Lm* adhesion and invasion into the intestinal epithelial cells, which was further supported by a proteomic analysis that indicated downregulation of SigB-regulated proteins (Mata et al. 2015).

Interestingly, *prfA* mRNA in *Lm* F45, a strong biofilm-former, was expressed at a similar level for both sessile and in planktonic cells; however, its level was down-regulated by 25% in *Lm* F4244 (a moderate biofilm-former) sessile cells than that of the planktonic cells (**Fig. 2.7**). These observations differ from a previous study where PrfA is reported to positively regulate biofilm formation(Lemon et al. 2010) and a strain (*Lm*10403S) overexpressing *prfA* showed higher biofilm-forming ability than the WT. Our data further imply that PrfA-regulated biofilm formation may vary from strain to strain which requires further investigation. Although PrfA is a key regulator for the expression of multiple virulence factors including InlA (Scortti et al. 2007), our qRT-PCR results further suggest that decreased expression of *inlA* in sessile cells is not always coupled with decreased expression of *prfA* (**Figs. 2.5** and **2.7**) since InlA can be expressed independently of PrfA regulation (Lingnau et al. 1995).

To confirm *in vitro* cell culture results in a mouse model, I challenged mice orally with 48 h-old sessile cells or 24 h-old planktonic cells of moderate biofilm-forming clinical strain (F4244) and a strong biofilm-forming food isolated strain (F45). At 12-24 hpi in mice, sessile cell burden

in intestinal and extra-intestinal tissues was undetectable or very low while the planktonic burden was significantly high and infectivity was comparable to the *in vitro* cell culture data indicating sessile cells are less invasive. However, at 48 hpi, burdens of both sessile and planktonic cells in mouse tissues were comparable suggesting that sessile cells are equally invasive as planktonic cells after the early stage (12 – 24 hpi) of the gastrointestinal phase of infection; however, the rate of bacterial tissue distribution and disease progression was variable (**Figs. 2.10** and **2.11**). To explain such discrepancy in intestinal epithelial cell invasion in the early stage (12-24 hpi) of infection, I hypothesized that possibly sessile cells are highly susceptible to antimicrobials present in intestinal fluids or expression of adhesion and invasion-related proteins are suppressed in intestinal fluids. Therefore, I examined survival and protein expression in sessile cells suspended in SGF (pH 3) and SIF (pH 7.0) that contain HCl, enzymes and bile salts (Mathipa and Thantsha 2015). In SGF+SIF, I did not observe any significant difference in *Lm* viability between sessile and planktonic cells but observed differential expressions of LAP and InlA, the two key virulence factors that are responsible for *Lm* translocation across the gut epithelial barrier (Nikitas et al. 2011; Drolia et al. 2018; Drolia and Bhunia 2019). Though the expression of both LAP and InlA were significantly upregulated in sessile cells in SGF and SIF, overall expression in planktonic cells was significantly higher than the sessile cells (**Fig. 2.15e**). These findings suggest that the gastrointestinal environment may help the sessile cells to quickly transition to a fully virulent state and may also explain the observed similar intestinal and extra-intestinal tissue burdens for both biofilm and planktonic cells at 48 hpi.

Our hypothesis is also supported by the observation that *inlA* and *lap* mRNA in sessile cells were upregulated after they arrive in the mouse intestine for 12 h (**Fig. 2.15g**). However, the expression of *inlA* mRNA maintained at a similar level and the expression of *lap* even decreased at 48 hpi (**Fig. 2.15g**), suggesting the expression of the virulence genes may not continue to increase with increasing residence time in the intestine. During this period, expression of regulatory genes, *prfA* was unaffected while the *sigB* level increased several-fold consistent with a previous report which showed SigB-mediated upregulation of several virulence genes, including *inlA*, is critical for *Lm* to switch global transcription from saprophytism to virulence while residing in the intestine (Toledo-Arana et al. 2009). This study further reinforces the importance of *sigB* in virulence gene expression in sessile cells during the intestinal phase of infection. Although the gastrointestinal environment is known to upregulate both LAP (Santiago et al. 1999; Jaradat and

Bhunia 2002; Burkholder et al. 2009) and InlA expression (Sue et al. 2004; Mata et al. 2015; Gilmartin et al. 2016), here, I provide evidence for the expression of these two proteins in biofilm-isolated cells.

In mice, InlA-mediated transcytosis is absent due to a lack of interaction between InlA and its cognate receptor, E-cadherin (Lecuit et al. 1999a), thus LAP-mediated *Lm* translocation is considered the predominant gut-barrier crossing mechanism in mice during the early (12-24 h) stage of infection (Drolia et al. 2018; Drolia and Bhunia 2019; Drolia et al. 2020). Hence, the observed reduction in LAP expression in sessile cells is considered a major contributory factor towards impaired *Lm* translocation in the intestinal and extra-intestinal tissues early in the infection process (12-24 h) (**Fig. 2.10**).

To further investigate the role of InlA in sessile cell infection in the mouse model, I generated $InlA^m$ strain (Wollert et al. 2007) and the intestinal and extra-intestinal tissue distribution of sessile and planktonic cells of $InlA^m$, surprisingly followed the same trend as the WT strain at 12, 24 and 48 hpi (**Table 2.4, Fig. 2.13**). The $InlA^m$ strain still did not show increased tissue distribution of either sessile or planktonic cells at 48 hpi compared to the WT. This result was expected since previous studies have shown that differential tissue distribution of $InlA^m$ and WT strains occur only after 72-96 h infection in mice (Wollert et al. 2007; Monk et al. 2010) and this was again verified in our study (**Fig. 2.13e**).

Furthermore, this experiment was conducted with mice that were even pretreated with streptomycin for 32 h in the drinking water to disrupt resident microflora (Becattini et al. 2017) and I still did not observe increased tissue distribution of either sessile or planktonic cells of $InlA^m$ strain at 48 hpi compared to the WT (**Fig. 2.13i**). The failure to observe increased tissue distribution is believed to be due to increased sensitivity of F4244 strain to streptomycin (MIC, 2.5 μg/ml) (**Fig. 2.14e**) used in the drinking water thus possibly affected its survival and tissue distribution. On the other hand, the previous study (Becattini et al. 2017), used the 10403S strain which is highly resistant to streptomycin (~1 mg/ml) (**Fig. 2.14e**), thus ensuring its survival and increased tissue dissemination (2-4 log) in the animal pretreated with streptomycin. To study bacterial invasiveness in an antibiotic-pretreated animal model, it is imperative to use a pathogen that is resistant to the same antibiotic used for microbiota disruption. For example, van der Waaij et al (van der Waaij et al. 1972) demonstrated that the dissemination and persistence of infectious *E. coli* in mice was facilitated only when the bacterium is resistant to the pre-exposed antibiotics.

Similarly, Hentges et al (Hentges et al. 1985) reported that the burdens of clindamycin sensitive *Pseudomonas aeruginosa* in MLN and liver of clindamycin-treated mice were lower than the burdens in untreated mice. Further experiments may be necessary to validate the antibiotic effect of our *Lm* strain (F4244) invasion by using a streptomycin-resistant strain which I plan to investigate in the future.

LLO is an important virulence factor required for *Lm* persistence during intracellular lifestyle (Schnupf and Portnoy 2007) and is also responsible for epithelial and lymphocyte apoptosis (Rogers et al. 1996; Bhunia and Feng 1999b; Menon et al. 2003a; Gray et al. 2005). In addition, LLO has been implicated to aid *Lm* dissemination from the gastrointestinal tract to extra-intestinal tissues (Roll and Czuprynski 1990). In this study, I observed reduced LLO expression in sessile cells (**Figs. 2.5** and **2.7**), which agrees with one study (Mata et al. 2015), but contradicts with another (Arevalos-Sánchez et al. 2012), where researchers report that biofilm formation does not affect bacterial ability to produce LLO. Interestingly, in another pathogen (*Bacillus cereus*), researchers (Arevalos-Sánchez et al. 2012) observed reduced expression of Hemolysin BL and other enterotoxins (CytK and EntC) in biofilm cells and consequently reduced cytotoxicity on both HeLa and MDA cells (Caro-Astorga et al. 2020). Collectively, these data imply that impaired toxin synthesis in biofilm cells affects bacterial virulence.

In summary, our data indicate that sessile cells are less invasive in cultured cell lines and during the early stage (12-24 h) of infection in an animal model possibly due to reduced expression of regulatory proteins (PrfA and SigB) and virulence factors (LAP, InlA, and LLO). However, both sessile and the planktonic cells showed similar extra-intestinal tissue burdens at 48 hpi and sessile cells are equally infective as planktonic cells but the dynamics of infection may vary between sessile and planktonic cells with possible differential disease onset or incubation period. Furthermore, *in vitro* cell culture experiment routinely used for virulence potential determination was found to be unreliable for assessing the pathogenic potential of biofilm-forming cells because it measures the pathogenic event over a short period (1-2 h). On the other hand, an animal model provides comprehensive pathogenic events over a prolonged period in physiologically relevant conditions and thus, is most reliable for studying the pathogenesis of biofilm-isolated cells.

CHAPTER 3. INACTIVATION OF MULTI-PATHOGEN BIOFILMS USING FOOD-GRADE NANOPARTICLE-CONJUGATED ANTIMICROBIALS

3.1 Abstract

Capacities of foodborne pathogens to form a mixed culture biofilm help their persistence in the food processing environment and consequent repeated product contamination. Inactivation and eradication of biofilms from food processing environments are achieved by using harsh disinfectants, but their toxicity and environmentally hostile characteristics make them undesirable. This study aims to use food-grade natural antimicrobials to control mixed-culture biofilms. I used chitosan, a natural antimicrobial biopolymer (polysaccharide) from crustaceans and derivatized it to produce chitosan nanoparticles (ChNP) for improved accessibility of biofilm architecture and as a carrier for other active molecules. ChNP was conjugated to another broad-spectrum antimicrobial agent, ε-poly-L-lysine (PL) and the ChNP-PL activity was tested against mixed-culture biofilms. ChNP-PL dimension was estimated to be around 100 nm and it exhibited a synergistic antimicrobial and anti-biofilm effect against five foodborne pathogens, including *Listeria monocytogenes*, *Staphylococcus aureus*, *Salmonella enterica* serovar Enteritidis, *Escherichia coli* O157:H7 and *Pseudomonas aeruginosa*. ChNP-PL, not only prevented the biofilm formation but also inactivated pre-formed biofilms when analyzed by crystal violet staining and plate counting. *In vitro* mammalian cell-based cytotoxicity analysis (LDH and WST-based assay) indicated ChNP-PL to be non-toxic. In conclusion, our results show ChNP-PL has strong potential to prevent the formation or inactivation of preformed polymicrobial biofilms of foodborne pathogens in the food processing environment.

3.2 Introduction

A major public health concern for the food industry is foodborne illnesses and the associated recalls of food products leading to loss of food and economic burden. To prevent foodborne disease outbreaks, the US government has passed the Food Safety Modernization Act (FSMA) in 2011 which emphasizes critical preventive measures through five broad focus areas: Prevention, Inspection and Compliance, Response, Imports, and Enhanced partnership. One key

element is science-based preventive control across the food supply chain. Intervention strategies to eliminate or reduce pathogen load in food processing environments and on products is an integral step for implementing FSMA.

Globally, foodborne pathogens are responsible for two billion illnesses and over one million deaths annually (Kirk et al. 2015), while in the US, about 48 million illnesses, 128,000 hospitalizations, and 3,000 deaths happen annually with an estimated economic burden of about 78 billion dollars (Scallan et al. 2011; Scharff 2012). The top five foodborne pathogens responsible for most fatalities include *Listeria monocytogenes, Salmonella enterica*, *Toxoplasma gondii*, Norovirus, and *Campylobacter* spp. In the US, *L. monocytogenes* alone is responsible for nearly 1,600 illnesses, and 250 deaths each year (Scallan et al. 2011). Numerous *Listeria* fatal outbreaks were associated with ready-to-eat meat, dairy, fish, and fruits and vegetables (Silk et al. 2012). *S. enterica* can cause severe gastrointestinal diseases and is a major foodborne pathogen of concern (Hendriksen et al. 2011) and is responsible for about 1 million illnesses and 378 (12.6%) deaths annually in the US (Scallan et al. 2011; Jackson et al. 2013). *S. enterica* is frequently transmitted through poultry products (Vandeplas et al. 2010) or products containing raw eggs, unpasteurized milk, beef, nuts, sprouted seeds, fruits, and unpasteurized fruit juices. Shiga-toxin producing *Escherichia coli* (STEC) strains are regarded as serious foodborne pathogens, and meat is the common source for *E. coli* O157:H7, a major STEC serovar (Mathusa et al. 2010). In addition, ice cream, milk, sprouts, lettuce, and cucumber are also involved in the outbreak. Although STEC O157 is the most widely recognized, other serogroups including O26, O45, O103, O111, O121 and O145 have been increasingly implicated in cases of foodborne human diseases (Mathusa et al. 2010; Valilis et al. 2018).

The persistence of pathogens in food processing facilities has been treated as the single most critical factor in product contamination (Ferreira et al. 2014; Wang 2019). Persistence is facilitated by biofilm formation (Carpentier and Cerf 2011). In a sessile physiological state, pathogens tend to form biofilms that is more recalcitrant to antimicrobials compared to the suspension or planktonic cells (Bonsaglia et al. 2014). From raw or undercooked food materials, pathogens find a harborage site or niche in food production facilities or product surfaces and form biofilms (Srey et al. 2013), which then serves as a source for foodborne outbreaks especially in cafeterias, hospitals, cruise ships, and commercial food processing facilities (Hall-Stoodley et al. 2004).

Biofilm formation is common strategy of bacteria to survive in nature when they encounter a solid surface in an effort to compete efficiently with other microbial cells for space and nutrients, and to resist any unfavorable environmental conditions (Flemming and Wingender 2010). Bacteria produce an extracellular polymeric substance (EPS) forming a three-dimensional biofilm scaffold on solid surfaces in the development of biofilms (Flemming and Wingender 2010). Biofilms can be comprised of single or mixed bacterial species. On solid surfaces, microbial attachment and biofilm formation provide significant protection to the cells living in the structure against desiccation, resistance to antibiotics or biocides (sanitizers), ultraviolet radiation, metallic cations, and physical removal of the cells by washing and cleaning.

Biofilm formation is comprised of several stages: (i) attachment, (ii) microcolony formation, (iii) maturation, and (iv) detachment or dispersion. In a biofilm, microorganisms express fimbriae, curli, flagella, adhesion proteins, and capsules to firmly attach to the surface (Flemming and Wingender 2010). The cells grow in close proximity and cell-to-cell communication (quorum sensing) occurs through the production of autoinducers such as N-acyl homoserine lactone or other molecules, which also regulate gene expression for survival, growth, cell density, resistance to antimicrobials, and tolerance to desiccation. As the microcolony continues to grow, cells accumulate forming a matured biofilm with three-dimensional scaffolds. Loose cells are then sloughed off from the matured biofilm and are converted into planktonic cells, which attach to a new surface preconditioned by food particles or substrates, completing the life cycle of a biofilm. The cells from biofilms become a continuous source for food contamination during food preparation.

Therefore, suitable intervention methods must be applied to develop anti-biofilm agents for food processing environments with food-compatible technologies. Chemical sanitizers are routinely used, but their toxicity to the handlers, potential residue in finished products, and environmentally hostile characteristics make them not a perfect solution to all application (Simões et al. 2010). Thus, alternative food-grade safe approaches are routinely being investigated. Chitosan, a natural biopolymer from crustaceans (shrimp, crab), is a polysaccharide, and has shown no negative health effects; therefore it has been proposed as an effective alternative bioactive polymer in the food industry (Rampino et al. 2013). It is a polycationic polymer (from about 10,000 to 1 million kDa) and possesses broad-spectrum antimicrobial effect at certain

molecular and in a different configuration, such as nanoparticles and films, against both Gram-positive and Gram-negative bacteria (Tsai et al. 2004; Luo and Wang 2013; Yang et al. 2016).

Chitosan is an inexpensive, nontoxic polycationic natural biopolymer industrially produced by alkaline (40-50% NaOH) deacetylation of chitin from shrimp and crab shells (Rabea et al. 2003). It is a technologically important and ubiquitous polysaccharide biopolymer and contains more than 5000 glucosamine units (*N*-acetyl glucosamine polymer). Previous studies have reported that binding of chitosan to cell wall teichoic acids, follwed with a potential extraction of membrane lipids (mainly lipoteichoic acid) leading to bacterial inactivation (Raafat and Sahl 2009). The antimicrobial effect of chitosan nanoparticles (ChNP) has been studied on *Streptococcus mutans* biofilm, where low molecular weight chitosan nanoparticles were more effective than the high molecular weight nanoparticles as an antibacterial agent (Chavez de Paz et al. 2011).

Nanoparticles with an overall dimension of <100 nm are shown to have characteristics that are desirable for the delivery of antimicrobial agents, drugs, functional bioactive molecules in the field of medicine, agriculture and food (Luo and Wang 2013). Though the antimicrobial activity of ChNP against certain bacterial species is reported (Mu et al. 2014; Fang et al. 2015), their effectiveness against pre-formed biofilms or prevention of biofilms of mixed culture foodborne pathogens is not known. Furthermore, I also explored, if the antibiofilm activity of ChNP could be augmented with the addition of another broad-spectrum food-grade antimicrobial peptide, such as ε-poly-L-lysine (Ye et al. 2013).

ε-Poly-L-lysine (PL) is water-soluble, biodegradable, edible, and nontoxic homo-poly-amino acids (25 - 35 lysine residues, 2.85-3.98 kDa), characterized by the peptide bond between the carboxyl and ε-amino groups of L-lysine (Yoshida and Nagasawa 2003). It is produced by *Streptomyces albulus* and inhibitory against both Gram-positive and Gram-negative bacteria, yeast and fungi (Hyldgaard et al. 2014). PL has been generally recognized as safe (GRAS) by the FDA at levels of up to 50 mg/kg in food (GRAS No. 000135). A recent study showed that the combination of both chitosan and PL as a coating on Pacific white shrimp is more effective than using each separately in extending the shelf life (Na et al. 2018). Besides, another study also found applying the combination of ChNP and nisin can effectively inhibit the white blush of fresh-cut carrots (Song et al. 2017).

However, the effectiveness of ChNP with PL conjugates on inactivation of multi-pathogen biofilms is not known thus it was investigated in this study. Data show ChNP-PL with an average

dimension of 100 nm showed synergistic antimicrobial effect against polymicrobial biofilms of *Listeria monocytogenes*, *Staphylococcus aureus*, *Salmonella enterica* serovar Enteritidis, *Escherichia coli* O157:H7 and *Pseudomonas aeruginosa*.

3.3 Materials and Methods

3.3.1 Bacterial and mammalian cell lines used in this study

Bacteria used in this study are listed in **Table 3.1**. Before experiments, bacteria were inoculated in Tryptic Soybean Broth supplemented with 0.6% yeast extract (TSBYE) from glycerol frozen stocks in -80°C and incubated at 37°C for overnight. A human ileocecal cell line, HCT-8 (ATCC), was used for assessing cytotoxicity of antimicrobial components. HCT-8 cells were recovered from frozen stocks in liquid nitrogen and seeded in T-25 flasks (TPP, Switzerland) with high glucose DMEM (HyClone, Logan, UT) supplemented with 10% (v/v) fetal bovine serum (Atlanta Biologicals). Cells were kept at 37°C with 7% CO_2 and 95% relative humidity. Medium in the T-25 flasks was changed for every three day until about 95% confluence, then the cell monolayers were trypsinized, counted, and seeded in microtiter plates for experiments.

3.3.2 Synthesis of chitosan nanoparticles (ChNP) and nanoconjugates of chitosan and ε-poly-L-lysine (ChNP-PL)

Chitosan (0.1% or 1 mg/mL) (low molecular weight, Sigma-Aldrich) dissolved in an aqueous solution of acetic acid (1% v/v) in deionized (DI) water was adjusted to pH 4.6 with NaOH and stored in an autoclaved glass bottle at 4°C. Solution of 1 mg/mL sodium tripolyphosphate (TPP) (Fisher Chemical) in DI water was also added with 1% acetic acid, adjusted to pH 4.6, filter sterilized through a 0.22 µm nitrocellulose filter membrane (Fisherbrand) and stored in the same conditions as chitosan solution. ChNP was synthesized using the ionic gelation method (de Paz et al. 2011; Joseph et al. 2018) with modifications. The chitosan solution (15 mL) and a magnetic stir bar were added into a sterile petri dish which was placed on a magnetic stirrer (Thermolyne Cimarec) operating at speed level 8. TPP solution (5 mL) was added into the petri dish from a funnel at an approximate rate of one drop per 25s. The final weight ratio of chitosan and TPP was 3:1. After all TPP was added, ChNP solution was stirred for another 30 min and then transferred into a 50 mL conical tube (Fisherbrand) on ice to be sonicated (Branson Sonifier) for 10 cycles of

30s with 30s break between each cycle. Then, ChNP solution was filtered through a 0.45 μm filter. To conjugate ε-poly-L-lysine (PL) to the ChNP, 0.1 or 0.2% PL was added into the 0.1% TPP solution and used for ChNP synthesis. After filtration through a 0.45 μm filter, free unbound PL was separated by ultrafiltration (30 kDa cut-off membrane, Amicon Ultra-15) and the retentate containing ChNP-PL was reconstituted to the volume before ultrafiltration with H_2O adjusted to pH4.6 with HCl (**Fig. 3.1e**). The size of nanoparticles was characterized using photo correlation spectroscope, Malvern Zetasizer.

3.3.3 Characterization of antibacterial activity of chitosan and PL

Bacterial inhibition zone tests were carried out on brain-heart infusion (BHI) medium soft agar plates. BHI (Thermo Scientific, Frederick, MD) soft agar plates were prepared by dissolving vendor-suggested amount of BHI medium and 0.8% (w/v) agar (Thermo Fisher Scientific) in DI water and autoclaved. After cooling down the soft agar in a 50°C water bath, 30 mL of the soft agar was transferred into a 50 mL sterile conical tube (Fisherbrand) and kept at ambient temperature for approximately 3 min. Then, 10 μL of fresh overnight bacteria cultures grown in BHI was added into the tube which was immediately shaken and poured into a sterile petri dish (10 cm X 10 cm, round, Fisher). After the soft agar in the petri dish solidified, wells were made using a cork borer and filled with 10 μL non-solidified soft agar to seal the bottom. Eight microliter of test samples were added into a well, and the whole plate was incubated at 37°C for 24 h.

To specifically quantify the minimal inhibition concentration (MIC) of a sample, I adopted the method described by Zhu et al. (2018). Briefly, bacterial cultures were incubated in BHI at 37°C for overnight and diluted in 2X Mueller Hinton Broth (MHB, Beckton Dickinson). One hundred microliter MHB containing approximately 10^3 CFU/mL bacteria were added in each well on a 96-well microtiter plate. A serially diluted antibacterial substance and sterile DI water were added into each well to make up to 200 μL. Bacterial growth was determined by a spectrometer (BioTek) at wavelength 595 nm or plating.

3.3.4 Cell proliferation and cytotoxicity tests of ChNP-PL on HCT-8 cells

HCT-8 cells (ATCC, Manassas, VA) cultured in D10F were trypsinized (HyClone) and seeded into tissue culture treated 96-well microtiter plates (TPP, Switzerland). The cells were

incubated at 37°C with 7% CO_2 and 95% relative humidity for a week with one medium change after three days. Before the experiment, cells in three wells were detached by trypsinization and counted using a hemocytometer. Cells had medium was changed with 100 µL fresh D10F and added with 10 µL ChNP-PL and/or fresh *Lm* F4244 at MOI of 1:10 (*Lm*:HCT-8). Non-treated cells and cells only treated with *Lm* F4244 were used as negative and positive controls, respectively. After incubating cells for 13 h, and 10 µL of WST-8 substrate (Millipore Sigma) for 2 h, the optical density of the wells was measured at 450 nm using a spectrometer. For cytotoxicity assay, 100 µL of cell supernatant after the 13-h incubation was collected and subjected to lactate dehydrogenase (LDH) assay (Thermo Scientific, Frederick, MD) following the vendor's instruction. Measurements from the supernatant of cells lysed by 0.1% Triton-X and non-treated cells were used as 0% and 100% cytotoxicity for calculation (Singh et al. 2018).

3.3.5 Formation and Assessment of single and mixed culture biofilms

Bacterial cultures were recovered from frozen stocks in -80°C, inoculated into Tryptic Soy Broth (TSB), and incubated under 37°C for 24 h. The cultures were standardized to 1.2 at OD_{595nm} and diluted by 1:200 into 45 ml TSB. Then, the cultures were transferred to a tissue culture-treated petri dish (TPP, Swizerland) to provide enough surface area for biofilm formation and incubating for 24 h at 30°C. To detach bacteria in biofilm after incubation, the medium was removed, and biofilm was washed once with 5 ml sterile PBS to remove loosely attached cells. Another 5 ml PBS was added to the biofilm, and the petri dish was sonicated for 15 min in a cold-water bath. To detach high biofilm formers, *S. aureus* ATCC25923 or *P. aeruginosa* PRI99, a sterile cell scraper was used. The bacteria in PBS were further diluted and plated on appropriate agar plates. Samples of mixed culture biofilms were plated on BHI agar and Modified Oxford medium (MOX) agar plates. The *Listeria* counts were determined by subtracting counts on MOX plates from the total counts on BHI. The remaining counts represent either *S. aureus* or *P. aeruginosa*.

3.3.6 Prevention of biofilm formation and inactivation of preformed biofilms

L. monocytogenes F4244, *S. aureus* ATCC25923, *P. aeruginosa* PRI99, *S.* Enteritidis 18ENT1344, and *E. coli* EDL933 were inoculated into tryptic soy broth (TSB, Thermo Scientific, Frederick, MD) at 37°C for about 18 h before use. Each culture was diluted to about 10^3 CFU/mL

in fresh TSB, and three wells on a 24-well tissue culture-treated microtiter plate (TPP, Switzerland) were added with 800 μL of the diluted culture. For mixed culture biofilms, about 10^3 CFU/mL of each culture contained 800 μL TSB were added in a well. For the biofilm prevention test, 200 μL antimicrobial substance, ChNP or ChNP-PL, was added to each well. After incubating the plates at 30°C for 24 h, TSB medium was removed, and each well was rinsed twice with 500 μL PBS to remove loosely attached bacteria. To detach sessile bacteria from biofilm, 200 μL PBS was added into each well, then the plate was sealed with parafilm and sonicated for 15 min in a water bath sonicator (iSonic, Chicago, IL). Sessile bacteria in the PBS were diluted and plated on BHI agar plates for quantification. For mixed culture biofilms, the dilution was plated on both MOX and BHI agar plates to enumerate the concentration of *L. monocytogenes* and total bacteria, respectively. The concentration of the non-*L. monocytogenes* bacteria was calculated by subtracting the amount of *L. monocytogenes* from the count of total bacteria.

In addition, biofilms were stained by crystal violet assay (Djordjevic et al. 2002) to visually present the prevention effect. The same procedures were followed in 96-well tissue culture treated microtiter plates (TPP, Switzerland) except the volumes of TSB and antimicrobial substance applied in each well were reduced to 200 and 50 μL, respectively. After 24 h incubation at 30°C, biofilms were rinsed twice with 100 μL PBS, air-dried for 15 min, and stained with 200 μL 0.1% crystal violet (CV) solution for 45 min at room temperature. After staining, CV solution was removed, and the CV residue was removed by rinsing twice with 100 μL PBS. For the biofilm inactivation test, bacteria were inoculated in 24-well microtiter plates as mentioned above except ChNP-PL was not added. After incubation at 30°C for 24 h to form biofilms, wells were gently rinsed once with 500 μL PBS to remove loosely attached bacteria. Then, 800 μL MHB and 200 μL antibacterial substance (ChNP or ChNP-PL) were added to the wells, and the plates were further incubated at 30°C for another 24 h. After incubation, biofilms were gently rinsed twice with 500 μL PBS, and sessile bacteria in biofilms were quantified as above mentioned.

3.4 Results

3.4.1 Synthesis of chitosan nanoparticles conjugated with ε-poly-L-lysine (ChNP-PL)

In acetic acid (1%) solution, chitosan forms a positively charged chain-like structure, thus negatively charged tripolyphosphate (TPP) is added as an anionic linker to crosslink chitosan

molecules by binding to their positively charged amino groups to form chitosan nanoparticle (ChNP) (Carvalho et al. 2009). After testing various combinations of chitosan and TPP, I determined that 1 volume of 0.1% TPP solution with 3 volumes of 0.1% chitosan solution (final weight ratio of Ch:TPP equals 3:1) produced ChNP with a dimension of about 100-200 nm measured by Malvern Zetasizer (**Fig. 3.1a**). After passing the preparation through a 0.45 μm filter, ChNP with uniform size (164 nm) was achieved (**Fig. 3.1a and b**). Interestingly, application of a sonication step (10 cycles, 30s each) before filtration, reduced ChNP dimension from about 164 nm to 91 nm (**Fig. 3.1c**) which were used for further studies. Note, a weight ratio of 4:1 or 6:1 (Ch:TPP) using 0.2% chitosan did not yield a desirable dimension rather it produced particles that are greater than 1000 nm (**Fig. 3.2a**), thus this approach was no longer pursued.

Next, ε-poly-L-Lysine (PL, 2%) was dissolved in TPP and the mixture was used for synthesizing ChNP-PL, however, the size of the complex increased from about 96 nm to 370 nm (**Fig. 3.1d**), suggesting complexation of PL with ChNP produced larger nanoconjugates (ChNP-PL). Consequent, sonication treatment, however, reduced the median size of ChNP-PL to 330 nm (**Fig. 3.1d**). To further reduce the dimension of ChNP-PL, the PL concentration was reduced from 2% to 1%, which helped lower the median size from 330 nm to 220 nm (**Fig. 3.1d and f**). Next, the extra unbound PL was removed by ultrafiltration (30 kDa cut-off membrane) (**Fig. 3.1e**), which resulted in a dimension that was close to our desirable size of 100 nm in the retentate (**Fig. 3.1f**). While the average diameter of the molecules in the filtrate was determined to be 5 nm, which was mostly consisted of free PL further indicating that a larger ChNP-PL complex was retained in the retentate and did not pass through the 30 kDa cut-off membrane (**Fig. 3.1f**).

Antimicrobial activity testing by well diffusion assay against a lawn of *L. monocytogenes* F4244 on an agar plate demonstrated that the activity (zone of inhibition) of ChNP-PL in retentate was about 1.96-fold of the activity observed for the filtrate, which consisted of mostly the free PL. To verify the antimicrobial activity of the filtrate, I tested the antimicrobial activity of 1% PL solution after passing through the membrane, and the activity of free PL molecules in the filtrate was observed to be higher than the retentate (**Fig. 3.1g**). Furthermore, by comparing the antimicrobial activity of ChNP-PL and free PL, I estimated that ChNP is bound to about 64% of PL (**Fig 3.1g**) which was used in our subsequent experiments. Because I found ChNP alone did not inhibit the growth of *L. monocytogenes* F4244 in soft BHI agar (**Fig. 3.2c**). I used the inhibition zone method to estimate the amount of PL in ChNP-PL after ultrafiltration. According to the

correlation function (R^2=0.995) between the PL concentration and the size of inhibition zone on *L. monocytogenes* F4244 (**Fig. 3.2d**), I estimated the concentration of PL in the retentate after filtering ChNP-PL, compared it with the original concentration of PL before ultrafiltration, and found about 63.7% of PL was still remained in the ChNP-PL preparation (**Fig. 3.2g**).

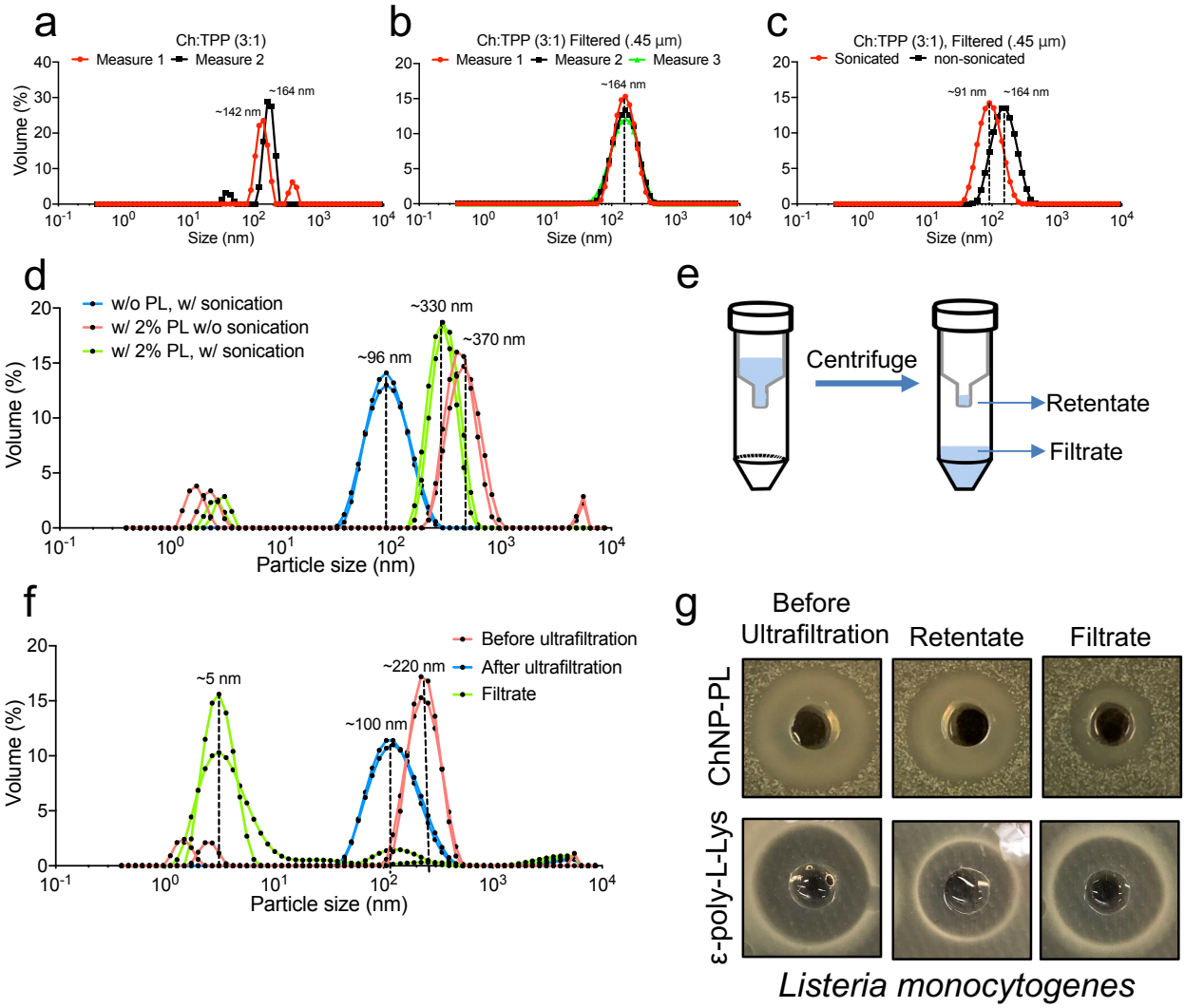

Figure 3.1. Synthesis and characterization of chitosan nanoparticles (ChNP) and chitosan nanoparticles with ε-poly-L-Lysine (ChNP-PL). (a) Zetasizer measurement of ChNP synthesized with TPP (Ch:TPP 3:1). Zetasizer measurement of ChNP after filtration through 0.45 µm syringe filters (b) and after 10 cycles of 30s sonication (c). (d) Size comparison of ChNP synthesized with or without 0.2% PL. (e) Removing unbound PL after ChNP-PL synthesis by ultrafiltration (30 kDa cutoff). (f) Zetasizer measurement of ChNP-PL synthesized with 0.1% PL before and after ultrafiltration. The median size of particles in filtrate (~5 nm) suggests that ChNP-PL cannot pass through the ultrafiltration (30 kDa cutoff). (g) ChNP-PL and PL-mediated inhibition of *L. monocytogenes* F4244 in soft BHI agar, demonstrating the formation of ChNP-PL.

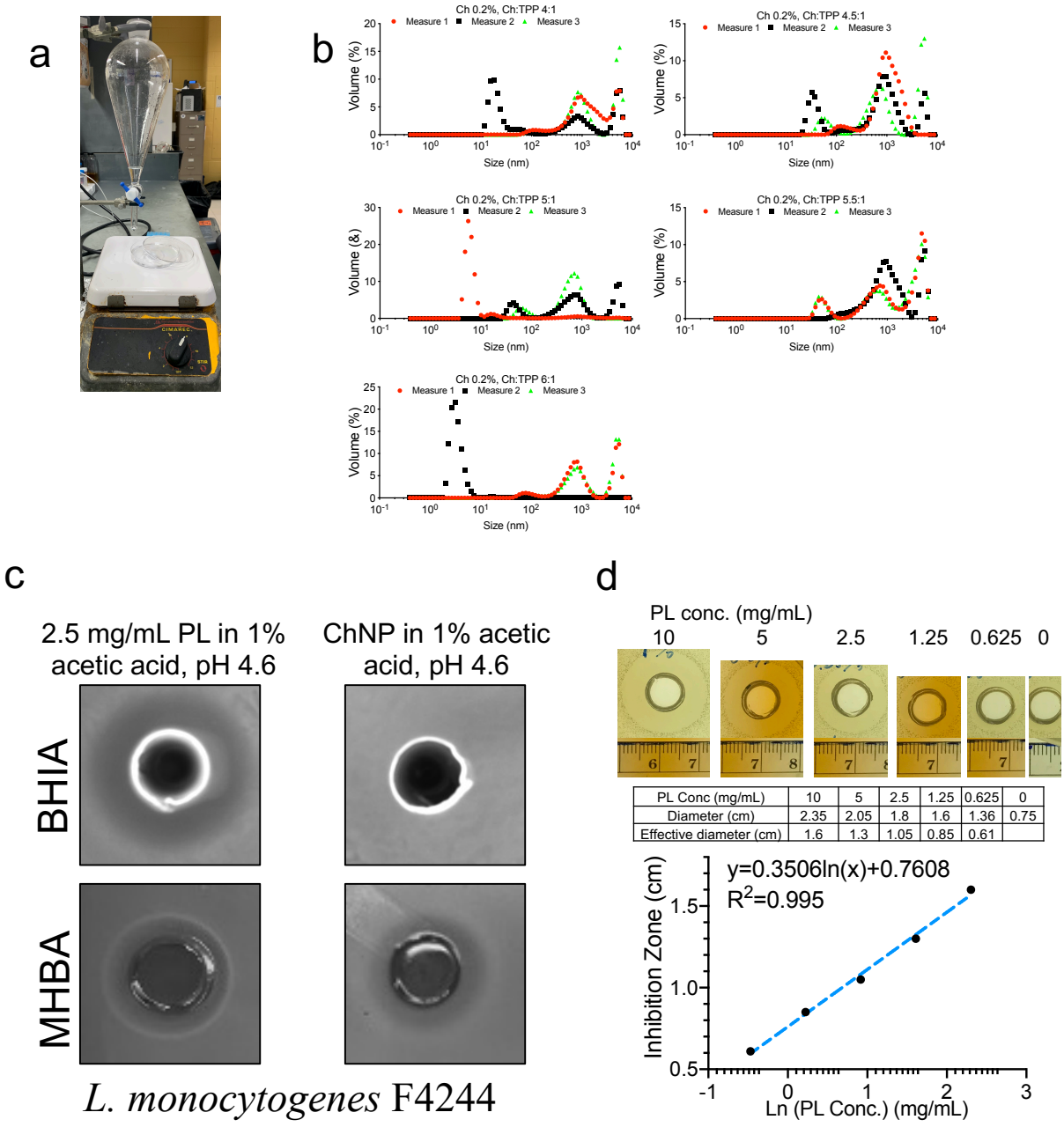

Figure 3.2 (a) A photo presentation of the setup for chitosan nanoparticles synthesis; (b) Size distribution of chitosan nanoparticle synthesized with 0.2% chitosan and various chitosan:TPP ratios; (c) Inhibition zone of 0.25% ε-Poly-L-lysine (PL) in 1% acetic acid pH4.6 or 0.1% chitosan in 1% acetic acid pH4.6 on *L. monocytogenes* F4244 in soft BHI or MHB agar. Since ChNP alone did not form inhibition zone on BHIA inoculated with *L. monocytogenes*, the concentration of PL in ChNP-PL can be reflected the size of inhibition zone on BHIA inoculated with *L. monocytogenes*; (d) Correlation between the concentration of PL and its inhibition zone size was constructed to estimate concentration of PL in ChNP.

3.4.2 ChNP and PL exhibited synergistic antimicrobial activity on foodborne pathogens

First, antimicrobial activity of chitosan polymer and ChNP was compared by using the minimal inhibition concentration (MIC) assay using a microdilution method (Singh et al. 2018) against five foodborne pathogens, including *L. monocytogenes* F4244, *S. aureus* ATCC25923, *P. aeruginosa* PRI99, *S.* Enteritidis 13ENT1344, and *E. coli* EDL933 (O157:H7). Bacterial growth inhibition results (OD_{595nm}) showed that the MIC of chitosan and ChNP were very similar depending on the strains tested (**Fig. 3.3**). MIC of chitosan and ChNP against *L. monocytogenes, S. aureus*, and *P. aeruginosa* were estimated to be 12.5 μg/mL; and 25 μg/mL for *E. coli* O157:H7. In addition, the MIC of chitosan against *S.* Enteritidis was 37.5 μg/mL while ChNP was 25 μg/mL (**Fig. 3.3**). By plating bacterial cultures in the sublethal concentration, however, I found the concentration of viable bacteria of *P. aeruginosa*, *S.* Enteritidis, and *E. coli* treated by ChNP were significantly ($P<0.05$) less than those bacteria treated by chitosan polymer (**Fig. 3.3**), suggesting nanoparticles (ChNP) has improved inhibitory activity than the chitosan polymer at certain concentration on some bacterial species.

Next, to test the synergistic antimicrobial effects of ChNP and PL on these pathogens, I conducted MIC tests by adding the decreasing concentration of both substances in each well on a 96-well microtiter plate. Results showed that the MIC of a mixture of ChNP and PL is lower than the MIC of each used separately, suggesting they do have synergistic antimicrobial effects (**Fig. 3.4 a-e**).

Next, I compared the MIC of ChNP and ChNP-PL conjugate by using microdilution methods against several pathogenic or nonpathogenic species/strains. Results showed that the MIC of ChNP-PL is lower than ChNP on all the 19 cultures tested (**Table 3.1**, **Fig. 3.5**). Compared to the MICs of ChNP, MICs of ChNP-PL on *Pseudomonas* (2 species) and *Salmonella enterica* (3 serovars) reduced by 3-fold, and *Listeria* (4 species), *S. aureus* (2 strains) and *E. coli* (3 strains) reduced by 10-fold, suggesting conjugation with PL significantly improves the inhibitory effect of ChNP.

Further, I tested the stability of ChNP-PL stored at ambient temperature for 16 days. Both freshly prepared and 16-day stored ChNP-PL produced a similar zone of inhibition when tested against lawns of *Salmonella*, *E. coli* O157:H7, and *L. monocytogenes* by well-diffusion method (**Fig. 3.6**). This suggests the antibacterial activity of ChNP-PL is maintained at least for 16 days in ambient conditions.

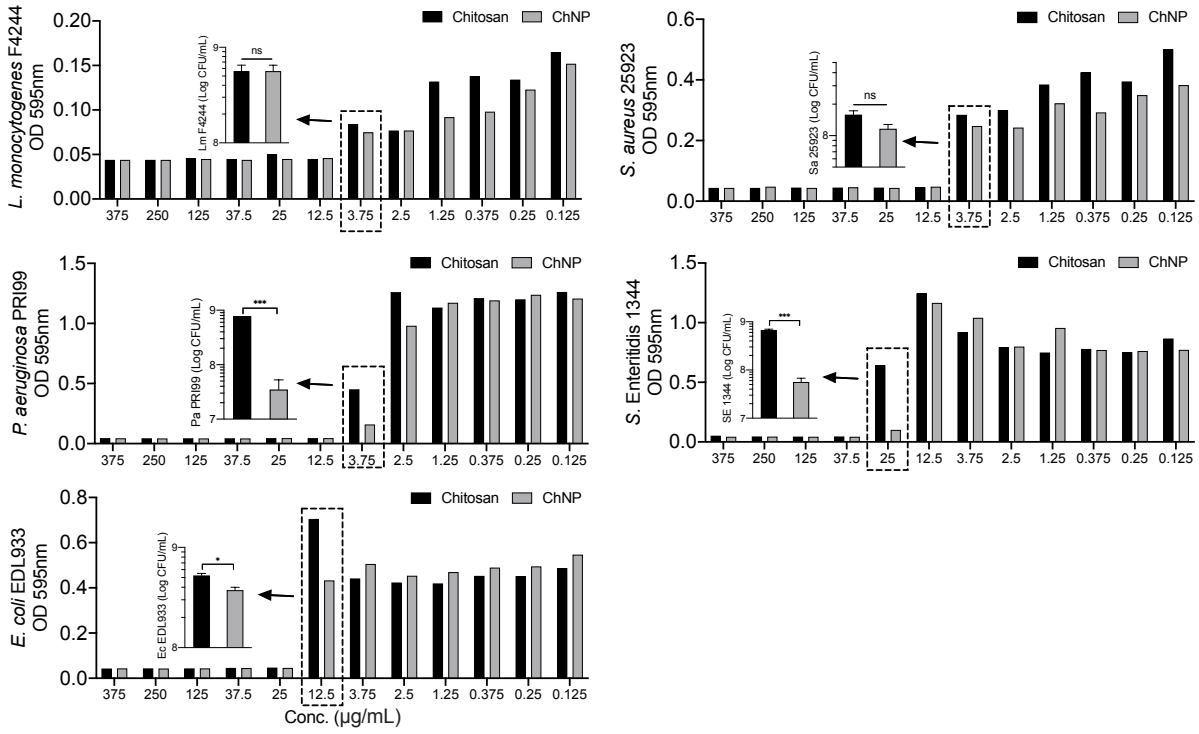

Figure 3.3 Comparing the minimal inhibition concentration (MIC) of chitosan and chitosan nanoparticles (ChNP) on *L. monocytogenes* F4244*, S. aureus* ATCC25923, *P. aeruginosa* PRI99, *S.* Enteritidis 13ENT1344, and *E. coli* EDL933 in MHB medium.

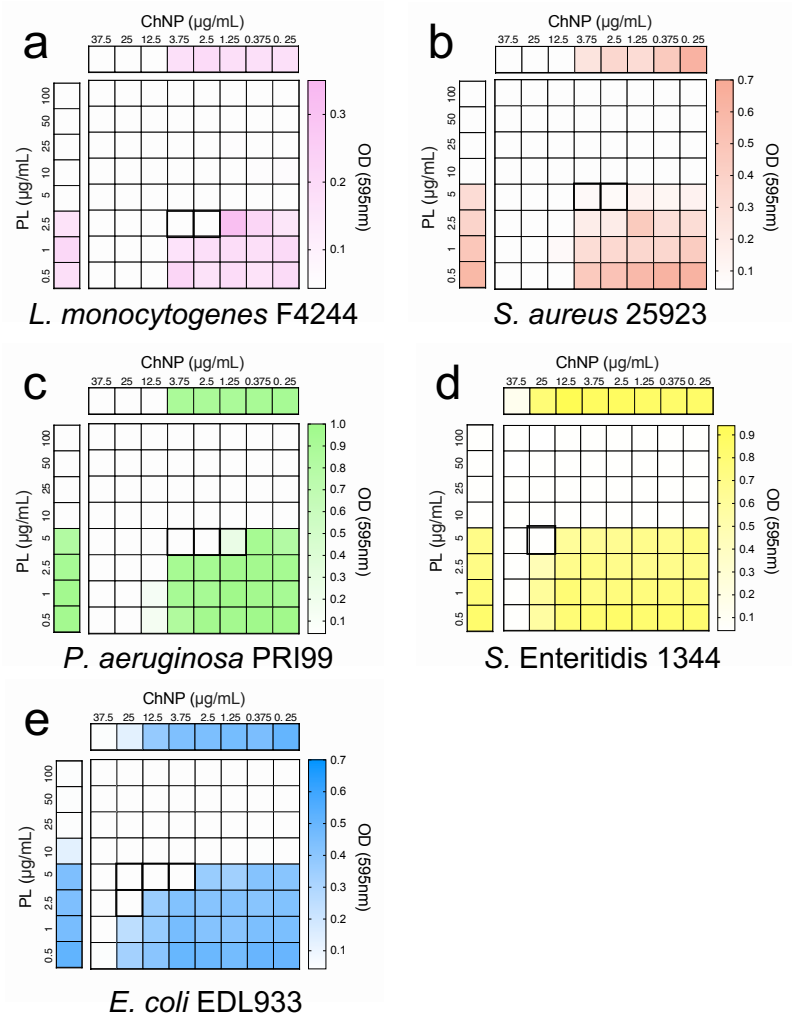

Figure 3.4 Synergistic MICs of ChNP and PL on *L. monocytogenes* F4244 (a), *S. aureus* ATCC25923 (b), *P. aeruginosa* PRI99 (c), *S.* Enteritidis 13ENT1344 (d), and *E. coli* EDL933 (e) was lower than the individual MIC of ChNP or PL presented in the top or left bar. The boxes with bold boundary indicate the reduced concentration of ChNP and PL when they act synergistically to the pathogens.

Table 3.1 Comparison of antimicrobial activity of ChNP and ChNP-PL

Bacteria	MIC (μg/mL)	
	ChNP	ChNP-PL
P. aeruginosa ATCC10145	>37.5	12.5-25
P. putida PRI107	>37.5	12.5-25
P. aeruginosa PRI99	25-37.5	2.5-3.75
L. ivanovii ATCC19119	25-37.5	2.5-3.75
L. seeligeri ATCC 35967	25-37.5	2.5-3.75
L. marthii ATCC BAA-1595	25-37.5	2.5-3.75
L. monocytogenes F40	25-37.5	2.5-3.75
L. monocytogenes F4244	25-37.5	1.25-2.5
S. Enteritidis PT21	>37.5	3.75-12.5
S. Typhimurium ST1	>37.5	12.5-25
S. Heidelberg 18ENT1418	>37.5	12.5-25
S. Enteritidis 18ENT1344	>37.5	3.75-12.5
S. aureus NRRL B767	>37.5	3.75-12.5
S. aureus ATCC25923	25-37.5	2.5-3.75
S. aureus ATCC29213	25-37.5	2.5-3.75
E. coli K12	>37.5	2.5-3.75
E. coli O157:H7 SEA13A72	>37.5	2.5-3.75
E. coli O157:H7 PT23	>37.5	1.25-2.5
E. coli EDL933	>37.5	2.5-3.75

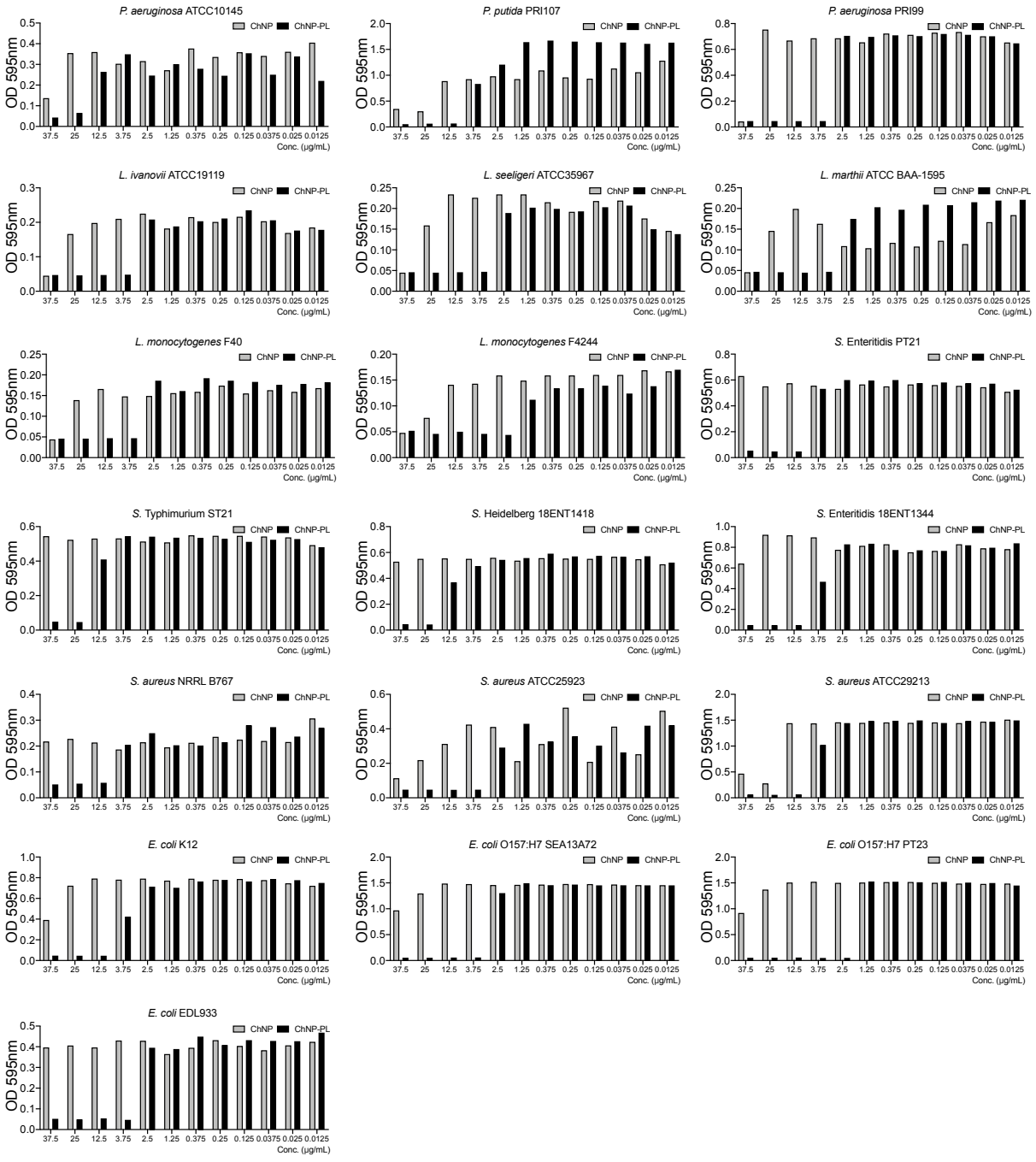

Figure 3.5 MICs of ChNP and ChNP-PL of 19 strains of *L. monocytogenes*, *S. aureus*, *P. aeruginosa*, *S. enterica*, and *E. coli*.

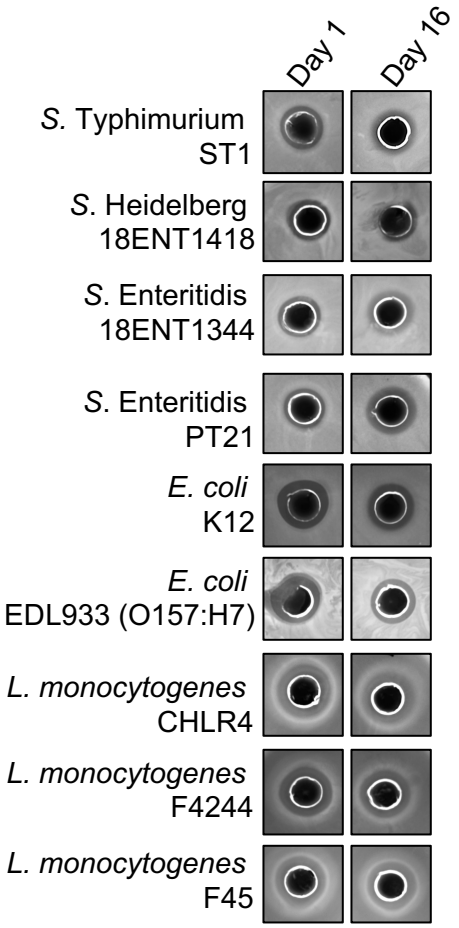

Figure 3.6 Comparison of the antimicrobial effect of fresh ChNP-PL and ChNP-PL stored at ambient temperature for 16 days using inhibition zone method.

3.4.3 ChNP-PL is nontoxic to intestinal epithelial cells

Cytotoxicity effects of ChNP-PL were tested on HCT-8 cell line, a human ileocecal colorectal adenocarcinoma cell line, using both WST-8 (2-(2-methoxy-4- nitrophenyl)-3-(4-nitrophenyl)-5-(2,4-disulfophenyl)-2Htetrazolium) (Chamchoy et al. 2019) and LDH (lactate dehydrogenase) (Roberts et al. 2001) assay. WST-8 assay measures cell proliferation by reacting with NADH from live cells and generating red color after reaction with formazan dye. After incubating HCT-8 cells with 1:10 diluted ChNP-PL for 13 h and WST-8 substrate for another 2 h, the proliferation of treated HCT-8 cells did not show any significance ($P>0.05$) difference with untreated cells (**Fig. 3.7a**). When *L. monocytogenes* F4244 was added to HCT-8 cells together with ChNP-PL at MOI of 1:10 (*Lm*:HCT-8), there was no significant ($P>0.05$) difference between

WST activity relative to untreated or ChNP-PL-treated HCT-8 cells (**Fig. 3.7a**). In contrast, when HCT-8 cells were treated with *L. monocytogenes* at the same MOI for 15 h in total without ChNP-PL treatment showed about a 50% increase in WST activity which was significantly ($P<0.0005$) higher than the other three treatments (**Fig. 3.7a**). These data indicate, in the absence of ChNP-PL, *L. monocytogenes* caused substantial HCT-8 cell damage which released intracellular enzymes and NADH.

Microscopic comparison of cell monolayers after WST-8 assay indicated maintenance of cell monolayer integrity when treated with ChNP-PL while cell rounding and the detached monolayer were evident when treated with *L. monocytogenes* (**Fig. 3.7b**). These data indicate ChNP-PL is non-toxic and could protect epithelial cells from *L. monocytogenes*-induced cell damage.

We also verified ChNP-PL effect on HCT-8 cells using a second cytotoxicity assay that assesses the membrane damage by monitoring the release of an intracellular enzyme, lactate dehydrogenase (LDH). After 13 h incubation with ChNP-PL, the cytotoxicity value was below zero while ChNP-PL plus *L. monocytogenes* F4244 treatment produced a cytotoxicity value of 10% and there was no significant difference ($P>0.05$) between the two treatments (**Fig. 3.7c**). While HCT-8 cells treated with *L. monocytogenes* alone for 13 h showed about 50% LDH release which was significantly ($P<0.0001$) higher than the values from the other two treatments (**Fig. 3.7c**). These results suggest that ChNP-PL has little or no cytotoxicity effects and would not affect the normal proliferation of HCT-8 cells in 13 h. Furthermore, ChNP-PL can also protect epithelial cells from the damage caused by *L. monocytogenes*.

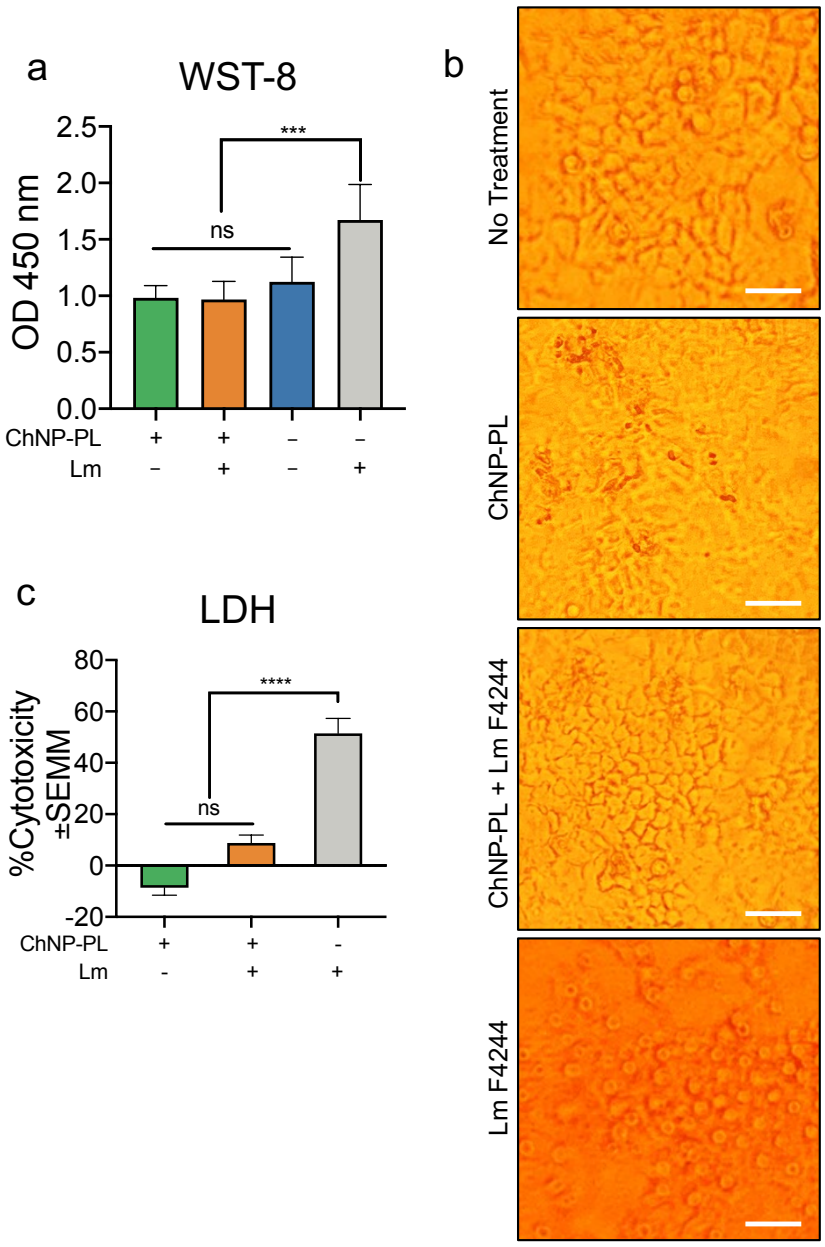

Figure 3.7 Cytotoxicity assessment of ChNP-PL on HCT-8, an intestinal epithelial cell line, using WST-8 (a) or Lactate Dehydrogenase (LDH) (c) assay. Cells were incubated with or without 1:10 diluted ChNP-PL and *L. monocytogenes* F4244 (Lm, MOI of 1:10, Lm:cell) for 13 h. Then, for WST-8 assay, substrates were added to the cells and incubated for another 2 h, and cell morphology after WST-8 incubation was captured with microscope (b). For LDH assay, supernatant was collected and subjected to LDH assay. Scale bars represent 50 µm. A pairwise Student's t-test used for statistical analysis. ***P<0.0005, ****P<0.0001.

3.4.4 Biofilm formation by *Listeria monocytogenes* is augmented in the presence of *Staphylococcus aureus* and *Pseudomonas aeruginosa*

We examined the dynamics of biofilm formation by *L. monocytogenes* in the presence of two strong biofilm-forming bacterial species, *S. aureus* and *P. aeruginosa*. In monoculture biofilm formed from the initial inoculum of about 3.5×10^6 CFU/mL, *L. monocytogenes* F4244 counts were about 4.0×10^8 CFU/mL after 24 h incubation at 30°C, while in the mixed culture biofilm with *S. aureus* ATCC25923, under the same growth conditions, *L. monocytogenes* counts were significantly ($P<0.005$) increased to 2.12×10^9 CFU/mL, i.e., a five-fold increase (**Fig. 3.8a** and **3.8b**). Interestingly, the *S. aureus* counts decreased by 10-fold (4.23×10^8 CFU/mL) when compared with its monoculture biofilm (4.70×10^9 CFU/mL) (**Fig. 3.8a** and **3.8b**).

When the initial inoculum of *L. monocytogenes* was increased from 3.3×10^6 to 1.6×10^8 CFU/mL in mixed culture biofilms with *S. aureus* initial inoculum of 3.5×10^7 CFU/mL, the *L. monocytogenes* counts also increased from 5.2×10^8 to 2.12×10^9 CFU/mL (**Fig. 3.8f**). Besides, it was also observed that *S. aureus* counts in the mixed culture biofilm were lower than the counts in its monoculture biofilms when the initial concentration of *S. aureus* was lower than *L. monocytogenes* (**Fig. 3.8e**). On the other hand, the counts of *S. aureus* in mixed biofilms significantly increased when there were more *S. aureus* cells in the initial inoculum than *L. monocytogenes* (**Fig. 3.8e**). In planktonic culture, I also found that the growth of *S. aureus* was slightly suppressed when more *L. monocytogenes* cells were present and its growth was not affected by *S. aureus* (**Fig. 3.8g**). Furthermore, I tested the mixed culture biofilm of *L. monocytogenes* F4244 and *S. aureus* 2747 whose biofilm-forming capabilities are lower than *S. aureus* ATCC25923, and it turned out that the counts for both bacteria (2.1×10^8 CFU/ml for *S. aureus* 2747 and 1.1×10^8 CFU/ml for *L. monocytogenes* F4244) were lower than the counts (3.0×10^8 CFU/ml for *S. aureus* 2747 and 3.2×10^8 CFU/ml for *L. monocytogenes* F4244) in their monoculture biofilm (**Table 3.2**, **Fig. 3.8h**).

In the mixed culture biofilm of *P. aeruginosa* PRI99 and *L. monocytogenes* F4244, the counts (4.7×10^9 CFU/ml) of *L. monocytogenes* increased significantly ($P<0.0005$) than its counts (4.0×10^8 CFU/ml) in the monoculture biofilm (**Fig. 3.8c**). Although the counts of *P. aeruginosa* PRI99 (7.2×10^9 CFU/ml) in the mixed biofilm was significantly ($P<0.005$) lower than its counts (4.6×10^9 CFU/ml) in the monoculture biofilm (**Fig. 3.8c**), the relative reduction was about 40% (**Fig. 6d**). I also tested the mixed culture biofilm of *L. monocytogenes* F4244 and *S.* Enteritidis

1344 or *E. coli* EDL933, however, the concentration of *L. monocytogenes* was not increased in either of those biofilms (**Table 3.2**, **Fig. 3.8i and 3.8j**).

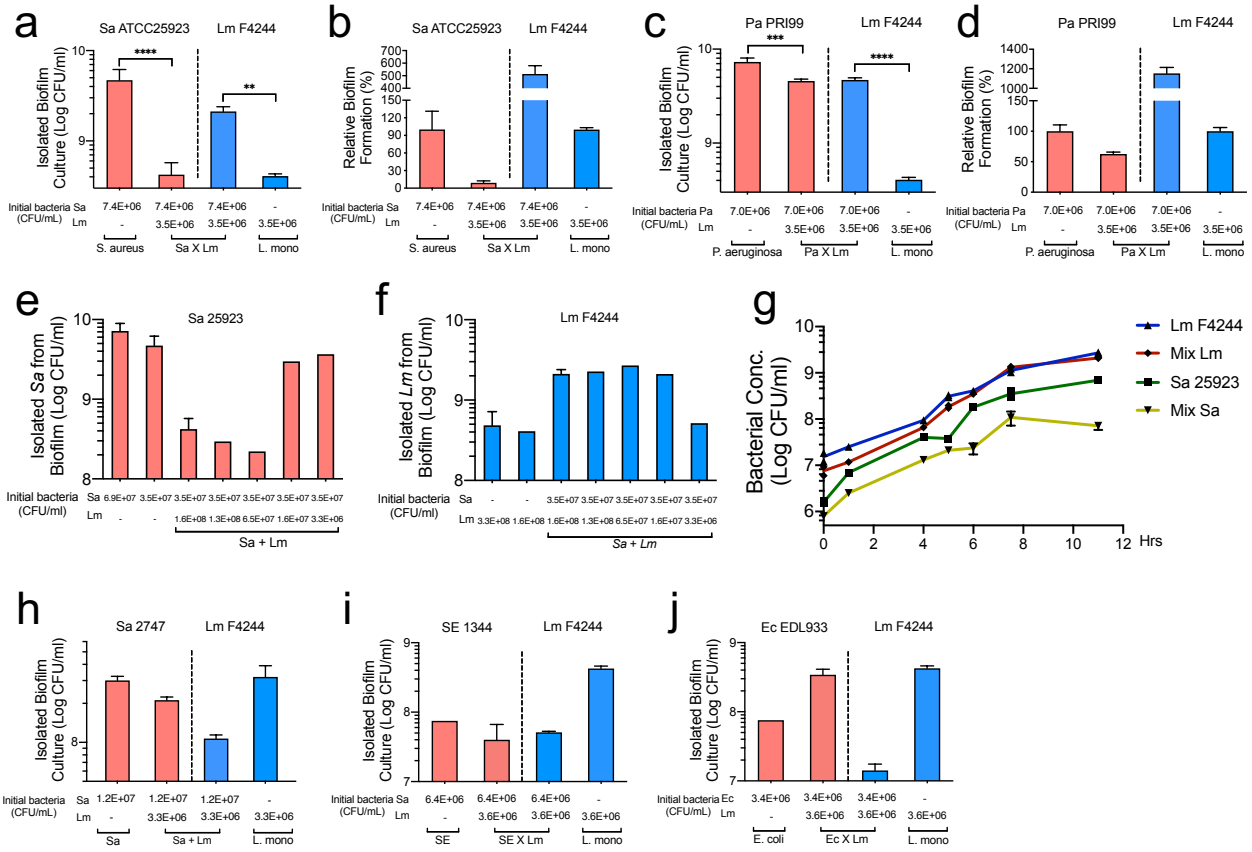

Figure 3.8 Quantification of bacterial counts in single and mixed culture biofilms. The exact concentrations of *L. monocytogenes* F4244 and *S. aureus* ATCC25923 (a) or *P. aeruginosa* PRI99 (c) in their single or mixed biofilms. Relative comparison of bacteria in their single and mixed culture biofilms (b and d). The counts of *S. aureus* ATCC25923 (e) and *L. monocytogenes* F4244 (f) in their mixed culture biofilms with different initial *L. monocytogenes* F4244 cells. (g) Growth rate of *S. aureus* ATCC25923 and *L. monocytogenes* F4244 in their single or mixed planktonic culture. The exact concentrations of *L. monocytogenes* F4244 and *S. aureus* 2747 (h), *S.* Enteritidis 18ENT1344 (i), or *E. coli* O157:H7 EDL933 (j) in their single or mixed biofilms. A pairwise Student's t-test used for statistical analysis. **P<0.005, ***P<0.0005, ****P<0.0001.

Table 3.2 Bacterial counts in mixed culture biofilms

Bacteria*	Avg CFU/ml			Fold-change
	Initial inoculum	Monoculture biofilm	Mixed culture biofilm	
Lm F4244	3.5×10^6	4.1×10^8	2.1×10^9	5-fold ↑
Sa ATCC25923	7.4×10^6	4.7×10^9	4.2×10^8	10-fold ↓
Lm F4244	3.5×10^6	4.1×10^8	4.7×10^9	11-fold ↑
Pa PRI99	7.0×10^6	7.3×10^9	4.6×10^9	1.6-fold ↓
Lm F4244	3.3×10^6	3.2×10^8	1.1×10^8	2.9-fold ↓
Sa 2747	1.2×10^7	3.0×10^8	2.1×10^8	1.4-fold ↓
Lm F4244	3.6×10^6	4.2×10^8	5.1×10^7	8.4-fold ↓
SE 1344	6.4×10^6	7.5×10^7	4.0×10^7	1.9-fold ↓
Lm F4244	3.6×10^6	4.2×10^8	1.4×10^7	30-fold ↓
Ec EDL933	3.4×10^6	7.6×10^7	3.4×10^8	4.5-fold ↑

**Lm*, *L. monocytogenes*; *Pa*, *Pseudomonas aeruginosa*; *Sa*, *Staphylococcus aureus*; SE, *Salmonella* Enteritidis; *Ec*, *E. coli* O157:H7

3.4.5 Prevention of biofilm formation by ChNP-PL

We tested the ability of ChNP-PL to prevent monoculture biofilm formation by each of the five pathogens, including *L. monocytogenes* F4244, *S. aureus* ATCC25923, *P. aeruginosa* PRI99, *S.* Enteritidis 18ENT1344, and *E. coli* EDL933 and the inhibition data were compared with ChNP-mediated inhibition. Each bacterium inoculated at about 1×10^3 CFU/mL in fresh TSB containing ChNP or ChNP-PL in wells of a 24-well microtiter plate and incubated at 30°C for 24 h to form biofilms. Then, crystal violet staining and plate counting were used to assess biofilm formation. ChNP-PL treatment prevented biofilm formation by *L. monocytogenes*, *P. aeruginosa,* and *E. coli* and bacterial counts were below the detection limit, while it caused 5-log reduction in *S.* Enteritidis counts and 3.5 log reduction in *S. aureus* counts (**Table 3.3**, **Fig. 3.9a**). Though ChNP prevented biofilm formation by *L. monocytogenes*, it showed only 1 log reduction in *S. aureus* counts and about 1.7 log reduction in *P. aeruginosa* counts (**Table 3.3**, **Fig. 3.9a**). In contrast, it had no inhibitory effect against *S.* Enteritidis or *E. coli*, rather it promoted bacterial growth with about 0.5 log increase in bacterial counts for both (**Table 3.3**, **Fig. 3.9a**).

Crystal violet staining provided a strong visual corroborating evidence for inhibitory activity of ChNP-PL against all tested organisms (**Fig. 3.9b**). Untreated control biofilms showed

intense dye-binding appearing dark blue, while partially inhibited biofilms showed moderate dye-binding while the wells without biofilms appeared clear. As stated above, ChNP appears to promote biofilm formation by *S*. Enteritidis and *E. coli* O157 showing intense dye-binding after ChNP treatment compared to the untreated controls, which showed partial dye-binding again suggesting ChNP appears to promote biofilm formation by these two pathogens. In contrast, ChNP-PL prevented biofilm formation by these pathogens and the wells appeared color-less or with a hint of stain (**Fig. 3.9b**).

Inhibitory activity of ChNP-PL against the mixed-culture biofilm of *L. monocytogenes* and *P. aeruginosa*, and *L. monocytogenes* and *S. aureus* were examined (**Fig. 3.9c**). Similar to the monoculture experiment, ChNP-PL completely inhibited the *L. monocytogenes* since the bacterial counts were below the detection limit while it caused about a 3.5-log reduction in *S. aureus* counts. In *L. monocytogenes* and *P. aeruginosa* mixed culture biofilms, ChNP-PL also completely inhibited biofilm formation by both pathogens since the counts were below the detection limit. In these experiments, ChNP abolished *L. monocytogenes* growth and reduced *P. aeruginosa* growth by 4.5 logs; however, ChNP did not show any inhibition of biofilm formation by *S. aureus* (**Table 3.3**, **Fig. 3.9c**). Crystal violet staining images corroborated with the plate counting data (**Table 3.3**, **Fig 3.9d**). These data again demonstrate that ChNP-PL is highly effective in preventing mixed culture biofilm formation by *L. monocytogenes* and *P. aeruginosa* or *L. monocytogenes* and *S. aureus*. Collectively, our data show ChNP-PL is highly effective in preventing single or mixed culture biofilms of five pathogens tested.

Figure 3.9 Assessment of the biofilm-preventing function of chitosan nanoparticles (ChNP) and nanoconjugates of chitosan nanoparticles and ε-Poly-L-lysine (ChNP-PL) on five foodborne pathogens. Comparison of biofilm preventing formation of ChNP and ChNP-PL on (a) single culture biofilms of *L. monocytogenes* F4244, *S. aureus* ATCC25923, *P. aeruginosa* PRI99, *S.* Enteritidis 18ENT1344, or *E. coli* O157:H7 EDL933, and (c) mixed culture biofilms of *L. monocytogenes* F4244 and *S. aureus* ATCC25923, or *L. monocytogenes* F4244 and *P. aeruginosa* PRI99. Bacteria isolated from biofilms were quantified by plating method. (b and d) Biofilms with no treatment, treated with ChNP, or treated with ChNP-PL were visualized by crystal violet staining. A pairwise Student's t-test used for statistical analysis. *P<0.005, **P<0.005, ***P<0.0005, ****P<0.0001.

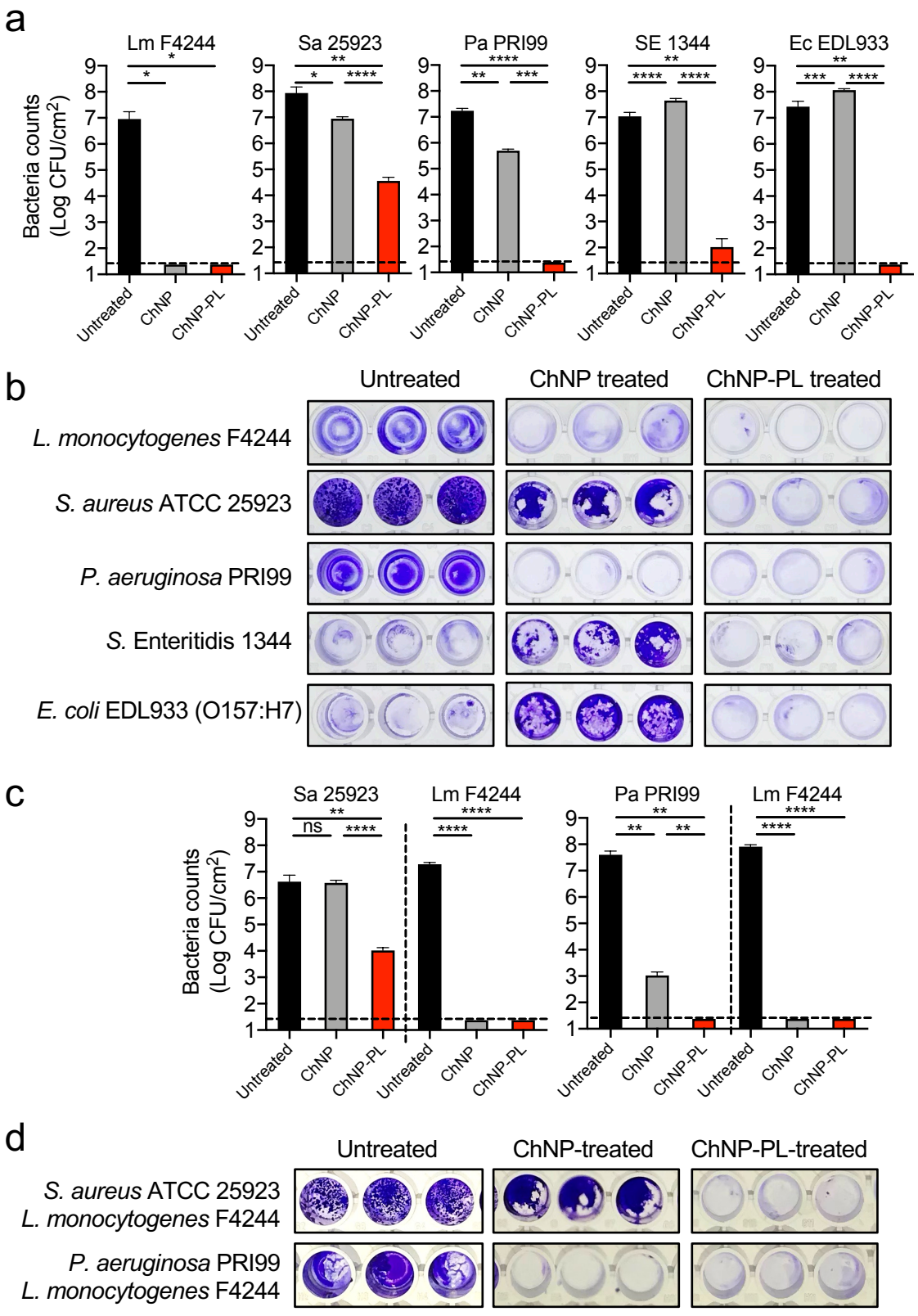
a
Lm F4244
Sa 25923
Pa PRI99
SE 1344
Ec EDL933
Bacteria counts (Log CFU/cm2)
Untreated
ChNP
ChNP-PL
b
Untreated
ChNP treated
ChNP-PL treated
L. monocytogenes F4244
S. aureus ATCC 25923
P. aeruginosa PRI99
S. Enteritidis 1344
E. coli EDL933 (O157:H7)
c
Sa 25923
Lm F4244
Pa PRI99
Lm F4244
Bacteria counts (Log CFU/cm2)
ns
d
Untreated
ChNP-treated
ChNP-PL-treated
S. aureus ATCC 25923
L. monocytogenes F4244
P. aeruginosa PRI99
L. monocytogenes F4244

Table 3.3 Prevention of biofilm formation by ChNP-PL

Bacteria	Avg CFU/cm^2		
	Untreated	ChNP treated	ChNP-PL treated
Lm	9.2×10^6	< 50 (>184,000-fold ↓)	< 50 (>184,000-fold ↓)
Sa	8.7×10^7	8.9×10^6 (9.8-fold ↓)	3.6×10^4 (2400-fold ↓)
Pa	1.7×10^7	5.0×10^5 (34-fold ↓)	< 50 (>184,000-fold ↓)
SE	1.1×10^7	4.4×10^7 (4-fold ↑)	103 (110,000-fold ↓)
EC	2.7×10^7	1.2×10^8 (4.4-fold ↑)	< 50 (>184,000-fold ↓)
Lm & Sa mixed biofilms			
Lm	1.9×10^7	< 50 (>184,000-fold ↓)	< 50 (>184,000-fold ↓)
Sa	4.2×10^6	3.8×10^6 (1.1-fold ↓)	1.0×10^4 (420-fold ↓)
Lm & Pa mixed biofilms			
Lm	8.2×10^7	< 50 (>184,000-fold ↓)	< 50 (>184,000-fold ↓)
Pa	4.0×10^7	1.0×10^3 (40,000-fold ↓)	< 50 (>184,000-fold ↓)

**Lm*, *L. monocytogenes*; *Pa*, *Pseudomonas aeruginosa*; *Sa*, *Staphylococcus aureus*; SE, *Salmonella* Entritidis; *Ec*, *E. coli* O157:H7

3.4.6 Inactivation of preformed biofilm by ChNP-PL

We also tested the ability of ChNP-PL to inactivate/disrupt preformed mono- or multi-pathogen biofilms and data were compared with ChNP-mediated activity. After pathogens were incubated in wells for 24 h to form biofilms, ChNP-PL or ChNP was diluted by 1:5 (v/v) in MHB and added to the wells for another 24 h and incubated at 37ºC. Then, sessile bacterial counts in treated and untreated biofilms were enumerated. In monoculture biofilm, ChNP-PL treatment reduced *L. monocytogenes* F4244 counts by 4.5 logs, *S.* Enteritidis by 2 logs, *E. coli* by 2 logs, and *S. aureus* by 0.5 logs while ChNP-PL had no inhibitory activity on *P. aeruginosa* (**Fig. 3.10a**). In contrast, ChNP had no inhibitory effect against *L. monocytogenes*, *S. aureus* and *P. aeruginosa* but showed a slight inhibitory effect against *S*. Enteritidis and *E. coli* (**Fig. 3.10a**). These data indicate that ChNP-PL is highly effective in inactivating preformed biofilms though the response was variable depending on the bacterial species tested.

In mixed culture biofilms of *L. monocytogenes* and *S. aureus*, ChNP-PL reduced *L. monocytogenes* counts by 0.3 logs and *S. aureus* by 0.1 log (**Fig. 3.10b**). In *L. monocytogenes* and *P. aeruginosa* mixed biofilms, ChNP-PL reduced *L. monocytogenes* counts by 2 logs but did not show any inhibitory effect against *P. aeruginosa*. Surprisingly, ChNP did not show any inhibitory effect against none of the pathogens in the mixed culture biofilms (**Fig. 3.10b**).

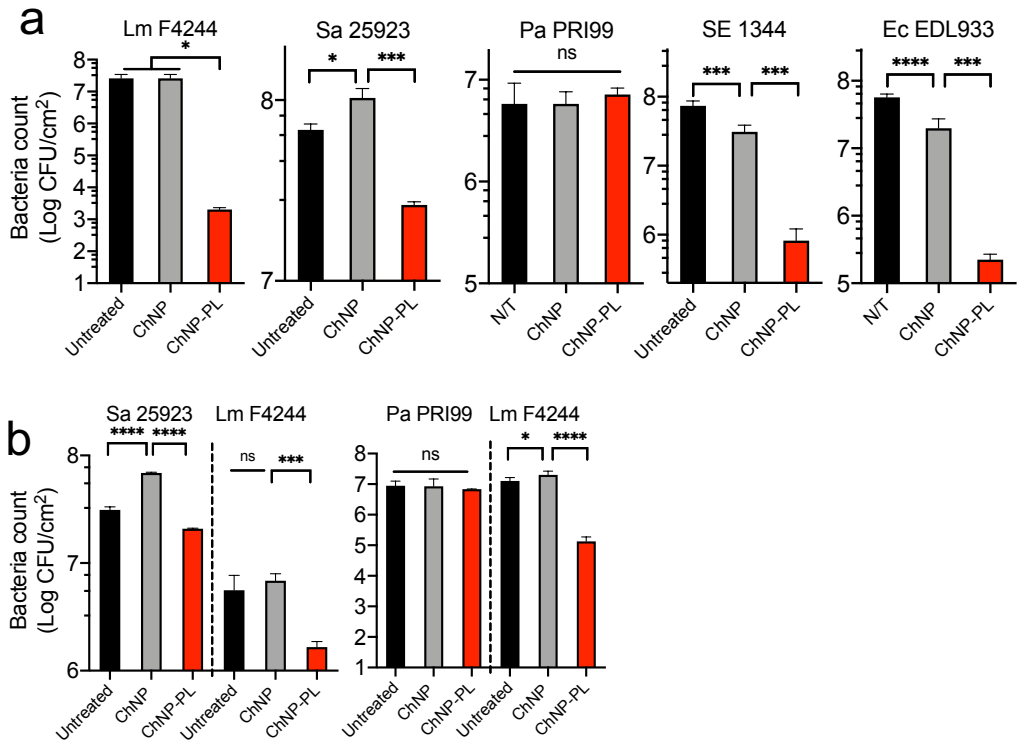

Figure 3.10 Assessment of the biofilm-inactivating function of chitosan nanoparticles (ChNP) and nanoconjugates of chitosan nanoparticles and ε-Poly-L-lysine (ChNP-PL) on five foodborne pathogens. Comparison of biofilm inactivating function of ChNP and ChNP-PL on (a) single culture biofilms of *L. monocytogenes* F4244, *S. aureus* ATCC25923, *P. aeruginosa* PRI99, *S.* Enteritidis 18ENT1344, or *E. coli* O157:H7 EDL933, and (b) mixed culture biofilms of *L. monocytogenes* F4244 and *S. aureus* ATCC25923, or *L. monocytogenes* F4244 and *P. aeruginosa* PRI99. Bacteria isolated from biofilms were quantified by plating method. A pairwise Student's t-test used for statistical analysis. *P<0.005, **P<0.005, ***P<0.0005, ****P<0.0001.

3.5 Discussion

Metaphorically speaking, biofilm can be described as a "house" that has a structure made up of bacteria-made EPS protecting bacterial cells living inside from harsh conditions (Bridier et al. 2011). Biofilm formation is also a strategy for microbes to expand their habitat and colonize new biotic or abiotic surfaces. For instance, *L. monocytogenes* can adhere and form biofilm on abiotic surfaces including stainless steel, PVC, and polystyrene (Haynes et al. 2003). Therefore, once bacteria are transmitted into food processing facilities, hospitals, cafeterias, or cruise ships through raw foods, they could attach to surfaces and start forming biofilms, which can become a consistent contamination source due to inadequate sanitation. Carpentier and Cerf (2011) reviewed multiple

cases that *L. monocytogenes* strains with the same pulsotypes were isolated multiple times from the same food processing environment throughout a year, suggesting some pathogens are capable of escaping or surviving routine sanitation regiment and could recurrently contaminate food products. Here, I aimed to use two natural antimicrobials and develop a solution to control biofilm formation by a broad spectrum of bacteria.

Biofilms in nature have also consisted of bacterial communities with great diversity instead of single culture biofilm (Lee et al. 2014). Zhang et al. (2012) used pyrosequencing and showed 1183-3567 operational taxonomic units in activated sludge from 14 sewage treatment plants, suggesting those locations contain a large bacterial diversity (Zhang et al. 2012). Some reported that mixed culture biofilms can provide better protection than monoculture. A nosocomial *Bacillus subtilis* isolate was tested to be resistant to peracetic acid because its biofilm prevents the penetration of the biocide (Bridier et al. 2012). When a peracetic acid-sensitive *S. aureus* strain forms mixed culture biofilm with the *B. subtilis* isolate, the former cells were also protected by the biofilm produced by the latter. Another study also showed that *L. monocytogenes* and *Lactobacillus plantarum* in their mixed culture biofilms were most resistant to 15-min treatment with benzalkonium chloride or peracetic acid than the bacteria in their monoculture biofilms (Van der Veen and Abee 2011). My results showed that *L. monocytogenes* in the mixed-culture biofilm with *S. aureus* or *P. aeruginosa* were reduced by less than 1 log or about 2 logs, respectively, after being treated by ChNP-PL (**Fig. 3.10b**), whereas *L. monocytogenes* in its mono-culture biofilm were reduced by about 3 logs by the same treatment (**Fig. 3.10a**). The improved survival of *L. monocytogenes* in the mixed biofilms may be because of the protection of *S. aureus* or *P. aeruginosa* produced biofilms.

In this study, I specifically investigated the mixed culture biofilm of *S. aureus* and *L. monocytogenes* because they not only were frequently isolated from the food processing environment but also isolated from the same location (Frank et al. 1990; Carpentier and Cerf 2011; Schirmer et al. 2013). Similar to our finding that the counts of *L. monocytogenes* in mixed biofilms with *S. aureus* were higher than the counts in monoculture biofilms of *L. monocytogenes*. Carpentier et al. (2004) also isolated more *L. monocytogenes* cells in the mixed biofilm with a food plant isolated *Staphylococcus capitis* strain than in the monoculture biofilm.

Although the various type of antimicrobial disinfectants, like benzalkonium chloride and peracetic acid, have been used in food processing environments for years, some drawbacks and

risks in applying those chemicals should be carefully analyzed. Peracetic acid is a strong oxidative organic acid that has been popularly used in situations including the food industry, hospitals, and households. Similar to other oxidizing agents, peracetic acid can inactivate microbial enzymes and other functional proteins, thus kills microbes (Batt and Tortorello 2014). A critical advantage of peracetic acid is that it does not generate harmful byproducts but produces acetic acid, water, oxygen and hydrogen peroxide (Bennett et al. 2014). However, peracetic acid is a strong oxidizer, thus requires careful handling with proper personal protection equipment. Mishandling and exposure could irritate eyes and membrane of the respiratory tract, and skin. A high concentration of peracetic acid can cause lethal hemorrhage and edema (NRC 2010). Benzalkonium chloride is another popular disinfectant used in the food industry. However, several studies have shown that exposing *L. monocytogenes* to sub-lethal concentration of benzalkonium chloride rendered the pathogen be more resistant to the chemical (Aase et al. 2000; To et al. 2002). A recent study reported that *L. monocytogenes* with induced resistance to benzalkonium chloride were also more resistant to other antimicrobial agents, including cefotaxime, cephalothin, ciprofloxacin, and ethidium bromide (Yu et al. 2018). More importantly, using one type of disinfectant in certain situations will consistently select the microbes with increasing resistance. Therefore, a good practice of sanitation is frequently switching to new disinfectants, which drive the development of new antimicrobial agents.

In recent decades, the surge of multiple antimicrobial-resistant pathogens drove not only the discovery of new antimicrobials but also more effective methods of applying current ones. The synergistic effect of applying multiple antimicrobial components of the same or different types has been reported. For example, essential oils can enhance the antimicrobial function of antibiotics and metal nanoparticles. Essential oils are produced through complicated metabolic reactions in plants to protect the plants from microbial infection (Rai et al. 2017). Because of the broad-spectrum antimicrobial function, essential oils have been tested on multi-antibiotics resistant bacteria, foodborne pathogens, and fungi and showed good efficacy (Friedman 2006; Fournomiti et al. 2015; Knezevic et al. 2016; Mekonnen et al. 2016). Though the fundamental antimicrobial mechanism of essential oils has not been fully revealed, some evidence suggests that cell membranes can be permeabilized with essential oils (Huang et al. 2014). In addition, combined application of essential oils and other antimicrobials showed further improved efficacy. For instance, Duarte et al. (2016) found that the addition of essential oils from *Rhaphiodon echinus*

significantly lowered the MICs of gentamicin, amikacin, and ciprofloxacin on *P. aeruginosa*. Karpanen et al. (2008) reported that applying the combination of multiple essential oils with chlorhexidine digluconate, a common disinfectant and antiseptic has lowered MICs for each component compared with applying them separately, suggesting the synergistic effect of the combination. Esmaeili et al. (2015) compared the size of inhibition zones generated by *Carum copticum* essential oils, chitosan nanoparticles, and chitosan nanoparticles loaded with *Carum copticum* essential oils on six bacterial species. Results showed that the essential oil-loaded chitosan nanoparticles generated the largest inhibition zone. The superior antimicrobial function of combining antimicrobials as indicated by numerous studies inspired us to combine chitosan and ε-Poly-L-lysine to combat bacterial biofilms.

As natural antimicrobials, both chitosan and ε-Poly-L-lysine have been extensively studied for their inhibitory effect on microbes. In 1992, (Sudarshan et al.) have demonstrated that water-soluble chitosan derivatives can cause membrane permeabilization in *E. coli*. Later, broad-spectrum antimicrobial activities of chitosan or its derivatives were demonstrated on bacteria, yeast, and mold (No et al. 2007). Because of its safety, biocompatibility, and biodegradability, chitosan has been tested and applied as a preservative in meat, eggs, vegetables, fruits, and their products (No et al. 2007; Duan et al. 2019). In 2013, U.S. Food and Drug Administration conferred GRAS on shrimp-derived chitosan for its application in the food industry (FDA 2013).

On the other hand, ε-Poly-L-lysine has also been given GRAS status to be used in sushi rice at 50 mg/kg (Chheda and Vernekar 2015). To test its antimicrobial action in the food matrix, Geornaras et al. (2007) showed that ε-Poly-L-lysine completely inhibited or reduced the growth of *E. coli* O157:H7, *S.* Typhimurium, and *L. monocytogenes* in several food products, including beef, rice, and vegetables, stored at 12°C for six days. Recently, You et al. (2017) demonstrated that daily consumption of ε-Poly-L-lysine for weeks did not cause permanent changes to gut microbiome in a mouse model, which provides another critical evidence for the safety of ε-Poly-L-lysine. Here, I aimed to produce nanoconjugates of the two antimicrobials and test their function specifically in controlling and inactivating bacterial biofilms.

I applied the ionotropic gelation method to synthesize chitosan nanoparticles using a "bottom-up" approach (Sanguansri and Augustin 2006; Sullivan et al. 2018). Generally, chitosan molecules are bound to each other with a small linker molecule and form larger nanoscale gel particles. Chitosan molecules are positively charged after being dissolved in a weak acid solution,

and triphenylphosphonium (TPP) is dissolved into a Penta-anion in water. After adding TPP in the chitosan solution, chitosan molecules are spontaneously attracted to TPP, bound with other chitosan molecules, and immediately forming gel nanoparticles. Not only the ratio of chitosan and TPP, but also the ionic strength, modification of chitosan, pH, and mixing rate affect the size distribution of ChNP (Sawtarie et al. 2017). Based on our experience of adapting published conditions for synthesis, minor differences in each laboratory could significantly affect the results, therefore each parameter should be optimized to produce the ChNP with a desirable dimension. After trying several ratios of chitosan and TPP, I was eventually able to synthesize ChNP with an median dimension of 150 nm using a ratio of 3:1 (**Fig. 3.1b** and **Fig. 3.2b**). Sullivan et al. (2018) used the same ratio and generated ChNP of 96.52 nm. Furthermore, Sawtarie et al. (2017) used a similar ratio of ~2.6:1, three different synthesis methods, and multiple concentrations of NaCl to synthesize ChNP with dimensions ranging from 100 nm to 800 nm.

After the synthesis of nanoparticles, I also found that membrane filtration of ChNP preparation through a 0.45 μm filter improved the size distribution of ChNP (**Fig. 3.1b**). It may be because filtration removed some undissolved particles in chitosan solution since it is the only material that was not filtered before synthesis. In addition, I found the application of the sonication step can also reduce the median size from 164 nm to 91 nm (44% reduction, **Fig. 3.1c**). After incorporating 2% PL into the matrix, the average size of ChNP dramatically increased to more than 300 nm (**Fig. 3.1d**), suggesting PL may enhance the coagulation of chitosan molecules in the presence of TPP. I eventually reduced the size of ChNP-PL nanoconjugates to about 100 nm by reducing the concentration of PL and introducing a sonication step (**Fig. 3.1f**). Using a previously established nanoparticles-based inhibition method (Singh et al. 2018), I determined that 63.7% PL were incorporated in the ChNP-PL matrix (**Fig. 3.1g** and **Fig. 3.2d**).

Chitosan has been applied in various foods as a natural preservative and is highly inhibitory against foodborne pathogens. I compared the MICs of chitosan polymer and ChNP on five bacterial pathogens and both showed similar MIC values on *L. monocytogenes*, *S. aureus*, *P. aeruginosa*, *S.* Enteritidis, and *E. coli* (**Fig. 3.3**). I also counted the viable bacterial numbers by plating and found that the counts of three bacteria (*P. aeruginosa*, *S.* Enteritidis, and *E. coli* EDL933) in the presence of ChNP were lower than their counts in the presence of chitosan (**Fig. 3.3**), suggesting ChNP may have better activity in slowing the growth of certain bacteria at the sublethal concentration. A recent study reported the MIC of chitosan and ChNP to be identical

when tested against four bacterial species (Sullivan et al. 2018), two (*S. aureus* and *E. coli*) of which were also tested in our study.

Furthermore, I compared the MIC of the mixture of ChNP and PL with each tested separately to determine whether they exhibit synergistic antimicrobial effects. Results on five tested strains clearly showed a synergistic effect (**Fig. 3.4a-e**). A recent study also reported the synergistic effect of Ch and PL against *Pseudomonas* spp. and H_2S-producing bacteria when applied on Pacific white shrimp (Na et al. 2018). This treatment significantly reduced total volatile basic nitrogen formation and extended the shelf life of shrimp without affecting the sensory perception (Na et al. 2018).

To ensure consistent delivery of two antimicrobials for inactivation of bacteria in biofilms, I synthesized the ChNP conjugated with PL and tested their MICs against a panel of 19 strains representing species of *Pseudomonas*, *Listeria*, *Salmonella*, *Staphylococcus*, and *E. coli*. Data show ChNP-PL to be highly inhibitory against the test strains and exhibited lower MIC than that of ChNP (**Table 3.1, Fig. 3.5**). Therefore, ChNP-PL was used in our subsequent experiments. Furthermore, I also observed that ChNP-PL maintained its antimicrobial activity even after 16 days of storage at ambient temperature (**Fig. 3.6**).

I also examined the safety of ChNP-PL by using *in vitro* cell culture (HCT-8) experiment and I did not observe any cytotoxicity when analyzed for the arrest of cell metabolism or cell membrane damage after 13 h of exposure to ChNP (**Fig. 3.7**). I also tested if ChNP-PL could protect HCT-8 cells from *L. monocytogenes* induced cell damage, and, interestingly, the fitness of HCT-8 cells was maintained, and cellular morphology was not affected in ChNP-PL treated cells (**Fig. 3.7**).

Though, research on chitosan as a carrier for drugs, DNA, and peptides has been conducted for decades (Illum et al. 2001; Janes et al. 2001; Mao et al. 2001), the safety of nanoparticulated form still requires a thorough assessment. Various models have been used to determine the safety of both chitosan and PL. Huang et al. (2004) thoroughly tested the cytotoxicity of chitosan with different molecular weights and chitosan nanoparticles. They reported that both chitosan polymer and ChNP exhibited significant cytotoxic effects on A549 cell line (lung cancer cell line) when used at a concentration above 0.741 mg/mL which is much higher than the MIC used in our study (**Fig. 3.5**). To test the safety of PL, Hiraki et al (2003) used an absorption, distribution, metabolism, and excretion (ADME) experiment using ^{14}C-labeled PL in a rat model and showed that 94% of

PL that entered the gastrointestinal tract, passed through the feces and no PL was accumulated in any tissues based on whole-body radiography (Hiraki et al. 2003). This study provided critical evidence as to the foundation for GRAS approval by FDA.

The inactivation of sessile bacteria in biofilm faces two significant challenges. Firstly, the biofilm matrix, or EPS, is largely made up with polysaccharides, extracellular DNA, and proteins, which provides a dense architecture protecting sessile bacteria from being removed by physical impacts or accessed by large molecules (Fong and Yildiz 2015; Limoli et al. 2015; Rabin et al. 2015). Secondly, sessile bacteria globally alter their gene expression, which usually gives them better resistance to antibiotics and several disinfectants (Høiby et al. 2010; Bridier et al. 2011). The strategies that can be applied to control biofilms in the food processing environment not only have to address the two challenges, also need to consider additional factors. For instance, the applied chemicals could be easily cleaned off and their residues in food should not raise any safety concern. Therefore, I was motivated to investigate the potential of using two food-grade molecules, chitosan and ε-poly-l-lysine, to control the formation of biofilms on food processing or touching surfaces. I tested the efficacy of preventing and inactivating the biofilms of five foodborne pathogens. ChNP-PL treatment completely prevented the biofilm formation by *L. monocytogenes*, *P. aeruginosa*, *S.* Enteritidis and *E. coli* O157:H7 and bacterial counts were undetectable after plating while it partially affected *S. aureus* biofilm formation. ChNP on the other hand completely inhibited biofilm formation by *L. monocytogenes* but showed some inhibitory effect against *S. aureus* and *P. aeruginosa* albeit much lower than ChNP-PL treatment. ChNP treatment surprisingly increased the bacterial counts in biofilms of *S.* Enteritidis 18ENT1344 and *E. coli* EDL933, which suggests low concentration of ChNP in TSB probably helps promote biofilm formation by these pathogens. It is interesting to note that ChNP in MHB is inhibitory towards planktonic cells of some *Salmonella* and *E. coli* strains (**Table 3.1**).

ChNP-PL is also inhibitory towards these pathogens in mixed culture biofilm and totally prevented the biofilm formation by *L. monocytogenes* when cocultured with *P. aeruginosa* and *S. aureus* and it also completely inhibited the growth of *P. aeruginosa* but partially inhibited *S. aureus* (**Fig. 3.9**). These data indicate ChNP-PL is effective in preventing biofilm formation by mono- or multi-pathogens. I also tested the inactivation of preformed biofilm by ChNP-PL and data show ChNP-PL was highly effective in eliminating monoculture biofilms of *L. monocytogenes*, *S.* Enteritidis, *E. coli* O157:H7 and moderately effective against *S. aureus* but not

against *P. aeruginosa* (**Fig. 3.10**). In the mixed culture biofilm, ChNP-PL is inhibitory towards *L. monocytogenes* and moderately towards *S. aureus* but none towards *P. aeruginosa*. In summary, our results showed the combination of two natural antimicrobials have great potential to be applied as a safe method to control broad spectrum of foodborne pathogens in food processing facilities.

APPENDIX A. PURIFICATION OF TAG-FREE RECOMBINANT LAP OF *L. INNOCUA*

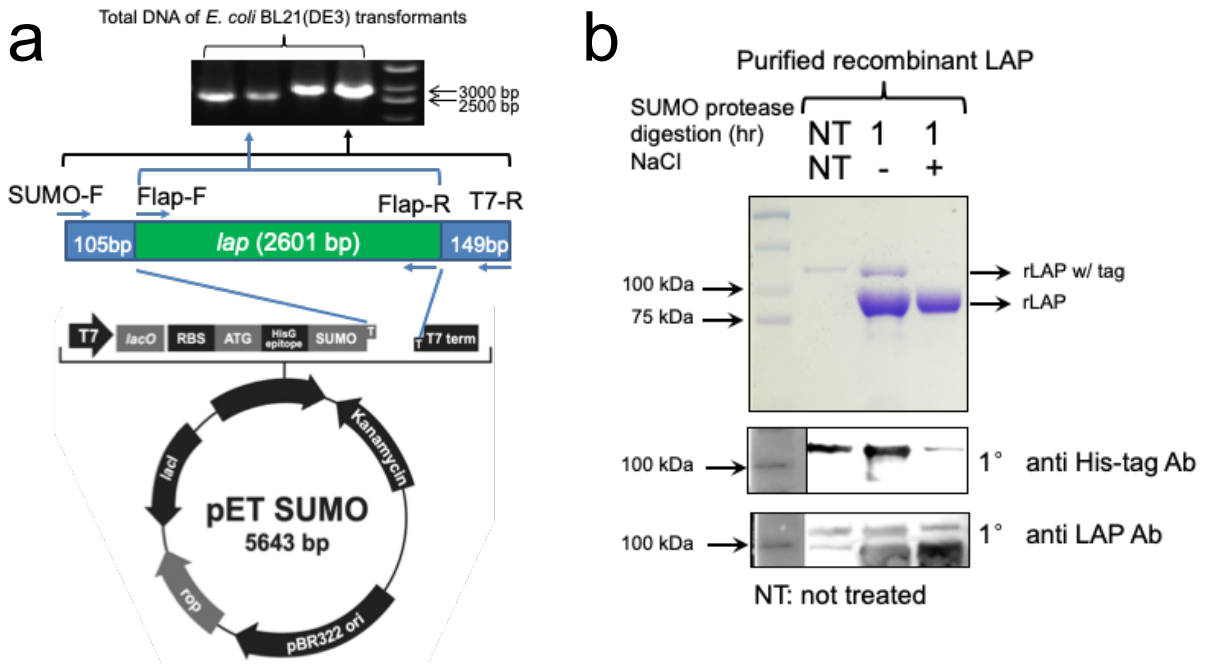

Lap gene from *L. innocua* F4248 was amplified with primers Flap-F and Flap-R (a), and the amplicon was cloned into pET SUMO vector (Thermo Fisher) through TA cloning following the vendor's protocol. Then, pET SUMO::*lap* was transfected into *E. coli* BL21(DE3), and the presence of *lap* gene and the vector in kanamycin resistant transformants were confirmed by PCR using two primer sets, Flap-F/Flap-R and SUMO-F/T7-R (a). After incubation and induction with IPTG, whole cell protein was extracted from *E. coli* BL21(DE3) pET SUMO::*lap*. Recombinant LAP was purified by its His tag and immobilized metal affinity chromatograph, then the recombinant LAP was treated with SUMO protease with or without NaCl to remove extra N-terminal tags. Finally, western blots using anti-His tag and anti-LAP antibody showed 1 h SUMO protease treatment with NaCl can effectively remove the N-terminal tags of the majority of recombinant LAP (b).

APPENDIX B. IDENTIFICATION OF *L. MONOCYTOGENES* ISOLATES WITH ABNORMAL INLA EXPRESSION

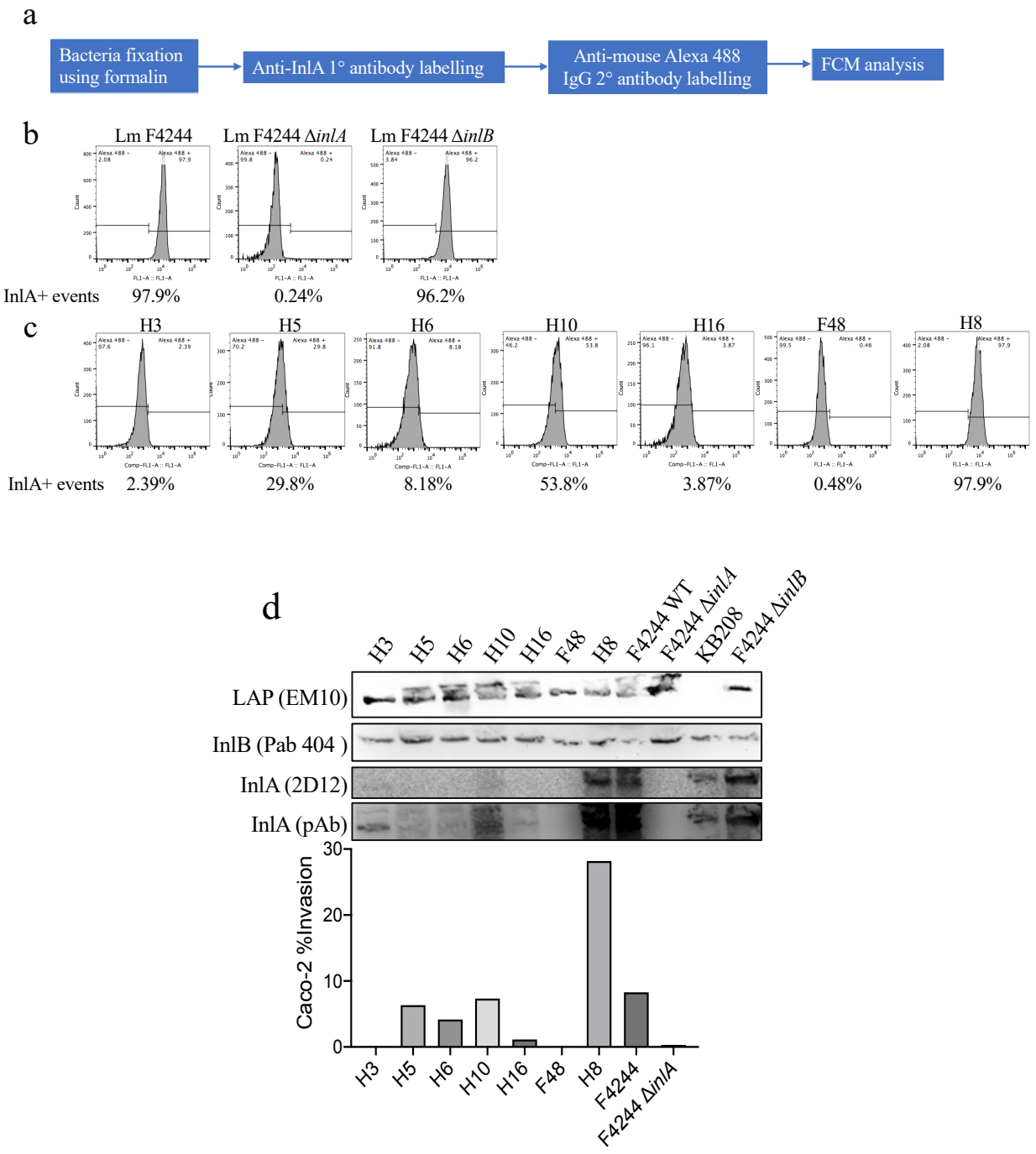

L. monocytogenes isolates and mutants were labeled with anti-InlA primary antibody and fluorescence tagged secondary antibody before flow cytometry (FCM) analysis (a). Comparison

between *Lm* F4244, *Lm* F4244 Δ*inlA*, and *Lm* F4244 Δ*inlB* showed that the FCM method can differentiate the expression of InlA in the bacteria (b). Same analysis on seven isolates showed six of them have abnormally low InlA expression, 0.48-53.8%, compared to *Lm* F4244 (**c**). In addition, Western blot also showed consistently low InlA expression (d). *In vitro* invasion assay using Caco-2 cells showed three isolates, *Lm* H3, H16, and F48, showed invasion rates of about 0.03%, 1.12%, and 0.03%, respectively. At the same time, the invasion rate of *Lm* F4244 is about 8.28%.

REFERENCES

Aase, B., Sundheim, G., Langsrud, S. and Rørvik, L.M. (2000) Occurrence of and a possible mechanism for resistance to a quaternary ammonium compound in *Listeria monocytogenes*. *International Journal of Food Microbiology* **62**, 57-63.

Abdelhamed, H., Lawrence, M.L. and Karsi, A. (2015) A novel suicide plasmid for efficient gene mutation in *Listeria monocytogenes*. *Plasmid* **81**, 1-8.

Allesen-Holm, M., Barken, K.B., Yang, L., Klausen, M., Webb, J.S., Kjelleberg, S., Molin, S., Givskov, M. and Tolker-Nielsen, T. (2006) A characterization of DNA release in *Pseudomonas aeruginosa* cultures and biofilms. *Molecular Microbiology* **59**, 1114-1128.

Archer, N.K., Mazaitis, M.J., Costerton, J.W., Leid, J.G., Powers, M.E. and Shirtliff, M.E. (2011) *Staphylococcus aureus* biofilms: properties, regulation, and roles in human disease. *Virulence* **2**, 445-459.

Arciola, C.R., Campoccia, D. and Montanaro, L. (2018) Implant infections: adhesion, biofilm formation and immune evasion. *Nature Revews Microbiology* **16**, 397-409.

Arevalos-Sánchez, M., Regalado, C., Martin, S.E., Domínguez-Domínguez, J. and García-Almendárez, B.E. (2012) Effect of neutral electrolyzed water and nisin on *Listeria monocytogenes* biofilms, and on listeriolysin O activity. *Food Control* **24**, 116-122.

Arnqvist, A., Olsén, A. and Normark, S. (1994) σS-dependent growth-phase induction of the csgBA promoter in *Escherichia coli* can be achieved *in vivo* by σ70 in the absence of the nucleoid-associated protein H-NS. *Molecular Microbiology* **13**, 1021-1032.

Austin, J.W., Sanders, G., Kay, W.W. and Collinson, S.K. (1998) Thin aggregative fimbriae enhance *Salmonella enteritidis* biofilm formation. *FEMS Microbiology Letters* **162**, 295-301.

Bailey, T.W., do Nascimento, N.C. and Bhunia, A.K. (2017) Genome sequence of *Listeria monocytogenes* strain F4244, a 4b serotype. *Genome Announcements* **5**, e01324-01317.

Baker, B. (2018) How to avoid food poisoning from *E. coli* and *Salmonella*
PennToday.

Banerjee, P. and Bhunia, A.K. (2010) Cell-based biosensor for rapid screening of pathogens and toxins. *Biosensors and Bioelectronics* **26**, 99-106.

Barbosa, J., Borges, S., Camilo, R., Magalhães, R., Ferreira, V., Santos, I., Silva, J., Almeida, G. and Teixeira, P. (2013) Biofilm formation among clinical and food isolates of *Listeria monocytogenes*. *International Journal of Microbiology* **2013**.

Barken, K.B., Pamp, S.J., Yang, L., Gjermansen, M., Bertrand, J.J., Klausen, M., Givskov, M., Whitchurch, C.B., Engel, J.N. and Tolker-Nielsen, T. (2008) Roles of type IV pili, flagellum-mediated motility and extracellular DNA in the formation of mature multicellular structures in *Pseudomonas aeruginosa* biofilms. *Environmental Microbiology* **10**, 2331-2343.

Barnhart, M.M. and Chapman, M.R. (2006) Curli biogenesis and function. *Annual Review of Microbiology* **60**, 131-147.

Batt, C.A. and Tortorello, M.-L. (2014) *Encyclopedia of Food Microbiology*: Academic press.

Becattini, S., Littmann, E.R., Carter, R.A., Kim, S.G., Morjaria, S.M., Ling, L., Gyaltshen, Y., Fontana, E., Taur, Y. and Leiner, I.M. (2017) Commensal microbes provide first line defense against *Listeria monocytogenes* infection. *Journal of Experimental Medicine* **214**, 1973-1989.

Behari, J. and Youngman, P. (1998) Regulation of hly Expression in *Listeria monocytogenes* by Carbon Sources and pH Occurs through Separate Mechanisms Mediated by PrfA. *Infection and Immunity* **66**, 3635-3642.

Bennett, J.E., Dolin, R. and Blaser, M.J. (2014) *Mandell, Douglas, and Bennett's Principles and Practice of Infectious Diseases*: Elsevier Health Sciences.

Bennett, S.D., Walsh, K.A. and Gould, L.H. (2013) Foodborne disease outbreaks caused by *Bacillus cereus*, *Clostridium perfringens*, and *Staphylococcus aureus*—United States, 1998–2008. *Clinical Infectious Diseases* **57**, 425-433.

Berche, P., Gaillard, J. and Sansonetti, P. (1987) Intracellular growth of Listeria monocytogenes as a prerequisite for in vivo induction of T cell-mediated immunity. *The Journal of Immunology* **138**, 2266-2271.

Bhunia, A., Steele, P., Westbrook, D., Bly, L., Maloney, T. and Johnson, M. (1994) A six-hour in vitro virulence assay for *Listeria monocytogenes* using myeloma and hybridoma cells from murine and human sources. *Microbial Pathogenesis* **16**, 99-110.

Bhunia, A.K. (2018) Animal and Cell Culture Models to Study Foodborne Pathogens. In *Foodborne Microbial Pathogens*. pp.117-132: Springer.

Bhunia, A.K. and Feng, X. (1999a) Examination of cytopathic effect and apoptosis in *Listeria monocytogenes*-infected hybridoma B-lymphocyte (Ped-2E9) line *in vitro*. *Journal of Microbiology and Biotechnology* **9**, 398-403.

Bhunia, A.K. and Feng, X. (1999b) Examination of cytopathic effect and apoptosis in *Listeria monocytogenes*-infected hybridoma B-lymphocyte (Ped-2E9) line *in vitro*. *Journal of Microbiology and Biotechnology* **9**, 398-403.

Bian, Z. and Normark, S. (1997) Nucleator function of CsgB for the assembly of adhesive surface organelles in *Escherichia coli*. *The EMBO Journal* **16**, 5827-5836.

Bierne, H. and Cossart, P. (2007) Listeria monocytogenes surface proteins: from genome predictions to function. *Microbiology and Molecular Biology Reviews* **71**, 377-397.

Boll, E.J., Ayala-Lujan, J., Szabady, R.L., Louissaint, C., Smith, R.Z., Krogfelt, K.A., Nataro, J.P., Ruiz-Perez, F. and McCormick, B.A. (2017) Enteroaggregative *Escherichia coli* adherence fimbriae drive inflammatory cell recruitment via interactions with epithelial MUC1. *MBio* **8**.

Bonazzi, M., Lecuit, M. and Cossart, P. (2009) *Listeria monocytogenes* internalin and E-cadherin: from structure to pathogenesis. *Cellular Microbiology* **11**, 693-702.

Bonsaglia, E.C.R., Silva, N.C.C., Fernades, A., Araujo, J.P., Tsunemi, M.H. and Rall, V.L.M. (2014) Production of biofilm by *Listeria monocytogenes* in different materials and temperatures. *Food Control* **35**, 386-391.

Borucki, M.K., Peppin, J.D., White, D., Loge, F. and Call, D.R. (2003) Variation in biofilm formation among strains of *Listeria monocytogenes*. *Applied and Environmental Microbiology* **69**, 7336-7342.

Brady, R.A., Leid, J.G., Camper, A.K., Costerton, J.W. and Shirtliff, M.E. (2006) Identification of *Staphylococcus aureus* proteins recognized by the antibody-mediated immune response to a biofilm infection. *Infection and Immunity* **74**, 3415-3426.

Bridier, A., Briandet, R., Thomas, V. and Dubois-Brissonnet, F. (2011) Resistance of bacterial biofilms to disinfectants: a review. *Biofouling* **27**, 1017-1032.

Bridier, A., del Pilar Sanchez-Vizuete, M., Le Coq, D., Aymerich, S., Meylheuc, T., Maillard, J.-Y., Thomas, V., Dubois-Brissonnet, F. and Briandet, R. (2012) Biofilms of a *Bacillus subtilis* hospital isolate protect *Staphylococcus aureus* from biocide action. *PLoS One* **7**, e44506.

Bueno, V.F., Banerjee, P., Banada, P.P., José de Mesquita, A., Lemes-Marques, E.G. and Bhunia, A.K. (2010) Characterization of *Listeria monocytogenes* isolates of food and human origins from Brazil using molecular typing procedures and *in vitro* cell culture assays. *International Journal of Environmental Health Research* **20**, 43-59.

Burkholder, K.M. and Bhunia, A.K. (2010) *Listeria monocytogenes* uses *Listeria* adhesion protein (LAP) to promote bacterial transepithelial translocation and induces expression of LAP receptor Hsp60. *Infection and Immunity* **78**, 5062-5073.

Burkholder, K.M., Kim, K.-P., Mishra, K., Medina, S., Hahm, B.-K., Kim, H. and Bhunia, A.K. (2009) Expression of LAP, a SecA2-dependent secretory protein, is induced under anaerobic environment. *Microbes and Infection* **11**, 859-867.

Camejo, A., Buchrieser, C., Couvé, E., Carvalho, F., Reis, O., Ferreira, P., Sousa, S., Cossart, P. and Cabanes, D. (2009) *In vivo* transcriptional profiling of *Listeria monocytogenes* and mutagenesis identify new virulence factors involved in infection. *PLoS Pathogens* **5**, e1000449.

Camejo, A., Carvalho, F., Reis, O., Leitao, E., Sousa, S. and Cabanes, D. (2011) The arsenal of virulence factors deployed by *Listeria monocytogenes* to promote its cell infection cycle. *Virulence* **2**, 379-394.

Camilli, A., Goldfine, H. and Portnoy, D.A. (1991) *Listeria monocytogenes* mutants lacking phosphatidylinositol-specific phospholipase C are avirulent. *Journal of Experimental Medicine* **173**, 751-754.

Cao, H., Krishnan, G., Goumnerov, B., Tsongalis, J., Tompkins, R. and Rahme, L.G. (2001) A quorum sensing-associated virulence gene of *Pseudomonas aeruginosa* encodes a LysR-like transcription regulator with a unique self-regulatory mechanism. *Proceedings of the National Academy of Sciences* **98**, 14613-14618.

Caro-Astorga, J., Frenzel, E., Perkins, J.R., Álvarez-Mena, A., de Vicente, A., Ranea, J.A.G., Kuipers, O.P. and Romero, D. (2020) Biofilm formation displays intrinsic offensive and defensive features of *Bacillus cereus*. *NPJ Biofilms and Microbiomes* **6**, 3.

Carpentier, B. and Cerf, O. (2011) Review - Persistence of *Listeria monocytogenes* in food industry equipment and premises. *International Journal of Food Microbiology* **145**, 1-8.

Carpentier, B. and Chassaing, D. (2004) Interactions in biofilms between *Listeria monocytogenes* and resident microorganisms from food industry premises. *International Journal of Food Microbiology* **97**, 111-122.

Carvalho, E.L.S., Grenha, A., Remuñán-López, C., Alonso, M.J. and Seijo, B. (2009) Chapter 15 Mucosal Delivery of Liposome-Chitosan Nanoparticle Complexes. *Methods in Enzymology* **465**, 289-312.

CDC (2012) Multistate Outbreak of Listeriosis Linked to Whole Cantaloupes from Jensen Farms, Colorado (FINAL UPDATE). https://www.cdc.gov/listeria/outbreaks/cantaloupes-jensen-farms/index.html

CDC (2013) Vital Signs: *Listeria* Illnesses, Deaths, and Outbreaks — United States, 2009–2011. https://www.cdc.gov/mmwr/preview/mmwrhtml/mm6222a4.htm

CDC (2019) *Pseudomonas aeruginosa*. https://www.cdc.gov/hai/organisms/pseudomonas.html

CDC (2020) Outbreak of *Salmonella Newport* Infections Linked to Onions. https://www.cdc.gov/salmonella/newport-07-20/index.html

CDC (2021) *Listeria* Outbreaks. https://www.cdc.gov/media/releases/2021/s0224-listeria-outbreak.html

Ceri, H., Olson, M., Stremick, C., Read, R., Morck, D. and Buret, A. (1999) The Calgary Biofilm Device: new technology for rapid determination of antibiotic susceptibilities of bacterial biofilms. *Journal of Clinical Microbiology* **37**, 1771-1776.

Chamchoy, K., Pakotiprapha, D., Pumirat, P., Leartsakulpanich, U. and Boonyuen, U. (2019) Application of WST-8 based colorimetric NAD(P)H detection for quantitative dehydrogenase assays. *BMC Biochemistry* **20**, 4.

Chapman, M.R., Robinson, L.S., Pinkner, J.S., Roth, R., Heuser, J., Hammar, M., Normark, S. and Hultgren, S.J. (2002) Role of *Escherichia coli* curli operons in directing amyloid fiber formation. *Science* **295**, 851-855.

Charlton, B.R., Kinde, H. and Jensen, L.H. (1990) Environmental survey for *Listeria* species in California milk processing plants. *Journal of Food Protection* **53**, 198-201.

Chavez de Paz, L.E., Resin, A., Howard, K.A., Sutherland, D.S. and Wejse, P.L. (2011) Antimicrobial effect of chitosan nanoparticles on streptococcus mutans biofilms. *Applied and Environmental Microbiology* **77**, 3892-3895.

Cheng, M.I., Chen, C., Engström, P., Portnoy, D.A. and Mitchell, G. (2018) Actin-based motility allows *Listeria monocytogenes* to avoid autophagy in the macrophage cytosol. *Cellular Microbiology* **20**, e12854.

Chheda, A. and Vernekar, M. (2015) A natural preservative ε-poly-L-lysine: fermentative production and applications in food industry. *International Food Research Journal* **22**.

Chi, E., Mehl, T., Nunn, D. and Lory, S. (1991) Interaction of *Pseudomonas aeruginosa* with A549 pneumocyte cells. *Infection and Immunity* **59**, 822-828.

Chirwa, N.T. and Herrington, M.B. (2003) CsgD, a regulator of curli and cellulose synthesis, also regulates serine hydroxymethyltransferase synthesis in *Escherichia coli* K-12. *Microbiology* **149**, 525-535.

Christensen, B.B., Sternberg, C., Andersen, J.B., Eberl, L., Møller, S., Givskov, M. and Molin, S. (1998) Establishment of new genetic traits in a microbial biofilm community. *Applied and Environmental Microbiology* **64**, 2247-2255.

Ciofu, O. and Tolker-Nielsen, T. (2019) Tolerance and Resistance of *Pseudomonas aeruginosa* Biofilms to Antimicrobial Agents—How *P. aeruginosa* Can Escape Antibiotics. *Frontiers in Microbiology* **10**.

Clausen, M., Koomey, M. and Maier, B. (2009) Dynamics of type IV pili is controlled by switching between multiple states. *Biophysical Journal* **96**, 1169-1177.

Collinson, S., Doig, P., Doran, J., Clouthier, S. and Kay, W. (1993) Thin, aggregative fimbriae mediate binding of *Salmonella* Enteritidis to fibronectin. *Journal of Bacteriology* **175**, 12-18.

Collinson, S., Emödy, L., Müller, K. and Kay, W. (1991) Purification and characterization of thin, aggregative fimbriae from *Salmonella* enteritidis. *Journal of Bacteriology* **173**, 4773-4781.

Comolli, J.C., Waite, L.L., Mostov, K.E. and Engel, J.N. (1999) Pili binding to asialo-GM1 on epithelial cells can mediate cytotoxicity or bacterial internalization by *Pseudomonas aeruginosa*. *Infection and Immunity* **67**, 3207-3214.

Costerton, J.W., Stewart, P.S. and Greenberg, E.P. (1999) Bacterial biofilms: a common cause of persistent infections. *Science* **284**, 1318-1322.

Cornelis, P. (2020). Putting an end to the *Pseudomonas aeruginosa* IQS controversy. *Microbiologyopen*, 9(2), e962.

Craig, L., Forest, K.T. and Maier, B. (2019) Type IV pili: dynamics, biophysics and functional consequences. *Nature Reviews Microbiology* **17**, 429-440.

Cramton, S.E., Gerke, C., Schnell, N.F., Nichols, W.W. and Götz, F. (1999) The intercellular adhesion (ica) locus is present in *Staphylococcus aureus* and is required for biofilm formation. *Infection and Immunity* **67**, 5427-5433.

Cramton, S.E., Ulrich, M., Götz, F. and Döring, G. (2001) Anaerobic conditions induce expression of polysaccharide intercellular adhesin in *Staphylococcus aureus* and *Staphylococcus epidermidis*. *Infection and Immunity* **69**, 4079-4085.

Cucarella, C., Solano, C., Valle, J., Amorena, B., Lasa, Í. and Penadés, J.R. (2001) Bap, a *Staphylococcus aureus* surface protein involved in biofilm formation. *Journal of Bacteriology* **183**, 2888-2896.

Czeczulin, J.R., Balepur, S., Hicks, S., Phillips, A., Hall, R., Kothary, M.H., Navarro-Garcia, F. and Nataro, J.P. (1997) Aggregative adherence fimbria II, a second fimbrial antigen mediating aggregative adherence in enteroaggregative *Escherichia coli*. *Infection and Immunity* **65**, 4135-4145.

Czeczulin, J.R., Whittam, T.S., Henderson, I.R., Navarro-Garcia, F. and Nataro, J.P. (1999) Phylogenetic analysis of enteroaggregative and diffusely adherent *Escherichia coli*. *Infection and Immunity* **67**, 2692-2699.

D'Argenio, D.A., Calfee, M.W., Rainey, P.B. and Pesci, E.C. (2002) Autolysis and autoaggregation in *Pseudomonas aeruginosa* colony morphology mutants. *Journal of Bacteriology* **184**, 6481-6489.

Davies, D.G., Parsek, M.R., Pearson, J.P., Iglewski, B.H., Costerton, J.W. and Greenberg, E.P. (1998) The involvement of cell-to-cell signals in the development of a bacterial biofilm. *Science* **280**, 295-298.

de las Heras, A., Cain, R.J., Bielecka, M.K. and Vazquez-Boland, J.A. (2011) Regulation of *Listeria* virulence: PrfA master and commander. *Current Opinion in Microbiology* **14**, 118-127.

de Paz, L.E.C., Resin, A., Howard, K.A., Sutherland, D.S. and Wejse, P.L. (2011) Antimicrobial effect of chitosan nanoparticles on *Streptococcus mutans* biofilms. *Applied and Environmental Microbiology* **77**, 3892-3895.

Déziel, E., Comeau, Y. and Villemur, R. (2001a) Initiation of biofilm formation by *Pseudomonas aeruginosa* 57RP correlates with emergence of hyperpiliated and highly adherent phenotypic variants deficient in swimming, swarming, and twitching motilities. *Journal of Bacteriology* **183**, 1195-1204.

Déziel, E., Comeau, Y. and Villemur, R.J.J.o.b. (2001b) Initiation of biofilm formation by *Pseudomonas aeruginosa* 57RP correlates with emergence of hyperpiliated and highly adherent phenotypic variants deficient in swimming, swarming, and twitching motilities. *Journal of Bacteriology* **183**, 1195-1204.

Di Bonaventura, G., Piccolomini, R., Paludi, D., D'Orio, V., Vergara, A., Conter, M. and Ianieri, A. (2008) Influence of temperature on biofilm formation by *Listeria monocytogenes* on various food-contact surfaces: Relationship with motility and cell surface hydrophobicity. *Journal of Applied Microbiology* **104**, 1552-1561.

Di Ciccio, P., Conter, M., Zanardi, E., Ghidini, S., Vergara, A., Paludi, D., Festino, A. and Ianieri, A. (2012) *Listeria monocytogenes*: Biofilms in food processing. *Italian Journal of Food Science* **24**, 203.

Dibb-Fuller, M., Allen-Vercoe, E., Thorns, C. and Woodward, M.J. (1999) Fimbriae-and flagella-mediated association with and invasion of cultured epithelial cells by *Salmonella* Enteritidis. *Microbiology* **145**, 1023-1031.

Diggle, S., Winzer, K., Chhabra, S., Worrall, K., Cámara, M. and Williams, P. (2003) The *Pseudomonas aeruginosa* quinolone signal molecule moderates the production of rhl-dependent quorum sensing phenotypes and promotes biofilm development. *Molecular Microbiology* **50**, 29-43.

Djordjevic, D., Wiedmann, M. and McLandsborough, L. (2002) Microtiter plate assay for assessment of *Listeria monocytogenes* biofilm formation. *Applied and environmental microbiology* **68**, 2950-2958.

Donelli, G. (2014) *Biofilm-based healthcare-associated infections: Volume II*: Springer.

Donlan, R., Murga, R., Carpenter, J., Brown, E., Besser, R. and Fields, B. (2001) Monochloramine disinfection of biofilm-associated *Legionella pneumophila* in a potable water model system. *Legionella*, 406-410.

Donlan, R.M. (2002) Biofilms: microbial life on surfaces. *Emerging Infectious Dieases* **8**, 881.

Doumith, M., Buchrieser, C., Glaser, P., Jacquet, C. and Martin, P. (2004) Differentiation of the major *Listeria monocytogenes* serovars by multiplex PCR. *Journal of Clinical Microbiology* **42**, 3819-3822.

Drake, D. and Montie, T.C. (1988) Flagella, motility and invasive virulence of *Pseudomonas aeruginosa*. *Microbiology* **134**, 43-52.

Dramsi, S., Biswas, I., Maguin, E., Braun, L., Mastroeni, P. and Cossart, P. (1995) Entry of *Listeria monocytogenes* into hepatocytes requires expression of InlB, a surface protein of the internalin multigene family. *Molecular Microbiology* **16**, 251-261.

Drolia, R., Amalaradjou, M.A.R., Ryan, V., Tenguria, S., Liu, D., Bai, X., Xu, L., Singh, A.K., Cox, A.D., Bernal-Crespo, V., Schaber, J.A., Applegate, B.M., Vemulapalli, R. and Bhunia, A.K. (2020) Receptor-targeted engineered probiotics mitigate lethal *Listeria* infection. *Nature Communications* **11**, 6344.

Drolia, R. and Bhunia, A.K. (2019) Crossing the intestinal barrier via *Listeria* adhesion protein and internalin A. *Trends in Microbiology* **27**, 408-425.

Drolia, R., Tenguria, S., Durkes, A.C., Turner, J.R. and Bhunia, A.K. (2018) Listeria Adhesion Protein Induces Intestinal Epithelial Barrier Dysfunction for Bacterial Translocation. *Cell Host and Microbe* **23**, 470-484.e477.

Duan, C., Meng, X., Meng, J., Khan, M.I.H., Dai, L., Khan, A., An, X., Zhang, J., Huq, T. and Ni, Y. (2019) Chitosan as a preservative for fruits and vegetables: a review on chemistry and antimicrobial properties. *Journal of Bioresources and Bioproducts* **4**, 11-21.

Duarte, A.E., De Menezes, I.R.A., Bezerra Morais Braga, M.F., Leite, N.F., Barros, L.M., Waczuk, E.P., Pessoa da Silva, M.A., Boligon, A., Teixeira Rocha, J.B. and Souza, D.O. (2016) Antimicrobial activity and Modulatory effect of essential oil from the leaf of *Rhaphiodon echinus* (Nees & Mart) Schauer on some antimicrobial drugs. *Molecules* **21**, 743.

Elias, S. and Banin, E. (2012) Multi-species biofilms: living with friendly neighbors. *FEMS Microbiology Reviews* **36**, 990-1004.

Ellison, C.K., Kan, J., Dillard, R.S., Kysela, D.T., Ducret, A., Berne, C., Hampton, C.M., Ke, Z., Wright, E.R. and Biais, N. (2017) Obstruction of pilus retraction stimulates bacterial surface sensing. *Science* **358**, 535-538.

Esmaeili, A. and Asgari, A. (2015) In vitro release and biological activities of Carum copticum essential oil (CEO) loaded chitosan nanoparticles. *International Journal of Biological Macromolecules* **81**, 283-290.

Fang, L., Wolmarans, B., Kang, M., Jeong, K.C. and Wright, A.C. (2015) Application of chitosan microparticles for reduction of Vibrio species in seawater and live oysters (Crassostrea virginica). *Applied and Environmental Microbiology* **81**, 640-647.

Farrow, J.M., Sund, Z.M., Ellison, M.L., Wade, D.S., Coleman, J.P. and Pesci, E.C. (2008) PqsE functions independently of PqsR-*Pseudomonas* quinolone signal and enhances the rhl quorum-sensing system. *Journal of Bacteriology* **190**, 7043-7051.

Favero, M., Carson, L., Bond, W. and Petersen, N. (1971) *Pseudomonas aeruginosa*: growth in distilled water from hospitals. *Science* **173**, 836-838.

FDA (2013) GRAS notices: shrimp-derived chitosan. https://www.fda.gov/food/generally-recognized-safe-gras/gras-notice-inventory

Feldman, M., Bryan, R., Rajan, S., Scheffler, L., Brunnert, S., Tang, H. and Prince, A. (1998) Role of flagella in pathogenesis of *Pseudomonas aeruginosa* pulmonary infection. *Infection and immunity* **66**, 43-51.

Ferreira, V., Wiedmann, M., Teixeira, P. and Stasiewicz, M.J. (2014) *Listeria monocytogenes* persistence in food-associated environments: Epidemiology, strain characteristics, and implications for public health. *Journal of Food Protection* **77**, 150-170.

Flemming, H.-C., Neu, T.R. and Wozniak, D.J. (2007) The EPS matrix: the "house of biofilm cells". *Journal of Bacteriology* **189**, 7945-7947.

Flemming, H.-C. and Wingender, J. (2010) The biofilm matrix. *Nature Reviews Microbiology* **8**, 623-633.

Flemming, H.-C., Wingender, J., Szewzyk, U., Steinberg, P., Rice, S.A. and Kjelleberg, S. (2016) Biofilms: an emergent form of bacterial life. *Nature Reviews Microbiology* **14**, 563.

Fong, J.N. and Yildiz, F.H. (2015) Biofilm matrix proteins. *Microbial Biofilms*, 201-222.

Fournomiti, M., Kimbaris, A., Mantzourani, I., Plessas, S., Theodoridou, I., Papaemmanouil, V., Kapsiotis, I., Panopoulou, M., Stavropoulou, E. and Bezirtzoglou, E.E. (2015) Antimicrobial activity of essential oils of cultivated oregano (Origanum vulgare), sage (Salvia officinalis), and thyme (Thymus vulgaris) against clinical isolates of *Escherichia coli*, *Klebsiella oxytoca*, and *Klebsiella pneumoniae*. *Microbial Ecology in Health and Disease* **26**, 23289.

Francois, P., Tu Quoc, P.H., Bisognano, C., Kelley, W.L., Lew, D.P., Schrenzel, J., Cramton, S.E., Götz, F. and Vaudaux, P. (2003) Lack of biofilm contribution to bacterial colonisation in an experimental model of foreign body infection by *Staphylococcus aureus* and *Staphylococcus epidermidis*. *FEMS Immunology & Medical Microbiology* **35**, 135-140.

Frank, C., Werber, D., Cramer, J.P., Askar, M., Faber, M., an der Heiden, M., Bernard, H., Fruth, A., Prager, R. and Spode, A. (2011) Epidemic profile of Shiga-toxin–producing *Escherichia coli* O104: H4 outbreak in Germany. *New England Journal of Medicine* **365**, 1771-1780.

Frank, J.F., Gillett, R.A. and Ware, G.O. (1990) Association of Listeria spp. contamination in the dairy processing plant environment with the presence of staphylococci. *Journal of Food Protection* **53**, 928-932.

Freitag, N.E., Port, G.C. and Miner, M.D. (2009) *Listeria monocytogenes* from saprophyte to intracellular pathogen. *Nature Reviews Microbiology* **7**, 623-628.

Friedman, L. and Kolter, R. (2004a) Genes involved in matrix formation in *Pseudomonas aeruginosa* PA14 biofilms. *Molecular Microbiology* **51**, 675-690.

Friedman, L. and Kolter, R. (2004b) Two genetic loci produce distinct carbohydrate-rich structural components of the *Pseudomonas aeruginosa* biofilm matrix. *Journal of Bacteriology* **186**, 4457-4465.

Friedman, M. (2006) Antibiotic activities of plant compounds against non-resistant and antibiotic-resistant foodborne human pathogens. Advances in Microbial Food Safety, Chapter 12, pp 167-183

Frost, L. and Paranchych, W.J.J.o.b. (1977) Composition and molecular weight of pili purified from *Pseudomonas aeruginosa* K. *Journal of Bacteriology* **131**, 259-269.

Fu, Y., Deering, A.J., Bhunia, A.K. and Yao, Y. (2017) Pathogen biofilm formation on cantaloupe surface and its impact on the antibacterial effect of lauroyl arginate ethyl. *Food Microbiol* **64**, 139-144.

Galié, S., García-Gutiérrez, C., Miguélez, E.M., Villar, C.J. and Lombó, F. (2018) Biofilms in the food industry: Health aspects and control methods. *Frontiers in Microbiology* **9**.

Gallagher, L.A., McKnight, S.L., Kuznetsova, M.S., Pesci, E.C. and Manoil, C. (2002) Functions required for extracellular quinolone signaling by *Pseudomonas aeruginosa. Journal of Bacteriology* **184**, 6472-6480.

Geornaras, I., Yoon, Y., Belk, K., Smith, G. and Sofos, J. (2007) Antimicrobial activity of ε-polylysine against *Escherichia coli* O157: H7, *Salmonella* Typhimurium, and *Listeria monocytogenes* in various food extracts. *Journal of Food Science* **72**, M330-M334.

Gerke, C., Kraft, A., Süßmuth, R., Schweitzer, O. and Götz, F. (1998) Characterization of theN-Acetylglucosaminyltransferase Activity Involved in the Biosynthesis of the *Staphylococcus epidermidis* Polysaccharide Intercellular Adhesin. *Journal of Biological Chemistry* **273**, 18586-18593.

Gilmartin, N., Gião, M.S., Keevil, C.W. and O'Kennedy, R. (2016) Differential internalin A levels in biofilms of *Listeria monocytogenes* grown on different surfaces and nutrient conditions. *International Journal of Food Microbiology* **219**, 50-55.

Goldsworthy, M.J.H. (2008) Gene expression of Pseudomonas aeruginosa and MRSA within a catheter-associated urinary tract infection biofilm model. *Bioscience Horizons* **1**, 28-37.

González, J.E. and Keshavan, N.D. (2006) Messing with bacterial quorum sensing. *Microbiology and Molecular Biology Reviews* **70**, 859-875.

Gouin, E., Adib-Conquy, M., Balestrino, D., Nahori, M.-A., Villiers, V., Colland, F., Dramsi, S., Dussurget, O. and Cossart, P. (2010) The *Listeria monocytogenes* InlC protein interferes with innate immune responses by targeting the I kappa B kinase subunit IKK alpha. *Proceedings of National Academy of Science U S A* **107**, 17333-17338.

Gray, K.M., Banada, P.P., O'Neal, E. and Bhunia, A.K. (2005) Rapid Ped-2E9 cell-based cytotoxicity analysis and genotyping of *Bacillus* species. *Journal of Clinical Microbiology* **43**, 5865-5872.

Gray, M.L. and Killinger, A. (1966) *Listeria monocytogenes* and listeric infections. *Bacteriological Reviews* **30**, 309.

Guilbaud, M., Piveteau, P., Desvaux, M., Brisse, S. and Briandet, R. (2015) Exploring the diversity of *Listeria monocytogenes* biofilm architecture by high-throughput confocal laser scanning microscopy and the predominance of the honeycomb-like morphotype. *Applied and Environmental Microbiology* **81**, 1813-1819.

Hahn, H.P.J.G. (1997) The type-4 pilus is the major virulence-associated adhesin of *Pseudomonas aeruginosa*–a review. *Gene* **192**, 99-108.

Hall-Stoodley, L., Costerton, J.W. and Stoodley, P. (2004) Bacterial biofilms: From the natural environment to infectious diseases. *Nature Reviews Microbiology* **2**, 95-108.

Hammar, M.r., Arnqvist, A., Bian, Z., Olsén, A. and Normark, S. (1995) Expression of two csg operons is required for production of fibronectin-and congo red-binding curli polymers in *Escherichia coli* K-12. *Molecular Microbiology* **18**, 661-670.

Hamon, M., Bierne, H. and Cossart, P. (2006) *Listeria monocytogenes*: a multifaceted model. *Nature Reviews Microbiology* **4**, 423-434.

Harmsen, M., Lappann, M., Knøchel, S. and Molin, S. (2010) Role of extracellular DNA during biofilm formation by *Listeria monocytogenes*. *Applied and Environmental Microbiology* **76**, 2271-2279.

Haynes, S., Darby, A., Daniell, T., Webster, G., Van Veen, F., Godfray, H., Prosser, J.I. and Douglas, A. (2003) Diversity of bacteria associated with natural aphid populations. *Applied and Environmental Microbiology* **69**, 7216-7223.

Hendriksen, R.S., Vieira, A.R., Karlsmose, S., Wong, D.M.A.L.F., Jensen, A.B., Wegener, H.C. and Aarestrup, F.M. (2011) Global Monitoring of *Salmonella* serovar distribution from the World

Health Organization global foodborne infections network country data bank: Results of quality assured laboratories from 2001 to 2007. *Foodborne Pathogens and Disease* **8**, 887-900.

Henry, R., Shaughnessy, L., Loessner, M.J., Alberti-Segui, C., Higgins, D.E. and Swanson, J.A. (2006) Cytolysin-dependent delay of vacuole maturation in macrophages infected with *Listeria monocytogenes*. *Cellular Microbiology* **8**, 107-119.

Hentges, D.J., Stein, A.J., Casey, S.W. and Que, J.U. (1985) Protective role of intestinal flora against infection with *Pseudomonas aeruginosa* in mice: influence of antibiotics on colonization resistance. *Infection and Immunity* **47**, 118-122.

Hiraki, J., Ichikawa, T., Ninomiya, S.-i., Seki, H., Uohama, K., Seki, H., Kimura, S., Yanagimoto, Y. and Barnett Jr, J.W. (2003) Use of ADME studies to confirm the safety of ε-polylysine as a preservative in food. *Regulatory Toxicology and Pharmacology* **37**, 328-340.

Høiby, N., Bjarnsholt, T., Givskov, M., Molin, S. and Ciofu, O. (2010) Antibiotic resistance of bacterial biofilms. *International Journal of Antimicrobial Agents* **35**, 322-332.

Horn, N. and Bhunia, A.K. (2018) Food-Associated Stress Primes Foodborne Pathogens for the Gastrointestinal Phase of Infection. *Frontiers in Microbiology* **9**, 1962.

Huang, D., Xu, J.-G., Liu, J.-X., Zhang, H. and Hu, Q. (2014) Chemical constituents, antibacterial activity and mechanism of action of the essential oil from Cinnamomum cassia bark against four food-related bacteria. *Microbiology* **83**, 357-365.

Huang, M., Khor, E. and Lim, L.-Y. (2004) Uptake and cytotoxicity of chitosan molecules and nanoparticles: effects of molecular weight and degree of deacetylation. *Pharmaceutical Research* **21**, 344-353.

Hyldgaard, M., Mygind, T., Vad, B.S., Stenvang, M., Otzen, D.E. and Meyer, R.L. (2014) The antimicrobial mechanism of action of epsilon-poly-L-lysine. *Applied and Environmental Microbiology* **80**, 7758-7770.

Ibusquiza, P.S., Herrera, J.J.R. and Cabo, M.L. (2011) Resistance to benzalkonium chloride, peracetic acid and nisin during formation of mature biofilms by *Listeria monocytogenes*. *Food Microbiology* **28**, 418-425.

Illum, L., Jabbal-Gill, I., Hinchcliffe, M., Fisher, A. and Davis, S. (2001) Chitosan as a novel nasal delivery system for vaccines. *Advanced Drug Delivery Reviews* **51**, 81-96.

Islam, M., Doyle, M.P., Phatak, S.C., Millner, P. and Jiang, X. (2004) Persistence of enterohemorrhagic *Escherichia coli* O157: H7 in soil and on leaf lettuce and parsley grown in fields treated with contaminated manure composts or irrigation water. *Journal of Food Protection* **67**, 1365-1370.

Ivanek, R., Gröhn, Y.T., Tauer, L.W. and Wiedmann, M. (2005) The cost and benefit of *Listeria monocytogenes* food safety measures. *Critical Reviews in food Scince and Nutrition* **44**, 513-523.

Jackson, B.R., Griffin, P.M., Cole, D., Walsh, K.A. and Chai, S.J. (2013) Outbreak-associated *Salmonella enterica* serotypes and food commodities, United States, 1998-2008. *Emerging Infectious Diseases* **19**, 1239-1244.

Jagadeesan, B., Fleishman Littlejohn, A.E., Amalaradjou, M.A.R., Singh, A.K., Mishra, K.K., La, D., Kihara, D. and Bhunia, A.K. (2011) N-Terminal Gly_{224} - Gly_{411} domain in *Listeria* adhesion protein interacts with host receptor Hsp60. *PLoS One* **6**, e20694.

Jagadeesan, B., Koo, O.K., Kim, K.P., Burkholder, K.M., Mishra, K.K., Aroonnual, A. and Bhunia, A.K. (2010) LAP, an alcohol acetaldehyde dehydrogenase enzyme in *Listeria* promotes bacterial adhesion to enterocyte-like Caco-2 cells only in pathogenic species. *Microbiology-SGM* **156**, 2782-2795.

Janes, K.A., Fresneau, M.P., Marazuela, A., Fabra, A. and Alonso, M.a.J. (2001) Chitosan nanoparticles as delivery systems for doxorubicin. *Journal of Controlled Release* **73**, 255-267.

Jaradat, Z., Schutze, G. and Bhunia, A. (2002) Genetic homogeneity among *Listeria monocytogenes* strains from infected patients and meat products from two geographic locations determined by phenotyping, ribotyping and PCR analysis of virulence genes. *International Journal of Food Microbiology* **76**, 1-10.

Jaradat, Z.W. and Bhunia, A.K. (2002) Glucose and nutrient concentrations affect the expression of a 104-kilodalton *Listeria* adhesion protein in *Listeria monocytogenes*. *Applied and Environmental Microbiology* **68**, 4876-4883.

Jennings, L.K., Storek, K.M., Ledvina, H.E., Coulon, C., Marmont, L.S., Sadovskaya, I., Secor, P.R., Tseng, B.S., Scian, M. and Filloux, A. (2015) Pel is a cationic exopolysaccharide that cross-links extracellular DNA in the Pseudomonas aeruginosa biofilm matrix. *Proceedings of the National Academy of Sciences* **112**, 11353-11358.

Joseph, D., Cruz-romero, M., Collins, T., Cummins, E., Kerry, J.P. and Morris, M.A. (2018) Synthesis of monodisperse chitosan nanoparticles. *Food Hydrocolloids* **83**, 355-364.

Karpanen, T.J., Worthington, T., Hendry, E., Conway, B.R. and Lambert, P.A. (2008) Antimicrobial efficacy of chlorhexidine digluconate alone and in combination with eucalyptus oil, tea tree oil and thymol against planktonic and biofilm cultures of *Staphylococcus epidermidis*. *Journal of Antimicrobial Chemotherapy* **62**, 1031-1036.

Kazmierczak, M.J., Wiedmann, M. and Boor, K.J. (2006) Contributions of *Listeria monocytogenes* SigB and PrfA to expression of virulence and stress response genes during extra- and intracellular growth. *Microbiology* **152**, 1827-1838.

Kim, K.P., Jagadeesan, B., Burkholder, K.M., Jaradat, Z.W., Wampler, J.L., Lathrop, A.A., Morgan, M.T. and Bhunia, A.K. (2006) Adhesion characteristics of Listeria adhesion protein (LAP)-expressing *Escherichia coli* to Caco-2 cells and of recombinant LAP to eukaryotic receptor Hsp60 as examined in a surface plasmon resonance sensor. *FEMS Microbiology Letters* **256**, 324-332.

Kirk, M.D., Pires, S.M., Black, R.E., Caipo, M., Crump, J.A., Devleesschauwer, B., Doepfer, D., Fazil, A., Fischer-Walker, C.L., Hald, T., Hall, A.J., Keddy, K.H., Lake, R.J., Lanata, C.F., Torgerson, P.R., Havelaar, A.H. and Angulo, F.J. (2015) World Health Organization estimates of the global and regional disease burden of 22 foodborne bacterial, protozoal, and viral diseases, 2010: A data synthesis. *Plos Medicine* **12**, e1001921.

Kisluk, G. and Yaron, S. (2012) Presence and persistence of *Salmonella enterica serotype* Typhimurium in the phyllosphere and rhizosphere of spray-irrigated parsley. *Applied and Environmental Microbiology* **78**, 4030-4036.

Klausen, M., Heydorn, A., Ragas, P., Lambertsen, L., Aaes-Jørgensen, A., Molin, S. and Tolker-Nielsen, T.J.M.m. (2003) Biofilm formation by *Pseudomonas aeruginosa* wild type, flagella and type IV pili mutants. *Molecular Microbiology* **48**, 1511-1524.

Knezevic, P., Aleksic, V., Simin, N., Svircev, E., Petrovic, A. and Mimica-Dukic, N. (2016) Antimicrobial activity of Eucalyptus camaldulensis essential oils and their interactions with conventional antimicrobial agents against multi-drug resistant Acinetobacter baumannii. *Journal of Ethnopharmacology* **178**, 125-136.

Kobayashi, S.D. and DeLeo, F.R. (2013) *Staphylococcus aureus* protein A promotes immune suppression. *MBio* **4**.

Kocks, C., Gouin, E., Tabouret, M., Berche, P., Ohayon, H. and Cossart, P. (1992) *L. monocytogenes*-induced actin assembly requires the actA gene product, a surface protein. *Cell* **68**, 521-531.

Kokare, C., Chakraborty, S., Khopade, A. and Mahadik, K.R. (2009) Biofilm: Importance and applications. *Indian Journal of Biotechnology* **8**, 159-168.

Kortebi, M., Milohanic, E., Mitchell, G., Péchoux, C., Prevost, M.-C., Cossart, P. and Bierne, H. (2017) *Listeria monocytogenes* switches from dissemination to persistence by adopting a vacuolar lifestyle in epithelial cells. *PLoS Pathogens* **13**, e1006734.

Kreft, J. and Vázquez-Boland, J.A. (2001) Regulation of virulence genes in *Listeria*. *International Journal of Medical Microbiology* **291**, 145-157.

Kubota, H., Senda, S., Tokuda, H., Uchiyama, H. and Nomura, N. (2009) Stress resistance of biofilm and planktonic *Lactobacillus plantarum subsp. plantarum* JCM 1149. *Food Microbiol* **26**, 592-597.

Landini, P., Antoniani, D., Burgess, J.G. and Nijland, R. (2010) Molecular mechanisms of compounds affecting bacterial biofilm formation and dispersal. *Applied Microbiology and Biotechnology* **86**, 813-823.

Larsen, P., Nielsen, J.L., Otzen, D. and Nielsen, P.H. (2008) Amyloid-like adhesins produced by floc-forming and filamentous bacteria in activated sludge. *Applied and Environmental Microbiology* **74**, 1517-1526.

Lasa, I., Gouin, E., Goethals, M., Vancompernolle, K., David, V., Vandekerckhove, J. and Cossart, P. (1997) Identification of two regions in the N-terminal domain of ActA involved in the actin comet tail formation by *Listeria monocytogenes*. *The EMBO Journal* **16**, 1531-1540.

Latasa, C., Roux, A., Toledo-Arana, A., Ghigo, J.M., Gamazo, C., Penadés, J.R. and Lasa, I. (2005) BapA, a large secreted protein required for biofilm formation and host colonization of *Salmonella enterica serovar* Enteritidis. *Molecular Microbiology* **58**, 1322-1339.

Lathrop, A.A., Jaradat, Z.W., Haley, T. and Bhunia, A.K. (2003) Characterization and application of a *Listeria monocytogenes* reactive monoclonal antibody C11E9 in a resonant mirror biosensor. *Journal of Immunological Methods* **281**, 119-128.

Lawrence, J., Korber, D., Hoyle, B., Costerton, J.W. and Caldwell, D. (1991) Optical sectioning of microbial biofilms. *Journal of Bacteriology* **173**, 6558-6567.

Lebeaux, D., Chauhan, A., Rendueles, O. and Beloin, C. (2013) From *in vitro* to *in vivo* models of bacterial biofilm-related infections. *Pathogens* **2**, 288-356.

Lecuit, M., Dramsi, S., Gottardi, C., Fedor-Chaiken, M., Gumbiner, B. and Cossart, P. (1999a) A single amino acid in E-cadherin responsible for host specificity towards the human pathogen *Listeria monocytogenes*. *EMBO Journal* **18**, 3956 - 3963.

Lecuit, M., Dramsi, S., Gottardi, C., Fedor-Chaiken, M., Gumbiner, B. and Cossart, P. (1999b) A single amino acid in E-cadherin responsible for host specificity towards the human pathogen *Listeria monocytogenes*. *The EMBO Journal* **18**, 3956 - 3963.

Lecuit, M., Ohayon, H., Braun, L., Mengaud, J. and Cossart, P. (1997) Internalin of *Listeria monocytogenes* with an intact leucine-rich repeat region is sufficient to promote internalization. *Infection and Immunity* **65**, 5309-5319.

Lecuit, M., Vandormael-Pournin, S., Lefort, J., Huerre, M., Gounon, P., Dupuy, C., Babinet, C. and Cossart, P. (2001) A transgenic model for listeriosis: role of internalin in crossing the intestinal barrier. *Science* **292**, 1722-1725.

Lee, J., Wu, J., Deng, Y., Wang, J., Wang, C., Wang, J., Chang, C., Dong, Y., Williams, P. and Zhang, L.-H. (2013) A cell-cell communication signal integrates quorum sensing and stress response. *Nature Chemical Biology* **9**, 339.

Lee, J. and Zhang, L. (2015) The hierarchy quorum sensing network in *Pseudomonas aeruginosa*. *Protein & Cell* **6**, 26-41.

Lee, K.W.K., Periasamy, S., Mukherjee, M., Xie, C., Kjelleberg, S. and Rice, S.A. (2014) Biofilm development and enhanced stress resistance of a model, mixed-species community biofilm. *The ISME Journal* **8**, 894-907.

Leimeister-Wächter, M., Domann, E. and Chakraborty, T. (1992) The expression of virulence genes in *Listeria monocytogenes* is thermoregulated. *Journal of Bacteriology* **174**, 947-952.

Lemon, K.P., Freitag, N.E. and Kolter, R. (2010) The virulence regulator PrfA promotes biofilm formation by *Listeria monocytogenes*. *Journal of Bacteriology* **192**, 3969-3976.

Lépine, F., Milot, S., Déziel, E., He, J. and Rahme, L.G. (2004) Electrospray/mass spectrometric identification and analysis of 4-hydroxy-2-alkylquinolines (HAQs) produced by *Pseudomonas aeruginosa*. *Journal of the American Society for Mass Spectrometry* **15**, 862-869.

Limoli, D.H., Jones, C.J. and Wozniak, D.J. (2015) Bacterial extracellular polysaccharides in biofilm formation and function. *Microbial Biofilms*, 223-247.

Lingnau, A., Domann, E., Hudel, M., Bock, M., Nichterlein, T., Wehland, J. and Chakraborty, T. (1995) Expression of the *Listeria monocytogenes* EGD *inlA* and *inlB* genes, whose products mediate bacterial entry into tissue culture cell lines, by PrfA-dependent and PrfA-independent mechanisms. *Infection and Immun* **63**, 3896-3903.

Liu, D. (2008) *Handbook of Listeria monocytogenes*: CRC press.

Lopes-Luz, L., Mendonça, M., Bernardes Fogaça, M., Kipnis, A., Bhunia, A.K. and Bührer-Sékula, S. (2021) *Listeria monocytogenes*: review of pathogenesis and virulence determinants-targeted immunological assays. *Critical Reviews in Microbiology*, 1-20.

Louie, A., Zhang, T., Becattini, S., Waldor, M.K. and Portnoy, D.A. (2019) A multiorgan trafficking circuit provides purifying selection of *Listeria monocytogenes* virulence genes. *Mbio* **10**.

Lourenço, A., de Las Heras, A., Scortti, M., Vazquez-Boland, J., Frank, J.F. and Brito, L. (2013a) Comparison of *Listeria monocytogenes* exoproteomes from biofilm and planktonic state: Lmo2504, a protein associated with biofilms. *Applied and Environmental Microbiology* **79**, 6075-6082.

Lourenço, A., de Las Heras, A., Scortti, M., Vazquez-Boland, J., Frank, J.F. and Brito, L. (2013b) Comparison of *Listeria monocytogenes* exoproteomes from biofilm and planktonic state: Lmo2504, a protein associated with biofilms. *Appllied and Environmental Microbiology* **79**, 6075-6082.

Luo, Q., Shang, J., Feng, X., Guo, X., Zhang, L. and Zhou, Q. (2013) PrfA led to reduced biofilm formation and contributed to altered gene expression patterns in biofilm-forming *Listeria monocytogenes*. *Current Microbiology* **67**, 372-378.

Luo, Y. and Wang, Q. (2013) Recent advances of chitosan and its derivatives for novel applications in food science. *Journal of Food Processing & Beverages* **1**, 1-13.

Luque-Sastre, L., Fox, E.M., Jordan, K. and Fanning, S. (2018) A comparative study of the susceptibility of *Listeria* species to sanitizer treatments when grown under planktonic and biofilm conditions. *Journal of Food Protection* **81**, 1481-1490.

Lydon, M. and Rahme, L.G. (2011) Production of *Pseudomonas aeruginosa* Intercellular Small Signaling Molecules in Human Burn Wounds. *Journal of Pathogens*. Volume 2011 |Article ID 549302

Mack, D., Fischer, W., Krokotsch, A., Leopold, K., Hartmann, R., Egge, H. and Laufs, R. (1996) The intercellular adhesin involved in biofilm accumulation of *Staphylococcus epidermidis* is a linear beta-1, 6-linked glucosaminoglycan: purification and structural analysis. *Journal of Bacteriology* **178**, 175-183.

Mannarreddy, P., Denis, M., Munireddy, D., Pandurangan, R., Thangavelu, K.P. and Venkatesan, K. (2017) Cytotoxic effect of Cyperus rotundus rhizome extract on human cancer cell lines. *Biomedicine & Pharmacotherapy* **95**, 1375-1387.

Mao, H.-Q., Roy, K., Troung-Le, V.L., Janes, K.A., Lin, K.Y., Wang, Y., August, J.T. and Leong, K.W. (2001) Chitosan-DNA nanoparticles as gene carriers: synthesis, characterization and transfection efficiency. *Journal of Controlled Release* **70**, 399-421.

Marco, A.J., Altimira, J., Prats, N., Lopez, S., Dominguez, L., Domingo, M. and Briones, V. (1997) Penetration of *Listeria monocytogenes* in mice infected by the oral route. *Microbial Pathogenesis* **23**, 255-263.

Martins, K.B., Ferreira, A.M., Pereira, V.C., Pinheiro, L., Oliveira, A.d. and Cunha, M.d.L.R.d.S.d. (2019) *In vitro* effects of antimicrobial agents on planktonic and biofilm forms of *Staphylococcus saprophyticus* isolated from patients with urinary tract infections. *Frontiers in Microbiology* **10**, 40.

Mata, M.M., da Silva, W.P., Wilson, R., Lowe, E. and Bowman, J.P. (2015) Attached and planktonic *Listeria monocytogenes* global proteomic responses and associated influence of strain genetics and temperature. *Journal of Proteome Research* **14**, 1161-1173.

Mathipa, M.G. and Thantsha, M.S. (2015) Cocktails of probiotics pre-adapted to multiple stress factors are more robust under simulated gastrointestinal conditions than their parental counterparts and exhibit enhanced antagonistic capabilities against *Escherichia coli* and *Staphylococcus aureus*. *Gut Pathogens* **7**, 5.

Mathusa, E.C., Chen, Y.H., Enache, E. and Hontz, L. (2010) Non-O157 Shiga toxin-producing *Escherichia coli* in foods. *Journal of Food Protection* **73**, 1721-1736.

Maurice, N.M., Bedi, B. and Sadikot, R.T. (2018) *Pseudomonas aeruginosa* biofilms: host response and clinical implications in lung infections. *American Journal of Respiratory Cell and Molecular Biology* **58**, 428-439.

McGann, P., Wiedmann, M. and Boor, K.J. (2007) The alternative sigma factor B and the virulence gene regulator PrfA both regulate transcription of *Listeria monocytogenes* internalins. *Applied and Environmental Microbiology* **73**, 2919-2930.

McKenney, D., Pouliot, K.L., Wang, Y., Murthy, V., Ulrich, M., Döring, G., Lee, J.C., Goldmann, D.A. and Pier, G.B. (1999) Broadly protective vaccine for *Staphylococcus aureus* based on an *in vivo*-expressed antigen. *Science* **284**, 1523-1527.

McKnight, S.L., Manoil, C., Kuznetsova, M.S., Gallagher, L.A. and Pesci, E.C. (2002) Functions Required for Extracellular Quinolone Signaling by *Pseudomonas aeruginosa*. *Journal of Bacteriology*.

Mead, P.S., Slutsker, L., Dietz, V., McCaig, L.F., Bresee, J.S., Shapiro, C., Griffin, P.M. and Tauxe, R.V. (1999) Food-related illness and death in the United States. *Emerging Infectious Diseases* **5**, 607.

Mekonnen, A., Yitayew, B., Tesema, A. and Taddese, S. (2016) *In vitro* antimicrobial activity of essential oil of *Thymus schimperi*, *Matricaria chamomilla*, *Eucalyptus globulus*, and *Rosmarinus officinalis*. *International Journal of Microbiology* **2016**.

Mendez, E., Walker, D.K., Vipham, J. and Trinetta, V. (2020) The use of a CDC biofilm reactor to grow multi-strain *Listeria monocytogenes* biofilm. *Food Microbiology* **92**, 103592.

Mendonca, M., Conrad, N., Conceicao, F., Moreira, A., da Silva, W., Aleixo, J. and Bhunia, A. (2012) Highly specific fiber optic immunosensor coupled with immunomagnetic separation for detection of low levels of *Listeria monocytogenes* and *L. ivanovii*. *BMC Microbiology* **12**, 275.

Menon, A., Shroyer, M.L., Wampler, J.L., Chawan, C.B. and Bhunia, A.K. (2003a) *In vitro* study of *Listeria monocytogenes* infection to murine primary and human transformed B cells. *Comparative Immunology and Microbiology and Infectious Diseases* **26**, 157-174.

Menon, A., Shroyer, M.L., Wampler, J.L., Chawan, C.B. and Bhunia, A.K. (2003b) *In vitro* study of *Listeria monocytogenes* infection to murine primary and human transformed B cells. *Comparative Immunology, Microbiology and Infectious Diseases* **26**, 157-174.

Merino, N., Toledo-Arana, A., Vergara-Irigaray, M., Valle, J., Solano, C., Calvo, E., Lopez, J.A., Foster, T.J., Penadés, J.R. and Lasa, I. (2009) Protein A-mediated multicellular behavior in Staphylococcus aureus. *Journal of Bacteriology* **191**, 832-843.

Miao, J., Liang, Y., Chen, L., Wang, W., Wang, J., Li, B., Li, L., Chen, D. and Xu, Z. (2017) Formation and development of *Staphylococcus* biofilm: with focus on food safety. *Journal of Food Safety* **37**, e12358.

Mitchell, G., Ge, L., Huang, Q., Chen, C., Kianian, S., Roberts, M.F., Schekman, R. and Portnoy, D.A. (2015) Avoidance of autophagy mediated by PlcA or ActA is required for *Listeria monocytogenes* growth in macrophages. *Infection and Immunity* **83**, 2175-2184.

Molin, S. and Tolker-Nielsen, T. (2003) Gene transfer occurs with enhanced efficiency in biofilms and induces enhanced stabilisation of the biofilm structure. *Current Opinion in Biotechnology* **14**, 255-261.

Moltz, A.G. and Martin, S.E. (2005) Formation of biofilms by *Listeria monocytogenes* under various growth conditions. *Journal of Food Protection* **68**, 92-97.

Monk, I.R., Casey, P.G., Hill, C. and Gahan, C.G.M. (2010) Directed evolution and targeted mutagenesis to murinize *Listeria monocytogenes* internalin A for enhanced infectivity in the murine oral infection model. *BMC Microbiology* **10**, 318.

Moradali, M.F., Ghods, S. and Rehm, B.H. (2017) *Pseudomonas aeruginosa* lifestyle: a paradigm for adaptation, survival, and persistence. *Frontiers in Cellular and Infection Microbiology* **7**, 39.

Mu, H., Guo, F., Niu, H., Liu, Q., Wang, S. and Duan, J. (2014) Chitosan improves anti-biofilm efficacy of gentamicin through facilitating antibiotic penetration. *International Journal of Molecular Sciences* **15**, 22296-22308.

Mulvihill, E., van Pee, K., Mari, S.A., Müller, D.J. and Yildiz, O.z. (2015) Directly observing the lipid-dependent self-assembly and pore-forming mechanism of the cytolytic toxin listeriolysin O. *Nano Letters* **15**, 6965-6973.

Murray, E.G.D., Webb, R.A. and Swann, M.B.R. (1926) A disease of rabbits characterised by a large mononuclear leucocytosis, caused by a hitherto undescribed bacillus Bacterium monocytogenes *The Journal of Pathology and Bacteriology* **29**, 407-439.

Na, S., Kim, J.-H., Jang, H.-J., Park, H.J. and Oh, S.-W. (2018) Shelf life extension of Pacific white shrimp (*Litopenaeus vannamei*) using chitosan and ε-polylysine during cold storage. *International Journal of Biological Macromolecules* **115**, 1103-1108.

Newell, D.G., Koopmans, M., Verhoef, L., Duizer, E., Aidara-Kane, A., Sprong, H., Opsteegh, M., Langelaar, M., Threfall, J. and Scheutz, F. (2010) Food-borne diseases—the challenges of 20 years ago still persist while new ones continue to emerge. *International Journal of Food Microbiology* **139**, S3-S15.

Nguyen, P.Q., Botyanszki, Z., Tay, P.K.R. and Joshi, N.S. (2014) Programmable biofilm-based materials from engineered curli nanofibres. *Nature Communications* **5**, 1-10.

Nikitas, G., Deschamps, C., Disson, O., Niault, T., Cossart, P. and Lecuit, M. (2011) Transcytosis of *Listeria monocytogenes* across the intestinal barrier upon specific targeting of goblet cell accessible E-cadherin. *Journal of Experimental Medicine* **208**, 2263-2277.

No, H., Meyers, S.P., Prinyawiwatkul, W. and Xu, Z. (2007) Applications of chitosan for improvement of quality and shelf life of foods: a review. *Journal of Food Science* **72**, R87-R100.

NRC (2010) *National Research Council: Acute Exposure Guideline Levels for Selected Airborne Chemicals*. Washington (DC): National Academies Press (US).

O'Toole, G.A. and Kolter, R. (1998) Flagellar and twitching motility are necessary for Pseudomonas aeruginosa biofilm development. *Molecular Microbiology* **30**, 295-304.

Olsén, A., Jonsson, A. and Normark, S. (1989) Fibronectin binding mediated by a novel class of surface organelles on *Escherichia coli*. *Nature* **338**, 652-655.

Oozeer, R., Furet, J.P., Goupil-Feuillerat, N., Anba, J., Mengaud, J. and Corthier, G. (2005) Differential activities of four *Lactobacillus casei* promoters during bacterial transit through the gastrointestinal tracts of human-microbiota-associated mice. *Applied and Environmental Microbiology* **71**, 1356-1363.

Osborne, S.E. and Brumell, J.H. (2017) Listeriolysin O: from bazooka to Swiss army knife. *Philosophical Transactions of the Royal Society B: Biological Sciences* **372**, 20160222.

Pan, Y., Breidt, F. and Kathariou, S. (2006) Resistance of *Listeria monocytogenes* biofilms to sanitizing agents in a simulated food processing environment. *Applied and Environmental Microbiology* **72**, 7711-7717.

Pan, Y., Breidt, F. and Kathariou, S. (2009) Competition of *Listeria monocytogenes* serotype 1/2a and 4b strains in mixed-culture biofilms. *Applied and Environmental Microbiology* **75**, 5846-5852.

Pasteur, I. (2015) TOOL-Biofilm Microfermenters: Institut Pasteur.

Pier, G.B., Meluleni, G. and Goldberg, J.B. (1995) Clearance of *Pseudomonas aeruginosa* from the murine gastrointestinal tract is effectively mediated by O-antigen-specific circulating antibodies. *Infection and Immunity* **63**, 2818-2825.

Pillsbury, A., Chiew, M., Bates, J. and Sheppeard, V. (2013) An outbreak of staphylococcal food poisoning in a commercially catered buffet. *Communicable Diseases Intelligence* **37**, E144-E148.

Ponniah, J., Robin, T., Paie, M.S., Radu, S., Ghazali, F.M., Kqueen, C.Y., Nishibuchi, M., Nakaguchi, Y. and Malakar, P.K. (2010) *Listeria monocytogenes* in raw salad vegetables sold at retail level in Malaysia. *Food Control* **21**, 774-778.

Portnoy, D.A., Auerbuch, V. and Glomski, I.J. (2002) The cell biology of *Listeria monocytogenes* infection: the intersection of bacterial pathogenesis and cell-mediated immunity. *The Journal of Cell Biology* **158**, 409-414.

Portnoy, D.A., Chakraborty, T., Goebel, W. and Cossart, P. (1992) Molecular determinants of *Listeria monocytogenes* pathogenesis. *Infection and Immunity* **60**, 1263-1267.

Prigent-Combaret, C., Prensier, G., Le Thi, T.T., Vidal, O., Lejeune, P. and Dorel, C. (2000) Developmental pathway for biofilm formation in curli-producing *Escherichia coli* strains: role of flagella, curli and colanic acid. *Environmental Microbiology* **2**, 450-464.

Raafat, D. and Sahl, H.G. (2009) Chitosan and its antimicrobial potential–a critical literature survey. *Microbial Biotechnology* **2**, 186-201.

Rabea, E.I., Badawy, M.E.T., Stevens, C.V., Smagghe, G. and Steurbaut, W. (2003) Chitosan as antimicrobial agent: Applications and mode of action. *Biomacromolecules* **4**, 1457-1465.

Rabin, N., Zheng, Y., Opoku-Temeng, C., Du, Y., Bonsu, E. and Sintim, H.O. (2015) Biofilm formation mechanisms and targets for developing antibiofilm agents. *Future Medicinal Chemistry* **7**, 493-512.

Radoshevich, L. and Cossart, P. (2018) *Listeria monocytogenes*: towards a complete picture of its physiology and pathogenesis. *Nature Reviews Microbiology* **16**, 32-46.

Ragimbeau, C. (2002) Characterization of *Listeria monocytogenes* populations in the smoked fish sector: genetic diversity, influence of the food matrix on virulence expression: Université des sciences et technologies.

Rai, M., Paralikar, P., Jogee, P., Agarkar, G., Ingle, A.P., Derita, M. and Zacchino, S. (2017) Synergistic antimicrobial potential of essential oils in combination with nanoparticles: Emerging trends and future perspectives. *International Journal of Pharmaceutics* **519**, 67-78.

Rampino, A., Borgogna, M., Blasi, P., Bellich, B. and Cesaro, A. (2013) Chitosan nanoparticles: Preparation, size evolution and stability. *International Journal of Pharmaceutics* **455**, 219-228.

Rasamiravaka, T., Labtani, Q., Duez, P. and El Jaziri, M. (2015) The formation of biofilms by *Pseudomonas aeruginosa*: a review of the natural and synthetic compounds interfering with control mechanisms. *BioMed Research International* **2015**.

Rashid, M.H. and Kornberg, A. (2000) Inorganic polyphosphate is needed for swimming, swarming, and twitching motilities of *Pseudomonas aeruginosa*. *Proceedings of the National Academy of Sciences* **97**, 4885-4890.

Ray, B. and Bhunia, A. (2007) *Fundamental Food Microbiology*: CRC press.

Reis-Teixeira, F.B.d., Alves, V.F. and Martinis, E.C.P.d. (2017) Growth, viability and architecture of biofilms of *Listeria monocytogenes* formed on abiotic surfaces. *Brazilian Journal of Microbiology* **48**, 587-591.

Renier, S., Hébraud, M. and Desvaux, M. (2011) Molecular biology of surface colonization by *Listeria monocytogenes*: an additional facet of an opportunistic Gram-positive foodborne pathogen. *Environmental Microbiology* **13**, 835-850.

Rice, K.C., Firek, B.A., Nelson, J.B., Yang, S.-J., Patton, T.G. and Bayles, K.W. (2003) The *Staphylococcus aureus* cidAB operon: evaluation of its role in regulation of murein hydrolase activity and penicillin tolerance. *Journal of Bacteriology* **185**, 2635-2643.

Rice, K.C., Mann, E.E., Endres, J.L., Weiss, E.C., Cassat, J.E., Smeltzer, M.S. and Bayles, K.W. (2007) The cidA murein hydrolase regulator contributes to DNA release and biofilm development in *Staphylococcus aureus*. *Proceedings of the National Academy of Sciences* **104**, 8113-8118.

Roberts, P.H., Davis, K.C., Garstka, W.R. and Bhunia, A.K. (2001) Lactate dehydrogenase release assay from Vero cells to distinguish verotoxin producing *Escherichia coli* from non-verotoxin producing strains. *Journal of Microbiological Methods* **43**, 171-181.

Rodríguez-López, P., Rodríguez-Herrera, J., Vázquez-Sánchez, D. and Lopez Cabo, M. (2018) Current knowledge on *Listeria monocytogenes* biofilms in food-related environments: Incidence, resistance to biocides, ecology and biocontrol. *Foods* **7**, 85.

Rogers, H.W., Callery, M.P., Deck, B. and Unanue, E.R. (1996) *Listeria monocytogenes* induces apoptosis of infected hepatocytes. *Journal of Immunology* **156**, 679-684.

Roll, J. and Czuprynski, C. (1990) Hemolysin is required for extraintestinal dissemination of *Listeria monocytogenes* in intragastrically inoculated mice. *Infection and Immunity* **58**, 3147 - 3150.

Rumbaugh, K.P., Griswold, J.A. and Hamood, A.N. (2000) The role of quorum sensing in the *in vivo* virulence of *Pseudomonas aeruginosa*. *Microbes and Infection* **2**, 1721-1731.

Rupp, M.E., Ulphani, J.S., Fey, P.D., Bartscht, K. and Mack, D. (1999) Characterization of the importance of polysaccharide intercellular adhesin/hemagglutinin of *Staphylococcus epidermidis* in the pathogenesis of biomaterial-based infection in a mouse foreign body infection model. *Infection and Immunity* **67**, 2627-2632.

Rychli, K., Guinane, C.M., Daly, K., Hill, C. and Cotter, P.D. (2014) Generation of nonpolar deletion mutants in *Listeria monocytogenes* using the "SOEing" method. In *Listeria monocytogenes*. pp.187-200: Springer.

Sakuragi, Y. and Kolter, R. (2007) Quorum-sensing regulation of the biofilm matrix genes (pel) of *Pseudomonas aeruginosa*. *Journal of Bacteriology* **189**, 5383-5386.

Saldaña, Z., Xicohtencatl-Cortes, J., Avelino, F., Phillips, A.D., Kaper, J.B., Puente, J.L. and Girón, J.A. (2009) Synergistic role of curli and cellulose in cell adherence and biofilm formation of attaching and effacing *Escherichia coli* and identification of Fis as a negative regulator of curli. *Environmental Microbiology* **11**, 992-1006.

Sanguansri, P. and Augustin, M.A. (2006) Nanoscale materials development–a food industry perspective. *Trends in Food Science & Technology* **17**, 547-556.

Santiago, N.I., Zipf, A. and Bhunia, A.K. (1999) Influence of temperature and growth phase on expression of a 104-kilodalton *Listeria* adhesion protein in *Listeria monocytogenes*. *Applied and Environmental Microbiology* **65**, 2765-2769.

Sawtarie, N., Cai, Y. and Lapitsky, Y. (2017) Preparation of chitosan/tripolyphosphate nanoparticles with highly tunable size and low polydispersity. *Colloids and Surfaces B: biointerfaces* **157**, 110-117.

Scallan, E., Hoekstra, R., Angulo, F., Tauxe, R. and Griffin, P. (2011) Foodborne Illness Acquired in the United States-Major Pathogens. *Emerging Infectious Diseases* **17**, 7-15.

Scharff, R. (2012) Economic burden from health losses due to foodborne illness in the United States. *Journal of Food Protection* **75**, 123-131.

Schertzer, J.W., Boulette, M.L. and Whiteley, M. (2009) More than a signal: non-signaling properties of quorum sensing molecules. *Trends in Microbiology* **17**, 189-195.

Schirmer, B., Heir, E., Møretrø, T., Skaar, I. and Langsrud, S. (2013) Microbial background flora in small-scale cheese production facilities does not inhibit growth and surface attachment of *Listeria monocytogenes*. *Journal of Dairy Science* **96**, 6161-6171.

Schnupf, P. and Portnoy, D.A. (2007) Listeriolysin O: a phagosome-specific lysin. *Microbes and Infection* **9**, 1176-1187.

Scortti, M., Monzó, H.J., Lacharme-Lora, L., Lewis, D.A. and Vázquez-Boland, J.A. (2007) The PrfA virulence regulon. *Microbes and Infection* **9**, 1196-1207.

Sheikh, J., Hicks, S., Dall'Agnol, M., Phillips, A.D. and Nataro, J.P. (2001) Roles for Fis and YafK in biofilm formation by enteroaggregative *Escherichia coli*. *Molecular Microbiology* **41**, 983-997.

Shirron, N., Kisluk, G., Zelikovich, Y., Eivin, I., Shimoni, E. and Yaron, S. (2009) A comparative study assaying commonly used sanitizers for antimicrobial activity against indicator bacteria and a *Salmonella* Typhimurium strain on fresh produce. *Journal of Food Protection* **72**, 2413-2417.

Silk, B.J., Date, K.A., Jackson, K.A., Pouillot, R., Holt, K.G., Graves, L.M., Ong, K.L., Hurd, S., Meyer, R., Marcus, R., Shiferaw, B., Norton, D.M., Medus, C., Zansky, S.M., Cronquist, A.B., Henao, O.L., Jones, T.F., Vugia, D.J., Farley, M.M. and Mahon, B.E. (2012) Invasive listeriosis

in the foodborne diseases active surveillance network (FoodNet), 2004-2009: Further targeted prevention needed for higher-risk groups. *Clinical Infectious Diseases* **54**, S396-S404.

Simões, M., Simões, L.C. and Vieira, M.J. (2010) A review of current and emergent biofilm control strategies. *LWT - Food Science and Technology* **43**, 573-583.

Singh, A.K., Bai, X., Amalaradjou, M.A.R. and Bhunia, A.K. (2018) Antilisterial and antibiofilm activities of pediocin and LAP functionalized gold nanoparticles. *Frontiers in Sustainable Food Systems* **2**, 74.

Sokolovic, Z., Fuchs, A. and Goebel, W. (1990) Synthesis of species-specific stress proteins by virulent strains of *Listeria monocytogenes*. *Infection and immunity* **58**, 3582-3587.

Song, Z., Li, F., Guan, H., Xu, Y., Fu, Q. and Li, D. (2017) Combination of nisin and ε-polylysine with chitosan coating inhibits the white blush of fresh-cut carrots. *Food Control* **74**, 34-44.

Sørensen, S.J., Bailey, M., Hansen, L.H., Kroer, N. and Wuertz, S. (2005) Studying plasmid horizontal transfer in situ: a critical review. *Nature Reviews Microbiology* **3**, 700-710.

Srey, S., Jahid, I.K. and Ha, S.-D. (2013) Biofilm formation in food industries: A food safety concern. *Food Control* **31**, 572-585.

Stewart, P.S. and Franklin, M.J. (2008) Physiological heterogeneity in biofilms. *Nature Reviews Microbiology* **6**, 199.

Sudarshan, N.R., Hoover, D.G. and Knorr, D. (1992) Antibacterial action of chitosan. *Food Biotechnology* **6**, 257-272.

Sue, D., Fink, D., Wiedmann, M. and Boor, K.J. (2004) SigB-dependent gene induction and expression in *Listeria monocytogenes* during osmotic and acid stress conditions simulating the intestinal environment. *Microbiology* **150**, 3843-3855.

Sullivan, D.J., Cruz-Romero, M., Collins, T., Cummins, E., Kerry, J.P. and Morris, M.A. (2018) Synthesis of monodisperse chitosan nanoparticles. *Food Hydrocolloids* **83**, 355-364.

Swaminathan, B. and Gerner-Smidt, P. (2007b) The epidemiology of human listeriosis. *Microbes and Infection* **9**, 1236-1243.

Taglialegna, A., Navarro, S., Ventura, S., Garnett, J.A., Matthews, S., Penades, J.R., Lasa, I. and Valle, J. (2016) Staphylococcal Bap proteins build amyloid scaffold biofilm matrices in response to environmental signals. *PLoS Pathog* **12**, e1005711.

Tang, Y.-W. and Sails, A. (2014) *Molecular Medical Microbiology*: Academic press.

Tattoli, I., Sorbara, M.T., Yang, C., Tooze, S.A., Philpott, D.J. and Girardin, S.E. (2013) *Listeria* phospholipases subvert host autophagic defenses by stalling pre-autophagosomal structures. *The EMBO Journal* **32**, 3066-3078.

Thi, M.T.T., Wibowo, D. and Rehm, B.H. (2020) *Pseudomonas aeruginosa* Biofilms. *International Journal of Molecular Sciences* **21**, 8671.

Tiensuu, T., Andersson, C., Rydén, P. and Johansson, J. (2013) Cycles of light and dark co-ordinate reversible colony differentiation in *Listeria monocytogenes*. *Molecular microbiology* **87**, 909-924.

Tilney, L.G., Connelly, P.S. and Portnoy, D.A. (1990) Actin filament nucleation by the bacterial pathogen, *Listeria monocytogenes*. *The Journal of Cell Biology* **111**, 2979-2988.

Tilney, L.G. and Portnoy, D.A. (1989) Actin filaments and the growth, movement, and spread of the intracellular bacterial parasite, *Listeria monocytogenes*. *The Journal of Cell Biology* **109**, 1597-1608.

To, M.S., Favrin, S., Romanova, N. and Griffiths, M.W. (2002) Postadaptational resistance to benzalkonium chloride and subsequent physicochemical modifications of *Listeria monocytogenes*. *Applied and Environmental Microbiology* **68**, 5258-5264.

Toledo-Arana, A., Dussurget, O., Nikitas, G., Sesto, N., Guet-Revillet, H., Balestrino, D., Loh, E., Gripenland, J., Tiensuu, T., Vaitkevicius, K., Barthelemy, M., Vergassola, M., Nahori, M.-A., Soubigou, G., Regnault, B., Coppee, J.-Y., Lecuit, M., Johansson, J. and Cossart, P. (2009) The *Listeria* transcriptional landscape from saprophytism to virulence. *Nature* **459**, 950-956.

Toledo-Arana, A., Merino, N., Vergara-Irigaray, M., Débarbouillé, M., Penadés, J.R. and Lasa, I. (2005) *Staphylococcus aureus* develops an alternative, ica-independent biofilm in the absence of the arlRS two-component system. *Journal of Bacteriology* **187**, 5318-5329.

Tolker-Nielsen, T. (2014) *Pseudomonas aeruginosa* biofilm infections: from molecular biofilm biology to new treatment possibilities. *APMIS* **122**, 1-51.

Toutain, C.M., Caizza, N.C., Zegans, M.E. and O'Toole, G.A. (2007) Roles for flagellar stators in biofilm formation by Pseudomonas aeruginosa. *Research in Microbiology* **158**, 471-477.

Travier, L., Guadagnini, S., Gouin, E., Dufour, A., Chenal-Francisque, V., Cossart, P., Olivo-Marin, J.-C., Ghigo, J.-M., Disson, O. and Lecuit, M. (2013a) ActA promotes *Listeria monocytogenes* aggregation, intestinal colonization and carriage. *PLoS Pathogens* **9**, e1003131.

Travier, L., Guadagnini, S., Gouin, E., Dufour, A., Chenal-Francisque, V., Cossart, P., Olivo-Marin, J.-C., Ghigo, J.-M., Disson, O. and Lecuit, M. (2013b) ActA promotes *Listeria monocytogenes* aggregation, intestinal colonization and carriage. *PLoS Pathog* **9**, e1003131.

Tremoulet, F., Duche, O., Namane, A., Martinie, B., European Listeria Genome, C. and Labadie, J.C. (2002) Comparison of protein patterns of *Listeria monocytogenes* grown in biofilm or in planktonic mode by proteomic analysis. *FEMS Microbiology Letters* **210**, 25-31.

Tsai, G.-J., Zhang, S.-L. and Shieh, P.-L. (2004) Antimicrobial activity of a low-molecular-weight chitosan obtained from cellulase digestion of chitosan. *Journal of Food Protection* **67**, 396-398.

Tsai, Y.-H., Disson, O., Bierne, H. and Lecuit, M. (2013) Murinization of internalin extends its receptor repertoire, altering *Listeria monocytogenes* cell tropism and host responses. *PLoS Pathogens* **9**, e1003381.

Valilis, E., Ramsey, A., Sidiq, S. and DuPont, H.L. (2018) Non-O157 Shiga toxin-producing *Escherichia coli*—A poorly appreciated enteric pathogen: Systematic review. *International Journal of Infectious Diseases* **76**, 82-87.

van der Veen, S. and Abee, T. (2010) Importance of SigB for *Listeria monocytogenes* static and continuous-flow biofilm formation and disinfectant resistance. *Applied and Environmental Microbiology* **76**, 7854-7860.

Van der Veen, S. and Abee, T. (2011) Mixed species biofilms of *Listeria monocytogenes* and *Lactobacillus plantarum* show enhanced resistance to benzalkonium chloride and peracetic acid. *International Journal of Food Microbiology* **144**, 421-431.

van der Waaij, D.a., Berghuis, J. and Lekkerkerk, J. (1972) Colonization resistance of the digestive tract of mice during systemic antibiotic treatment. *Epidemiology & Infection* **70**, 605-610.

Vandeplas, S., Dauphin, R.D., Beckers, Y., Thonart, P. and Thewis, A. (2010) *Salmonella* in chicken: Current and developing strategies to reduce contamination at farm level. *Journal of Food Protection* **73**, 774-785.

Vasseur, P., Vallet-Gely, I., Soscia, C., Genin, S. and Filloux, A. (2005) The pel genes of the *Pseudomonas aeruginosa* PAK strain are involved at early and late stages of biofilm formation. *Microbiology* **151**, 985-997.

Vial, P.A., Robins-Browne, R., Lior, H., Prado, V., Kaper, J.B., Nataro, J.P., Maneval, D., Elsayed, A.-e.-d. and Levine, M.M. (1988) Characterization of enteroadherent-aggregative *Escherichia coli*, a putative agent of diarrheal disease. *Journal of Infectious Diseases* **158**, 70-79.

Vidal, O., Longin, R., Prigent-Combaret, C., Dorel, C., Hooreman, M. and Lejeune, P. (1998) Isolation of an *Escherichia coli* K-12 mutant strain able to form biofilms on inert surfaces: involvement of a new *ompR* allele that increases curli expression. *Journal of Bacteriology* **180**, 2442-2449.

Vitale, M., Scatassa, M.L., Cardamone, C., Oliveri, G., Piraino, C., Alduina, R. and Napoli, C. (2015) Staphylococcal food poisoning case and molecular analysis of toxin genes in

Staphylococcus aureus strains isolated from food in Sicily, Italy. *Foodborne Pathogens and Disease* **12**, 21-23.

Wampler, J.L., Kim, K.P., Jaradat, Z. and Bhunia, A.K. (2004a) Heat shock protein 60 acts as a receptor for the *Listeria* adhesion protein in Caco-2 cells. *Infection and Immunity* **72**, 931-936.

Wampler, J.L., Kim, K.P., Jaradat, Z. and Bhunia, A.K. (2004b) Heat shock protein 60 acts as a receptor for the *Listeria* adhesion protein in Caco-2 cells. *Infection and Immunity* **72**, 931-936.

Wang, J., Wang, C., Yu, H.B., Dela Ahator, S., Wu, X., Lv, S. and Zhang, L.H. (2019) Bacterial quorum-sensing signal IQS induces host cell apoptosis by targeting POT1–p53 signalling pathway. *Cellular Microbiology* **21**, e13076.

Wang, M., Gao, Z., Zhang, Z., Pan, L. and Zhang, Y. (2014) Roles of M cells in infection and mucosal vaccines. *Human Vaccines and Immunotherapeutics* **10**, 3544-3551.

Wang, R. (2019) Biofilms and meat safety: a mini-review. *Journal of food protection* **82**, 120-127.

Watts, T.H., Scraba, D.G. and Paranchych, W. (1982) Formation of 9-nm filaments from pilin monomers obtained by octyl-glucoside dissociation of Pseudomonas aeruginosa pili. *Journal of Bacteriology* **151**, 1508-1513.

Weigel, L.M., Donlan, R.M., Shin, D.H., Jensen, B., Clark, N.C., McDougal, L.K., Zhu, W., Musser, K.A., Thompson, J., Kohlerschmidt, D., Dumas, N., Limberger, R.J. and Patel, J.B. (2007) High-level vancomycin-resistant *Staphylococcus aureus* isolates associated with a polymicrobial biofilm. *Antimicrob Agents Ch* **51**, 231.

Werbrouck, H., Grijspeerdt, K., Botteldoorn, N., Van Pamel, E., Rijpens, N., Van Damme, J., Uyttendaele, M., Herman, L. and Van Coillie, E. (2006) Differential inlA and inlB expression and interaction with human intestinal and liver cells by *Listeria monocytogenes* strains of different origins. *Applied and Environmental Microbiology* **72**, 3862-3871.

Whitchurch, C.B., Tolker-Nielsen, T., Ragas, P.C. and Mattick, J.S. (2002) Extracellular DNA required for bacterial biofilm formation. *Science* **295**, 1487-1487.

Wollert, T., Pasche, B., Rochon, M., Deppenmeier, S., van den Heuvel, J., Gruber, A.D., Heinz, D.W., Lengeling, A. and Schubert, W.D. (2007) Extending the host range of *Listeria monocytogenes* by rational protein design. *Cell* **129**, 891-902.

Wu, S., Wu, Q., Zhang, J., Chen, M. and Hu, H. (2015) *Listeria monocytogenes* prevalence and characteristics in retail raw foods in China. *PLoS One* **10**, e0136682.

Xiao, G., Déziel, E., He, J., Lépine, F., Lesic, B., Castonguay, M.H., Milot, S., Tampakaki, A.P., Stachel, S.E. and Rahme, L.G. (2006a) MvfR, a key *Pseudomonas aeruginosa* pathogenicity LTTR-class regulatory protein, has dual ligands. *Molecular Microbiology* **62**, 1689-1699.

Xiao, G., He, J. and Rahme, L.G. (2006b) Mutation analysis of the *Pseudomonas aeruginosa* mvfR and pqsABCDE gene promoters demonstrates complex quorum-sensing circuitry. *Microbiology* **152**, 1679-1686.

Yamada, F., Ueda, F., Ochiai, Y., Mochizuki, M., Shoji, H., Ogawa-Goto, K., Sata, T., Ogasawara, K., Fujima, A. and Hondo, R. (2006) Invasion assay of *Listeria monocytogenes* using Vero and Caco-2 cells. *Journal of Microbiological Methods* **66**, 96-103.

Yang, Y., Yang, S., Wang, Y., Yu, Z., Ao, H., Zhang, H., Qin, L., Guillaume, O., Eglin, D. and Richards, R.G. (2016) Anti-infective efficacy, cytocompatibility and biocompatibility of a 3D-printed osteoconductive composite scaffold functionalized with quaternized chitosan. *Acta Biomaterialia* **46**, 112-128.

Yaron, S. and Romling, U. (2014) Biofilm formation by enteric pathogens and its role in plant colonization and persistence. *Microbial Biotechnology* **7**, 496-516.

Ye, R., Xu, H., Wan, C., Peng, S., Wang, L., Xu, H., Aguilar, Z.P., Xiong, Y., Zeng, Z. and Wei, H. (2013) Antibacterial activity and mechanism of action of ε-poly-L-lysine. *Biochemical and Biophysical Research Communications* **439**, 148-153.

Yoshida, T. and Nagasawa, T. (2003) epsilon-Poly-L-lysine: microbial production, biodegradation and application potential. *Applied Microbiology and Biotechnology* **62**, 21-26.

You, X., Einson, J.E., Lopez-Pena, C.L., Song, M., Xiao, H., McClements, D.J. and Sela, D.A. (2017) Food-grade cationic antimicrobial ε-polylysine transiently alters the gut microbial community and predicted metagenome function in CD-1 mice. *NPJ Science of Food* **1**, 1-10.

Yu, T., Jiang, X., Zhang, Y., Ji, S., Gao, W. and Shi, L. (2018) Effect of benzalkonium chloride adaptation on sensitivity to antimicrobial agents and tolerance to environmental stresses in *Listeria monocytogenes*. *Frontiers in Microbiology* **9**, 2906.

Zhang, T., Shao, M.-F. and Ye, L. (2012) 454 Pyrosequencing reveals bacterial diversity of activated sludge from 14 sewage treatment plants. *The ISME Journal* **6**, 1137-1147.

Zhu, X., Liu, D., Singh, A.K., Drolia, R., Bai, X., Tenguria, S. and Bhunia, A.K. (2018) Tunicamycin mediated inhibition of wall teichoic acid affects *Staphylococcus aureus* and *Listeria monocytogenes* cell morphology, biofilm formation and virulence. *Frontiers in Microbiology* **9**, 1352-1352.

Zogaj, X., Nimtz, M., Rohde, M., Bokranz, W. and Römling, U. (2001) The multicellular morphotypes of *Salmonella typhimurium* and *Escherichia coli* produce cellulose as the second component of the extracellular matrix. *Molecular Microbiology* **39**, 1452-1463.

PUBLICATIONS

1. Bai, X., Liu, D., Xu, L., Tenguria, S., Drolia, R., Gallina, N.L., Cox, A.D., Koo, O.-K. and Bhunia, A.K. (2021) Biofilm-isolated *Listeria monocytogenes* exhibits reduced systemic dissemination at the early (12–24 h) stage of infection in a mouse model. NPJ Biofilms and Microbiomes 7, 18.
2. Drolia, R., Amalaradjou, M.A.R., Ryan, V.E., Tenguria, S., Liu, D., Bai., X., Xu, L., Singh, A.K., Cox, A.D., Bernal-Crespo, V., Schaber, J.A., Applegate, B.M., Vemulapalli, R., and Bhunia, A.K. 2020. Receptor-targeted engineered probiotics mitigate lethal *Listeria* infection. Nature Communications 11, 6344.
3. Kim, K.-P., Singh, A.K., Bai, X., Leprun, L. and Bhunia, A.K. (2015) Novel PCR assays complement laser biosensor-based method and facilitate *Listeria* species detection from food. Sensors 15, 22672-22691.
4. Singh, A.K., Bai, X., Amalaradjou, M.A.R. and Bhunia, A.K. (2018) Antilisterial and antibiofilm activities of Pediocin and LAP functionalized gold nanoparticles. Frontiers in Sustainable Food Systems 2, 74.
5. Singh, A.K., Drolia, R., Bai, X. and Bhunia, A.K. (2015) Streptomycin induced stress response in *Salmonella enterica serovar* Typhimurium shows distinct colony scatter signature. PloS One 10, e0135035.
6. Singh, A.K., Leprun, L., Drolia, R., Bai, X., Kim, H., Aroonnual, A., Bae, E., Mishra, K.K. and Bhunia, A.K. (2016) Virulence gene-associated mutant bacterial colonies generate differentiating two-dimensional laser scatter fingerprints. Applied and Environmental Microbiology 82, 3256-3268.
7. Singh, A.K., Sun, X., Bai, X., Kim, H., Abdelhaseib, M.U., Bae, E. and Bhunia, A.K. (2015) Label-free, non-invasive light scattering sensor for rapid screening of *Bacillus* colonies. Journal of Microbiological Methods 109, 56-66.
8. Sun, Q., Wu, S., Yin, R., Bai, X., Bhunia, A.K., Liu, C., Zheng, Y., Wang, F. and Blatchley III, E.R. (2021) Effects of fulvic acid size on microcystin-LR photodegradation and detoxification in the chlorine/UV process. Water Research 193, 116893.
9. Xu, L., Bai, X. and Bhunia, A.K. (2021) Current State of Biosensors Development and their Application in Foodborne Pathogen Detection. Journal of Food Protection. In Press.

10. Xu, L., Bai, X., Tenguria, S., Liu, Y., Drolia, R. and Bhunia, A.K. (2020) Mammalian Cell-Based Immunoassay for Detection of Viable Bacterial Pathogens. Frontiers in Microbiology 11, 575615.
11. Zhu, X., Liu, D., Singh, A.K., Drolia, R., Bai, X., Tenguria, S. and Bhunia, A.K. (2018) Tunicamycin mediated inhibition of wall teichoic acid affects *Staphylococcus aureus* and *Listeria monocytogenes* cell morphology, biofilm formation and virulence. Frontiers in Microbiology 9, 1352.